University of Windsor
Scholarship at UWindsor

Electronic Theses and Dissertations

2001

Evaluation of impact factors of straight and horizontally curved composite concrete deck-steel cellular bridges.

Xuesheng. Zhang
University of Windsor

Follow this and additional works at: http://scholar.uwindsor.ca/etd

Recommended Citation
Zhang, Xuesheng., "Evaluation of impact factors of straight and horizontally curved composite concrete deck-steel cellular bridges." (2001). *Electronic Theses and Dissertations.* Paper 1980.

This online database contains the full-text of PhD dissertations and Masters' theses of University of Windsor students from 1954 forward. These documents are made available for personal study and research purposes only, in accordance with the Canadian Copyright Act and the Creative Commons license—CC BY-NC-ND (Attribution, Non-Commercial, No Derivative Works). Under this license, works must always be attributed to the copyright holder (original author), cannot be used for any commercial purposes, and may not be altered. Any other use would require the permission of the copyright holder. Students may inquire about withdrawing their dissertation and/or thesis from this database. For additional inquiries, please contact the repository administrator via email (scholarship@uwindsor.ca) or by telephone at 519-253-3000ext. 3208.

INFORMATION TO USERS

This manuscript has been reproduced from the microfilm master. UMI films the text directly from the original or copy submitted. Thus, some thesis and dissertation copies are in typewriter face, while others may be from any type of computer printer.

The quality of this reproduction is dependent upon the quality of the copy submitted. Broken or indistinct print, colored or poor quality illustrations and photographs, print bleedthrough, substandard margins, and improper alignment can adversely affect reproduction.

In the unlikely event that the author did not send UMI a complete manuscript and there are missing pages, these will be noted. Also, if unauthorized copyright material had to be removed, a note will indicate the deletion.

Oversize materials (e.g., maps, drawings, charts) are reproduced by sectioning the original, beginning at the upper left-hand corner and continuing from left to right in equal sections with small overlaps.

ProQuest Information and Learning
300 North Zeeb Road, Ann Arbor, MI 48106-1346 USA
800-521-0600

NOTE TO USERS

This reproduction is the best copy available.

UMI

EVALUATION OF IMPACT FACTORS OF STRAIGHT AND HORIZONTALLY CURVED COMPOSITE CONCRETE DECK-STEEL CELLULAR BRIDGES

BY

XUESHENG ZHANG

A Thesis
submitted to the Faculty of Graduate Studies and Research through
the Department of Civil and Environmental Engineering
in Partial Fulfillment of the Requirements for the
Degree of Master of Applied Science at the
University of Windsor

Windsor, Ontario, Canada
2001

National Library of Canada
Acquisitions and Bibliographic Services
395 Wellington Street
Ottawa ON K1A 0N4
Canada

Bibliothèque nationale du Canada
Acquisitions et services bibliographiques
395, rue Wellington
Ottawa ON K1A 0N4
Canada

Your file Votre référence

Our file Notre référence

The author has granted a non-exclusive licence allowing the National Library of Canada to reproduce, loan, distribute or sell copies of this thesis in microform, paper or electronic formats.

The author retains ownership of the copyright in this thesis. Neither the thesis nor substantial extracts from it may be printed or otherwise reproduced without the author's permission.

L'auteur a accordé une licence non exclusive permettant à la Bibliothèque nationale du Canada de reproduire, prêter, distribuer ou vendre des copies de cette thèse sous la forme de microfiche/film, de reproduction sur papier ou sur format électronique.

L'auteur conserve la propriété du droit d'auteur qui protège cette thèse. Ni la thèse ni des extraits substantiels de celle-ci ne doivent être imprimés ou autrement reproduits sans son autorisation.

0-612-67578-5

Canada

945470

Xuesheng Zhang
© 2001
All Rights Reserved

I hereby declare that I am the sole author of this document.

I authorize the University of Windsor to lend this document to other institutions or individuals for the purpose of scholarly research.

Xuesheng Zhang

I further authorize the University of Windsor to reproduce the document by photocopying or by other means, in total or part, at the request of other institutions or individuals for the purpose of scholarly research.

Xuesheng Zhang

THE UNIVERSITY OF WINDSOR requires the signatures of all persons using or photocopying this document.

Please sign below, and give address and date.

ABSTRACT

The use of horizontally curved composite bridges in interchanges of modern highway systems has become increasingly popular for economic as well as aesthetic considerations. A cellular steel section composite with a concrete deck is one of the most suitable structures in resisting torsional and warping effects induced by highway curvature. This type of structure has inherently created new design problems for engineers in estimating its dynamic impact factors as well as dynamic characteristics when subjected to moving vehicle loading. North American codes of practice have recommended some provisions for impact factors; however, they do not include this type of straight and curved bridges. To meet the practical requirements arising during the design process, a simple design method is needed for straight and curved composite multi-cell bridges in the form of impact factors for moment, reaction and deflection.

A theoretical investigation of the dynamic impact factors for straight and curved composite cellular bridges is performed in this thesis. The bridges are modelled as three-dimensional solid structures using commercially available software "ABAQUS" to simulate the bridge geometry and vehicle loading. The vehicle loads are modelled as a pair of two concentrated forces moving along in circumferential paths.

Extensive parametric study is conducted, in which 120 composite multi-cell bridge prototypes are analyzed to: (1) evaluate their first natural frequencies; (2) evaluate their impact factors for moment, reaction, and deflection under truck loading conditions. The key parameters considered in this study are: number and area of cross-bracing and top-chord systems, number of cells, number of lanes, degree of curvature, span length, and loading conditions.

Based on the data generated from the parametric study, expressions for dynamic impact factors for moment, reaction, and deflection are proposed. Moreover, expressions for

the first flexural frequency are developed. The proposed equations for impact factors are compared against those based on other codes for verification. The results from this practical-design-oriented thesis would enable the bridge engineer to design curved composite cellular bridges more reliably and economically.

TO MY FAMILY

ACKNOWLEDGEMENTS

The author wishes to express his deep appreciation to his advisors Dr. John B. Kennedy, University Distinguished Professor, and Dr. Khaled M. Sennah, Assistant Professor, for their constant support and valuable supervision during the development of this research. Dr. Kennedy and Dr. Sennah devoted their time and effort to make this study a success. Their most helpful supervision is greatly appreciated.

The author wishes to acknowledge the financial support provided by the Natural Sciences and Engineering Research Council of Canada.

The author is also very grateful to his parents and his wife for their great support, understanding, and patience throughout the course of this study.

TABLE OF CONTENTS

ABSTRACT vi

ACKNOWLEDGEMENTS ix

LIST OF TABLES. xiii

LIST OF FIGURES xiv

NOTATION xix

CHAPTER

I- INTRODUCTION
- 1.1 General 1
- 1.2 The Problem 3
- 1.3 Objectives and Scope 4
- 1.4 Contents and Arrangement of the Thesis 6

II- LITERATURE REVIEW
- 2.1 General 7
- 2.2 Elastic Analysis of Box Girder Bridges 7
  - 2.2.1 Orthotropic Plate Theory Method 8
  - 2.2.2 Grillage Analogy Method 8
  - 2.2.3 Folded Plate Method 9
  - 2.2.4 Finite-Strip Method 9
  - 2.2.5 Finite-Element Method 11
  - 2.2.6 Thin-Walled Curved Beam Theory 13
- 2.3 Dynamic Response and Codes of Practice for Box Girder Bridges 15

III- FINITE ELEMENT ANALYSIS
- 3.1 General 20
- 3.2 Finite Element Method 21
- 3.3 Description of the Finite Element Program ABAQUS 25
  - 3.3.1 Static Analysis 25
  - 3.3.2 Dynamic Analysis 26
    - (a) Free Vibration Analysis 26
    - (b) Transient modal dynamic analysis (mode superposition method) 28
    - (c) Direct integration dynamic analysis 29
- 3.4 Finite Element Modelling of straight and Curved Composite Multi-Cell Bridges 30
  - 3.4.1 Geometric Modelling 30
    - (a) Modelling of Deck Slab, Webs, Bottom Flange, and End-Diaphragms ... 30
    - (b) Modelling of Steel Top Flanges, Top-chords, and Cross-Bracings 31

3.4.2 Boundary Conditions 32
3.4.3 Material Modelling 32
3.5 Finite Element Analysis of the Bridges and the Prototype Bridges 33
3.5.1 Finite Element Mesh of Bridges 33
3.5.2 Description of the Bridge Prototypes Used in the Parametric Studies 34

IV- METHODOLOGY FOR DYNAMIC IMPACT FACTOR
4.1 General 38
4.2 Truck Idealization 38
4.3 Truck Loading Conditions 40
4.4 Dynamic Impact Factor 42
4.5 Impact Factor Selection Criterion 44

V- DEFINITION AND VERIFICATION OF DYNAMIC ANALYSIS
5.1 General 47
5.2 Free Vibration Analysis 47
5.3 Forced Response Analysis 50
5.3.1 Mode Superposition Method 50
5.3.2 Direct Integration Method 54
5.4 Comparison of Dynamic Analysis Methods 56
5.4.1 Natural Frequency Extraction 57
5.4.2 Parametric Study of Direct Integration Method 58
5.4.3 Comparison of dynamic responses using different methods 59
5.5 Summary 59

VI- FUNDAMENTAL FREQUENCY OF STRAIGHT AND CURVED COMPOSITE CELLULAR BRIDGES
6.1 General 61
6.2 Effect of Cross-Bracing Systems 62
6.3 Effect of Span-to-Depth Ratio 63
6.4 Effect of Span 64
6.5 Effect of Curvature 64
6.6 Effect of Number of Cells and Number of Lanes 65
6.7 Empirical Formulas for the Fundamental Frequency 65

VII- ANALYSIS OF IMPACT FACTORS
7.1 General 68
7.2 Analysis of Effects of Bridges and Vehicle Variables 69
7.2.1 Effect of Cross-Bracing Systems 69
a. Effect of number of cross-bracing systems 69
b. Effect of area of cross-bracing systems 71
7.2.2 Effect of Number of Lanes 72
7.2.3 Effect of Number of Cells 73
7.2.4 Effect of Curvature 73
7.2.5 Effect of Span 74

7.2.6 Effect of Truck Speed 75
7.2.7 Effect of Truck Loading Conditions 76
7.3 Empirical Formulas for Impact Factors 78
7.3.1 Impact Factor as Function of Fundamental Natural Frequency 79
7.3.2 Impact Factor as Function of Span Length 81
7.3.3 Impact Factor as Function of Span-to-curvature Ratio 83
7.4 Verification of Results 84

VIII- SUMMARY AND CONCLUSIONS
8.1 Summary 88
8.2 Conclusions 89
8.3 Recommendations for Future Research 91

REFERENCES 92

TABLES 102

FIGURES 111

APPENDIX

1. Impact Factors Recommended by AASHTO for Horizontally Curved Box Girder Bridges (1980 Edition) 195
2. Impact Factors Recommended by AASHTO for Horizontally Curved Box Girder Bridges (1993 Edition) 196
3. Typical 'ABAQUS' Input Data 198
4. Program for Processing Output Data from ABAQUS 207
5. CD-ROM Input Files

VITA AUCTORIS 217

LIST OF TABLES

Table		Page
3.1	Material properties for concrete and steel	102
3.2.1	Geometry of bridge prototypes of 20 m span	103
3.2.2	Geometry of bridge prototypes of 40 m span	104
3.2.3	Geometry of bridge prototypes of 60 m span	105
3.2.4	Geometry of bridge prototypes of 80 m span	106
3.2.5	Geometry of bridge prototypes of 100 m span	107
5.1	Extracted natural frequencies of *2l-2c-60* straight bridge	108
5.2	Effective mass percentage to the total mass (%) of *2l-2c-60* straight bridge	109
6.1	Comparison of fundamental frequency between proposed method and Sennah's method	109
7.1	Dynamic and static responses of outer girder of *2l-2c-40* straight and curved bridges subjected to different loading cases	110

LIST OF FIGURES

Figure		Page
1.1	Box girder cross-sections	111
1.2	Jacques Cartier I-girder bridge in Montreal, Quebec	112
1.3	Box girder bridge in downtown Toronto	112
1.4	Three-cell bridge cross-section	113
3.1	Shell element "S4R" used for plate modelling	114
3.2	Beam element "B31H" for beam in space	115
3.3	Finite-element discretization of cross-section of the bridge models	115
3.4	Typical finite-element mesh for bridges	116
3.5	Basic cross-section configurations and symbols	117
3.6	Cross-section configurations used in the parametric studies	118
4.1	Truck loading configuration according to AASHTO specifications	119
4.2	Moving load idealization	119
4.3	Loading cases considered I-n the parametric study	120
4.4	Idealized cross-section for analysis of impact factors	121
5.1	Normal stress-time history of edge-girder mid-span bottom-flange of *2l-2c-60* straight bridge by using direct integration method	122
5.2	Enlargement of Fig. 5.1	123
5.3	Normal stress-time history of edge-girder mid-span bottom-flange of *2l-2c-60* straight bridge	124
5.4	Maximum normal stress of edge-girder mid-span bottom-flange of *2l-2c-60* straight bridge	125
5.5	Normal stress-time history of outer-girder mid-span bottom-flange of *2l-2c-60* curved bridge by using direct integration method	126

5.6 Enlargement of Fig. 5.5 127

5.7 Normal stress-time history of outer-girder mid-span bottom-flange of *2l-2c-60* curved bridge 128

5.8 Maximum normal stress of outer-girder mid-span bottom flange of *2l-2c-60* curved bridge 129

6.1 Mode shapes of *2l-2c-40* straight bridge 130

6.2 Mode shapes of *2l-2c-40* curved bridge with L/R = 1.0 131

6.3a Normal stress-time history of edge-girder mid-span bottom-flange of *2l-2c-40* straight bridge 132

6.3b Reaction-time history of edge-web of *2l-2c-40* straight bridge 133

6.3c Deflection-time history of edge-web mid-span of *2l-2c-40* straight bridge 134

6.4a Normal stress-time history of mid-span bottom-flange of *2l-2c-40* curved bridge 135

6.4b Reaction-time history of *2l-2c-40* curved bridge 136

6.4c Deflection-time history of mid-span of *2l-2c-40* curved bridge 137

6.5 Effect of number of cross-bracing systems on fundamental frequency of *2l-2c-40* bridges 138

6.6 Effect of area of cross-bracing systems on fundamental frequency of *2l-2c-40* bridges 139

6.7 Effect of span-to-depth ratio on fundamental frequency of *2l-2c-40* bridges 140

6.8 Effect of span on fundamental frequency of *4l-4c* bridges 141

6.9 Effect of curvature on fundamental frequency of *4l-4c* bridges 142

6.10 Effect of number of cells on fundamental frequency of *3l-100* bridges 143

6.11 Effect of number of lanes on fundamental frequency of bridges with span 40 144

7.1 Effect of number of cross-bracing systems on moment impact factor of *2l-2c-40* bridges 145

7.2 Effect of number of cross-bracing systems on of reaction impact factor of *2l-2c-40* bridges 146

7.3 Effect of number of cross-bracing systems on deflection impact factor of *2l-2c-40* bridges 147

7.4 Effect of area of cross-bracing systems on moment impact factor of *2l-2c-40* bridges 148

7.5 Effect of area of cross-bracing systems on reaction impact factor of *2l-2c-40* bridges 149

7.6 Effect of area of cross-bracing systems on deflection impact factor of *2l-2c-40* bridges 150

7.7 Effect of number of lanes on moment impact factor of *4c-40* bridges 151

7.8 Effect of number of lanes on moment impact factor of *4c-100* bridges 152

7.9 Effect of number of lanes on reaction impact factor of *4c-40* bridges 153

7.10 Effect of number of lanes on reaction impact factor of *4c-100* bridges 154

7.11 Effect of number of lanes on deflection impact factor of *4c-40* bridges 155

7.12 Effect of number of lanes on deflection impact factor of *4c-100* bridges 156

7.13 Effect of number of cells on moment impact factor of *2l-40* bridges 157

7.14 Effect of number of cells on reaction impact factor of *2l-40* bridges 158

7.15 Effect of number of cells on deflection impact factor of *2l-40* bridges 159

7.16 Effect of curvature on moment impact factor of *4c-40* bridges 160

7.17 Effect of curvature on moment impact factor of *4c-100* bridges 161

7.18 Effect of curvature on reaction impact factor of *4c-40* bridges 162

7.19 Effect of curvature on reaction impact factor of *4c-100* bridges 163

7.20 Effect of curvature on deflection impact factor of *4c-40* bridges 164

7.21 Effect of curvature on deflection impact factor of *4c-100* bridges 165

7.22 Effect of span on moment impact factor of *3l-4c* bridges 166

7.23 Effect of span on reaction impact factor of *3l-4c* bridges 167

7.24 Effect of span on deflection impact factor of *3l-4c* bridges 168

7.25 Effect of span on moment impact factor of *2l-2c* bridges 169

7.26 Effect of span on reaction impact factor of *2l-2c* bridges 170

7.27 Effect of span on deflection impact factor of *2l-2c* bridges 171

7.28 Effect of truck speed on moment impact factor of *2l-2c-40* bridges 172

7.29 Effect of truck speed on reaction impact factor of *2l-2c-40* bridges 173

7.30 Effect of truck speed on deflection impact factor of *2l-2c-40* bridges 174

7.31 Effect of truck speed on impact factor of *3l-4c-60* bridges with L/R=0.4 175

7.32 Effect of truck speed on impact factor of *2l-2c-60* straight bridges 176

7.33 Effect of loading condition on moment impact factor of *2l-2c-40* bridges 177

7.34 Moment impact factor versus fundamental frequency of straight bridges 178

7.35 Reaction impact factor versus fundamental frequency of straight bridges 179

7.36 Deflection impact factor versus fundamental frequency of straight bridges 180

7.37 Moment impact factor versus fundamental frequency of curved bridges 181

7.38 Reaction impact factor versus fundamental frequency of curved bridges with L/R $\geq$ 1.0 182

7.39 Reaction impact factor versus fundamental frequency of curved bridges with L/R < 1.0 183

7.40 Deflection impact factor versus fundamental frequency of curved bridges 184

7.41 Moment impact factor versus bridge span of straight bridges 185

7.42 Reaction impact factor versus bridge span of straight bridges 186

7.43 Deflection impact factor versus bridge span of straight bridges 187

7.44 Moment impact factor versus bridge span of curved bridges 188

7.45 Reaction impact factor versus bridge span of curved bridges with curvature L/R $\geq$1.0 189

7.46 Reaction impact factor versus bridge span of curved bridges with curvature L/R<1.0 190

7.47 Deflection impact factor versus bridge span of curved bridges 191

7.48 Moment impact factor versus L/R of curved bridge 192

7.49 Reaction impact factor versus L/R of curved bridges 193

7.50 Deflection impact factor versus L/R of curved bridges 194

NOTATION

A	bridge width
[A]	transform matrix from local to global coordinates at the nodes
b	half bridge width
B	cell width
[B]	strain-displacement matrix
c	symbol of cells in designation of bridge type
C	steel top flange width
[C]	damping matrix
d	depth measured from the centre of the bottom flange to the centre line of the concrete deck slab
D	total depth of the steel cells
[D]	constitutive matrix or elasticity matrix
DLA	dynamic load allowance
e	pavement superelevation
E	modulus of Elasticity
f	dominant frequency, Hz coefficient of side friction between truck tire and road pavement
f_B	body forces
f_{BEAM}	first flexural frequency from beam theory, Hz
f_{CELL}	first flexural frequency for simply-supported curved multi-cell bridge
f_S	surface forces
F	total depth of composite bridge
F_C	centrifugal force

F_D	dynamic value of variable F
F_S	maximum static value of variable F
g	gravitational constant, 32.2 ft / sec^2
G	shear modulus
I	second moment of inertia, impact factor
I_D	deflection impact factor
I_F	dynamic impact factor for the variable F
I_M	moment impact factor
I_R	reaction impact factor
[K]	stiffness matrix
l	symbol of lanes in designation of bridge type
L	centre line, span of simply supported bridge
m	mass per unit length of the bridge
[M]	mass matrix
P	truck axle load
[P]	applied loads vector at the nodes
r	radius of the path along which the centre line of the truck is moving
R	radius of curvature measured from the centre of curvature to bridge centre line
R_C	concentrated forces at nodes
S	design speed of a highway (mile/hour)
t	time
t_l	thickness of steel top flange

t_2	thickness of steel web
t_3	thickness of steel bottom flange
t_4	thickness of concrete deck slab
t_f	flange thickness
t_w	web thickness
[u]	internal displacement vector at any point within an element
[u']	virtual displacement field
[U]	displacement vector at the nodes
v	design speed of a highway (km/h)
W_E	external virtual work
W_I	internal virtual work
X,Y & Z	intermediate factors to calculate the torsional constant of a section
α	correction factor for bridge geometry and curvature, artificial damping
$[\alpha]$	generalized coordinate vector
β	correction factor for bridge geometry and curvature
$[\varepsilon]$	strain matrix
$[\varepsilon']$	virtual strain matrix
ϕ	eigenvector
$[\Phi]$	displacement function, shape function
ρ	density
ω	circular frequency
$[\sigma]$	Cauchy stress matrix

CHAPTER I

INTRODUCTION

1.1 General

Modern highway bridges are often subject to tight geometric restrictions and, in many cases, must be built on curved alignment. Horizontally curved bridges have become important component in highway bridges, especially in densely populated cities where elevated freeways and multi-level interchange structures are necessary.

Curved bridges may be entirely of reinforced concrete, prestressed concrete, steel, or composite concrete deck-steel girders. Moreover, these curved bridges may take the form of a deck slab on I-girders or box girders. Concrete box girders are usually cast in-situ or precast in segments erected on falsework or launching frame and then prestressed. Steel box girders are frequently constructed as segmented cantilevers. In some cases, they are prefabricated in long lengths and lifted into position by climbing jacks and connected together. The decks could be of steel or reinforced concrete. For the case of curved steel plate girders, two methods of fabrications have been employed. One method involves prefabrication of straight webs followed by either cold-bent or heat-curved to achieve the required curvature. In the second method, the curved flanges are cut from straight plates and welded to the webs that are curved. This actual curving of girders has allowed greater

span lengths, fewer piers, and more aesthetically pleasing structures than straight girders used as chords in forming a curved alignment.

A typical curved box girder bridge consists of top and bottom flange plates connected together by cylindrical or conical webs to form the closed structure. Box girder cross-sections may be composed of one or more cells which are either contiguous or separated. Usually interior cell shape is rectangular while edge cells often have vertical, inclined, or rounded outside webs. As shown in Figure 1.1, a box girder cross-section may take the form of single cell (one box), multiple-spine (separate boxes), or multi-cell with a common bottom flange (contiguous cells or cellular shape).

On horizontally curved alignment of highways in rural and urban areas, where curvature is small, open-section bridges such as beam-slab structures have been used. However, as the curvature of the highway increases due to space limitation, bridges of cellular cross-section become more suitable. In addition to their lighter weight, shallower depth of cross-section, and significant longitudinal bending stiffness, cellular bridges are favored for their considerable torsional stiffness to resist applied loads when compared to open sections. The cross-section renders an efficient transverse load distribution as well as high resistance to torsional vibration caused by moving vehicles, wind, or seismic conditions. Such structures are also aesthetically pleasing and relatively inexpensive to maintain since the surface area vulnerable to environmental conditions is small compared to open-sections. In addition, the cells can be used to carry the required utilities.

The ramp shown in Figure 1.2 is a sharply curved part of the Jacques Cartier Bridge crossing the St. Lawrence River between Montreal Island and Longueuil in Quebec. It is

made of curved composite I-girders with small spans and massive vertical, horizontal, and diagonal bracings to increase its torsional stiffness to resist the applied loads. Also, Figure 1.3 shows a four-span continuous, twin-spine, box girder bridge crossing a railway in downtown Toronto. Composite cellular cross-sections, if used in the above mentioned prototype bridges, would have saved in the material content due to their excellent transverse distribution of loads which is nearly uniform in straight bridges. Proper design of straight and curved composite concrete deck-steel cellular bridges requires good understanding of their overall structural behavior in both static and dynamic conditions, as when a truck travels across the bridges. Thus a study of their dynamic characteristics and dynamic impact factors is necessary.

1.2 The Problem

The multi-cell bridge cross-section, shown in Figure 1.4, consists of composite construction of a concrete deck and steel cells. The steel cells consist of two, or more, top flanges and a common bottom flange connected to the top flanges by webs. Shear connectors connecting the steel top flanges with the concrete deck slab ensure full interaction between them. Solid end-diaphragms are used at the support lines of such bridges to seal off the end of the steel cells with an opening to access or lay the utility cables inside the cells. Cross-bracings and top chords (lateral ties between the steel top flanges) made of steel are used between the support lines inside the cells along the span.

The current design practices in North America recommend few analytical methods

for the design of straight and curved composite multi-cell box girder bridges to account for the dynamic effect of truck loading. The Canadian Highway Bridge Design Code, CHBDC 2000, (65) and the Ontario Highway Bridge Design Code, OHBDC 1993, (63) recommend an equation of dynamic load allowance to account for the dynamic effect on moment, reaction, and deflection. The AASHTO Standard Specification (5) recommends an impact factor equation for straight bridges as well. The AASHTO Guide Specification for Horizontally Curved Highway Bridges (4) recommends separate impact factor equations for moment, reaction, and deflection for curved bridges of multi-box cross-section. Therefore, a simplified design method in the form of expressions for moment, reaction and deflection impact factors is required for straight and curved cellular bridges of composite construction.

It is well known that the analytical dynamic response of structures is mainly given by the first few mode shapes and their corresponding natural frequencies. The major contributor is the first mode shape corresponding to the first natural frequency (fundamental frequency) of the system. Therefore, it is very important for designers to have also an idea about the fundamental frequency of the bridges they design to avoid resonance when subjected to external loading such as earthquake, wind, blast, or moving truck loading.

1.3 Objectives and Scope

The main objectives of the present research work are:

1. Investigate the key geometric parameters and loading conditions of straight and curved

composite cellular bridges that affect their dynamic characteristics and impact factors.

2. Develop a simplified design method for straight and curved composite cellular bridges in the form of dynamic impact factors for moment, reaction and deflection.
3. Deduce empirical expressions for the fundamental natural frequency to assist the design of the bridge for serviceability (deflection control).

In this practical-design-oriented thesis, a detailed analytical study on straight and curved composite cellular bridges is presented. Analysis is based on the finite element method, which is capable of including all the important factors influencing the structural behavior. The main parameters examined in the current research are: cross-bracing systems, number of lanes, number of cells, span-to-radius of curvature ratio, L/R, span, speed of truck and loading conditions.

The scope of this study thus includes the following:

1. A literature review of previous research work and codes of practice for straight and curved box girder bridges.
2. Comparative study of dynamic responses of bridges using both the mode superposition method and the direct integration method.
3. Parametric study on the key parameters that may affect (a) the fundamental natural frequency; (b) moment impact factor; (c) reaction impact factor; and (d) deflection impact factor. The study applies to both straight and curved simply-supported bridges.

1.4 Contents and Arrangement of the Thesis

The literature review and previous work on box girder bridges is presented in Chapter II. Chapter III describes the finite element program used in the analytical study. This includes the linear static, free vibration, forced vibration, idealization and modelling of the composite bridge components, and prototype bridges used in this study. Chapter IV deals with the idealization and modelling of truck loading and dynamic impact factor selection criterion. Chapter V discusses two dynamic analysis methods popularly used, i.e., mode superposition method and direct integration method, and comparing the two methods. Chapter VI presents the results of the parametric studies on fundamental natural frequency of bridge studied. Chapter VII presents the results of the parametric studies on the dynamic impact factors for straight and curved bridges. Chapter VIII gives a summery of this research, the conclusions reached, and recommendations for further research.

CHAPTER II

LITERATURE REVIEW

2.1 General

The curvilinear nature of box girder bridges along with the complex deformation patterns and stress fields developed for different boundary conditions and loading cases have compelled designers to adopt approximate and conservative methods for static and dynamic analyses. Recent literatures on straight and curved box girder bridges dealt with analytical formulations. The literature survey presented herein deals with: (*i*) elastic analysis of box girder bridges; (*ii*) dynamic response and codes of practice for box girder bridges.

2.2 Elastic Analysis of Box Girder Bridges

In the design of bridges, analysis is usually simplified by means of assumptions that establish the relationship between the behavior of single elements in the integrated structure. The combined response of these single elements is assumed to represent the response of the whole structure. The accuracy of such solutions depends on the validity of the assumptions made. The Canadian Highway Bridge Design Code, CHBDC 2000, (65) has recommended several methods of analysis for straight box girder bridges only. These

methods include: Orthotropic Plate Theory, Grillage Analogy, Folded Plate, Finite-Strip, and Finite-Element technique. Several authors have applied these methods along with the thin-walled beam theory to the analysis of straight and curved box girder bridges. In the following sections, these different approaches to box girder bridge idealizations and their limitations will be discussed.

2.2.1 Orthotropic Plate Theory Method

In the equivalent orthotropic plate theory method, the stiffness of the flanges and girders are lumped into an orthotropic plate of equivalent stiffness and the stiffness of diaphragms is distributed over the girder length. This method is suggested mainly for multi-I-girder straight and curved bridges. However, the 2000 CHBDC code (65) has recommended using this method for the analysis of only straight box girder bridges of multi-spine cross-section, but not for multi-cell cross-section.

2.2.2 Grillage Analogy Method

Canadian Highway Bridge Design Code of 2000 (65) limits the applicability of this method to voided slab and box girder bridges in which the number of cells or boxes is greater than two. In this method, the multi-cellular superstructure was idealized as a grid assembly by Hambly and Pennells (33). One difficulty of the grillage analogy method lies in the representation of torsional stiffness of the closed cells. Satisfactory, but

approximate representation can be achieved in modelling the torsional stiffness of a single closed cell by an equivalent I-beam torsional stiffness (Evans and Shanmugam, 25).

2.2.3 Folded Plate Method

The folded plate method utilizes the plane stress elasticity theory and the classical two-way plate bending theory to determine the membrane stresses and slab moments in each folded plate member. The folded plate system consists of an assemblage of longitudinal annular plate elements interconnected at joints along their longitudinal edges and simply-supported at the ends. No intermediate diaphragms are assumed. Solution of simply-supported straight or curved box girder bridges is obtained for any arbitrary longitudinal load function by using the direct stiffness harmonic analysis. The method has been applied to cellular structures by Al-Rifaie and Evans (3), Evans (24), and Meyer and Scordelis (59). However, it was evident that the method is complicated and time-consuming. Furthermore, the 2000 CHBDC code (65) restricted this method to bridges with support conditions closely equivalent to line supports at both ends of the bridge.

2.2.4 Finite-Strip Method

The finite-strip method may be regarded as a special form of the displacement formulation of the finite-element method. In principle, it employs the minimum total

potential energy theorem to develop the relationship between unknown nodal displacement parameters and the applied load. In this method, the box girders and plates are discretized into annular finite-strips running from one end-support to the other and connected transversely along their edges by longitudinal nodal lines. The displacement functions of the finite-strips are assumed as a combination of harmonics varying longitudinally and polynomials varying in the transverse direction. Cheung and Cheung (16), in 1971, applied the finite-strip method to curved box girder bridges. Kabir and Scordelis (48), in 1974, developed a finite-strip computer program to analyze curved continuous span cellular bridges, with interior radial diaphragms, on supporting planar frame bents. Cheung and Chan (15), in 1978, used the finite-strip method to determine the effective width of the compression flange of straight multi-spine and multi-cell box girder bridges. Cheung (14), in 1984, used a numerical technique based on the finite-strip method and the force method for the analysis of continuous curved multi-cell box girder bridges. Scordelis et al. (75), in 1985, extended the applicability of the available computer program (48) to take into account the effect of post-tension prestressing tendons. Li et al. (55), in 1988, presented the application of spline finite-strip method to the elasto-static analysis of circular and non-circular multi-cell box girder bridges. Bradford and Wong (8), in 1992, used the finite-strip method to study the local buckling of straight composite concrete deck-steel box section in negative bending. Compared to the finite-element method, the finite-strip method yields considerable savings in both computer time and effort, since only a small number of unknowns are generally required in the analysis. However, the drawback of the finite-strip method is that the method is limited to simply-supported prismatic structures

with simple line supports (65).

2.2.5 Finite-Element Method

During the past two decades, the finite-element method of analysis has rapidly become a very popular technique for the computer solution of complex problems in engineering. In structural analysis, the method can be regarded as an extension of earlier established analytical techniques, in which a structure is represented as an assemblage of discrete elements interconnected at a finite number of nodal points (93). Chapman et al. (13), in 1971, conducted a finite-element analysis on steel and concrete box girder bridges to investigate the effect of intermediate diaphragms on the warping and distortional stresses. Sisodiya et al. (79), in 1970, approximated the curvilinear boundaries of finite elements used to model the curved box girder bridges by a series of straight boundaries using parallelogram elements. This approximation would require a large number of elements enough to achieve a satisfactory solution. Such an approach is impractical especially for highly curved box bridges. Bazant and El Nimeiri (6), in 1974, attributed the problems associated with the neglect of curvilinear boundaries in elements used to model curved box beams by the loss of continuity at the end cross-sections of two adjunct elements meeting at an angle. They developed a skew-ended finite-element with shear deformation using straight elements and adopted a more accurate theory, which allows for transverse shear deformations.

Chu et al. (19), in 1971, developed a finite-element formulation of curved box girder

bridges consisting of horizontal sector plates and vertical cylindrical shell elements. Willam and Scordelis (91), in 1972, presented an elastic analysis of cellular structures of constant depth with arbitrary geometry in plan using quadrilateral elements. Fam and Turkstra (27), in 1975, Fam (26), and Turkstra and Fam (28) described a finite-element scheme for static and free-vibration analysis of box girders with orthogonal boundaries and arbitrary combinations of straight and horizontally curved sections using a four-node plate bending annular element with two straight radial boundaries, for the top and bottom flanges, and conical elements for the inclined web members. Turkstra and Fam (84) also demonstrated the importance of warping stresses in single-cell curved bridge, in relation to the longitudinal normal bending stresses obtained from curved beam theory.

Malcolm and Redwood (57) and Moffatt and Dowling (62) investigated the shear lag phenomena in steel box girder bridges. Sargious et al. (73), in 1979, studied the behavior of end-diaphragms with opening in single-cell concrete box girder bridges supported by a central pier. Ishac and Smith (46), in 1985, presented simple design approximations for determining the transverse moments in single-span single-cell concrete box girder bridges. Dilger et al. (22), in 1988, studied the effect of presence and orientation of diaphragms on the reaction, internal forces, and the behavior of skew, single cell, concrete box girder bridges. Galuta and Cheung (32), in 1995, developed a hybrid analytical solution, which combines the boundary element method (BEM) with the finite-element method (FEM) to analyze box girder bridges. The finite-element method was used to model the webs and bottom slab of the bridge, while the boundary element method was employed to model the top slab.

Recently, some authors have dealt with temperature effects on box girder bridges. Chan et al. (12), in 1990, presented temperature data collected continuously in three composite box-girder bridges over a one-to-two year period. The first bridge was the Portage Bridge spanning the Ottawa River between Hull, Quebec, and Ottawa, Ontario. This bridge is a three-lane, three-span continuous, composite concrete deck-steel five-box structure with a total length of 158.5 m. The second bridge was the St. Leonard Bridge, International Bridge over the St. John River connecting St. Leonard, New Brunswick and Van Buren, Maine. This bridge is a continuous, five-span, composite concrete deck-steel two-box girders with a total length of 222.5 m. The third bridge was the Robert Campbell Bridge spanning the Yukon River in the city of Whitehorse. It is a continuous two-span composite concrete deck-steel three-box girders with a total span of 109.7 m. Thermal stresses induced in these bridges were determined using the finite-element method, with input being the measured extreme temperature profiles. Elbadry and Ibrahim (23), in 1996, determined the time-dependent temperature variations within the cross-section and along the length of curved concrete single-cell box girder bridges using a three-dimensional finite-element model used in heat transfer.

2.2.6 Thin-Walled Curved Beam Theory

The curved beam theory was first established by Saint-Venant for the case of solid curved beams loaded in a direction normal to their plane of curvature. The theory is based on the usual beam assumption, i. e. cross-sectional dimensions are small compared to the

length; cross-sections do not distort and plane sections remain plane. Curved beam theory can only provide the designer with an accurate distribution of the resultant bending moments, torque, and shear at any section of a curved beam if the axial, torsional and bending rigidities of the section are accurately known. In general, curved beam theory cannot be applied to curved box girders bridges since it cannot account for the warping, distortion, and bending deformations of the individual wall elements of the box. Therefore, the thin-walled beam theory was developed by Vlasov (87) for axisymmetric sections, and then extended by Dabrowski (21) for asymmetric section, to account for warping deformations caused by the gradient of normal stresses in individual box elements. The theory assumes non-distortional cross-section and, hence, does not account for all warping or bending stresses. The theory cannot predict shear lag or the response of deck slabs due to local wheel loads. Using this theory, few authors (37, 39, 63, 64) have analyzed curved multi-spine box girder bridges under dead and live loads.

Hasebe et al. (34), in 1985, presented a detailed analytical study, based on the refined thin-walled beam theory by Kano et al. (49), taking into account shear deformation and shear lag, to examine the influence of various parameters on the effective width of curved box beams. Maisel (56), in 1989, extended Vlasov's thin-walled beam theory to treat torsional, distortional, and shear lag effects of straight, thin-walled cellular box beams. Mavaddat and Mirza (58), in 1989, used Maisel's formulations to develop computer programs to analyze straight concrete box beams with one, two, or three cells and side cantilevers over a simple span or two continuous spans with symmetric mid-span loadings. The structure is idealized as a beam and the normal and shear stresses are calculated using

the simple bending theory and St-Venant's theory of torsion. The secondary stresses, arising from torsional and distortional warping and shear lag, are then calculated.

Several investigators (6, 60, 86, 92, 85, 88, 90, 29, 83) have combined the thin-walled beam theory by Vlasov and the finite-element technique to develop a thin-walled box beam element for elastic analysis of cellular box girder bridges, in which transverse distortion and longitudinal torsional warping, and in some cases the shear lag effect, were accounted for. In 1992 and 1994, Li (54) and Razaqpur and Li (71) developed two thin-walled box beam finite elements, straight and curved, to model extension, flexure (including shear deformation), torsion, torsional warping, distortion, distortional warping, and shear lag effects. The two elements were developed by extending Vlasov's thin-walled beam theory, and used for the analysis of multi-cell box girder bridges with general geometry. Razaqpur and Li (69, 70) then extended the application of these two elements to the analysis of straight and curved multi-branch multi-cell box girder assemblages, respectively. The results using the proposed element compared well with the shell element analysis.

2.3 Dynamic Response and Codes of Practice for Box Girder Bridges

The use of high-strength materials over the past three decades has led to slender bridge members, resulting in vibration problems due to the passage of heavy vehicles, wind, and (or) seismic excitations. These vibration problems include excessive dynamic deflections and accelerations that can cause discomfort to motorists and pedestrians using

the bridge specially when the dominant mode of vibration is torsional. Bridge-vehicle interaction is another problem that affects the bridge dynamic response. Dynamic impact factors for straight and curved bridges under moving vehicle are therefore an interesting topic that attracts many researchers. Reasonable estimates for impact factors greatly improve the bridge design and reduce the computational cost of bridge analysis. Some analytical and experimental studies have been conducted in the past to study the dynamic response of box girder bridges.

Culver (20) and Shore and Chaudhuri (78) studied the effect of transverse shear deformation and flexural rotatory inertia on the natural frequencies of a horizontally circularly curved beam using closed form-solution of the equation of motion. Tan and Shore (81, 82), in 1968, modeled a simply-supported horizontally curved girder bridge by idealizing the bridge as a slender, prismatic curved beam subjected to a moving force. The differential equations that represent the out-of-plane vibrational motion of a horizontally curved beam were used. In 1966 and 1970, Komatsu and Nakai (52, 53) conducted several studies on the free-vibration and forced-vibration of horizontally curved single-, and twin-box girder bridges using the fundamental equation of motion along with the Vlasov's thin-walled beam theory. Cheung and Cheung (18), in 1972, described the application of the finite-strip method to the determination of the natural frequencies and mode shapes of vibration of straight and curved beam-slab or box-girder bridges.

In 1972 and 1973, Tabba (80) and Fam (26), respectively, studied the behavior of curved box section bridges using the finite-element method for applied dynamic loads. Results from testing two curved two-cell box girder plexiglas models were used to verify

the proposed method. Heins and Sahin (38), in 1979, evaluated the first natural frequency of, straight and curved, simply-supported and continuous, multi-spine box girder bridges using a finite-difference technique to solve the differential equations of motion based on Vlasov's thin walled beam theory. Heins and Lee (36), in 1981, presented the experimental results obtained from vehicle-induced dynamic field testing of a two-span continuous curved composite concrete deck-steel single cell bridge, located in Seoul, Korea.

The bridge code of the American Association of State Highway and Transportation Officials, AASHTO 1996, (5) has traditionally applied an impact factor depending only on the bridge span and states that the impact factor decreases with increase in the span. However, in 1994, Chang and Lee (11) found that impact factors are almost constant with span length.

Rabizadeh and Shore (68), in 1975, presented a finite-element method for the dynamic analysis of curved multiple box girder bridges, which formed the basis for the impact factors adopted by the 1980-edition AASHTO Guide Specification for Horizontally Curved Highway Bridges (4). The vehicle was simulated by two sets of concentrated forces, having components in the radial and transverse directions and moving with constant angular velocities on circumferential paths of the bridge. In 1988, 1990, and 1992, Galdos (30), Galdos et al. (31), and Schelling et al. (74) studied the dynamic response of horizontally curved multi-spine box girder bridges, of different spans, based on a planar grid finite-element analysis. The moving vehicle was represented by two constant forces, with no mass, travelling with constant angular velocity in a circumferential path. Their findings formed the basis for the impact factors currently used by the 1993-edition AASHTO Guide

Specification for Horizontally Curved Highway Bridges (4) for curved multi-spine box girder bridges. The impact factors adopted in this Guide Specification greatly reduced the magnitude in the previous specification. However, the span-to-radius of curvature ratio was limited to between 0.025 and 0.5.

Billing (7), in 1984, presented the results of dynamic tests conducted on 27 bridges of various configurations and span lengths in 1980. The results from these tests formed the basis for the dynamic load allowance adopted by the Ontario Highway Bridge Design Code, OHBDC second edition 1983, (66) and the Canadian Standard Association, CAN/CSA-S6-88, (9). This dynamic load allowance, DLA, depends on the bridge first flexural frequency calculated on the basis of the simple flexural beam theory. However, this dynamic load allowance/frequency relationship was revised in the third edition of the OHBDC code, 1992, (67) as well as in the CHBDC code, 2000, (65), to a constant value depending on the number of axles. This revision was questioned later by Akoussah et al in 1997 (2). Akoussah et al. used the three-dimensional finite element modelling to investigate the vehicle-bridge interaction and then the dynamic amplification factor of simply-supported reinforced concrete bridges of spans of 20 to 32 m.

Chang et al. (10) and Abdel-Salam and Heins (1) predicted the seismic response of curved composite girder and multiple-box girder bridges, respectively. Inbanathan and Wieland (45), in 1987, presented an analytical investigation on the dynamic response of a simply-supported box girder bridge due to a moving vehicle moving over a rough deck. In Cheung and Megnounif (17), in 1991, conducted an analytical investigation, using the finite-element method, to study the influence of diaphragms, cross-bracings, and bridge

aspect ratio on the dynamic response of a straight twin-box girder bridge of 45 m span. In 1990 and 1992, Kashif and Humar (51), and Kashif (50) developed a finite-element technique to analyze the dynamic response of simply-supported multiple box girder bridges considering vehicle-bridge interaction.

Richardson et al. (72), in 1993, presented the results of a field test, using simulated earthquake loads, on a curved highway overpass of box girder cross-section. Huang et al. (42), in 1995, studied the dynamic response of curved I-girder bridges due to truck loading. Moreover, they (43) also presented a procedure for obtaining the dynamic response of thin-walled box girder bridges due to truck loading over rough road-surface, based on a thin-walled beam finite-element model. Wang et al. (89), in 1996, studied the free-vibration characteristics and the dynamic response of three-span continuous and cantilever thin-walled single-cell box girder bridges when subjected to multi-vehicle load moving across a rough bridge deck. Senthilvasan et al. (77), in 1997, combined the spline finite-strip method of analysis and a horizontally curved folded-plate model to investigate the bridge-vehicle interaction in curved box girder bridges.

Most of the previous studies on bridge dynamics concentrated on multiple-spine box girder bridges while very little effort has been directed to the dynamic analysis of multi-cell box girder bridges. Dynamic impact factors for straight and curved composite cellular bridges are needed to fill the gap found in the literature as well as in bridge codes.

CHAPTER III

FINITE ELEMENT ANALYSIS

3.1 General

Of all the available methods of analysis, the finite element method is the most powerful, versatile, and flexible. Recent developments in the finite element analysis make it possible to model a bridge in a more realistic manner and to provide a full description of its structural response statically and dynamically. The most important advantage of this method is its capability to deal with problems that have arbitrary arrangements of structural elements, material properties, and boundary conditions. Therefore, the finite element method is especially suitable for the analysis of straight and curved composite cellular bridges. Thus, the finite element analysis program named ABAQUS (40) was used throughout this study to determine both the static and dynamic linear responses of the straight and curved composite multi-cell bridges. The finite element modelling of the different components of the composite cellular bridges (i.e., the reinforced concrete deck slab, the steel top flanges, the steel webs, the steel bottom flange, the solid end-diaphragms, the cross-bracings, and the top chords) is described in subsequent sections in this chapter. A general description of the ABAQUS program is presented in this chapter. The finite element method of structural analysis described herein was also employed to perform the

parametric studies on the fundamental frequency of both straight and curved composite concrete deck-steel multi-cell box girder bridges, described in detail in chapter VI, and the dynamic impact factors for straight and curved bridges in chapter VII.

3.2 Finite Element Method

The finite element method is a discretization technique in which the entire structure is discretized into a finite number of regions (elements) that are interconnected at certain points (nodes). With a displacement formulation, the stiffness matrix of each element is derived and the global stiffness matrix of the entire structure can be formulated by the direct stiffness method. This global matrix, along with the given displacement boundary conditions and applied loads, is solved and thus the displacements and stresses can be determined. The global stiffness matrix represents the nodal force-displacement relationships and can be expressed in the following matrix equation form:

$$[P] = [K][U] \tag{3.1}$$

in which *[P]* is the nodal load vector, *[K]* is the global stiffness matrix, and *[U]* is the nodal displacement vector. The steps for deriving the above equation can be summarized in the following basic relationships:

(a) $$[u(x,y)] = [\Phi(x,y)][\alpha] \tag{3.2}$$

where $[u]$ is the internal displacement vector of the element, $[\Phi]$ is the displacement function (shape function), and $[\alpha]$ is the generalized coordinate vector.

(b) $$[U] = [A][\alpha] \quad \text{then, } [\alpha] = [A]^{-1}[U] \tag{3.3}$$

where $[A]$ is the transformation matrix from local to global coordinates.

(c) $$[\varepsilon(x,y)] = [B(x,y)][\alpha] = [B(x,y)][A]^{-1}[U] \tag{3.4}$$

in which $[B(x, y)]$ is the strain-displacement matrix, and $[\varepsilon(x, y)]$ is the strain matrix.

The Cauchy stress matrix $[\sigma(x, y)]$ is given by:

(d) $$[\sigma(x,y)] = [D][\varepsilon(x,y)] = [D][B(x,y)][A]^{-1}[U] \tag{3.5}$$

where $[D]$ is the constitutive matrix or the elasticity matrix.

(e) When a virtual displacement field $[u']$ is imposed on the system ($[u']$ is consistent with the prescribed boundary conditions), the corresponding virtual strain is $[\varepsilon']$. Now,

$$(i)\ W_I = \int [\varepsilon']^T [\sigma] dV = [u']^T \int [A^{-1}]^T [B]^T [\sigma] dV$$

$$(ii)\ W_E = \int [u']^T f^B dV + \int [u']^T f^S dS + \sum u_i' R_C^i \tag{3.6}$$

where W_E is the external virtual work, and W_I is the internal virtual work.

According to the principle of virtual work, $W_E = W_I$, therefore, the system equilibrium equation can be expressed as:

$$\int [A^{-1}]^T [B]^T [D][B][A]^{-1} dV [u] = \int f^B dV + \int f^S dS + \sum R_C^i \tag{3.7}$$

thus the solution leads to

$$[P] = [K][U] \tag{3.1}$$

where

$$[P] = \int f^B dV + \int f^S dS + \sum R_C^i \tag{3.8}$$

$$[K] = \int [A^{-1}]^T [B]^T [D][B][A]^{-1} \tag{3.9}$$

f_B : body forces

f_S : surface forces

R_C : concentrated loads at nodes

(f) The solution of the equilibrium equation of the system, Equation (3.1), yields the values of nodal displacement *[U]*, and the internal forces for each element can be obtained by using Equations (3.4) and (3.5).

However, if some of the forces acted on the system are varied with time, the displacements are also changed with time, and Equation (3.1) is just a state of equilibrium at any specific time. Then following the same procedure, by applying the principle of virtual displacement as Equation (3.6), and using the d'Alambert's principle to include the inertia and damping forces as part of the body forces, the equilibrium equation for the system should be written as

$$[P] = [M][\ddot{U}] + [C][\dot{U}] + [K][U] \qquad (3.1a)$$

where *[M]*, *[C]*, and *[K]* are the mass, damping, and the stiffness matrix, respectively; *[P]* is the external load vector in which the element body forces f_B does not contain the inertia and damping forces, and *[U]*, $[\dot{U}]$, and $[\ddot{U}]$ are the displacement, velocity and acceleration vectors of the system, respectively. Equation (3.1a) is the motion equilibrium equation of a system. Several numerical techniques have been proposed for the solution of the equation. The techniques can be divided into two categories: mode superposition

method and direct integration method. These two methods have been employed in this study and compared. The detailed discussion is summarized in chapter V.

3.3 Description of the Finite Element Program ABAQUS

ABAQUS (40) is designed as a flexible tool for numerical modelling of structural response in both linear and nonlinear analysis. This computer program runs as a batch application to assemble a data deck that describes a problem so that it can provide an analysis. A data deck for this computer program contains model data and history data. Model data defines a finite element model: the elements, nodes, element properties, material definitions, nodal constraints, and any data that specify the model itself. History data define what happens to the model, the sequence of events or loads for which the model's response is sought. The computer program provides a *TRANSFORM option to specify a local coordinate system at nodes by setting up a rotated direction for displacements and rotations at individual nodes and node sets. This option was used to rotate the two horizontal displacements (U_x and U_y) to radial and tangential displacement to apply the boundary conditions at the radial supports of curved bridges.

3.3.1 Static Analysis

ABAQUS (40) uses the STATIC procedure, *STATIC option, to perform the elastic static analysis of structures. The concentrated loads are applied by the *CLOAD option.

3.3.2 Dynamic Analysis

ABAQUS (40) offers several methods for performing dynamic analysis of problems in which inertia effects should be taken into consideration. Direct i ntegration methods must be used when nonlinear dynamic response is being studied, or a great number of vibration modes should be taken into consideration. Modal methods are usually chosen for linear analysis firstly because in direct integration method, the global equations of motion of a system must be integrated through time, which makes direct integration methods significantly more expensive than modal methods.

Dynamic studies of linear problems are generally performed by using the eigenmodes of the system as a basis for calculating the response. In such cases, the necessary modes and frequencies are calculated first in a frequency extraction step (free vibration). The mode-based procedures are generally simple to use; and the dynamic response analysis itself is usually not expensive computationally, although the eigenmode extraction can become computationally intensive if many modes are required for a large model.

(a) Free Vibration Analysis

The FREQUENCY EXTRACTION procedure, *FREQUENCY option, in ABAQUS (40) uses an eigenvalue analysis to extract the frequencies of a system and the corresponding mode shapes. Frequency extraction is required prior to any of the mode-based procedures. Because damping just slightly reduces the values of natural

frequencies, the undamped system is usually used to extract the natural frequencies of a structure for simplicity.

The eigenvalue problem for the natural frequencies of an undamped finite element model is:

$$(-\omega^2 M^{ij} + K^{ij})\,\phi^j = 0 \tag{3.10}$$

where M^{ij} is the mass matrix (which is symmetric and positive definite); K^{ij} is the stiffness matrix; ϕ^j is the eigenvector (the mode of vibration); ω is the circular natural frequency needed to extract; and i and j are degrees of freedom.

ABAQUS offers two eigenvalue extraction methods, i.e., the Lanczos method and subspace iteration method. The Lanczos method is generally faster when a large number of eigenmodes is required for a system with many degrees of freedom. On the other hand, the subspace iteration method may be faster when only a few (less than 20) eigenmodes are needed.

The density of the materials forming the structure must be defined in the *DENSITY option in any dynamic analysis. The users need to specify the number of frequencies required in the FREQUENCY EXTRACTION procedure. In the computer program, the eigenvectors are normalized so that the largest displacement entry in each vector is unity. If the displacements are negligible, as in a torsional mode, the eigenvectors are normalized so that the largest rotation entry in each vector is unity. In addition to extracting the natural frequencies and mode shapes, the computer program automatically

calculates the participation factor which indicates how strongly motion in the global x-, y-, and z-directions or rigid body rotation about one of these axes is represented in the eigenvector of that mode.

(b) Transient modal dynamic analysis (mode superposition method)

Transient modal dynamic analysis procedure, presented by *MODAL DYNAMIC option in ABAQUS, gives the response of the model as a function of time based on a given time-depending loading. The structure's response is based on a subset of the eigenmodes of the system, which are extracted first during the FREQUENCY procedure in the previous step. The number of modes extracted must be sufficient to model the dynamic response of the system adequately, which is a matter of judgement on the part of the user. The modal amplitudes are integrated through time, and the response is synthesized from these modal responses. The user should ensure that the forcing function definition and the choice of time increment is consistent for this purpose. The *MODAL DYNAMIC option provides the time period of the analysis and the time increment to be used. The *MODAL DAMPING option is usually used in conjunction with a modal dynamic analysis to include the damping of the system. It provides the fraction of the critical damping assigned to certain modes.

The applied loads in modal dynamic analysis can be prescribed as concentrated nodal forces applied to the translation degree of freedom by using the *CLOAD option. The *AMPLITUDE option allows arbitrary time variations of load given throughout the step. The default of this option is to give the magnitude of the force as a multiple (fraction)

of the reference magnitude given on the data line of the loading. For a truck travelling across a bridge, the computer program specifies the amplitude with time at each nodal point in a tabular form. The user must define the amplitude curve as a table of values at constituent points on the time scale and the computer program interpolates linearly between these values of the time increment in the analysis if it is not the same as that in the amplitude curve. The output of the dynamic analysis includes the dynamic response of the structure due to the prescribed load-time history in the form of the straining action-time histories. These straining actions include accelerations, dynamic displacements, and dynamic stresses.

(c) Direct integration dynamic analysis

ABAQUS uses the *DYNAMIC option to perform a direct integration dynamic analysis procedure. The general direct integration method provided in ABAQUS, called the Hilber-Hughes-Taylor operator (41), is an extension of the trapezoidal rule. The operator is implicit: the integration operator matrix must be inverted, and a set of simultaneous dynamic equilibrium equations must be solved at each time increment. This solution is done iteratively using Newton's method, and the equation solving process is extremely expensive compared to mode superposition method especially when the time considered is longer.

The ALPHA parameter on the *DYNAMIC option is used to introduce artificial damping. This damping is purely numerical in order to keep the solution stable and convergent. Material damping is specified using the *DAMPING option. The

*DAMPING option can be used to introduce Rayleigh structural damping. The load is applied to the structure followed the same procedure as the transient modal dynamic analysis discussed in the previous section.

3.4 Finite Element Modelling of Straight and Curved Composite Multi-Cell Bridges

A three dimensional finite element analysis is used to model straight and curved composite concrete deck-steel cellular bridges in this study. The structure is first divided into several components, namely: concrete deck slab, steel webs, steel bottom flange, steel solid-end-diaphragms, steel top flanges, and cross-bracing and top-chord members. The reinforced concrete slab is rigidly connected to the steel top flanges by means of shear stud connectors. In this section, element types used for different components as well as material modelling in the elastic loading stage are presented. It should be noted that the model presented herein was verified and substantiated by Sennah (76).

3.4.1 Geometric Modelling

(a) Modelling of Deck Slab, Webs, Bottom Flange, and End-Diaphragms

A mesh of three-dimensional shell elements was used to model the reinforced concrete deck slab, steel webs, steel bottom flange, and steel solid-end-diaphragms. A four-node doubly-curved general purpose shell element named S4R in the ABAQUS

element library was used. The element has either straight or curved boundaries depending on node definitions. The element had six degrees of freedom at each node, namely three displacements (*U1*, *U2*, *U3*) and three rotations (*Φ1*, *Φ2*, *Φ3*). A detailed description of the shell element S4R is shown in Figure 3.1. The general-purpose shell element chosen herein uses thick shell theory as the shell thickness increases; it becomes discrete Kirchhoff thin shell elements as the thickness decreases; the transverse shear deformation becomes very small as the shell thickness decreases. The criterion for neglecting shear deformation occurs when the thickness of the shell is less than about 1/15 of a characteristic length on the surface of the shell, such as the distance between supports or the wave length of a significant eigenmode in dynamic analysis. However, the thickness of the shell may be larger than 1/15 of the element length. Element S4R accounts for finite membrane strains and allows for change in thickness caused by deformation. It is, therefore, suitable for large membrane strain analysis, besides large-rotation analysis, involving materials w ith Poisson's ratios.

(b) Modelling of Steel Top Flanges, Top-chords, and Cross-bracings

A three-dimensional two-node linear-interpolation element, named B31H in ABAQUS element library, was adopted to model the steel top flanges, top-chords, a nd cross-bracings. The element had two nodes with six degrees of freedom at each node, three displacements (*U1*, *U2*, *U3*) and three rotations (*Φ1*, *Φ2*, *Φ3*). A detailed description of the beam element B31H is shown in Figure 3.2. This hybrid element is designed to handle very slender situations, where the axial stiffness of the member is very

large compared to its bending stiffness. Therefore, because of their insignificant flexural and torsional stiffness, cross-bracing and top-chord members are considered as axial members loaded in tension and compression.

3.4.2 Boundary Conditions

Two different nodal constraints were used in the analysis, namely: boundary constraints and multi-point constraints. Boundary constraints of two different types were used in modelling the simply-supported bridges: the roller support at one end of the bridge constrained both vertical and radial displacements at the lower end nodes of each web; the hinge support at the other end of the bridge was modelled by restricting all possible translations at the lower end nodes of each web.

The multi-point constraint option in the ABAQUS, type * BEAM, which allows constraint between different degrees of freedom between different element types, was used between the shell nodes of the concrete deck and the beam element nodes of the steel top flanges. This multi-point constraint option ensured full interaction between the concrete deck slab and the steel cells, thus modelling the presence of the shear connectors. In this type of constraint, a linear set of constraint equations was utilized to couple the nodal degrees of freedom of the nodes of relevant elements as shown in Figure 3.3.

3.4.3 Material modelling

ABAQUS (40) requires that the material is sufficiently defined to provide suitable properties for those elements with which the material is associated, and for the analytical

procedures through which the model will be run. Thus a material associated with the structural elements must include a mechanical category option to define its mechanical (stress-strain) properties such as elastic modulus and Poisson's ratio.

In this study, the material is considered as isotropic, elastic and homogeneous material. The concrete deck slab is considered uncracked throughout the loading. The properties for the steel and reinforced concrete are listed in Table 3.1.

3.5 Finite Element Analysis of the Bridges and the Prototype Bridges

3.5.1 Finite Element Mesh of Bridges

The finite-element mesh is usually chosen based on pilot runs and is a compromise between economy and accuracy. The mesh size was selected mainly to accommodate different locations for the truck wheel loads due to different loading cases which will be discussed in chapter IV and to better integrate the stresses between girders to obtain the impact factors. Thus, in the finite element modelling, four elements were utilized on each side of the cells and on each side of the support diaphragms. Four elements were also used in webs along the depth of bridges. Moreover, 72 elements were used in the tangential direction of the simply-supported bridges. Figure 3.4 shows the finite element meshes of two typical straight and curved bridges, respectively. In the extensive parametric study of the bridges, shell elements of aspect ratios between 1 to 2, 2 to 3, 3 to 4, and 4 to 5 were 57%, 21%, 13%, and 9%, respectively, of those used in modelling bridges of spans 20, 40,

60, 80 and 100 m. This maximum limit of 5 would be enough when stress evaluation is of prime concern.

Pilot runs on the effect of vertical web stiffeners on the structural behavior proved that these thin stiffeners have an insignificant effect on structural responses. Therefore, they were not included in the finite element model. It was also proven that the steel reinforcement in the concrete deck slab has an insignificant effect in the bridge elastic and dynamic responses. In practice, the cross-bracing system should be as deep as possible to accomplish its effect. The top surface of the top-chord members should be very close to the steel top flanges with a vertical distance equal to half the concrete deck slab thickness to allow for concrete form work and to prevent lateral instability of the steel top flanges during construction. Therefore, the connections of the top-chord and cross-bracing members to the steel cells used in the finite element modelling were shifted to the points of intersection of the steel webs and the steel top flanges.

The finite element modelling was employed to perform several parametric studies on the structural response of straight and curved composite cellular bridge prototypes as shown in chapter VII. In this aspect, a wide range of prototype bridges was examined as described in the next section of this chapter. Appendix 3 shows a typical list of the finite-element computer program input data decks used in the dynamic analysis.

3.5.2 Description of the Bridge Prototypes Used in the Parametric Studies

In order to determine the parameters affecting the structural dynamic impact factors of straight and curved composite multi-cell bridges, it was necessary to define the geometric

parameters that may affect their dynamic behavior. These parameters include span length, number of cells, number of lanes, span-to-radius ratio, and cross-bracing and top-chord systems. For this study, the straight composite cellular bridges, presented in Table 3.2, which were designed according to AASHTO Bridge Specifications (5), formed the basis of the bridge prototypes used in the parametric studies. Figure 3.5 shows the basic cross-sectional configurations and symbols as presented in Table 3.2. The main geometry data of curved bridges is based on the corresponding straight bridges.

In the parametric studies, the span length of the bridges ranged from 20 m to 100 m, representing medium span bridges. The number of lanes was taken as 1, 2, 3, and 4. One-lane bridges are included in this study since the Geometric Design Standards for Ontario Highways, 1985, (61) as well as the CHBDC Code, 2000, (65) permit using single lane bridges for ramps and highway exit terminals. Furthermore, these specifications state that the lane widths for ramps of two or more lanes should be 3.75 m; the single lane bridges should be a minimum of 5.00 m roadway width except for single lane ramps; and the single lane ramp bridges should be a minimum of 4.75 m roadway width. According to these recommendations, the bridge width was 6.80 m in the case of one-lane, 9.30 m in the case of two-lane, 13.05 m in the case of three-lane, and 16.80 m in the case of four-lane bridges. The number of cells ranged from 1 to 4 in the case of one-lane, 1 to 7 in the case of two-lane, 3 to 9 in the case of three-lane, and 4 to 9 in the case of four-lane bridges. To change the number of cells for the same lane width, the thickness of the steel top flanges, webs, and bottom flange were changed to maintain the same shear stiffness of the webs and overall flexural stiffness of the cross-section. Figure 3.6 shows the number of cells along

with the number of lanes considered in the parametric studies.

For each bridge included in the parametric study, the transverse geometry (including number and stiffness of cross-bracing and top-chord systems) as well as radius of curvature were changed to study their effect on the impact factors. The number of cross-bracings as well as the top-chords was varied from 0 to 17. For roadways or ramps where structural depth is not severely limited, box girder, T-, or I-beam bridges have cost about the same for spans close to 24 m. For shorter spans, T- or I- beam bridges are usually cheaper, and for longer spans, box girder bridges tend to be more economical. However, in some cases, box girder bridges have been found to be economical for spans as short as 20 m when structural depth was restricted.

The curved bridges considered in this study are assumed to have constant elevations of concrete decks. The degree of curvature can be defined by the span-to-radius ratio, L/R, where the span of the bridge, L, is the arc length along the central line of its cross-section and the radius of curvature, R, is the distance from the origin of the circular arc to the central line of the cross-section. The L/R ratios used in this study ranged from 0.0 to 1.4. The higher values of L/R along with the lower value of the span length, 20 m, are theoretically possible to analyze but practically uncommon for curved highway bridges since the Geometric Design Standards for Ontario Highways, 1985, (61) only allow using curved bridges when a radius of curvature $\geq$ 45 m. However, the inclusion in this study of a smaller radius of curvature serves to show the trend of the structural response of curved bridges within certain limits of L/R.

It was mentioned that the full range of all the parameters used in this study is listed

in Table 3.2. These ranges were based on an extensive survey of actual designed bridges [Johanston et al., 1967, (47); Chapman et al., 1971, (13); Heins, 1978, (35)]. For the parametric studies, the material properties (modulus of elasticity, Poisson's ratio, and mass density) for the concrete deck, steel cells, diaphragms, and bracing systems were taken to be the same for all the cases studied and are listed in Table 3.1.

The key parameters investigated in this study are: number of cross-bracing and top-chord systems, number of cells, number of lanes, span, and degree of curvature. Solid end-diaphragms considered in this study were provided at both ends of the bridge in the radial direction. When investigating the effect of the number of cross-bracing systems, X-type bracings as well as top chords were provided inside the cells, in the radial direction, at different locations along the span. In practice, these bracings are made from single or back-to-back angles. Sensitivity study proved that replacing the area of angle cross-section by rectangular cross-section has no effect on the structural response. Moreover, changing the stiffness of these rectangular bracing systems or replacing the bracing system by an equivalent solid plate diaphragm of the same volume has no effect on the structural response, irrespective of the degree of curvature.

CHAPTER IV

METHODOLOGY FOR DYNAMIC IMPACT FACTOR

4.1 General

The method of dynamic analysis of straight and curved cellular bridges for finding the impact factor is described in this chapter. The AASHTO Guide Specifications (4) recommends that the dynamic analysis of straight and curved cellular bridges be done as a system. In this study, the dynamic analysis of the bridges is treated as systems. A criterion is proposed for selecting the impact factors for straight and curved bridges under various truck loading cases. The simulation of truck loading is also presented in this chapter.

4.2 Truck Idealization

Considerations were given to the effects of highway truck loading on the dynamic impact factor of straight and curved composite cellular bridges. The highway truck loading considered in this study is the HS20-44 highway standard design truck of AASHTO (5). Figure 4.1 summarizes the configurations of the AASHTO truck loading.

The truck is idealized as a pair of concentrated forces moving along the deck in a

circumferential path. The truck is assumed to move with constant velocity, with no mass, acting normal to the deck of the bridge and moving in two circumferential paths parallel to the curved centerline of the bridge. It is assumed that the truck moves smoothly with no slippage, and in constant contact with the surface of the bridge. The radial distance between the paths is taken to be 1.8 m. It should be mentioned that the interaction between the truck mass and that of the bridge is not considered herein since the weight ratio of the design truck and that of the bridge is less than or equal to 0.3 [Tan and Shore, 1968, (81, 82); Senthilvasan et al., 1997, (77)]. This condition is applicable to two-, three-, and four-lane bridges with span lengths between 30 to 100 m.

For curved bridges, the centrifugal force, F_c, is assumed to act horizontally and at right angles to the direction of the truck travelling, 2 m above the deck surface at the center of travel paths, and moving with the truck as indicated in the CHBDC code (65) and as shown in Figure 4.2.a. The force F_c is calculated as

$$F_c = \frac{P v^2}{127 r} \qquad (4.1a)$$

where P = the truck axle load (kN)

v = the design speed of a highway (km/h)

r = the radius of the path along which the truck is moving (m)

This is similar to the ASSHTO force

$$F_c = \frac{PS^2}{gr} \qquad (4.1b)$$

where P = the truck axle load (lbs or kips)

S = the design speed of a highway (miles per hour)

r = the radius of the path along which the truck is moving (ft)

g = Gravitational constant, 32.2 ft / sec^2

Figure 4.2.a shows the force system simulating the truck action. However, for analytical purposes, the static equivalent of the centrifugal force is used and the final truck force system applied to the bridge deck is shown in Figure 4.2.b.

4.3 Truck Loading Conditions

In the transverse direction of straight and curved bridges, three cases of truck loading were considered in the finite element modelling: (i) one or two trucks travelling in the inner lane close to the curb; (ii) one or two trucks travelling in the outer lane close to the curb; and, (iii) one, two, three, or four trucks travelling close to the middle of the bridge lanes. The detailed truck loading conditions considered in this study are illustrated in Figure 4.3.

The maximum safe allowable speed of trucks is restricted by two conditions: a 110km/h limit and the following equation

$$v = \sqrt{127r(e+f)} \tag{4.2}$$

where e = pavement superelevation (tangent of the angle), the value of e being positive if the pavement slopes toward the center of the curve

f = coefficient of side friction force between truck tire and road pavement

v = the design speed of a highway (km/h)

r = the radius of the path along which the truck is moving (m)

For straight bridges and bridges with large radius of curvature, the speed of 110 km/h will control, but for bridges with small radius of curvature the controlling speed is given by Equation (4.2).

The superelevation of curved bridges is governed by factors as slow-moving and fast-moving traffic for variable weather conditions. In regions free of ice and snow, a maximum rate for skid-resistant surface of 0.08 can be used. However, for regions subject to severe winter conditions, maximum slopes of 0.06 have been recommended (61). In this study, the maximum superelevation rate of 0.08 is used for all cases. This is because high superelevation rate yields higher maximum safe allowable speed, and higher speed usually produces larger dynamic impact factors, which will be discussed in detail in chapter VII.

The lateral friction of curved bridges is based on the truck travelling speed and the driver comfort. For a given curved bridge whose superelevation rate is fixed, the truck speed may exceed the design speed when the truck changes lanes and overtake. In these

cases, the truck travels along a path of smaller radius than the central line. In order to keep travelling along the circumferential path smoothly, therefore, the lateral friction should be taken larger than the normal condition. On the other hand, at higher speeds, if the centrifugal force required to maintain the vehicle on the curve was s upplied l argely b y lateral friction rather than superelevation, passengers would experience discomfort. In this study, the maximum friction coefficient of 0.18 is used for all cases (61).

4.4 Dynamic Impact Factor

AASHTO Guide Specifications (4) recommends that the dynamic impact factor for bridges under moving vehicles may be obtained from the following equation:

$$I_F = \frac{F_i(x_j, t, P) - F_i(x_j, P)}{MAXF_i(x_k, P)} \tag{4.3}$$

where I_F = dynamic increment factor for the variable F effects at station i at time t

$F_i(x_j, t, P)$ = dynamic value of F at station i when the vehicle of weight P moving with velocity v at station j at time t

$F_i(x_j, P)$ = static value of F at station i when the vehicle of weight P is at station j

$MAXF_I(x_k, P)$ = maximum static value of F at station i when the vehicle of weight P is at station k

According to Equation (4.3), in order to obtain the maximum dynamic impact factor of variable F, a great number of calculations should be done to compare the impact factors for different positions on the bridge. The calculations would include dynamic analysis and static analysis at every selected position. thus the computational cost becomes too high and unrealistic in 3-D modelling bridge analysis. In order to reduce the computational cost and obtain sufficient accuracy of the impact factor, a simple equation is proposed to calculate the dynamic impact factor of bridges in this study defined as

$$I_F = \frac{F_D - F_S}{F_S} \tag{4.4}$$

where I_F = dynamic impact factor for the variable F

F_S = maximum static value of variable F

F_D = dynamic value of variable F

The aim of this study is to investigate the impact factors for moment, reaction, and deflection of the studied bridges. For moment and deflection impact factors, the loading on the bridges was applied at the mid-span position in such a way as to produce maximum static longitudinal stresses and vertical displacements. It is reasonable to assume that the maximum dynamic response of longitudinal stresses and vertical displacement occur at the mid-span middle of bridge span too. However, in case of the impact factor for reaction, the truck was located very close to the support lines in the longitudinal direction in such a

way as to produce maximum support reactions with no wheel load applied directly over the support. Subsequently, three loading cases were considered for the sensitivity study of some bridge prototypes, shown in Figure 4.3. In the two partial loading cases, Figure 4.3.b and Figure 4.3.c, the wheel loads close to the curbs were applied at a distance of 0.6 m from the inside edge of the curbs.

4.5 Impact Factor Selection Criterion

The AASHTO Guide Specifications (4) recommends that the dynamic design values may be found using the following relationship,

$$\textit{Dynamic Value of } F = (1 + I)\,(\textit{Maximum static value of } F) \qquad (4.5)$$

where I would be the extreme value resulting from Equation (4.3). In this study, I would be the impact factor determined by Equation (4.4).

The cellular cross-section was divided into idealized I-beam shaped girders as shown in Figure 4.4. Each idealized girder consisted of the web, steel top flange, concrete deck slab, and bottom flange. For the inside girders, the width of the concrete deck slab and bottom flange equaled the web spacing. While for the edge girders, the width of concrete deck slab extends from mid-point between the webs and the side edge of the cantilever supporting the curbs and the parapet, and the bottom flange width is taken as half the web spacing. Based on the finite-element modelling, the distributions of the normal flexural

stresses at the bottom flange of mid-span section of bridges were obtained. These normal stresses were then integrated for each girder to obtain the static normal stress, S_S, for static analysis, and the dynamic normal stress, $S_D(t)$, at each increment for dynamic analysis. Then the moment impact factor can be written as:

$$I_M = \frac{MAX(S_D(t)) - S_S}{S_S} \tag{4.6}$$

The reaction and deflection of each web can be relatively easier to obtain directly from the static and dynamic finite element analyses in the same way. The form of reaction and deflection impact factors is the same as Equation (4.6).

The following criteria are presented for the selection of the theoretical dynamic impact factors for straight and curved composite cellular bridges under AASHTO truck loading:

(1) Sensitivity study to examine geometric parameters that affect the impact factors. These geometric parameters include number and area of cross-bracing systems, number of cells and lanes, spans, and the degree of bridge curvature.

(2) Sensitivity study to examine the aforementioned three truck loading conditions which produce maximum static response.

(3) Sensitivity study to examine the effect of the truck speed on the impact factors.

(4) The dynamic and static responses are obtained by using finite element and coded program (Appendix 4) for each of the prototype bridges.

(5) The dynamic impact factors are calculated by applying Equation (4.6) for each of bridges.

(6) Empirical expressions for the impact factors are deduced.

CHAPTER V

DEFINITION AND VERIFICATION

OF DYNAMIC ANALYSIS

5.1 General

As mentioned in chapter III, generally there are two methods to analyze the dynamic response of structures, namely: mode superposition method and direct integration method. In this chapter, the principle of the two methods is thoroughly discussed. Then both of them are utilized to investigate the dynamic response of one straight bridge prototype. By comparison of the results generated by the two methods, the direct integration method is chosen to investigate the dynamic impact factors of all bridges studied herein.

5.2 Free Vibration Analysis

The most important characteristic of a structure under dynamic loading is its natural frequencies and corresponding mode shapes, and especially the fundamental natural frequency and the mode shape. Free vibration analysis is used to extract the structural natural frequencies as well as the mode shapes. In addition, it is the first step for any of the

mode-based methods, such as the mode superposition method. The principle of free vibration analysis is discussed in detail in the following section.

Recall Equation (3.1a)

$$[P] = [M][\ddot{U}] + [C][\dot{U}] + [K][U] \tag{3.1a}$$

It was mentioned in chapter III that damping just slightly reduces the values of the natural frequencies. Therefore, damping is usually neglected when calculating the natural frequencies. By reducing the load vector $[P]$ to zero and neglecting the damping forces in Equation (3.1a), the equilibrium equation of undamped system is obtained,

$$[M][\ddot{U}] + [K][U] = 0 \tag{5.1}$$

A solution to Equation (5.1) can be taken in the form

$$[U] = [\phi]e^{i\omega t} \tag{5.2}$$

where $[\phi]$ is a vector of order n that represents the amplitude of displacements $[U]$, and ω is a constant that represents the frequency of vibration of the vector $[\phi]$.

The generalized solution to the eigenproblem is obtained for the unknowns $[\phi]$ and ω by substituting (5.2) into (5.1):

$$[K][\phi] = \omega^2 [M][\phi] \tag{5.3}$$

Solving Equation (5.3) yields n eigenpairs $(\omega_1^2, \phi^1), (\omega_2^2, \phi^2), \ldots, (\omega_n^2, \phi^n)$, where ω^2 are the eigenvalues, and ϕ^i are the eigenvectors. Since the matrices *[K]* and *[M]* are positive definite, all eigenvalues are greater than zero.

The structural eigenvalue problem has received considerable attention since the advent of finite element models. ABAQUS provides two methods to extract the natural frequencies and mode shapes of structures, i.e. subspace iteration method and Lanczos method.

The advantage of the subspace iteration method is the extraction of the eigenvalues in reduced space, which will cause a rapid convergence to the eigenvectors in full space. The subspace iteration method may be faster when only a few (less than 20) eigenmodes are needed. On the other hand, the implementation of the Lanczos method is a powerful tool for extraction of the extreme eigenvalues and the corresponding eigenvectors of a sparse symmetric generalized eigenproblem. The Lanczos method is generally faster when a large number of eigenmodes is required for a system with many degrees of freedom. In the next section of this chapter, over 200 natural frequencies are considered in the mode superposition method, which uses Lanczos method to extract the required natural frequencies. However, only a few natural frequencies are needed in chapter VI to collect the fundamental frequency of bridges, where the subspace iteration method is used.

5.3 Forced Response Analysis

5.3.1 Mode Superposition Method

Linear dynamic analysis using mode superposition is computationally inexpensive and can provide useful insight into the dynamic behavior of a system. With modern eigenvalue/eigenvector extraction techniques, such as the subspace iteration method and Lanczos method, discussed in the previous section of this chapter, the cost of obtaining a sufficient basis of eigensolutions is not excessive, and the subsequent computational effort involved in obtaining the dynamic response by mode superposition method is relatively small, especially when compared to the cost of the direct integration methods which will discussed in the next section of this chapter.

The basic concept of mode superposition method is that the response of the structure is expressed in terms of a relatively small number of eigenmodes of the system. The orthogonality of the eigenmodes uncouples this system. Furthermore, only eigenmodes that are close to the frequencies of interest are usually needed.

Generally Equation (3.1a) is coupled; that is, they cannot be solved independently, but only simultaneously. The mode superposition method can transform the coupled equations into uncoupled equations, and then they may be solved independently of one another. Finding a coordinate system that enable the decoupling of the equations of motion is the essence of the mode superposition method. The coordinates are called principal coordinates, or normal coordinates.

The normal (or principal) coordinates $[q]$ are defined by the following matrix transformation

$$[U] = [\Phi][q] \tag{5.4}$$

where $[\Phi]$ is then the modal matrix determined from the solution of the system eigenproblem. Therefore, the transformation of equations of motion from physical to normal coordinates is accomplished by the following matrix premultiplication of Equation (3.1a):

$$[\Phi]^T([M][\ddot{U}] + [C][\dot{U}] + [K][U]) = [\Phi]^T[P] \tag{5.5}$$

where $[\Phi]^T$ is the transpose of $[\Phi]$. Substituting (5.4) into (5.5) and using the orthonormality properties, the uncoupled equations of motion in normal coordinates are obtained as

$$[M^*][\ddot{q}] + [C^*][\dot{q}] + [K^*][q] = [P^*] \tag{5.6}$$

where $[M^*]$ and $[K^*]$ are modal mass matrix and modal stiffness matrix, respectively (which have been diagonalized by the modal transformation), and $[P^*]$ is the modal force vector.

Thus

$$[M^*] = [\Phi]^T [M][\Phi] \tag{5.7a}$$

$$[K^*] = [\Phi]^T [K][\Phi] \tag{5.7b}$$

$$[P^*] = [\Phi]^T [P] \tag{5.7c}$$

$$[C^*] = [\Phi]^T [C][\Phi] \tag{5.7d}$$

In the above transformation, it is assumed that $[C]$ is referred to as the classical damping or proportional damping, and $[C^*]$ being diagonal.

Therefore, Equation (5.6) can be written in the form of n uncoupled equations:

$$M_r \ddot{q}_r + C_r \dot{q}_r + K_r q_r = P_r \tag{5.8}$$

where,

$$M_r = [\Phi]_r^T [M][\Phi]_r \tag{5.9a}$$

$$K_r = [\Phi]_r^T [K][\Phi]_r \tag{5.9b}$$

$$P_r = [\Phi]_r^T [P] \tag{5.9c}$$

$$C_r = 2\xi_r M_r \omega_r \tag{5.9d}$$

Equation (5.8) can also be written in a simple form

$$\ddot{q}_r + 2\omega_r \xi_r \dot{q}_r + \omega_r^2 q_r = p_r \tag{5.10}$$

The *rth* typical equation in (5.10) is the equilibrium equation of a single degree of freedom system, from which the complete response of finite element nodal point displacements are obtained by the superposition of response in each mode

$$[U] = \sum_{r=1}^{n} [\Phi]_r [q_r] \tag{5.11}$$

The mode superposition method is a very popular dynamic analysis technique, but it has several important limitations. Firstly, the method is valid for linear systems only. Secondly, damping in the system must be proportional. Mode superposition method is most effective for large systems when the dynamic response can be accurately evaluated by consideration of only a few of the lowest modes of vibration. This is because the majority of the computational effort expended for a mode superposition analysis is associated with the eigenproblem solution, which extracts the system natural frequencies and vibration mode shapes. If it is necessary to calculate a large number of vibration modes to accurately represent the dynamic response of a system having several thousand degrees of freedom, then solution of the eigenproblem may be computationally prohibitive. Therefore, a mode superposition method is ideally suited for situations where the dynamic disturbance is confined to the lowest few modes of vibration of the system, and the duration of the disturbance is relatively long.

5.3.2 Direct Integration Method

A direct integration analysis, on the other hand, should be utilized in situations when a large number of vibration modes must be included in the response calculations. In addition, for nonclassically damped systems or systems exhibiting any nonlinear characteristics, a direct integration analysis is required. Besides, direct integration method can be applied to any kinds of dynamic analysis where the mode superposition method cannot work.

Direct dynamic integration operators are broadly characterized as implicit or explicit. Explicit schemes obtain values for dynamic quantities at $t+\Delta t$ based entirely on available values at time t. The major disadvantages of explicit schemes are that they are usually conditionally stable and that the time step size is rather small. On the other hand, implicit schemes solve for dynamic quantities at time $t+\Delta t$ based not only on values at t, but also on these same quantities at $t+\Delta t$. In structural problems, implicit integration schemes usually give acceptable solution with time steps typically one or two orders of magnitude larger than the stability limit of simple explicit schemes.

The implicit operator used for time integration of the dynamic problem in ABAQUS is the operator defined by Hilber, Hughes, and Taylor (41). This operator is a single parameter operator with controllable numerical damping, the damping being most valuable in the automatic time stepping scheme, because the small high frequency numerical noise inevitably introduced when the time step is changed is removed rapidly by a small amount

of numerical damping. The operator definition is completed by the following Newmark formulae (63a) for displacement and velocity integration:

$$U|_{t+\Delta t} = U|_t + \Delta t\ \dot{U}|_t + \Delta t^2((\frac{1}{2} - \beta)\ddot{U}|_t + \beta\ \ddot{U}|_{t+\Delta t}) \qquad (5.12a)$$

$$\dot{U}|_{t+\Delta t} = \dot{U}|_t + \Delta t((1-\gamma)\ddot{U}|_t + \gamma\ddot{U}|_{t+\Delta t}) \qquad (5.12b)$$

where

$$\beta = \frac{1}{4}(1-\alpha)^2, \quad \gamma = \frac{1}{2} - \alpha \quad and \quad -\frac{1}{3} \le \alpha \le 0. \qquad (5.12c)$$

Equations (5.12) and the equilibrium Equation (3.1a) at time $t+\Delta t$ can be considered as:

$$M\ddot{U}_{t+\Delta t} + C\dot{U}_{t+\Delta t} + KU_{t+\Delta t} = R_{t+\Delta t} \qquad (5.13)$$

After the Equation (5.13) is solved, the results of the structural system are accordingly obtained.

Hilber, Hughes, and Taylor (41) present cogent arguments for the use of Equation (5.12) for integrating structural dynamic problems. The main appeal of the operator is its controllable numerical damping and the form this damping takes, slowly growing at low frequencies, with more rapid growth in damping at high frequencies. Control over the

amount of numerical damping is provided by the parameter α : with $\alpha = 0$, there is no damping, and the operator is the trapezoidal rule (Newmark, β=1/4), while with α=-1/3, significant damping is available. The operator is used primarily because the slight numerical damping it offers is needed in the automatic time stepping scheme, since each time step change introduces some slight noise into the solution, and a little numerical damping quickly removes this high frequency noise without having any significant effect on the meaningful, lower frequency response. It will be seen from the later section of this chapter that the numerical damping α has an insignificant effect on the dynamic response when the time step is fixed.

5.4 Comparison of Dynamic Analysis Methods

Generally, in the solution of vibration problems, not enough emphasis has been given to the differences between mode superposition and direct integration solutions in many cases. However, Galdos and Schelling (30) reported the phenomenon of natural frequency clustering when the dynamic impact analysis of horizontally curved steel box-girder bridges was conducted. The curved bridges were modelled by using the two-dimensional planar grid analogy in that study. The vehicle is modelled as the same model as in this study. In that study, 28 natural frequencies were extracted and found to be very clustered. The 28th frequency (25.04 Hz) is only about 18 times greater than the fundamental natural frequency (1.34 Hz), and in many cases the difference between consecutive frequencies is less than 10% of the lower one. The maximum moment by the

mode superposition solution produced smaller value than that for the static solution. However, the direct integration method gives larger value than the other two solutions.

The aim of this section is to investigate the natural frequency clustering phenomenon of simply-supported straight composite multicell box-girder bridges, and to compare the dynamic results generated by the mode superposition method and by the direct integration method. One straight bridge prototype of *2l-2c-60* (two-lane two-cell 60-meter-span) under fully loaded truck loading is selected by using the three-dimensional modelling in this section. It should be noted that material damping is neglected.

5.4.1 Natural Frequency Extraction

Up to 200 natural frequencies are extracted by using Lanczos method in ABAQUS. Table 5.1 lists all the extracted natural frequencies. It is clearly shown that the natural frequencies of the bridge are clustered significantly. The first natural frequency is 1.71 Hz, and the 200^{th} natural frequency is only 31.55 Hz, which is indeed very low in structural dynamic analysis. It is well known that the effective mass of participated modes is an indication that the number of modes considered in the mode superposition method is sufficient or not for the dynamic analysis. Fortunately, accompanying with the natural frequency extraction, the effective mass of each mode is also an output by ABAQUS. Table 5.2 lists the effective mass percentage to the total mass in three translation directions with different number of participated modes. It can be observed that the percentage of the effective mass to the total mass is lower than 90 percent for each translation direction up to

50 modes considered. The effective mass percentage is only 81.61, 87.7, and 79.78 for Z-, X-, and Y-direction, respectively. When the number of participated modes increases to 200, the percentages are only 90.92 percent and 93.08 percent for the Z- and X-directions, respectively, while it is 96.54% for the Y-direction. It is said that the effective mass percentage of participated modes should be at least 95% for a relatively accurate solution. Therefore, it is still not enough for the dynamic analysis with 200 modes.

The fundamental frequency of the prototype bridges studied herein will be discussed in detail in chapter VI. The typical mode shapes will also be illustrated in chapter VI together with the typical time histories of structural responses.

5.4.2 Parametric Study of Direct Integration Method

For the forced transient dynamic analysis, time step is the key parameter affecting the accuracy of the results and the computational cost. Besides, the numerical damping, α, mentioned in previous sections may have a significant effect on the dynamic results when using the direct integration method in ABAQUS. In this section, the two parameters will be examined. Figure 5.1 shows the normal stress time histories at mid-span of the edge girder for different parameters, using the direct integration method. It can be observed that the three curves are almost the same. Figure 5.2 is an enlargement of Figure 5.1. It shows that the three curves have slight difference and the difference can be neglected because the difference among the maximum responses is only about 0.3%. Therefore, it can be concluded that, for this type of bridge, it is reasonable to neglect the

numerical damping, α, and assume the time step to be fixed at 0.01 second.

5.4.3 Comparison of dynamic responses using different methods

Figure 5.3 includes the normal stress time histories at mid-span of the edge girder by using different methods, i.e., one direct integration case, four mode superposition cases with 10, 50, 150, and 200 participated modes. Figure 5.4 shows the maximum responses together with the static response with the same loading imposed at the bridge mid-span. The time step is taken as 0.01 sec for all the dynamic analyses.

It can be observed that the maximum response by the direct integration method is higher than any of the cases using the mode superposition method. For the mode superposition method alone, the maximum response increases with increase in the number of participated modes. For the case where the number of mode shapes is less than 50, the maximum response is still smaller than that for the static one. Similar results are also obtained from the analysis of a *2l-2c-60* curved bridge with L/R = 1.0, shown in Figures 5.5 to 5.8. Therefore, based on this comparison it was decided to use the direct integration method to perform the dynamic analysis of prototype bridges studied herein.

5.5 Summary

For the dynamic analysis of simply-supported composite cellular straight and curved bridges, the following conclusions are drawn from the study reported in this chapter:

1. The phenomenon of natural frequency clustering is presented in the 3-D bridge study.
2. Clustering greatly affects the dynamic response when the mode superposition method with fewer modes is used.
3. The mode superposition method gives smaller and unsafe results when a few numbers of modes are taken into consideration for the kind of bridges to be studied herein.
4. The direct integration method is a more reliable method to study the dynamic response of bridges studied herein.
5. A reasonable time step can be considered without affecting the results.
6. Numerical damping has an insignificant effect on the dynamic response when fixed time step is used in the direct integration method.

CHAPTER VI

FUNDAMENTAL FREQUENCY OF STRAIGHT AND CURVED COMPOSITE CELLULAR BRIDGES

6.1 General

Excessive dynamic deflections and unusual vibration in bridges can cause discomfort to motorists and pedestrians especially when the dominant mode of vibration is torsional. Human biodynamic response to either wind-, earthquake-, or vehicle-excited motion is generally more influenced by the higher derivatives of displacements. Therefore, bridge design and occupant comfort can be affected by underestimating the dynamic response as a consequence of neglecting the contribution of higher modes of vibration. On the other hand, it is known that the dynamic response of vibrational phenomena in analytical solutions is mainly given by the first few mode shapes and their corresponding natural frequencies. The major contributor is the first mode shape corresponding to the first natural frequency (fundamental frequency) of a system. Figure 6.1 and Fig 6.2 show the first three mode shapes of one typical straight bridge prototype and one curved bridge prototype, respectively. It can be observed that the first mode shape is purely flexural for both of straight and curved bridges.

For the other two modes, mode shapes are complex being combination of torsional, warping and flexural modes. Figure 6.3 and Figure 6.4 show the time histories of mid-span bottom-flange normal stress, edge-web reaction and mid-span deflection for an exterior girder in straight and curved bridges, respectively. It can be observed that the maximum dynamic responses are reached when the trucks are traveling within the bridges. The bridges then vibrate freely almost at the frequency corresponding to the fundamental natural frequency after the trucks move out of the bridges. Therefore, the fundamental frequency is important in the dynamic analysis. Furthermore, it is also very important for bridge designers to have a reliable estimate of the fundamental frequency of any bridge being designed to avoid resonance with any external loadings such as earthquake, wind, blast, and moving trucks.

In the first part of this chapter, parameters affecting the fundamental frequency are examined. Then based on the numerous results generated, empirical formulas for the fundamental frequency for straight and curved bridges are derived by a regression analysis method.

6.2 Effect of Cross-Bracing Systems

X-type cross-bracings as well as top chords are normally used in the radial direction between cells during construction to minimize distortional, longitudinal warping, and transverse bending stresses encountered in an open-cell cross-section. To study the effect of this parameter on the fundamental frequency in composite cellular bridges, the number and the area of the cross-bracing systems are changed while the other parameters are kept constant. Figure 6.5 presents the fundamental frequency versus the number of cross-bracing systems

for *2l-2c-40* straight and curved bridges with curvature, L/R = 0.4 and 1.0. It can be observed that the presence of bracing systems does not influence the fundamental frequency for straight bridges. An increase in the number of cross-bracing systems does not affect the fundamental frequency, either. However, it does affect the fundamental frequency of curved bridges. The fundamental frequencies of curved bridges with three cross-bracing systems increase dramatically when compared to those in curved bridges with no cross-bracing system. This increase is augmented further by the curvature. The reason for this observation is that the presence of cross-bracing systems significantly increases the flexural stiffness of curved bridges. However, further increase in the number of cross-bracing systems has an insignificant effect on the fundamental frequency.

Figure 6.6 presents the variations in the fundamental frequency for *2l-2c-40* straight and curved bridges with different area of cross-bracing systems and different degrees of curvature. It can be observed that the area of cross-bracing systems has an insignificant effect on the fundamental frequency of straight and curved bridges. Thus, based on the results of the sensitivity study, it was decided to conduct extensive parametric study on the fundamental frequency of bridges with three or more cross-bracing systems, with spacing less than the maximum spacing of 7.5 m recommended by AASHTO code (5), and an area of 100*100 mm^2 for the cross-bracing system.

6.3 Effect of Span-to-Depth Ratio

Figure 6.7 shows the effect of the bridge span-to-depth ratio on the fundamental frequency of *2l-2c-40* straight and curved bridges with curvature, L/R = 1.0. It is observed

that the fundamental frequency decreases significantly with increase in the span-to-depth ratio, L/D, for both straight and curved bridges. The reason for this is that the stiffness of bridges decreases dramatically when the span-to-depth ratio increases. Furthermore, it can be also observed that the span-to-depth ratio has more influence on the fundamental frequency of curved than straight bridges.

6.4 Effect of Span

Figure 6.8 shows the effect of the span on the fundamental frequency of *4l-4c* straight and curved bridges with span-to-depth ratio, L/D = 25, and with L/R = 0.4, 1.0, and 1.4. Similar to the effect of bridge span-to-depth ratio, the fundamental frequency decreases significantly with increase in the span for all of straight and curved bridges. It can be also observed that the span has more influence on the fundamental frequency of curved bridges. With increase in the curvature of a bridge, the fundamental frequency decreases slightly. Whereas the fundamental frequency decreases more rapidly for straight bridges. It seems that in longer span bridges flexure is more dominant, thus leading to smaller fundamental frequencies.

6.5 Effect of Curvature

The fundamental frequency of a bridge is strongly affected by the degree of curvature. Figure 6.9 shows the effect of curvature on the fundamental frequency of *4l-4c* bridges of 20 m to 100 m span. For the same span length of a curved bridge, the smaller the radius of curvature produces the smaller fundamental frequency. It can be also observed that the

fundamental frequency of straight bridges is always larger than that of corresponding curved bridges. Furthermore, decrease in span of bridges causes significant decrease in the fundamental frequency of the bridges.

6.6 Effect of Number of Cells and Number of Lanes

Figure 6.10 shows the effect of the number of cells on the fundamental frequency of *3l-100* straight and curved bridges with L/R = 0.4, 1.0, and 1.4. It can be observed that the number of cells has no significant effect on the fundamental frequency for both straight and curved bridges. Figure 6.11 shows the effect of number of lanes on the fundamental frequency of straight and curved bridges of 40 m span with L/R = 0.4, 1, and 1.4. The number of cells for one-, two-, three-, and four-lane bridges is 2, 2, 4, and 4, respectively. Since the number of cells has an insignificant effect on the fundamental frequency, different number of cell bridges can be treated as the same type bridges. Thus, the fundamental frequency is also comparable for these selected bridges. It can be observed that the number of lanes has no significant effect on fundamental frequency for straight and curved bridges, irrespective of bridge curvature.

6.7 Empirical Formulas for the Fundamental Frequency

The parametric study revealed that number of lanes, span-to-radius of curvature ratio, span-to-depth ratio, and span length are the major parameters that affect the dynamic characteristics of straight and curved multi-cell bridges. Based on the data generated from the extensive parametric study, empirical expressions for the fundamental frequencies of straight

and curved bridges are deduced. A regression analysis was used to determine the constants in the expressions. Assuming that both the flexural rigidity, EI, and the mass per unit length of the structure, m, are constant along the span length, L, the first flexural frequency of vibration, f_{BEAM}, from the beam theory without considering shear deformation and torsional inertia, is given by Humar (44) as:

$$f_{BEAM} = \frac{\pi}{2L^2}\sqrt{\frac{EI}{m}} \tag{6.1}$$

It is assumed that the fundamental frequency of simply-supported straight and curved composite concrete deck-steel multi-cell bridges, f_{CELL}, may then be expressed in the following form:

$$f_{CELL} = \alpha\beta\, f_{BEAM} \tag{6.2}$$

where α and β are correction factors. The parametric study revealed that these factors depend on the bridge span, L, in meters and, L/R ratio as follows:

For straight bridges:

$$\alpha = 0.93 - \frac{0.76}{L} - \frac{18}{L^2} \tag{6.3a}$$

$$\beta = 1 \tag{6.3b}$$

For curved bridges:

For $N_L = 4$, L/R > 0.4, L < 40 m:

$$\alpha = 0.93 - \frac{0.76}{L} - \frac{18}{L^2} \tag{6.3a}$$

$$\beta = 1 - 0.23\left(\frac{L}{R}\right) - 0.06\left(\frac{L}{R}\right)^2 \tag{6.3c}$$

For other cases of curved bridges:

$$\alpha = 0.93 - \frac{0.76}{L} - \frac{18}{L^2} \tag{6.3a}$$

$$\beta = 1 - 0.04\left(\frac{L}{R}\right) - 0.15\left(\frac{L}{R}\right)^2 \tag{6.3d}$$

Sennah (76) suggested a set of equations to evaluate the fundamental frequency for straight and curved bridges. Table 6.1 presents the comparison between the values from Sennah's equations and those from the proposed equations.

When using Equation (6.2), it is assumed that end-diaphragms as well as at least three cross-bracing and top-chord systems are provided in the radial direction along the bridge span. For the purpose of design, the designer can easily calculate the fundamental frequency of designed bridge by using the proposed equations.

CHAPTER VII

ANALYSIS OF IMPACT FACTORS

7.1 General

This chapter presents the results from an extensive parametric study, using the finite element method, in which 120 simply-supported composite multi-cell bridge prototypes are analyzed, to investigate their dynamic impact factors when used in straight and curved alignments. The parametric study conducted herein includes the following aspects: (*i*) moment impact factor; (*ii*) reaction impact factor; and (*iii*) deflection impact factor in simply-supported straight and curved composite multi-cell bridges.

In the first part of this chapter, a sensitivity study of the bridge parameters and loading conditions that are hypothesized to influence the magnitude of the dynamic impact factor is carried out. These parameters include: (*i*) cross-bracing systems; (*ii*) number of lanes; (*iii*) number of cells; (*iv*) bridge curvature; (*v*) bridge span; (*vi*) speed of truck; and (*vii*) truck loading conditions. Based on the data generated from the extensive parametric study, simplified dynamic impact factor equations are proposed for analysis and design of straight and curved simply-supported composite multi-cell bridges under highway loading in the last part of this chapter. These equations are then compared to the impact factors presented in the AASHTO code (4, 5), the OHBDC (67) and the CHBDC (65). It should be noted that the dynamic analysis of curved bridges is greatly different from that of straight bridges because of the existence of the centrifugal force. Therefore, it was necessary to study the dynamic

impact factor for straight and curved bridges separately.

7.2 Analysis of Effects of Bridge Parameters and Vehicle Variables

7.2.1 Effect of Cross-Bracing Systems

The cross-bracing systems in bridges include the X-type cross-bracings within the cells and the top chords associated with the cross-bracings. In this section, selected types of bridges are chosen to examine the effects on bridges with various numbers of cross-bracing systems and various areas of cross-bracing systems. The number of cross-bracing systems is chosen as 0, 3, 5, 7, 11, and 17. The area of cross-bracing systems is chosen as 625, 2500, 5625, 10000, 15625 mm^2. The *2l-2c-40* bridges are chosen in the analysis for this section, with L/R ratios of 0.0 (straight bridge), 0.4, and 1.0 and with full truck loading at the maximum allowable safe speeds determined by the method proposed in chapter IV. These limitations are chosen as to reduce the influence of other parameters.

a. Effect of number of cross-bracing systems

Figures 7.1, 7.2 and 7.3 show the effect of number of cross-bracing systems on moment, reaction, and deflection impact factors, respectively, with different L/R = 0.0, 0.4 and 1.0. From Figure 7.1, it can be observed that adding three cross-bracing systems along the span reduces the moment impact factor by about 73% and 83% in the case of L/R = 0.4 and 1, respectively. It can also be observed that further increase the number of bracings has an insignificant effect on the moment impact factor. For straight bridges, it is observed that

the presence of cross-bracing systems has no influence on the moment impact factor.

It can be observed from Figure 7.2 that adding three cross-bracing systems along the span reduces reaction impact factor by about 13% in the case of L/R = 0.4. Beyond that, the reaction impact factor increases slightly with increase in the number of cross-bracing systems. For curved bridge with L/R = 1.0, it shows that number of cross-bracing systems has an insignificant effect on the reaction impact factor. For straight bridges, adding three cross-bracing systems along the span slightly increases the reaction impact factor. Beyond that, the reaction impact factor remains almost constant with increase in the number of cross-bracing systems.

Figure 7.3 shows similar trends for the deflection impact factor. It can be observed that adding three cross-bracing systems along the span reduces the deflection impact factor by about 43% in the case of L/R = 0.4. Then, the impact factor slightly decreases with increase in the number of cross-bracing systems. For curved bridges with L/R = 1.0, adding three cross-bracing systems along the span greatly increases the deflection impact factor. Beyond that, the impact factor slightly decreases with increase in the number of cross-bracing systems. For straight bridges, the deflection impact factor almost remains constant and not influenced by any cross-bracing system.

However, the presence of cross-bracing system is generally required for stability purposes at the construction phase, and it is important to enhance the bridge torsion stiffness. Thus AASHTO code (5) recommends at least three cross-bracings with spacing less than the maximum spacing of 7.5 m. For this reason and the discussion of the previous section, it was decided to conduct the parametric study with the number of bracing and top-chord systems of

3, 5, 7, 11, and 17 for bridge spans of 20, 40, 60, 80, and 100 m, respectively.

b. Effect of area of cross-bracing systems

Figures 7.4, 7.5 and 7.6 show the effect of area of cross-bracing systems on moment, reaction, and deflection impact factors, respectively, with different L/R = 0.0, 0.4 and 1.0. From Figure 7.4, it can be observed that the moment impact factor decreases with increase in the area of cross-bracing systems for curved bridges, but it decreases very slowly when the area is equal to or larger than 2500 mm^2. However, for straight bridges, the moment impact factor slightly increases with increase in the area of cross-bracing systems, and it is almost constant when the area is equal to or larger than 2500 mm^2. It can be observed from Figure 7.5 that the reaction impact factor increases slightly with increase in the area of cross-bracing system for both straight and curved bridges.

Figure 7.6 shows similar relationship for the deflection impact factor as with the moment impact factor. It can be observed that the deflection impact factor slightly decreases with increase in the area of cross-bracing systems in the case of L/R = 0.4. For curved bridges with L/R = 1.0, the deflection impact factor increases when the bracing area increases from 625 to 2500 mm^2. When the bracing area continues to increase, the impact factor slightly decreases.

Therefore, it was decided to conduct the parametric study with cross-bracings and top-chords having a 100x100 mm^2 rectangular cross-section in this study.

7.2.2 Effect of Number of Lanes

The number of lanes utilized in this study consists of one, two, three, and four lanes for all straight and curved prototype bridges. In this section, selected types of bridges are chosen to examine the effect of varying the number of lanes. The full truck loading at the maximum allowable safe speed is applied to the bridges in this section. The chosen bridges are *4c-40* and *4c-100* bridges with L/R = 0.0, 0.4, 1.0, and 1.4.

Figures 7.7 and 7.8 show the effect of the number of lanes on moment impact factor with span of 40 m and 100 m, respectively. For straight bridges, the moment impact factor is almost constant when the number of lanes changes for both spans. For curved bridges, the moment impact factor increases with increase in the number of lanes for bridges of 40 m span except when L/R = 0.4, in which it varies irregularly with increase in the number of lanes. However, the moment impact factor decreases with increase in the number of lanes for bridges of 100 m span except for one lane bridge with L/R = 1.4.

Figures 7.9 and 7.10 show the effect of number of lanes on the reaction impact factor of bridges of spans of 40 m and 100 m, respectively. For span of 40 m, it can be observed that the number of lanes has an insignificant effect on the reaction impact factor for straight and curved bridges except for L/R = 0.4, in which case, the reaction impact factor decreases with increase in the number of lanes. For 100-m-span bridges, Figure 7.10 shows that the number of lanes has an insignificant effect on the reaction impact factor for curved bridges. But it slightly increases with increase in the number of lanes.

Figures 7.11 and 7.12 show the effect of number of lanes on the deflection impact factor of bridge spans of 40 m and 100 m, respectively. For spans of 40 m, it can be observed

that the deflection impact factor slightly increases with increase in the number of lanes for curved bridges. For straight bridges, it is almost constant with increase in the number of lanes. For bridges of 100 m span, Figure 7.12 shows that the deflection impact factor is not sensitive to changes in the number of lanes except for curved bridges with L/R = 0.4, in which the impact factor decreases with increase in the number of lanes.

Therefore, the number of lanes has an unpatterned influence on the impact factors for curved bridges. For straight bridges, however, it has an insignificant influence on the impact factors other than the reaction impact factor.

7.2.3 Effect of Number of Cells

Similar to the study in the previous sections, the full truck loading at the maximum allowable safe speed is chosen in this section to examine the effect of the number of cells on the impact factors. The selected bridges are *2l-40* straight and curved bridges with L/R = 0.0, 0.4, 1.0, and 1.4. Figures 7.13, 7.14, and 7.15 show the effect of the number of cells on moment, reaction, and deflection impact factors with span of 40 m bridges, respectively. It can be observed that the impact factors are insensitive to changes in the number of cells for almost all cases except the reaction impact factor of straight bridges, in which the reaction impact factor significantly increases with increase in the number of cells.

7.2.4 Effect of Curvature

The effect of curvature on impact factors of curved bridges is examined in this section. The L/R ratios studied were 0.4, 1.0, and 1.4. The *4c-40* and *4c-100* bridges are chosen in

this section. The bridges are under full truck loading with the maximum allowable safe speed.

Figures 7.16 and 7.17 show the effect of curvature on moment impact factor of bridges of 40 m span and 100 span, respectively. It can be observed that the moment impact factor increases with increase in L/R for two-, three-, and four-lane bridges of both spans. For one-lane bridges, it increases with increase in the curvature for span of 40 m, but it decreases for span of 100 m.

Figures 7.18 and 7.19 show the effect of curvature on the reaction impact factor of bridges of 40 m span and 100 span, respectively. The reaction impact factor decreases sharply with increase in the curvature for all lanes.

The effect of curvature on the deflection impact factor of bridges of 40 m span and 100 span are presented in Figures 7.20 and 7.21, respectively. Figure 7.20 shows that the impact factor increases with increase in curvature for all cases of 40 m span bridges. On the other hand, the impact factor decreases with increase in curvature for bridges of 100 m span in Figure 7.21.

7.2.5 Effect of Span

In this section, the effect of span on impact factors of straight and curved bridges is presented. Selected bridges are *3l-4c* and *2l-2c* bridges with L/R = 0.0, 0.4, 1.0, and 1.4 under full truck loading at the maximum allowable safe speed.

Figures 7.22 and 7.25 show the effect of span on the moment impact factor of *3l-4c* and *2l-2c* bridges, respectively. It can be observed that the moment impact factor increases

with increase in the span for straight bridges for both cases. For curved bridges, the impact factors is very similar for bridges with L/R =1.0 and 1.4. The moment impact factor in the two cases decreases when the span increases from 20 m to 60 m, and then it begins to increase for 60 m span to 100 m span. However, for bridges of curvature L/R = 0.4, the moment impact factor behaves irregularly when the span increases.

Figures 7.23 and 7.26 show the effect of span on the reaction impact factor of *3l-4c* and *2l-2c* bridges, respectively. It can be observed that the reaction impact factor decreases when the span changes from 20 m to 60 m span for curved bridges with L/R = 1.0 and 1.4, but the impact factor slightly increases from 60 m span to 100 m span. For curved bridges with curvature L/R = 0.4, the impact factor slightly increases with increase in the span of *3l-4c* bridges, and it becomes almost constant for *2l-2c* bridges. For *3l-4c* straight bridges, the reaction impact factor increases when the span changes from 20 m to 60 m, and then it decreases for 60 m to 100 m spans. On the other hand, for *2l-2c* straight bridges, the reaction impact factor decreases with increase in the bridge span.

Figures 7.24 and 7.27 show the effect of span on the deflection impact factor of *3l-4c* and *2l-2c* bridges, respectively. It can be observed that the deflection impact factor behaves in a similar fashion as the moment impact factor when the bridge span changes for both straight and curved bridges.

7.2.6 Effect of Truck Speed

The purpose of this section is to analyze the influence of truck speed alone on the impact factors, where the speed is the independent variable. In chapter IV it was discussed

that curvature and speed are correlated and it appears that together they have a clear influence on the outcome of the impact factors for most cases because the curvature determines the maximum allowable safe speed for all curved bridges in this study. In this section, the effect of truck speed on impact factors is examined under full truck loading while the truck speed is selected within the maximum allowable safe speed.

Figures 7.28 to 7.30 show the effect of truck speed on the moment, reaction and deflection impact factors for *2l-2c-40* bridges, respectively. It can be clearly observed that the truck speed has a significant influence on impact factors. The impact factors increase significantly with increase in the truck speed for curved bridges with L/R = 1.0 and 1.4. Figure 7.31 presents the effect of truck speed on the moment and reaction impact factors of *3l-4c-60* bridges with L/R = 0.4. Trends are similar to those shown in Figure 7.28 to 7.30.

Figure 7.32 shows the effect of truck speed on the impact factors for *2l-2c-60* straight bridges. It is clearly demonstrated that the impact factors increase with increase in the truck speed.

7.2.7 Effect of Truck Loading Conditions

As explained in chapter IV, three types of truck loading are applied in this study, namely: (*i*) partially loading in the inner lane close to the curb; (*ii*) partially loading in the outer lane close to the curb; and, (*iii*) fully loading close to the middle of the bridge lanes. The maximum allowable safe speed is determined by the method in chapter IV. In this section, the effect of truck loading conditions on the impact factors is analyzed for *2l-2c-40* bridges. Furthermore, an additional loading case is used in the sensitivity study of this section, namely

two trucks travelling from the opposite directions in separate lanes at the same angular speed, and the maximum allowable safe speed is determined by the truck travelling in the outer lane of the curved bridge.

Figure 7.33 shows the effect of loading conditions on the moment impact factor for *2l-2c-40* straight and curved bridges with L/R = 0.4. Table 7.1 presents the dynamic and static responses of the outer girder of the selected bridges. It should be noted that, for straight bridges, partial loading case on the outer lane is the same as that on the inner lane. It is shown here just for comparison. It can be observed from Figure 7.33 that the moment impact factor under full truck loading is slightly smaller than that for partially loaded truck loading for straight bridges. However, the loading case of two trucks travelling from opposite directions yields higher moment impact factor for straight bridges. From Table 7.1, however, the maximum static normal stress was generated in the full truck loading case. Furthermore, for three-lane and four-lane bridges, the full truck loading case is much easier to be studied than other cases. For curved bridges, the moment impact factor for the full truck loading case is somewhat larger than that of the partially loaded case in inner lane, but is slightly smaller than that in the partially loaded case in outer lane. In addition, it is almost the same as that for the case of two trucks travelling from opposite directions. However, Table 7.1 shows that the static normal stresses of full loading case are larger than that of partially loading cases. Similar conclusions can be made for the reaction and deflection responses. Therefore, the full truck loading condition is the most important loading case for the impact factors. Thus, it was decided that the full truck loading case be used in the parametric study to investigate the impact factors of bridges.

7.3 Empirical Formulas for Impact Factors

The influence of various variables of bridge geometry and loading conditions on the impact factors has been discussed in the previous sections. As explained previously, the study of the influence of the variables was done in such a way as to reduce the influence of other effects to a minimum. Under these circumstances the impact factors, in most cases, showed a definite trend relative to the variables in question. However, these would have been valid under these conditions only, which would seriously limit their usefulness for general design. Furthermore, the effect of various parameters is cumulative and the impact factors will probably show higher degree of dispersion than those in the study of isolated cases. In fact this is what happened as will be shown in the following sections. For curved bridges, the situation is more complicated because the curvature determines the maximum allowable safe speed. For different spans and curvatures, the maximum allowable safe speed is always different. This indicates that a dynamic analysis of straight and curved bridges for impact factors with variable radii of curvature, number of cells, span lengths, etc., is very complex, and apparently the analysis of a large number of bridge cases is necessary to derive adequate estimates for impact factors that can be applicable to bridge design.

It was mentioned in chapter VI that the mode of fundamental natural frequency contributes more to the dynamic response than any other mode of natural frequencies. For a dynamic analysis, then, it becomes sensible to relate impact factors to the fundamental natural frequency. Thus, in this section, the impact factors are presented as a function of the fundamental natural frequency of the bridge. It will also be of interest to relate the dynamic impact factors to span length. Span length is an excellent proxy variable for the fundamental

natural frequency since they are related. Since the span length is known in any bridge design, impact equations are also derived as a function of bridge span. Since the span-to-radius ratio is the most important variable in curved bridges, impact factor equations are also derived in terms of the span-to-radius ratio. It should be mentioned that the impact factor equations derived are all upper bound.

7.3.1 Impact Factors as Function of Fundamental Natural Frequency

Figures 7.34 to 7.36 show the impact factors versus the fundamental natural frequency for straight bridges. Figures 7.37 to 7.40 present the impact factor versus the fundamental natural frequency for curved bridges. The derived equations for the impact factors are as follows:

For straight bridges:

(1) Moment impact factor

$$I_M = 0.16 - \frac{f}{36} \qquad f < 2 \text{ Hz} \qquad (7.1)$$

$$I_M = 0.11 \qquad f > 2 \text{Hz}$$

[NOTE: For a bridge with $f = 2$ Hz, the value of the moment impact factor is calculated from the two corresponding equations listed, and the larger value of the moment impact factor calculated is used for the conservative design. The following impact factor equations follow the same rule as in Equation (7.1)]

(2) Reaction impact factor

$$I_R = 0.59 \qquad f < 1.5\text{Hz}$$

$$I_R = 0.78 - \frac{f}{8} \qquad 1.5\text{ Hz} < f < 3.5\text{ Hz} \qquad (7.2)$$

$$I_R = 0.34 \qquad f > 3.5\text{Hz}$$

(3) Deflection impact factor

$$I_D = 0.18 - \frac{f}{30} \qquad f < 3\text{ Hz} \qquad (7.3)$$

$$I_D = 0.08 \qquad f > 3\text{Hz}$$

For curved bridges:

(1) Moment impact factor

$$I_M = 0.20 \qquad f < 2\text{ Hz} \qquad (7.4)$$

$$I_M = 0.28 - \frac{f}{24} \qquad f > 2\text{ Hz}$$

(2) Reaction impact factor

(a) L/R $\geqslant$ 1.0

$$I_R = 0.52 - \frac{f}{23} \qquad f < 3.5\text{ Hz} \qquad (7.5a)$$

$$I_R = 0.37 \qquad f > 3.5\text{Hz}$$

(b) L/R < 1.0

$$I_R = 0.61 \qquad f < 3.5 \text{ Hz} \qquad (7.5b)$$

$$I_R = 0.68 - \frac{f}{39} \qquad f > 3.5 \text{Hz}$$

(3) Deflection impact factor

$$I_D = 0.14 \qquad f < 3 \text{ Hz} \qquad (7.6)$$

$$I_D = 0.26 - \frac{f}{29} \qquad f > 3 \text{Hz}$$

7.3.2 Impact Factors as Function of Span Length

Figures 7.41 to 7.43 show the impact factors versus span length for straight bridges. Figures 7.44 to 7.47 show the impact factor versus span length for curved bridges. The derived equations for the impact factors are as follows:

For straight bridges:

(1) Moment impact factor

$$I_M = 0.12 \qquad L < 60 \text{ m} \qquad (7.7)$$

$$I_M = 0.11 + \frac{L}{4000} \qquad L > 60 \text{ m}$$

(2) Reaction impact factor

$$I_R = 0.31 + \frac{L}{282} \qquad L < 80\text{ m}$$

$$I_R = 0.97 - \frac{L}{210} \qquad L > 80\text{ m} \qquad (7.8)$$

(3) Deflection impact factor

$$I_D = 0.12 \qquad L < 40\text{ m} \qquad (7.9)$$

$$I_D = 0.09 + \frac{L}{1818} \qquad L > 40\text{ m}$$

For curved bridges:

(1) Moment impact factor

$$I_M = 0.15 \qquad L < 60\text{ m} \qquad (7.10)$$

$$I_M = 0.07 + \frac{L}{727} \qquad L > 60\text{ m}$$

(2) Reaction impact factor

(a) L/R $\geqslant$ 1.0

$$I_R = 0.42 - \frac{L}{354} \qquad L < 60\text{ m}$$

$$I_R = 0.22 + \frac{L}{1739} \qquad L > 60\text{ m} \qquad (7.11a)$$

(b) L/R < 1.0

$$I_R = 0.52 + \frac{L}{465} \qquad L < 60\text{ m}$$

$$I_R = 0.65 - \frac{L}{870} \qquad L > 60\text{ m} \qquad (7.11b)$$

(3) Deflection impact factor

$$I_D = 0.14 \qquad (7.12)$$

7.3.3 Impact Factors as Function of Span-to-curvature Ratio

Figures 7.48 to 7.50 show the impact factors versus span-to-curvature ratio (L/R) of curved bridges. The derived equations for the impact factors are as follows:

(1) Moment impact factor

$$I_M = 0.22 - \frac{1}{27}\frac{L}{R} \qquad (7.13)$$

(2) Reaction impact factor

$$I_R = 0.72 - 0.28\frac{L}{R} \qquad (7.14)$$

(3) Deflection impact factor

$$I_D = 0.12 + \frac{1}{60}\frac{L}{R} \qquad (7.15)$$

7.4 Verification of Results

The impact factors obtained in this study are compared to the values given by the Ontario Highway Bridge Design Code (OHBDC) (67), the AASHTO Guide Specifications (4, 5), and by the CHBDC (65).

First, the impact factor results are compared to those in the OHBDC (67). The OHBDC discarded the term "impact factor" in favor of the term "dynamic load allowance" for only straight bridges and its impact factor applies equally to moment, reaction, and deflection. Figures 7.34 to 7.36 show the impact factors for straight bridges with the OHBDC provisions. It is observed that the moment and deflection impact factors generated in this study are much smaller than the OHBDC provisions, especially for longer span bridges. However, for reaction, Figure 7.35, the impact factor found in this study is significantly higher than those in the OHBDC provision when the fundamental frequency is smaller than 2.5 Hz. For fundamental frequencies greater than 3.5 Hz, the impact factor derived herein is slightly lower than OHBDC provision.

The OHBDC is not applicable to bridges with curved alignment, but it is interesting to compare the impact factors of curved bridges derived herein to those in the OHBDC if they were applicable to curved bridges. Figures 7.37 to 7.40 present the impact factors of curved bridges showing the hypothetical values from the OHBDC provisions. For the moment and deflection impact factors, the values derived herein are much lower than those given by OHBDC for straight bridges, especially for higher frequencies. For higher L/R curved bridges (L/R / 1.0), the reaction impact factor is very close to the OHBDC values for straight bridges except for some larger impact factors in the lower frequency range. However, for

curved bridges with L/R < 1.0, the reaction impact factor is much higher than those proposed by OHBDC.

Next, the derived impact factors of straight bridges are compared with the equation given in AASHTO Standard Specification (5):

$$I = \frac{50}{125 + L} \tag{7.16}$$

where L is the span of simply-supported straight bridges in feet, and the maximum value for I is 30%.

Figures 7.41 to 7.43 present the derived impact factors for straight bridges and those given by the above AASHTO equation. It should be noted that the above AASHTO standard equation for impact factor is equally applicable to moment, reaction, and deflection calculations. From the results in Figures 7.41 and 7.43, it can be observed that the moment and deflection impact factors from this study are much smaller than those given by the AASHTO standard equation. Furthermore, the impact factors for moment and deflection increase with increase in the bridge span, which is opposite to the trends in the AASHTO standard equation in which the impact factor decreases with increase in the bridge span. The reaction impact factor, Figure 7.42, however, is significantly higher than those given by the AASHTO standard equation, especially for longer bridge spans.

The impact factors of curved bridges are compared with the values of the impact

factors based on the equations given in the Guide Specification for Horizontally Curved Highway Bridges (4). It should be noted that these equations in Guide Specification (4) were derived for curved multiple-spine box girder bridges using only planar-grid analysis, which is not as accurate as the 3-D analyses adopted in this study. Figures 7.44 to 7.47 show the derived impact factors of curved bridges and those given by the equations in Appendix 2 of 1993-edition of the Guide Specification (4). It is observed that the moment and deflection impact factors derived herein are smaller than the values given by the Guide Specification. For the reaction impact factor, however, the derived values are significantly higher than those based on 1993-edition of the Guide Specification, especially for lower L/R bridges. But these reaction impact factors are still smaller than the value given in the 1980-edition of the Guide Specification (Appendix 1), in which the reaction impact factor = 1.00. It is believed that three main reasons account for the difference. The first reason is that curved bridges are modelled as 3-D solid structures in this study, not 2-D structures (74, 31, 4) as in the Guide Specification. 3-D models are relatively more accurate than 2-D models, resulting in lower moment and deflection impact factors. The second reason is that the section of bridges in this study is cellular box, not multiple-spine box on which the impact factors in the Guide Specification are based. It is evident that cellular box section has higher torsional stiffness than that of multiple-spine box section. This implies that cellular box curved bridges would have lower moment and deflection impact factors than multiple-spine box curved bridges. The last reason is that the impact factor selection criterion is different. In this study, the moment and deflection impact factors are obtained from the maximum dynamic and static responses of the mid-span section of the bridge. However, the AASHTO Guide Specification

selects the maximum impact factors from all the positions studied on the bridge. Therefore, the impact factors recommended by AASHTO Guide Specification should be larger somewhat. For the reaction impact factor, the values derived herein are between those given by the two editions of Guide Specification for Horizontally Curved Highway Bridges of 1993 and 1980 (4). This implies that the 1993-edition Guide Specification may underestimate the reaction impact factors for multiple-spine bridges.

CHAPTER VIII

SUMMARY AND CONCLUSIONS

8.1 Summary

Extensive theoretical studies were carried out to investigate the static and dynamic responses of straight and curved composite concrete deck-steel cellular bridges. A literature review was conducted in order to establish the foundation for this study. It was observed that there is lack of information regarding the dynamic impact factors of this type of bridges. While the current design practices in North America recommend few analytical methods for the design of straight composite multi-cell box girder bridges, practical requirements in the design process call for a simplified design method in the form of expressions for moment, reaction and deflection impact factors for both straight and curved composite cellular bridges. Therefore, the current research described in this thesis was carried out with the goal to fill most of the gaps found in previous studies as well as in bridge codes.

One hundred and twenty simple-supported composite concrete deck-steel cellular box straight prototype bridges and over two hundred curved prototype bridges were considered in this study. For its analytical versatility, the finite element method was used throughout this study to describe the linear, static and dynamic responses of such bridges. It should be noted that the effects of temperature, vehicle-bridge interaction, and deck surface roughness were not considered herein because they are outside the scope of this study. In the extensive parametric study, the prototype bridges were subjected to AASHTO truck loadings in

different positions. Based on the data generated from the parametric studies, simplified design equations for impact factors were proposed for both straight and curved cellular bridges of composite construction. These equations involved dynamic impact factors for moment, reaction, and deflection. Empirical expressions for the fundamental frequency of such bridges were deduced to assist in the check for serviceability (deflection control).

8.2 Conclusions

The most important conclusions drawn from the results in this study are summarized below:

1. The phenomenon of natural frequency clustering is presented in simply-supported composite cellular box girder straight and curved bridges. This clustering greatly underestimates the dynamic response when the mode superposition method with fewer modes is used.
2. The mode superposition method gives smaller and unsafe results when a few numbers of modes are taken into consideration for this kind of bridges.
3. The direct integration method is a good and safe method to study the dynamic response of this type of bridges.
4. The time step can be taken as a relatively large value without affecting the results.
5. The numerical damping has an insignificant effect on the dynamic result when a fixed time step is used in the direct integration method.

6. The presence of end-diaphragms at the supports, with minimum thickness specified by the codes, and a minimum of three cross-bracings and top-chord systems, with a maximum spacing of 7.5 m, are adequate to enhance the fundamental frequency of simply-supported straight and curved bridges. The area of the cross-bracing systems has an insignificant effect on the fundamental frequency of straight and curved bridges.
7. The fundamental frequency of straight and curved bridges decreases with increase in the bridge span, span-to-depth ratio, and the degree of bridge curvature.
8. The number of lanes and cells has an insignificant effect on the fundamental frequency of straight and curved bridges.
9. The presence of end-diaphragms at the support lines along with a minimum of three bracing systems between the radial support lines, with a maximum spacing of 7.5 m, significantly affects the impact factors of curved bridges.
10. Increasing the area of cross-bracing systems has an insignificant effect on the impact factors for straight and curved bridges.
11. The number of lanes has an insignificant effect on the moment and deflection impact factors of straight bridges, but it has some effect on the reaction impact factor for straight bridges and impact factors for curved bridges.
12. The number of cells has an insignificant effect on the moment and deflection impact factors of straight and all impact factors for curved bridges, but it greatly affects the reaction impact factor for straight bridges.
13. Curvature and bridge span have a complicated effect on the impact factors for straight and curved bridges. For different combination of curvature and span, the trend of impact

factors is haphazard.

14. Truck speed is an important parameter that affects the impact factors of straight and curved bridges. An increase in the truck speed greatly increases the impact factors for bridges.

15. The moment and deflection impact factors for straight bridges increase with increase in bridge span.

8.3 Recommendations for Future Research

It is recommended that further research efforts be directed towards the following:

1. The axial force in the cross-bracing systems changes constantly from compression to tension and vice versa during truck motion. The corresponding impact factor is essential for the design of the cross-bracing system.
2. The study of the roughness of pavement on impact factors for straight and curved bridges is needed for possible evaluation of existing bridges.
3. A 3-D finite element analysis for the dynamic response of curved composite multiple-spine bridges to verify the available impact factor equations in the AASHTO Guide (4) which were based on a 2-D analysis.
4. Study vehicle-bridge interaction for bridges of short spans.
5. Field testing on actual bridges is required to verify the analytical modelling.

REFERENCES

1- Abdel-Salam, M. N., and Heins, C. P. 1988. **Seismic response of curved steel box girder bridges**. ASCE Journal of Structural Engineering, 114(12): 2790-2800.

2- Akoussah, K. E., Fafard, M., Talbot, M., and Beaulieu, D. 1997. **Parametric study of dynamic load amplification factor for simply-supported reinforced concrete bridges**, in French. Canadian Journal of Civil Engineering, 24(2): 313-322.

3- Al-Rifaie, W. N., and Evans, H. R. 1979. **An approximate method for the analysis of box girder bridges that are curved in plan**. Proceedings of International Association of Bridges and Structural Engineering, IABSE, 1-21.

4- American Association of State Highway and Transportation Officials, AASHTO. 1980 and 1993. **Guide specifications for horizontally curved highway bridges**. Washington, D.C.

5- American Association of State Highway and Transportation Officials, AASHTO. 1996. **Standard specifications for highway bridges**. Washington, D.C.

6- Bazant, Z. P., and El Nimeiri, M. 1974. **Stiffness method for curved box girders**. ASCE Journal of the Structural Division, 100(ST10): 2071-2090.

7- Billing, J. R. 1984. **Dynamic loading and testing of bridges in Ontario**. Canadian Journal of Civil Engineering, 11(4): 833-843.

8- Bradford, M. A., and Wong, T. C. 1992. **Local buckling of composite box girders under negative bending**. The Structural Engineer, 70(21): 377-380.

9- Canadian Standard Association. 1988. **Design of highway bridges (CAN/CSA-S6-88)**. Rexdale, Ontario, Canada.

10- Chang, P. C., Heins, C. P., Guohao, L., and Ding, S. 1985. **Seismic study of curved**

bridges using the Rayleigh-Ritz method. Computers & Structures, 21(6): 1095-1104.

11- Chang, D. and Lee, H. 1994. **Impact Factors for Simple-span Highway Girder Bridges**. Journal of Structural Engineering, 120(1): 704-715.

12- Chan, M. Y. T., Cheung, M. S., Beauchamp, J. C., and Hachem, H. M. 1990. **Thermal stresses in composite box-girder bridges**. Proceeding of the 3rd International Conference on Short and Medium Span Bridges, Toronto, Ontario, Canada, 2: 355-366.

13- Chapman, J. C., Dowling, P. J., Lim, P. T. K., and Billington, C. J. 1971. **The structural behaviour of steel and concrete box girder bridges**. The Structural Engineer, 49(3): 111-120.

14- Cheung, M. S. 1984. **Analysis of continuous curved box-girder bridges by the finite strip method**, In Japanese. Japanese Society of Civil Engineers, 1-10.

15- Cheung, M. S., and Chan, M. Y. T. 1978. **Finite strip evaluation of effective flange width of bridge girders**. Canadian Journal of Civil Engineering, 5(2): 174-185.

16- Cheung, M. S., and Cheung, Y. K. 1971. **Analysis of curved box girder bridges by the finite-strip method**. International Association of Bridges and Structural Engineering, IABSE, 31(I): 1-8.

17- Cheung, M. S., and Megnounif, A. 1991. **Parametric study of design variations on the vibration modes of box girder bridges**. Canadian Journal of Civil Engineering, 18(5): 789-798.

18- Cheung, Y. K., and Cheung, M. S. 1972. **Free vibration of curved and straight beam-slab or box-girder bridges**. International Association of Bridges and Structural Engineering, 32(2): 41-52.

19- Chu, K., and Pinjarkar, S. G. 1971. **Analysis of horizontally curved box girder bridges**. ASCE Journal of the Structural Division, 97(ST10): 2481-2501.

20- Culver, C. G. 1967. **Natural frequencies of horizontally curved beams.** ASCE Journal of the Structural Division, 93(ST2): 189-203.

21- Dabrowski, R. 1968. **Curved thin-walled girders, Theory and analysis.** Springer, New York.

22- Dilger, W. H., Ghoneim, G. A., and Tadros, G. S. 1988. **Diaphragms in skew box girder bridges.** Canadian Journal of Civil Engineering, 15(5): 869-878.

23- Elbadry, M. M., and Ibrahim, A. M. 1996. **Temperature distributions in curved concrete box-girder bridges.** 1st Structural Specialty Conference, Canadian Society of Civil Engineering, Edmonton, Alberta, Canada, 1-12.

24- Evans, H. R. 1982. **Simplified methods for the analysis and design of bridges of cellular cross-section.** Proceedings of the NATO Advanced Study Institute on Analysis and Design of Bridges,Cesme, Izmir, Turkey, 95-115.

25- Evans, H. R., and Shanmugam, N. E. 1984. **Simplified analysis for cellular structures.** ASCE Journal of the Structural Division. 110(ST3): 531-543.

26- Fam, A. R. M. 1973. **Static and free-vibration analysis of curved box bridges.** Structural Dynamic Series No. 73-2, Department of Civil Engineering and Applied Mechanics, McGill University, Montreal, Quebec, Canada.

27- Fam, A. R., and Turkstra, C. J. 1975. **A finite element scheme for box bridge analysis.** Computers and Structures Journal, Pergamon Press, 5: 179-186.

28- Fam, A. R., and Turkstra, C. J. 1976. **Model study of horizontally curved box girder.** ASCE Journal of the Structural Division, 102(ST5): 1097-1108.

29- Fu, C. C., and Hsu, Y. T. 1995. **The development of an improved curvilinear thin-walled Vlasov element.** Computers and Structures Journal, Pergamon Press, 54(1): 147-159.

30- Galdos, N. H. 1988. **A theoretical investigation of the dynamic behaviour of horizontally curved steel box girder bridges under truck loadings.** Thesis presented to the University of Maryland at Collage Park, Md., in partial fulfilment of the requirement for the degree of Doctor of Philosophy.

31- Galdos, N. H., Schelling, D. R., and Sahin, M. A. 1990. **Methodology for impact factor of horizontally curved box bridges.** A SCE Journal of Structural Engineering, 119(6): 1917-1934.

32- Galuta, E. M., and Cheung, M. S. 1995. **Combined boundary element and finite element analysis of composite box girder bridges.** Computers and Structures Journal, Pergamon Press, 57(3): 427-437.

33- Hambly, E. C., and Pennells, E. 1975. **Grillage analysis applied to cellular bridge decks.** The Structural Engineer, 53(7): 267-275.

34- Hasebe, K., Usuki, S., and Horie, Y. 1985. **Shear lag analysis and effective width of curved girder bridges.** ASCE Journal of Engineering Mechanics, 111(1): 87-92.

35- Heins, C. P. 1978. **Box girder bridge design-State-of-the-Art.** A ISC Engineering Journal, 2: 126-142.

36- Heins, C. P., and Lee, W. H. 1981. **Curved box-girder bridge: field test.** ASCE Journal of the Structural Division, 107(ST2): 317-327.

37- Heins, C. P., and Oleinik, J. C. 1976. **Curved box beam bridge analysis.** Computers and Structures Journal, Pergamon Press, London, 6(2): 65-73.

38- Heins, C. P., and Sahin, M. A. 1979. **Natural frequency of curved box girder bridges.** ASCE Journal of the Structural Division, 105(ST12): 2591-2600.

39- Heins, C. P., and Sheu, F. H. 1982. **Design/analysis of curved box girder bridges.** Computers and Structures Journal, 15(3): 241-258.

40- Hibbitt, H. D., Karlson, B. I., and Sorenson, E. P. 1996. **ABAQUS version 5.6, finite** element program. Hibbitt, Karlson & Sorenson, Inc, Providence, R. I.

41- Hilber, H. M., Hughes, T. J. R., and Taylor, R. L. 1978 **Collocation, Dissipation and "Overshoot" for Time Integration Schemes in Structural Dynamics.** Earthquake Engineering and Structural Dynamics, vol. 6: 99-117.

42- Huang, D., Wang, T., and Shahawy, M. 1995. **Dynamic behaviour of horizontally curved I-girder bridges.** Computers & Structures Journal, 57(4): 703-714.

43- Huang, D., Wang, T., and Shahaway, M. 1995. **Vibration of thin-walled box-girder bridges exited by vehicles.** ASCE Journal of Structural Engineering, 121(9): 1330-1337.

44- Humar, J. L. 1990. **Dynamic of structures.** Prentice-Hall Inc.

45- Inbanathan, M. J., and Wieland, M. 1987. **Bridge vibration due to vehicle moving over rough surface.** ASCE Journal of Structural Engineering, 113(9): 1994-2008.

46- Ishac, I. I., and Smith, T. R. G. 1985. **Approximations for moments in box girders.** ASCE Journal of Structural Engineering, 111(11): 2333-2342.

47- Johanston, S. B., and Mattock, A. H. 1967. **Lateral distribution of loads in composite box girder bridges.** Highway Research Record, Highway Research Board, 167: 25-33.

48- Kabir, A. F. and Scordelis, A. C. 1974. **Computer programs for curved bridges on flexible bents.** Structural Engineering and Structural Mechanics Report No. UC/SESM 74-10, University of California, Berkeley, CA.

49- Kano, T., Usuke, S., and Hasebe, K. 1982. **Theory of thin-walled curved members with shear deformation.** Ingenieur-Archiv, 51.

50- Kashif, A. M. 1992. **Dynamic response of highway bridges to moving vehicles.** Ph.D. Dissertation, Department of Civil Engineering, Carleton University, Ottawa, Canada.

51- Kashif, A. M., and Humar, J. L. 1990. **Analysis of the dynamic characteristics of box**

girder bridges. Proceedings of the Third International Conference on Short and Medium Span Bridges, Toronto, Ontario, 2: 367-378.

52- Komatsu, S., and Nakai, H. 1966. **Study on free vibrations of curved girder bridges.** Transactions, Japan Society of Civil Engineers, Tokyo, Japan, (136): 35-60.

53- Komatsu, S., and Nakai, H. 1970. **Fundamental study on forced vibration of curved girder bridges.** Transactions, Japan Society of Civil Engineers, Tokyo, Japan, 2(I): 37-42.

54- Li, H. G. 1992. **Thin-walled box beam finite elements for static analysis of curved haunched and skew multi-cell box girder bridges**. Ph.D. Thesis, Department of Civil Engineering, Carleton University, Ottawa, Ontario, Canada.

55- Li. W. Y., Tham, L. G., and Cheung, Y. K. 1988. **Curved box-girder bridges**. Journal of Structural Engineering, American Society of Civil Engineers, 114(6): 1324-1338.

56- Maisel, B. I. 1985. **Analysis of concrete box beams using small computer capacity**. Canadian Journal of Civil Engineering, 12(2): 265-278.

57- Malcolm, D. J., and Redwood, R. G. 1970. **Shear lag in stiffened box girders**. ASCE Journal of the Structural Division, 96(ST7): 1403-1419.

58- Mavaddat, S., and Mirza, M. S. 1989. **Computer analysis of thin walled concrete box beams**. Canadian Journal of Civil Engineering, 16(6): 902-909.

59- Meyer, C. and Scordelis, A. C. 1971. **Analysis of curved folded plate structures**. ASCE Journal of the Structural Division, 97(ST10): 2459-2480.

60- Mikkola, M., and Paavola, J. 1980. **Finite element analysis of box girders**. ASCE Journal of the structural Division, 106(ST6): 1343-1357.

61- Ministry of Transportation and Communications. 1985. **Geometric design standards for Ontario highways**. Downsview, Ontario, Canada.

62- Moffatt, K. R., and Dowling, P. J. 1975. **Shear lag in steel box girder bridges**. The

Structural Engineer, 53(10): 439-448.

63- Nakai, H., and Heins, C. P. 1977. **Analysis criteria for curved bridges.** ASCE Journal of Structural Division, 103(ST7):1419-1427.

63a- Newmark, N.M. 1959. **A method of computation for structural dynamics.** Proceeding of ASCE, Vol. 85, EM3: 67-94.

64- Oleinik, J. C., and Heins, C. P. 1975. **Diaphragms for curved box beam bridges.** ASCE Journal of the Structural Division, 101(ST10): 2161:2179.

65- Ontario Ministry of Transportation and Communications. 2000. **Canadian highway bridge design code, CHBDC.** Downsview, Ontario

66- Ontario Ministry of Transportation and Communications. 1983. **Ontario highway bridge design code, OHBDC.** Second edition, Downsview, Ontario.

67- Ontario Ministry of Transportation and Communications. 1992. **Ontario highway bridge design code, OHBDC.** Third edition, Downsview, Ontario

68- Rabizadeh, R. O., and Shore, S. 1975. **Dynamic analysis of curved box-girder bridges.** ASCE Journal of the Structural Division, 101(ST9): 1899-1912.

69- Razaqpur, A. G., and Li, H. G. 1997. **Analysis of curved multi-cell box girder assemblages.** Structural Engineering and Mechanics, 5(1): 33-49.

70- Razaqpur, A. G., and Li, H. G. 1990. **Analysis of multi-branch multi-cell box girder bridges.** Proceeding of the 3th International Conference on Short and Medium Span Bridges, Toronto, Ontario, Canada, 2: 153-164.

71- Razaqpur, A. G., and Li, H. G. 1994. **Refined analysis of curved thin-walled multi-cell box girders.** Computers and Structures Journal , Pergamon Press, 53(1): 131-142.

72- Richardson, J. A., and Douglas, B. N. 1993. **Results from field testing a curved box girder bridge using simulated earthquake loads.** Earthquake Engineering & Structural

Dynamics, 22(10): 905-922.

73- Sargious, M. A., Dilger, W. H., and Hawk, H. 1979. **Box girder diaphragms with openings.** ASCE Journal of the Structural Division, 105(ST1): 53-65.

74- Schelling, D. R., Galdos, N. H., and Sahin, M. A. 1992. **Evaluation of impact factors for horizontally curved steel box bridges.** ASCE Journal of Structural Engineering ,118(11): 3203-3221.

75- Scordelis, A. C., Chan, E. C., and Ketchum, M. A. 1985. **Computer program for prestressed concrete box girder bridges.** Report No. UCB/SESM 85/02, University of California, Berkeley, CA.

76- Sennah, K. M. 1998. **Load Distribution and Dynamic Characteristics of Curved Composite Concrete Deck-steel Cellular Bridges.** Ph.D. Dissertation, Civil and Environmental Engineering Program, University of Windsor, Windsor, Ontario, Canada.

77- Senthilvasan, J., Brameld, G. H., and Thambiratnam, D. P. 1997. **Bridge-vehicle interaction in curved box girder bridges.** Microcomputers in Civil Engineering, 12(3): 171-181.

78- Shore, S., and Chaudhuri, S. 1972. **Free-vibration of horizontally curved beams.** ASCE Journal of the Structural Division, 98(ST3): 793-796.

79- Sisodiya, R. G., Cheung, Y. K., and Ghali, A. 1970. **Finite-element analysis of skew, curved box girder bridges.** International Association of Bridges and Structural Engineering, IABSE, 30(II): 191-199.

80- Tabba, M. M. 1972. **Free-vibration of curved box girder bridges.** M.Eng. thesis, Department of Civil Engineering and Applied Mechanics, McGill University, Montreal, Quebec, Canada.

81- Tan, C. P., and Shore, S. 1968-a. **Dynamic response of a horizontally curved bridge.**

ASCE Journal of the Structural Division, 94(ST3): 761-781.

82- Tan, C. P., and Shore, S. 1968-b. **Response of horizontally curved bridge to moving load.** ASCE Journal of the Structural Division, 94(ST9): 2135-2151.

83- Tesar, A. 1996. **Shear lag in the behaviour of thin-walled box bridges.** Computers & Structures Journal, 59(4): 607-612.

84- Trukstra, C. J., and Fam, A. R. 1978. **Behaviour study of curved box bridges.** ASCE Journal of the Structural Division, 104(ST3): 453-462.

85- Usuki, T. 1987. **The theory of curved multi-cell box girder bridges under consideration of cross-sectional distortion.** Structural Engineering/Earthquake Engineering, 4(2): 277-287.

86- Van Zyl, S. 1978. **Analysis of curved segmentally erected prestressed concrete box girder bridges.** Structural Engineering and Structural Mechanics, Report No. UC/SESM 78-2, University of California, Berkeley, CA.

87- Vlasov, V. Z. 1965. **Thin-walled elastic beams.** OTS61-11400, National Science Foundation, Washington, D. C.

88- Waldron, P. 1988. **The significance of warping torsion in the design of straight concrete box-girder bridges.** Canadian Journal of Civil Engineering, 15(5): 879-889.

89 -Wang, T., Huang, D., and Shahawy, M. 1996. **Dynamic behaviour of continuous and cantilever thin-walled box girder bridges.** ASCE Journal of Bridge Engineering, 1(2): 67-75.

90- Williams, R. O. M., Cassell, A. C., and Boswell, L. F. 1992. **A computer design aid for prestressed box beams.** Proceedings of the Institute of Civil Engineering Structures & Bridges, 94: 61-72.

91- Willam, K. J., and Scordelis, A. C. 1972. **Cellular structures of arbitrary plan**

geometry. ASCE Journal of the Structural Division, 98(ST7): 1377-1394.

92- Zhang, S. H., and Lyons, L. P. R. 1984. **Thin-walled box beam finite element for curved bridge analysis**. Computers and Structures Journal, 18(6): 1035-1046.

93- Zienkiewicz, O. C. 1977. **The finite-element method**. McGraw-Hill Book Company, Third Edition.

Table 3.1. Material properties for concrete and steel

Material properties	Concrete	Steel
Modulus of elasticity, E (MPa)	27,000	200,000
Poisson's ratio, ν	0.20	0.30
Density, ρ (kg/m^3)	2400	7800

Table 3.2.1. Geometry of bridge prototypes of 20 m span

Span m	No. of lanes	No. of cells	Cross-sectional dimensions, mm								
			A	B	C	D	F	t_1	t_2	t_3	t_4
20	1	1	6800	3400	300	800	1025	24	15	13	225
20	1	2	6800	2267	300	800	1025	16	10	10	225
20	1	3	6800	1700	300	800	1025	12	8	9	225
20	1	4	6800	1360	300	800	1025	10	8	8	225
20	2	1	9300	4650	300	800	1025	32	20	15	225
20	2	2	9300	3100	300	800	1025	21	13	11	225
20	2	3	9300	2325	300	800	1025	16	10	10	225
20	2	4	9300	1860	300	800	1025	13	8	10	225
20	2	5	9300	1550	300	800	1025	11	8	9	225
20	2	6	9300	1328	300	800	1025	10	8	8	225
20	2	7	9300	1162	300	800	1025	10	8	8	225
20	3	3	13050	3262	300	800	1025	24	15	11	225
20	3	4	13050	2610	300	800	1025	20	12	10	225
20	3	5	13050	2175	300	800	1025	16	10	10	225
20	3	6	13050	1864	300	800	1025	14	9	10	225
20	3	7	13050	1631	300	800	1025	12	8	9	225
20	3	8	13050	1450	300	800	1025	10	8	9	225
20	3	9	13050	1305	300	800	1025	10	8	9	225
20	4	4	16800	3360	300	800	1025	26	16	11	225
20	4	5	16800	2800	300	800	1025	21	14	10	225
20	4	6	16800	2400	300	800	1025	18	12	10	225
20	4	7	16800	2100	300	800	1025	16	10	10	225
20	4	8	16800	1867	300	800	1025	14	10	10	225
20	4	9	16800	1680	300	800	1025	13	10	10	225

Note: Symbols A, B, C, D, F, t_1, t_2, t_3, t_4 are explained in Fig. 3.5.

Table 3.2.2. Geometry of bridge prototypes of 40 m span

Span m	No. of lanes	No. of cells	Cross-sectional dimensions, mm								
			A	B	C	D	F	t_1	t_2	t_3	t_4
40	1	1	6800	3400	375	1600	1825	42	21	16	225
40	1	2	6800	2267	375	1600	1825	28	14	12	225
40	1	3	6800	1700	375	1600	1825	21	10	11	225
40	1	4	6800	1360	375	1600	1825	17	8	10	225
40	2	1	9300	4650	375	1600	1825	56	28	18	225
40	2	2	9300	3100	375	1600	1825	37	19	14	225
40	2	3	9300	2325	375	1600	1825	28	14	12	225
40	2	4	9300	1860	375	1600	1825	22	12	11	225
40	2	5	9300	1550	375	1600	1825	19	10	11	225
40	2	6	9300	1328	375	1600	1825	16	8	11	225
40	2	7	9300	1162	375	1600	1825	14	8	10	225
40	3	3	13050	3262	375	1600	1825	42	20	14	225
40	3	4	13050	2610	375	1600	1825	34	17	13	225
40	3	5	13050	2175	375	1600	1825	28	14	12	225
40	3	6	13050	1864	375	1600	1825	24	12	12	225
40	3	7	13050	1631	375	1600	1825	21	11	11	225
40	3	8	13050	1450	375	1600	1825	19	10	11	225
40	3	9	13050	1305	375	1600	1825	17	10	10	225
40	4	4	16800	3360	375	1600	1825	45	22	13	225
40	4	5	16800	2800	375	1600	1825	37	19	13	225
40	4	6	16800	2400	375	1600	1825	32	16	12	225
40	4	7	16800	2100	375	1600	1825	28	14	12	225
40	4	8	16800	1867	375	1600	1825	25	13	12	225
40	4	9	16800	1680	375	1600	1825	22	11	12	225

Note: Symbols A, B, C, D, F, t_1, t_2, t_3, t_4 are explained in Fig. 3.5.

Table 3.2.3. Geometry of bridge prototypes of 60 m span

Span m	No. of lanes	No. of cells	Cross-sectional dimensions, mm								
			A	B	C	D	F	t_1	t_2	t_3	t_4
60	1	1	6800	3400	450	2400	2625	60	27	20	225
60	1	2	6800	2267	450	2400	2625	40	18	15	225
60	1	3	6800	1700	450	2400	2625	30	14	13	225
60	1	4	6800	1360	450	2400	2625	24	11	12	225
60	2	1	9300	4650	450	2400	2625	80	36	23	225
60	2	2	9300	3100	450	2400	2625	53	24	17	225
60	2	3	9300	2325	450	2400	2625	40	18	15	225
60	2	4	9300	1860	450	2400	2625	32	15	14	225
60	2	5	9300	1550	450	2400	2625	27	12	13	225
60	2	6	9300	1328	450	2400	2625	23	10	13	225
60	2	7	9300	1162	450	2400	2625	20	10	12	225
60	3	3	13050	3262	450	2400	2625	60	27	17	225
60	3	4	13050	2610	450	2400	2625	48	22	16	225
60	3	5	13050	2175	450	2400	2625	40	18	15	225
60	3	6	13050	1864	450	2400	2625	34	16	15	225
60	3	7	13050	1631	450	2400	2625	30	14	14	225
60	3	8	13050	1450	450	2400	2625	27	12	14	225
60	3	9	13050	1305	450	2400	2625	24	10	14	225
60	4	4	16800	3360	450	2400	2625	64	29	16	225
60	4	5	16800	2800	450	2400	2625	53	24	16	225
60	4	6	16800	2400	450	2400	2625	46	21	15	225
60	4	7	16800	2100	450	2400	2625	40	18	15	225
60	4	8	16800	1867	450	2400	2625	35	16	15	225
60	4	9	16800	1680	450	2400	2625	32	14	15	225

Note: Symbols A, B, C, D, F, t_1, t_2, t_3, t_4 are explained in Fig. 3.5.

Table 3.2.4. Geometry of bridge prototypes of 80 m span

Span m	No. of lanes	No. of cells	Cross-sectional dimensions, mm								
			A	B	C	D	F	t_1	t_2	t_3	t_4
80	1	1	6800	3400	530	3200	3425	78	33	23	225
80	1	2	6800	2267	530	3200	3425	52	22	17	225
80	1	3	6800	1700	530	3200	3425	39	17	15	225
80	1	4	6800	1360	530	3200	3425	31	13	14	225
80	2	1	9300	4650	530	3200	3425	104	44	24	225
80	2	2	9300	3100	530	3200	3425	70	29	19	225
80	2	3	9300	2325	530	3200	3425	52	22	17	225
80	2	4	9300	1860	530	3200	3425	42	18	16	225
80	2	5	9300	1550	530	3200	3425	35	15	15	225
80	2	6	9300	1328	530	3200	3425	30	13	15	225
80	2	7	9300	1162	530	3200	3425	26	11	14	225
80	3	3	13050	3262	530	3200	3425	78	33	19	225
80	3	4	13050	2610	530	3200	3425	62	26	18	225
80	3	5	13050	2175	530	3200	3425	52	22	17	225
80	3	6	13050	1864	530	3200	3425	45	19	17	225
80	3	7	13050	1631	530	3200	3425	40	17	16	225
80	3	8	13050	1450	530	3200	3425	35	15	16	225
80	3	9	13050	1305	530	3200	3425	31	13	16	225
80	4	4	16800	3360	530	3200	3425	83	35	19	225
80	4	5	16800	2800	530	3200	3425	69	29	18	225
80	4	6	16800	2400	530	3200	3425	59	25	17	225
80	4	7	16800	2100	530	3200	3425	52	22	17	225
80	4	8	16800	1867	530	3200	3425	46	20	17	225
80	4	9	16800	1680	530	3200	3425	42	18	16	225

Note: Symbols A, B, C, D, F, t_1, t_2, t_3, t_4 are explained in Fig. 3.5.

Table 3.2.5. Geometry of bridge prototypes of 100 m span

Span m	No. of lanes	No. of cells	Cross-sectional dimensions, mm								
			A	B	C	D	F	t_1	t_2	t_3	t_4
100	1	1	6800	3400	600	4000	4225	96	39	27	225
100	1	2	6800	2267	600	4000	4225	64	26	20	225
100	1	3	6800	1700	600	4000	4225	48	20	18	225
100	1	4	6800	1360	600	4000	4225	38	16	16	225
100	2	1	9300	4650	600	4000	4225	128	52	30	225
100	2	2	9300	3100	600	4000	4225	85	35	22	225
100	2	3	9300	2325	600	4000	4225	64	26	20	225
100	2	4	9300	1860	600	4000	4225	51	21	19	225
100	2	5	9300	1550	600	4000	4225	43	18	18	225
100	2	6	9300	1328	600	4000	4225	37	15	17	225
100	2	7	9300	1162	600	4000	4225	32	13	17	225
100	3	3	13050	3262	600	4000	4225	96	39	22	225
100	3	4	13050	2610	600	4000	4225	77	31	21	225
100	3	5	13050	2175	600	4000	4225	64	26	20	225
100	3	6	13050	1864	600	4000	4225	55	22	19	225
100	3	7	13050	1631	600	4000	4225	48	20	19	225
100	3	8	13050	1450	600	4000	4225	43	17	19	225
100	3	9	13050	1305	600	4000	4225	38	16	19	225
100	4	4	16800	3360	600	4000	4225	102	42	22	225
100	4	5	16800	2800	600	4000	4225	85	35	21	225
100	4	6	16800	2400	600	4000	4225	73	30	20	225
100	4	7	16800	2100	600	4000	4225	64	26	20	225
100	4	8	16800	1867	600	4000	4225	57	23	20	225
100	4	9	16800	1680	600	4000	4225	51	21	19	225

Note: Symbols A, B, C, D, F, t_1, t_2, t_3, t_4 are explained in Fig. 3.5.

Table 5.1. Extracted natural frequencies of *2l-2c-60* straight bridge

Mode No	Frequency Hz	Mode No	Frequency Hz	Mode No	Frequency Hz	Mode No	Frequency Hz	Mode No	Frequency Hz
1	1.71	41	12.43	81	21.00	121	24.13	161	28.00
2	4.52	42	12.53	82	21.11	122	24.17	162	28.09
3	6.18	43	12.84	83	21.11	123	24.27	163	28.17
4	8.34	44	12.89	84	21.13	124	24.28	164	28.22
5	8.69	45	13.17	85	21.24	125	24.46	165	28.34
6	8.73	46	13.38	86	21.30	126	24.51	166	28.46
7	8.78	47	13.53	87	21.33	127	24.57	167	28.58
8	8.82	48	13.54	88	21.39	128	24.67	168	28.69
9	8.86	49	13.95	89	21.41	129	24.77	169	28.74
10	8.92	50	13.95	90	21.48	130	24.81	170	28.81
11	8.92	51	14.29	91	21.58	131	24.85	171	28.96
12	9.59	52	14.41	92	21.68	132	24.88	172	28.97
13	9.67	53	14.91	93	21.73	133	25.13	173	29.04
14	9.79	54	15.10	94	21.86	134	25.15	174	29.21
15	9.80	55	15.34	95	22.05	135	25.20	175	29.27
16	9.96	56	15.43	96	22.18	136	25.32	176	29.46
17	9.96	57	15.77	97	22.19	137	25.35	177	29.46
18	10.14	58	15.98	98	22.32	138	25.43	178	29.54
19	10.35	59	16.50	99	22.42	139	25.52	179	29.60
20	10.36	60	16.62	100	22.47	140	25.53	180	29.69
21	10.48	61	17.11	101	22.55	141	25.75	181	29.75
22	10.55	62	17.28	102	22.65	142	25.98	182	29.94
23	10.58	63	17.30	103	22.73	143	26.05	183	29.96
24	10.61	64	18.04	104	22.74	144	26.16	184	30.19
25	10.63	65	18.12	105	22.78	145	26.22	185	30.21
26	10.65	66	18.83	106	22.80	146	26.27	186	30.26
27	10.66	67	18.85	107	22.94	147	26.37	187	30.30
28	10.85	68	19.02	108	22.95	148	26.48	188	30.40
29	11.00	69	19.55	109	23.12	149	26.60	189	30.46
30	11.10	70	19.69	110	23.15	150	26.69	190	30.56
31	11.22	71	19.76	111	23.18	151	26.82	191	30.57
32	11.37	72	19.89	112	23.23	152	26.90	192	30.66
33	11.37	73	19.96	113	23.29	153	26.91	193	30.75
34	11.41	74	19.99	114	23.35	154	27.14	194	30.89
35	11.56	75	20.00	115	23.36	155	27.35	195	30.95
36	11.66	76	20.53	116	23.40	156	27.38	196	31.03
37	11.79	77	20.76	117	23.41	157	27.38	197	31.08
38	12.00	78	20.83	118	23.67	158	27.63	198	31.40
39	12.03	79	20.90	119	23.78	159	27.82	199	31.51
40	12.11	80	20.99	120	24.05	160	27.93	200	31.55

Table 5.2. Effective mass percentage to the total mass (%) of *2l-2c-60* straight bridge

Number of modes	X-Direction	Percentage	Y-Direction	Percentage	Z-Direction	Percentage
10	5.68E+04	11.8	3.85E+05	79.7	3.81E+05	78.8
20	1.95E+05	40.2	3.85E+05	79.7	3.88E+05	80.3
30	3.06E+05	63.3	3.85E+05	79.7	3.93E+05	81.4
50	4.24E+05	87.7	3.86E+05	79.8	3.95E+05	81.6
100	4.61E+05	95.4	4.15E+05	85.8	4.31E+05	89.2
200	4.67E+05	96.5	4.50E+05	93.1	4.40E+05	90.9

Table 6.1. Comparison of fundamental frequency between proposed method and Sennah's method

Span,m	lanes	cells	L/R	Sennah	Proposed	L/R	Sennah	Proposed	L/R	Sennah	Proposed
20	1	1	0	0.60	0.85	0.4	0.49	0.81	1	0.36	0.69
20	1	2	0	0.70	0.85	0.4	0.62	0.81	1	0.47	0.69
20	1	3	0	0.93	0.85	0.4	0.87	0.81	1	0.73	0.69
20	2	1	0	0.55	0.85	0.4	0.46	0.81	1	0.34	0.69
20	2	2	0	0.61	0.85	0.4	0.54	0.81	1	0.41	0.69
20	2	3	0	0.61	0.85	0.4	0.54	0.81	1	0.41	0.69
20	3	4	0	0.61	0.85	0.4	0.54	0.81	1	0.41	0.69
20	4	4	0	0.61	0.85	0.4	0.54	0.81	1	0.41	0.60
40	1	1	0	0.79	0.90	0.4	0.65	0.86	1	0.48	0.73
40	1	2	0	0.87	0.90	0.4	0.78	0.86	1	0.59	0.73
40	1	3	0	0.96	0.90	0.4	0.90	0.86	1	0.76	0.73
40	2	1	0	0.73	0.90	0.4	0.61	0.86	1	0.45	0.73
40	2	2	0	0.76	0.90	0.4	0.68	0.86	1	0.52	0.73
40	2	3	0	0.76	0.90	0.4	0.68	0.86	1	0.52	0.73
40	3	4	0	0.76	0.90	0.4	0.68	0.86	1	0.52	0.73
40	4	4	0	0.76	0.90	0.4	0.68	0.86	1	0.52	0.73

Note: The values in this Table are the correction factors to the Equation (6.1) from the beam theory.

Table 7.1. Dynamic and static responses of outer girder of *2l-2c-40* straight and curved bridges subjected to different loading cases

Straight bridge

Response	Normal stress	Reaction	Deflection	Loading case
Dynamic	4.51E+05	2.33E+05	-1.03E-02	Partially loaded
Static	4.34E+05	2.30E+05	-9.97E-03	
Impact factor	0.037	0.013	0.035	
Dynamic	8.52E+05	1.62E+05	-1.91E-02	Fully loaded
Static	8.23E+05	1.56E+05	-1.84E-02	
Impact factor	0.035	0.038	0.036	
Dynamic	8.64E+05	1.53E+05	-1.95E-02	Two truck from
Static	8.19E+05	1.05E+05	-1.83E-02	opposite directions
Impact factor	0.055	0.455	0.064	

Curved bridge (L/R = 0.4)

Response	Normal stress	Reaction	Deflection	Loading case
Dynamic	4.02E+05	7.07E+04	-9.53E-03	Partially inner
Static	3.78E+05	3.38E+04	-9.16E-03	
Impact factor	0.063	1.092	0.041	
Dynamic	4.78E+05	3.14E+05	-1.23E-02	Partially outer
Static	4.49E+05	2.49E+05	-1.17E-02	
Impact factor	0.065	0.258	0.050	
Dynamic	8.83E+05	3.20E+05	-2.17E-02	Fully loaded
Static	8.30E+05	2.08E+05	-2.07E-02	
Impact factor	0.064	0.541	0.045	
Dynamic	8.83E+05	2.79E+05	-2.17E-02	Two truck from
Static	8.30E+05	2.06E+05	-2.07E-02	opposite directions
Impact factor	0.064	0.353	0.049	

a) Types of single-cell box girders

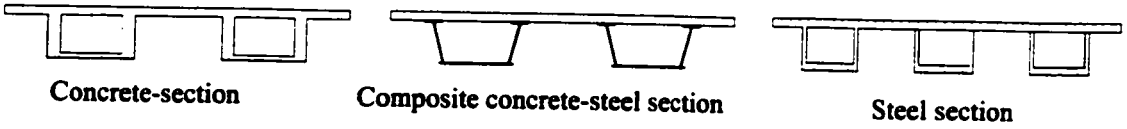

b)Types of multiple-spine (multi-box) box girders

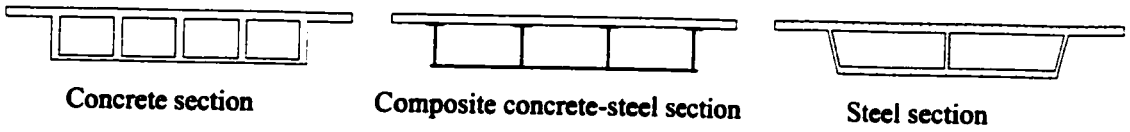

c) Types of multi-cell (cellular) box girders

Fig. 1.1. Box girder cross-sections

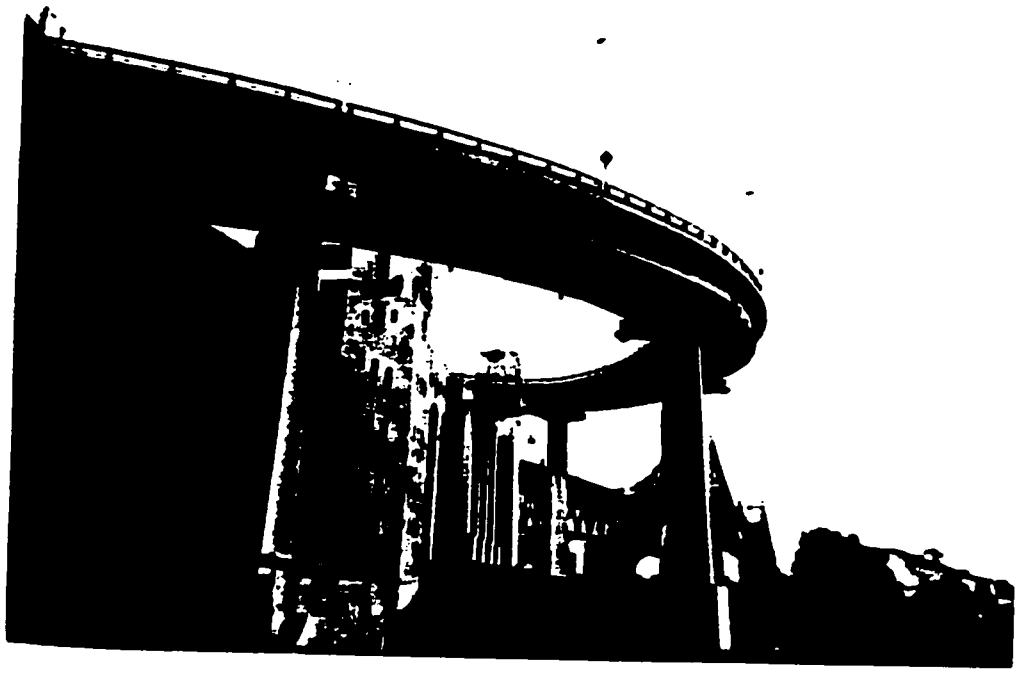

Fig. 1.2. Jacques Cartier I-girder bridge in Montreal, Quebec

Fig. 1.3. Box girder bridge in downtown Toronto

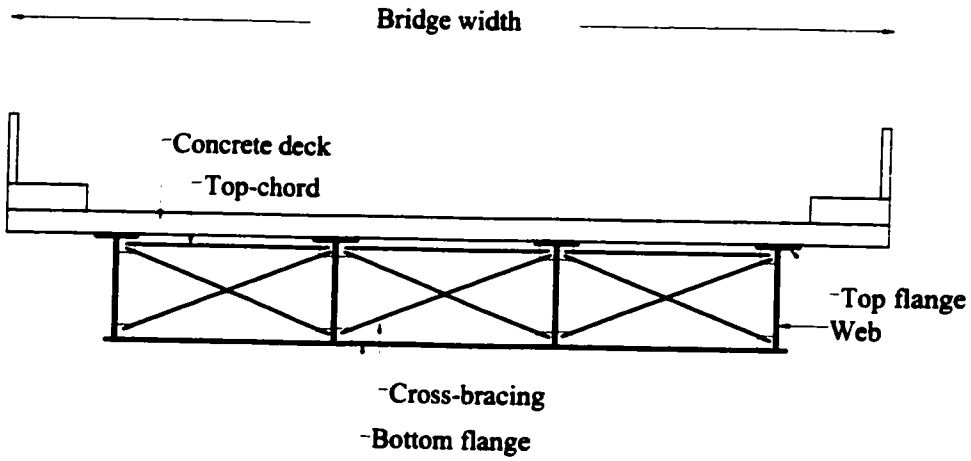

Fig. 1.4. Three-cell bridge cross-section

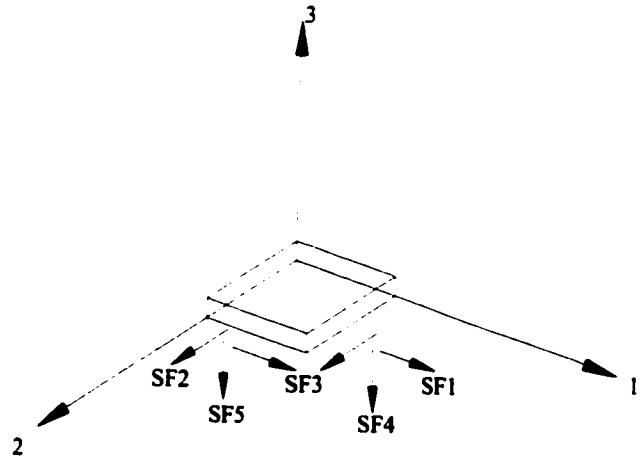

(a) Output forces

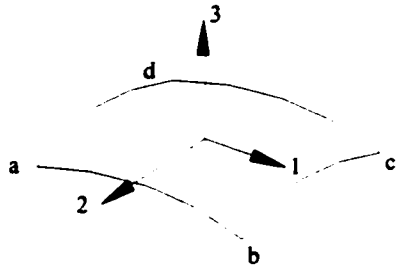

(c) Shell element "S4R"
(in ABAQUS)

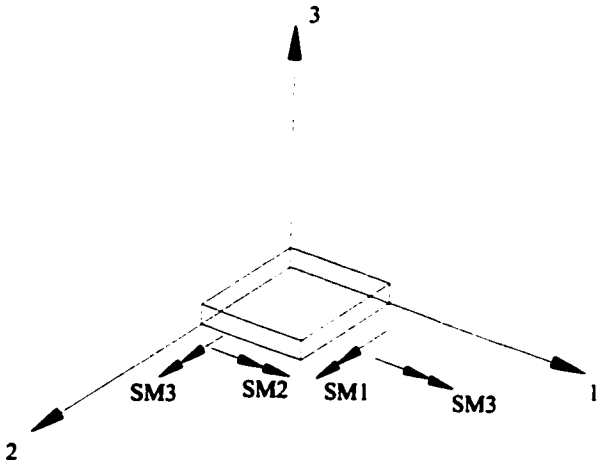

(b) Output moments

- Four-node element
- Degrees of freedom : U1, U2, U3, Φ1, Φ2, Φ3
- Output forces : SF1, SF2, SF3, SF4, SF5
- Output moments : SM1, SM2, SM3
- Stress components : S11, S22, S12

Fig. 3.1. Shell element "S4R" used for plate modelling

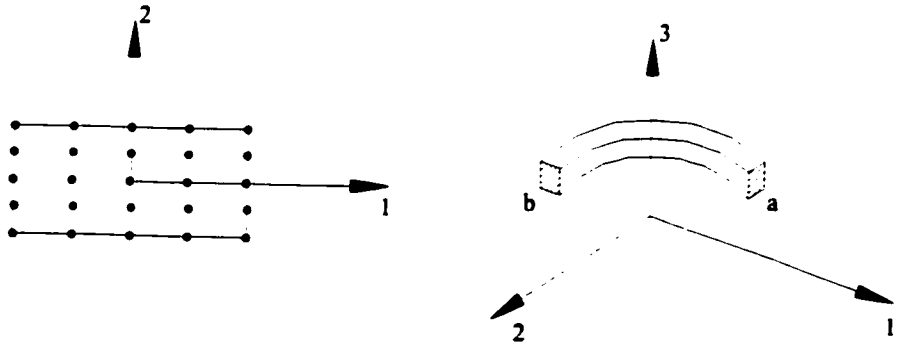

(b) Integration points of beam in space (for output results)

(b) Element B31H in ABAQUS

- Two-node element
- Degrees of freedom : U1, U2, U3, Φ1, Φ2, Φ3
- Output forces : SF1, SF2, SF3
- Output moments : SM1, SM2, SM3
- Stress components : S11, S12

Fig. 3.2. Beam element "B31H" for beam in space

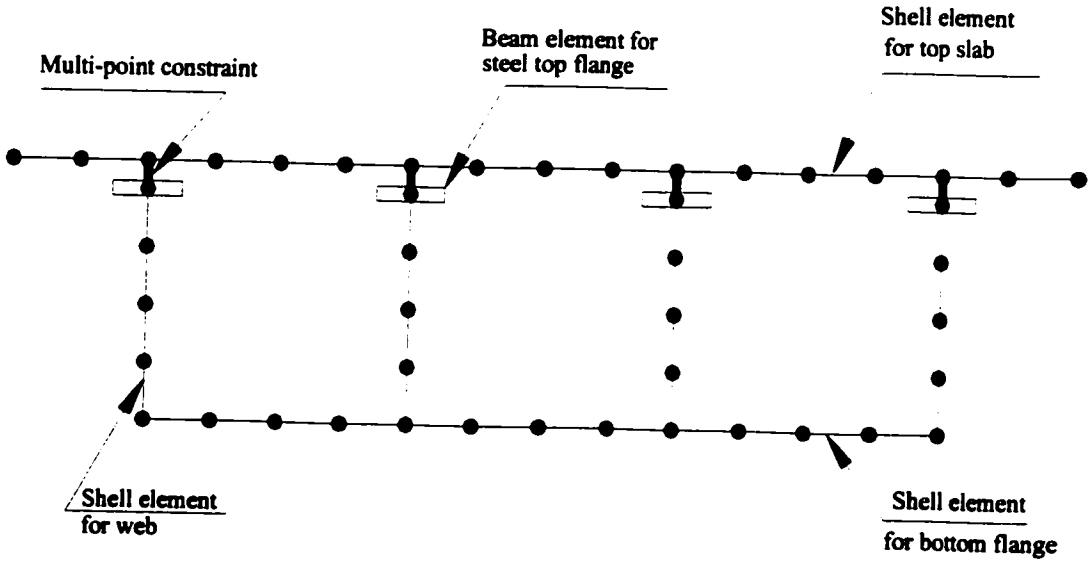

Fig. 3.3. Finite-element discretization of cross-section of the bridge

(a) Finite-element mesh of 2l-2c-40 straight bridge

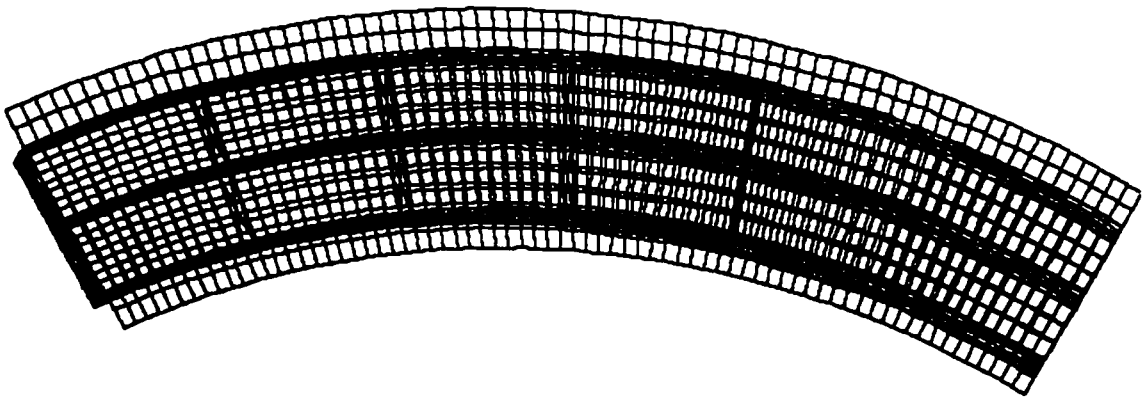

(b) Finite-element mesh of 2l-2c-40 curved bridge with L/R = 1.0

Fig. 3.4. Typical finite-element meshes for bridges

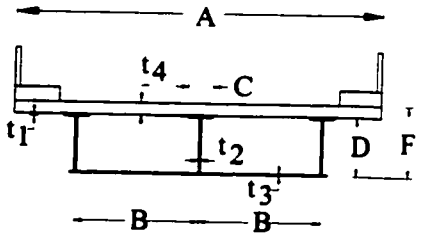

(a) One-lane two-cell cross-section

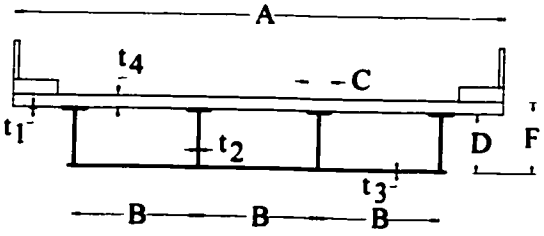

(b) Two-lane three-cell cross-section

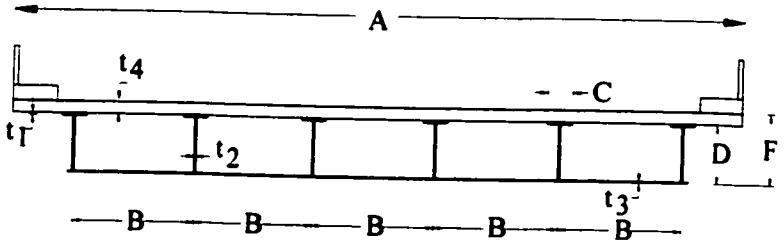

(c) Three-lane five-cell cross-section

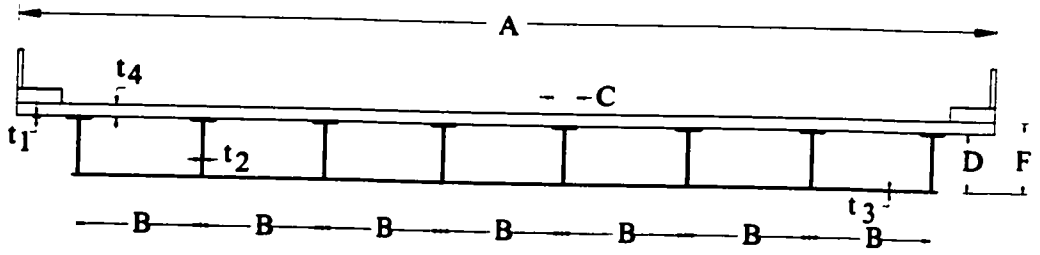

(d) Four-lane seven-cell cross-section

Fig. 3.5. Basic cross-section configurations and symbols

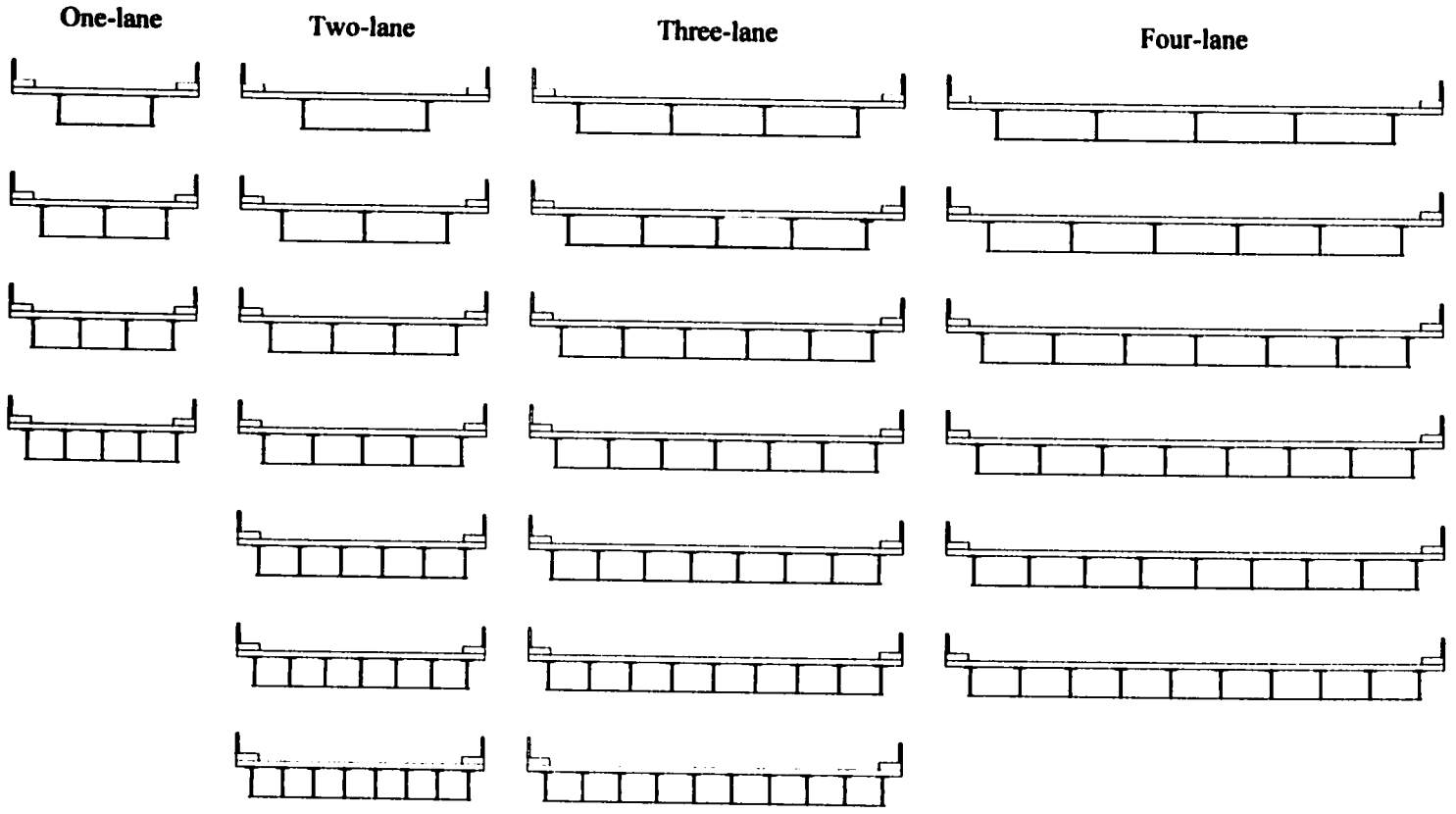

Fig. 3.6. Cross-section configurations used in the parametric studies

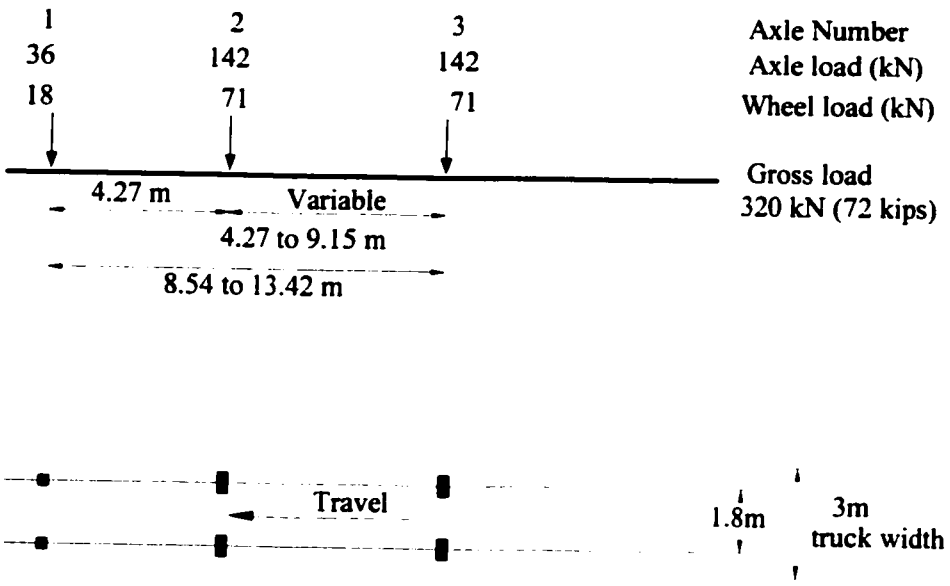

Fig. 4.1. Truck loading configuration according to AASHTO specifications (HS20-44 AASHTO loading truck)

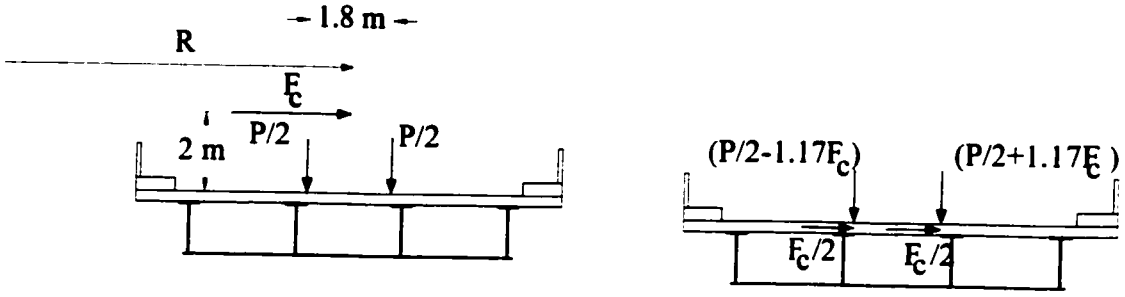

a) Moving load and the centrifugal force b) Static equivalent of the moving force

Fig. 4.2. Moving load idealization

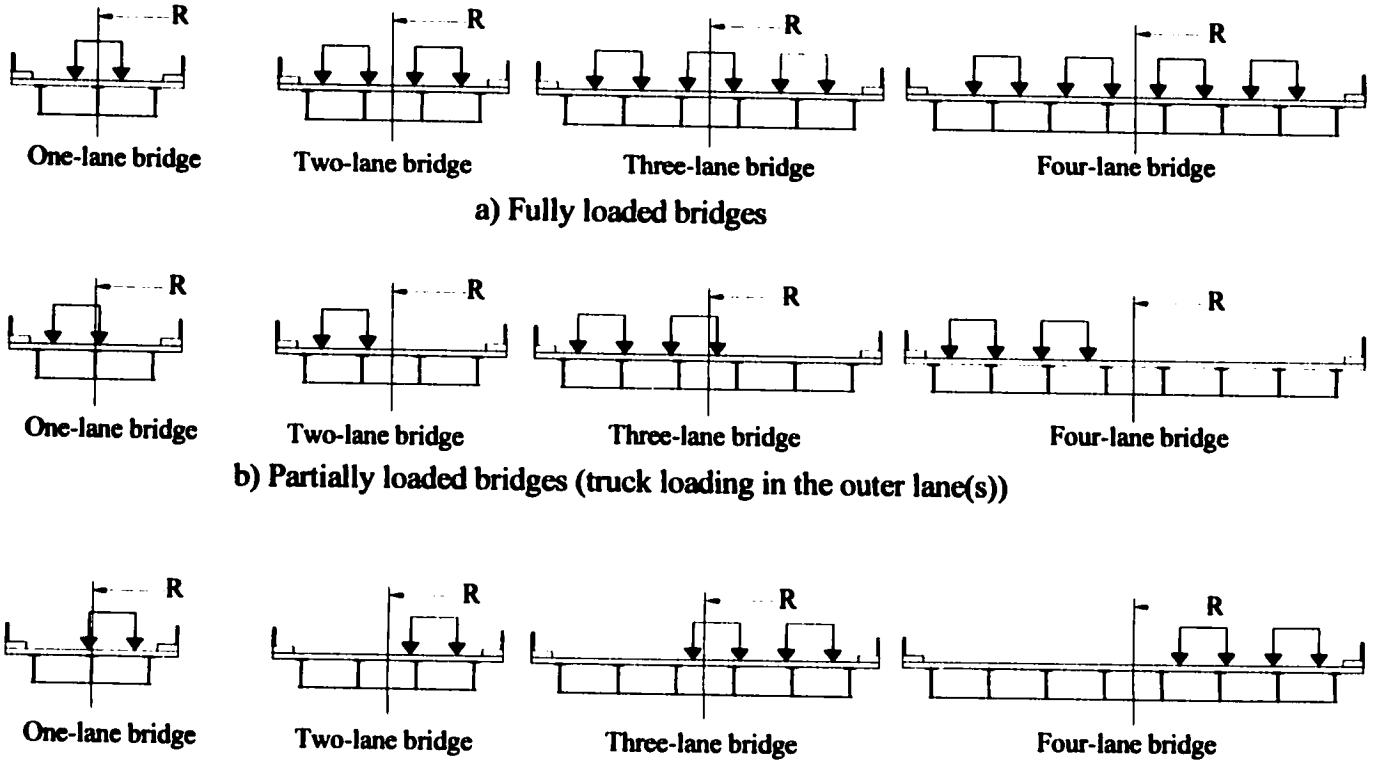

Fig. 4.3. Loading cases considered in the parametric study

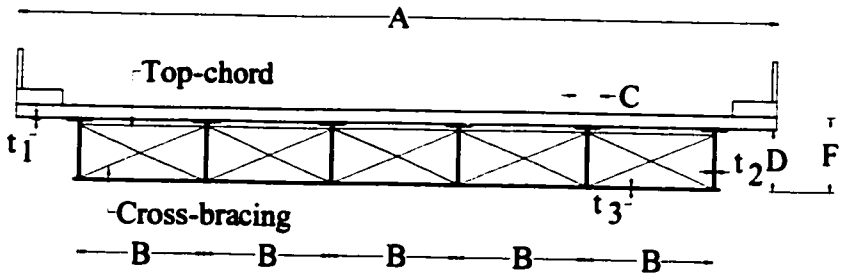

(a) Cross-section of five-cell bridge

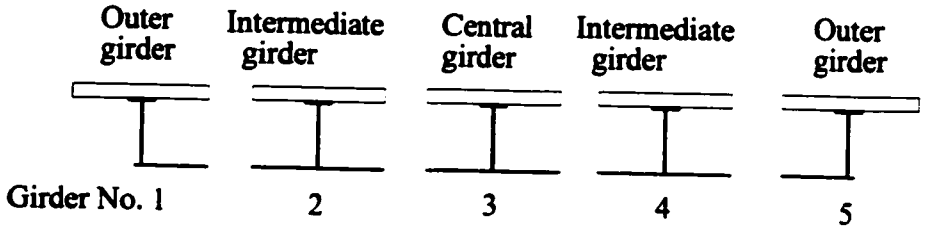

(b) Idealized cellular bridge for moment distribution

Fig. 4.4. Idealized cross-section for analysis of impact factors

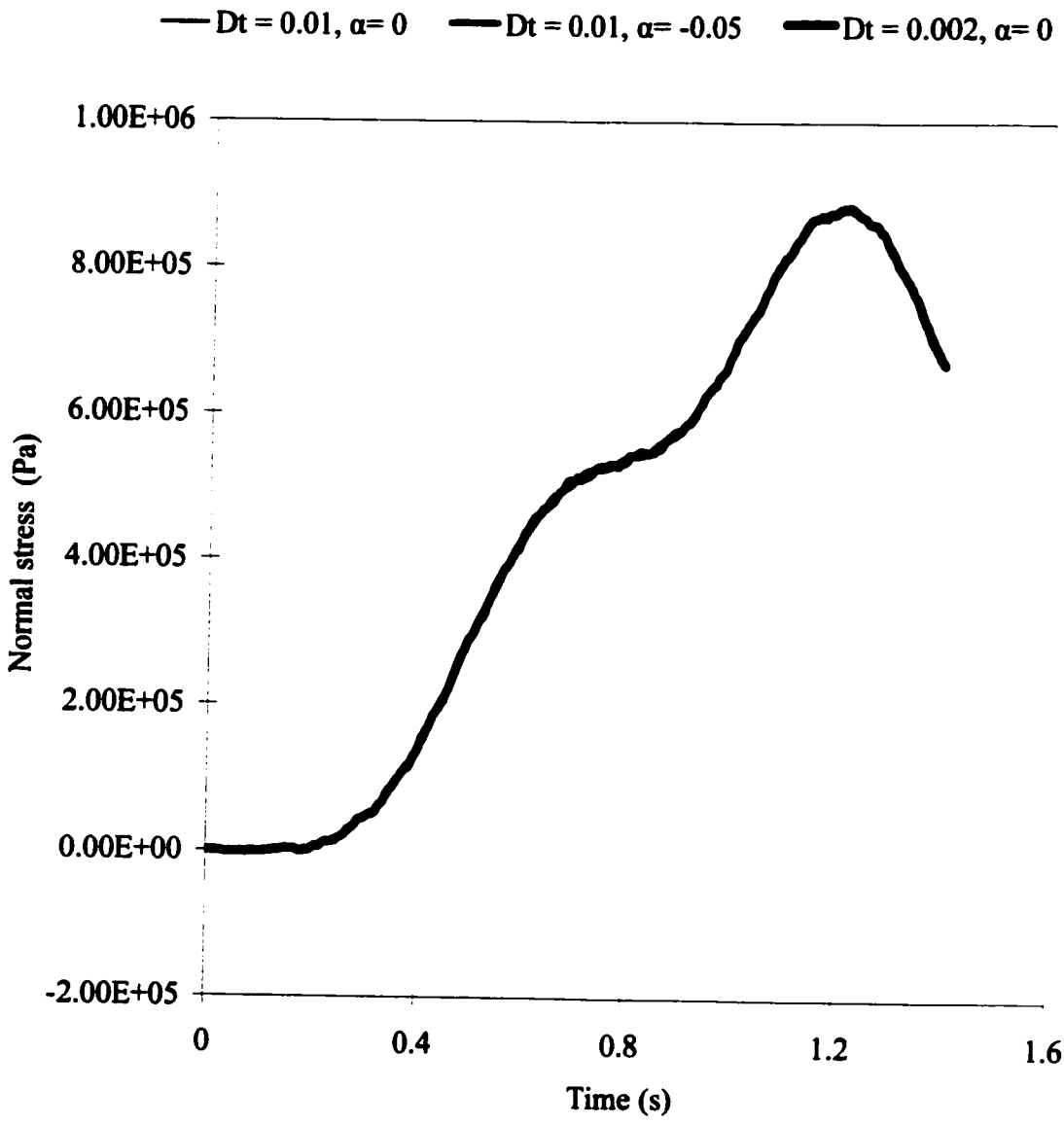

Fig. 5.1. Normal stress-time history of edge-girder mid-span bottom-flange of *2l-2c-60* straight bridge by using the direct integration method (v = 110km/h, full loading)
Dt - time step, α - artificial damping factor of ABAQUS

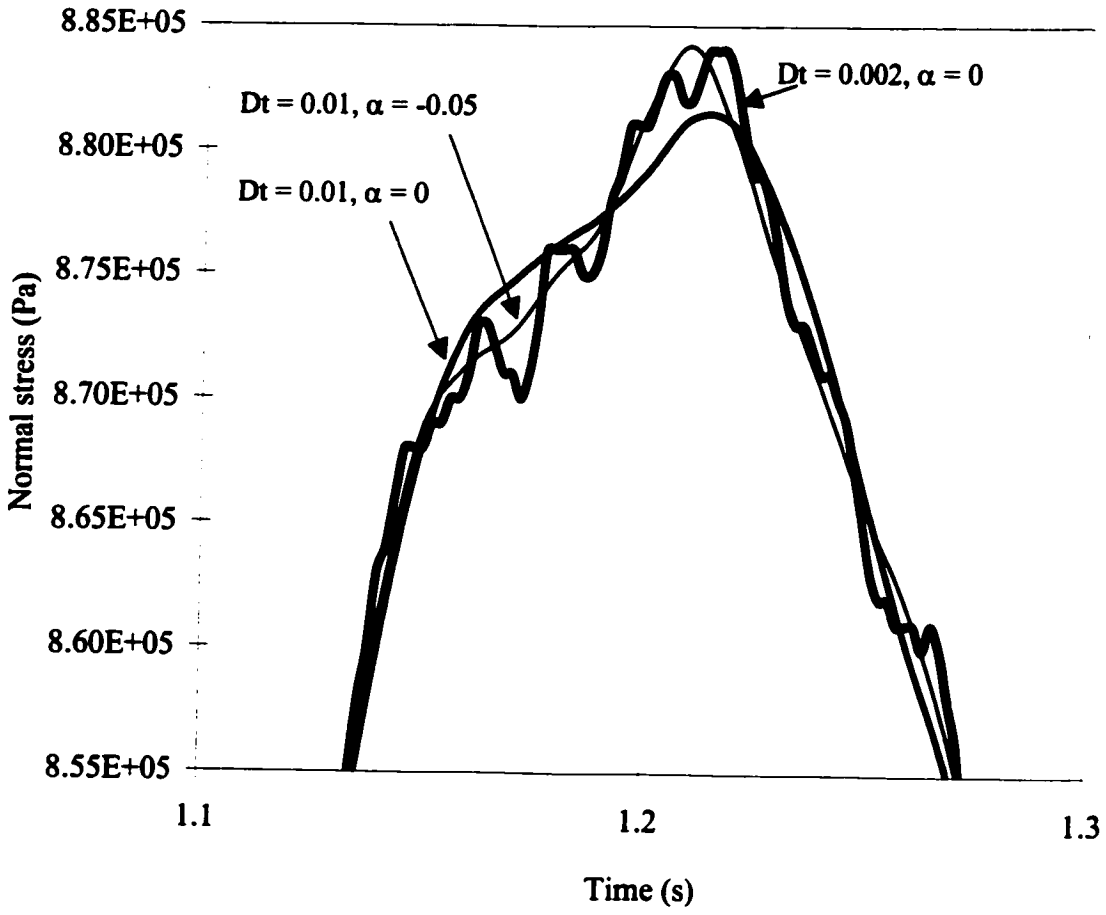

Fig. 5.2. Enlargement of Fig. 5.1

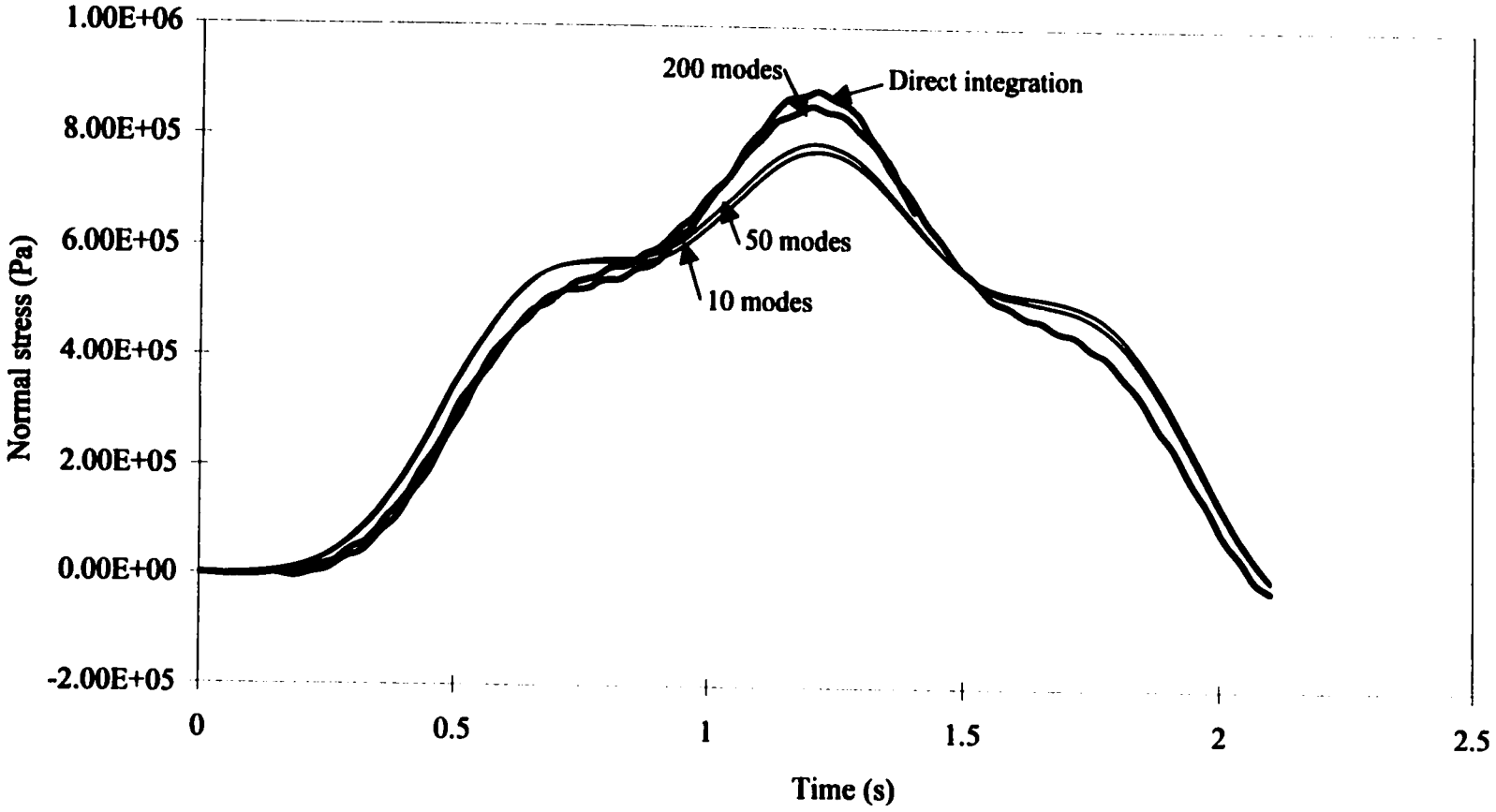

Fig. 5.3. Normal stress-time history of edge-girder mid-span bottom-flange of *2l-2c-60* straight bridge (v = 110 km/h, full loading)

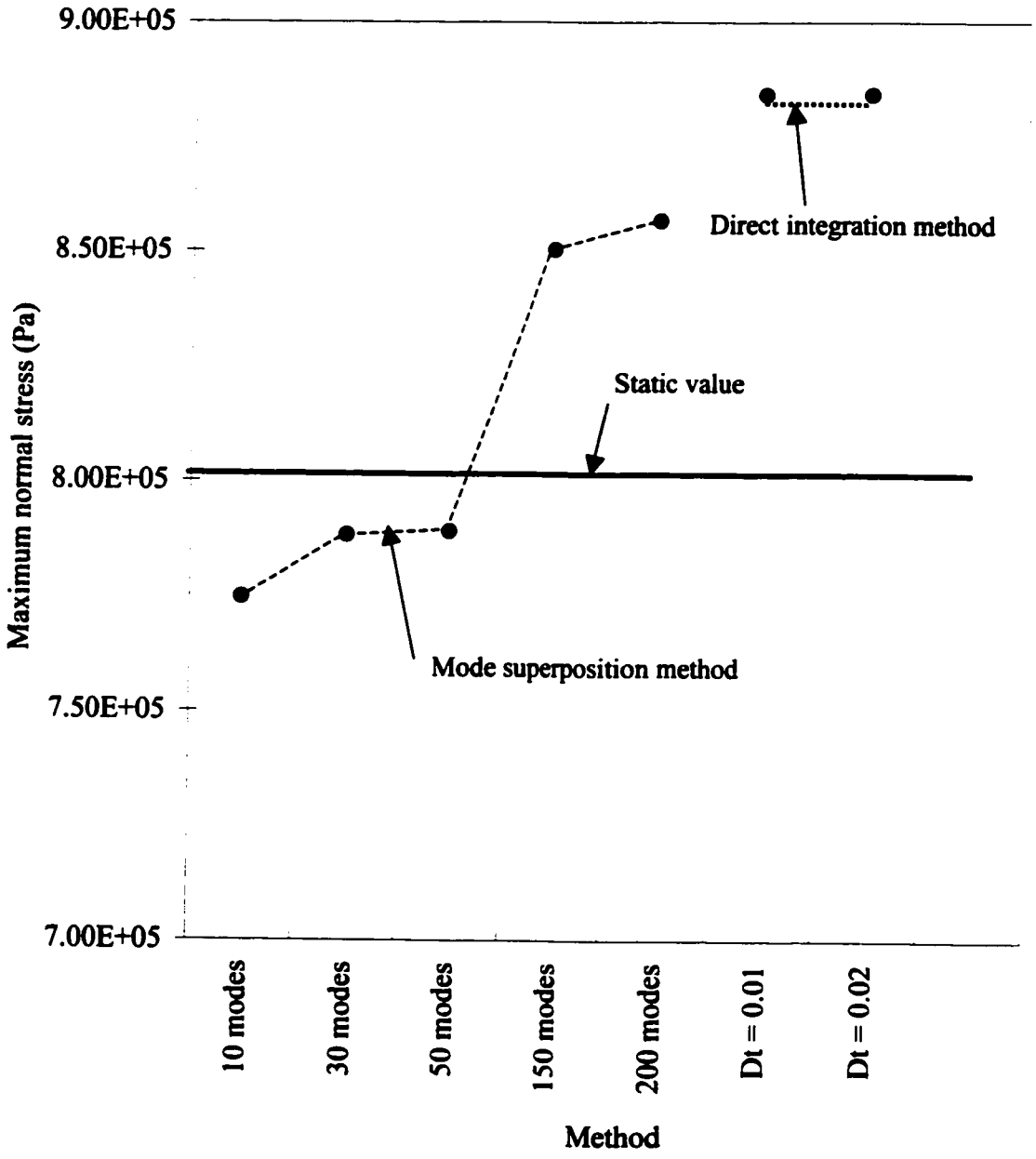

Fig. 5.4. Maximum normal stress of edge-girder mid-span bottom-flange of *2l-2c-60* straight bridge (v = 110km/h, full loading)

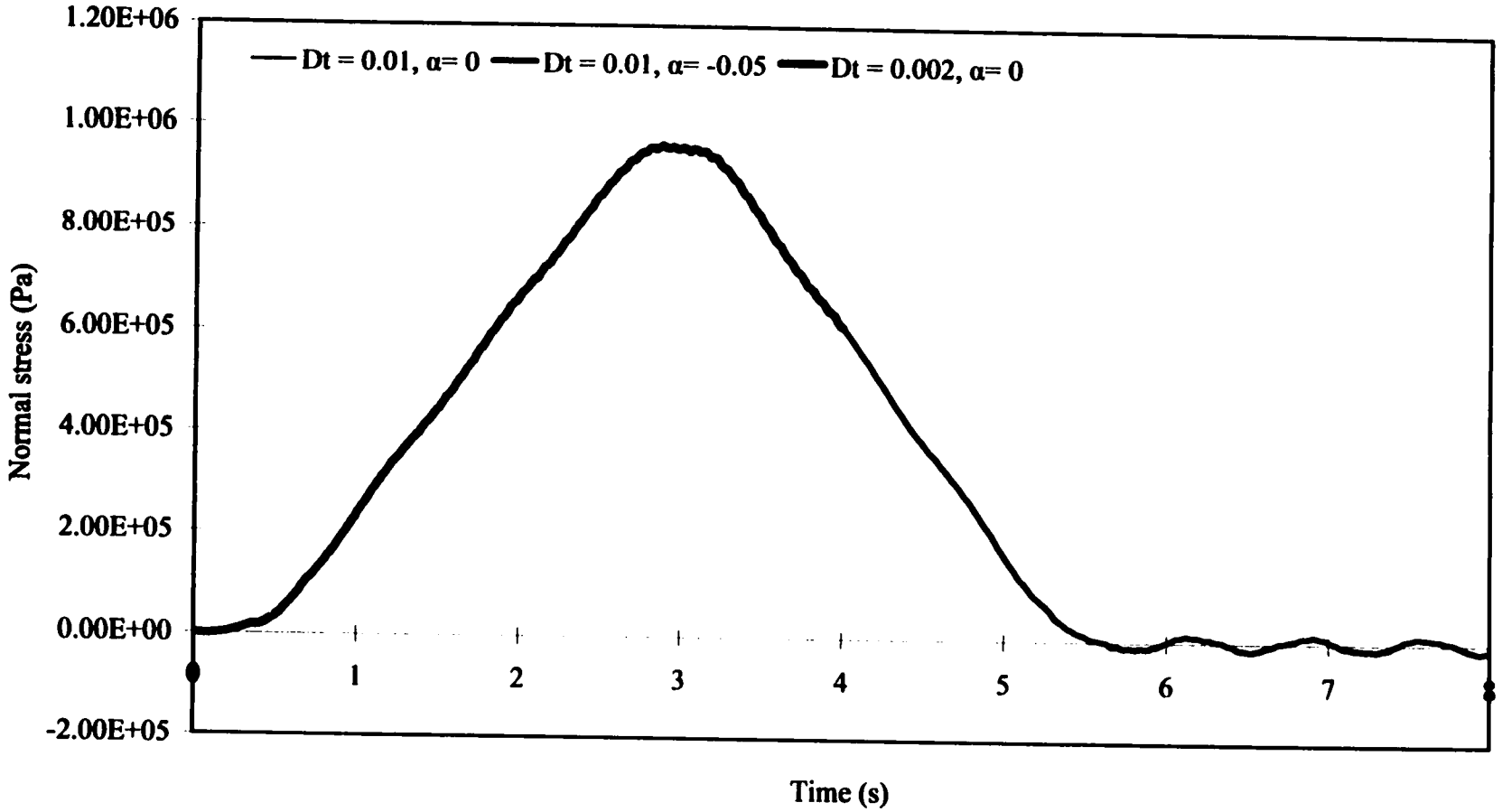

Fig. 5.5. Normal stress-time history of outer-girder mid-span bottom-flange of *2l-2c-60* curved bridge by using the direct integration method (L/R = 1.0, v = 45 km/h, full loading)

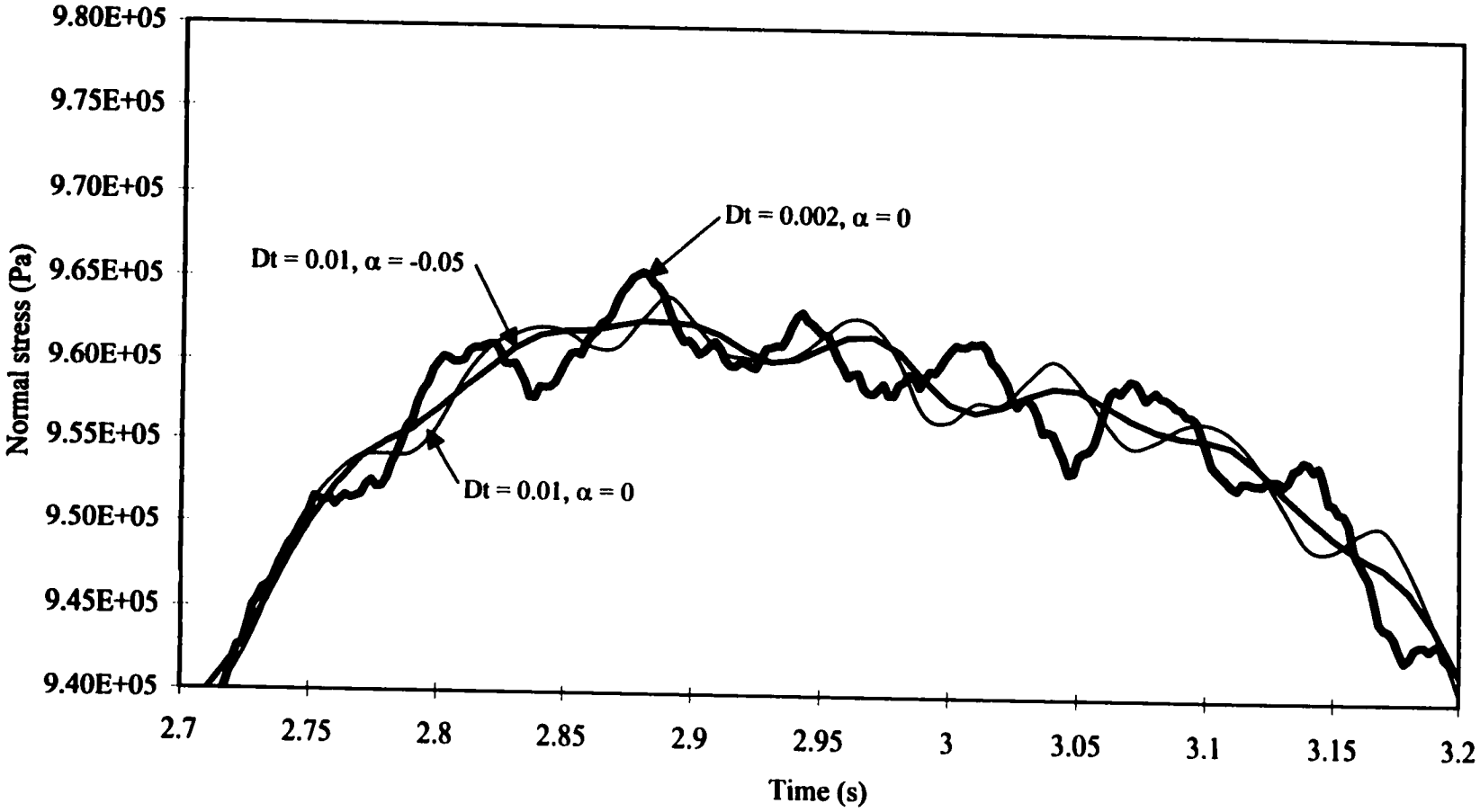

Fig. 5.6. Enlargement of Fig. 5.5

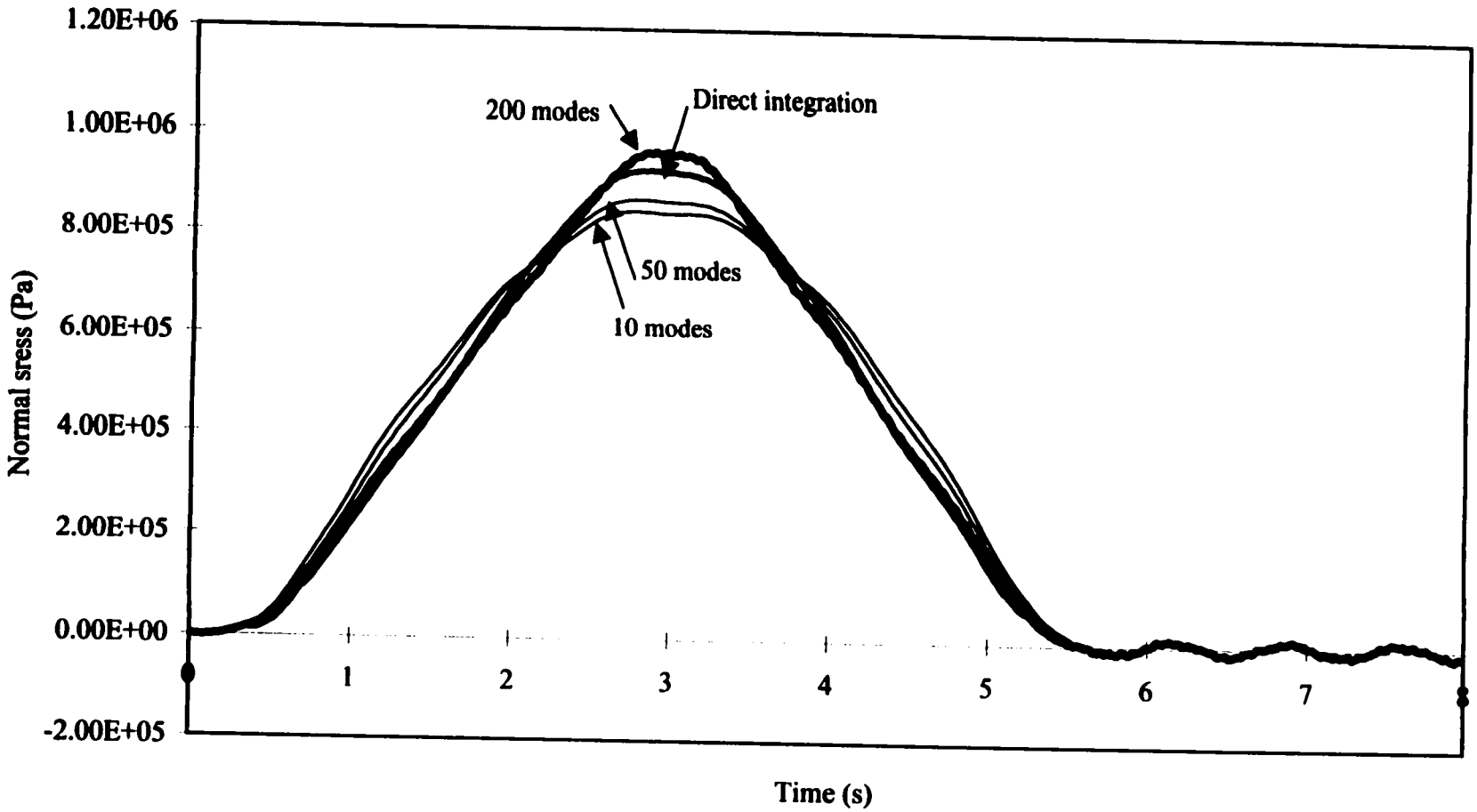

Fig. 5.7. Normal stress-time history of outer-girder mid-span bottom-flange of *2l-2c-60* curved bridge
(L/R = 1.0, v = 45 km/h, full loading)

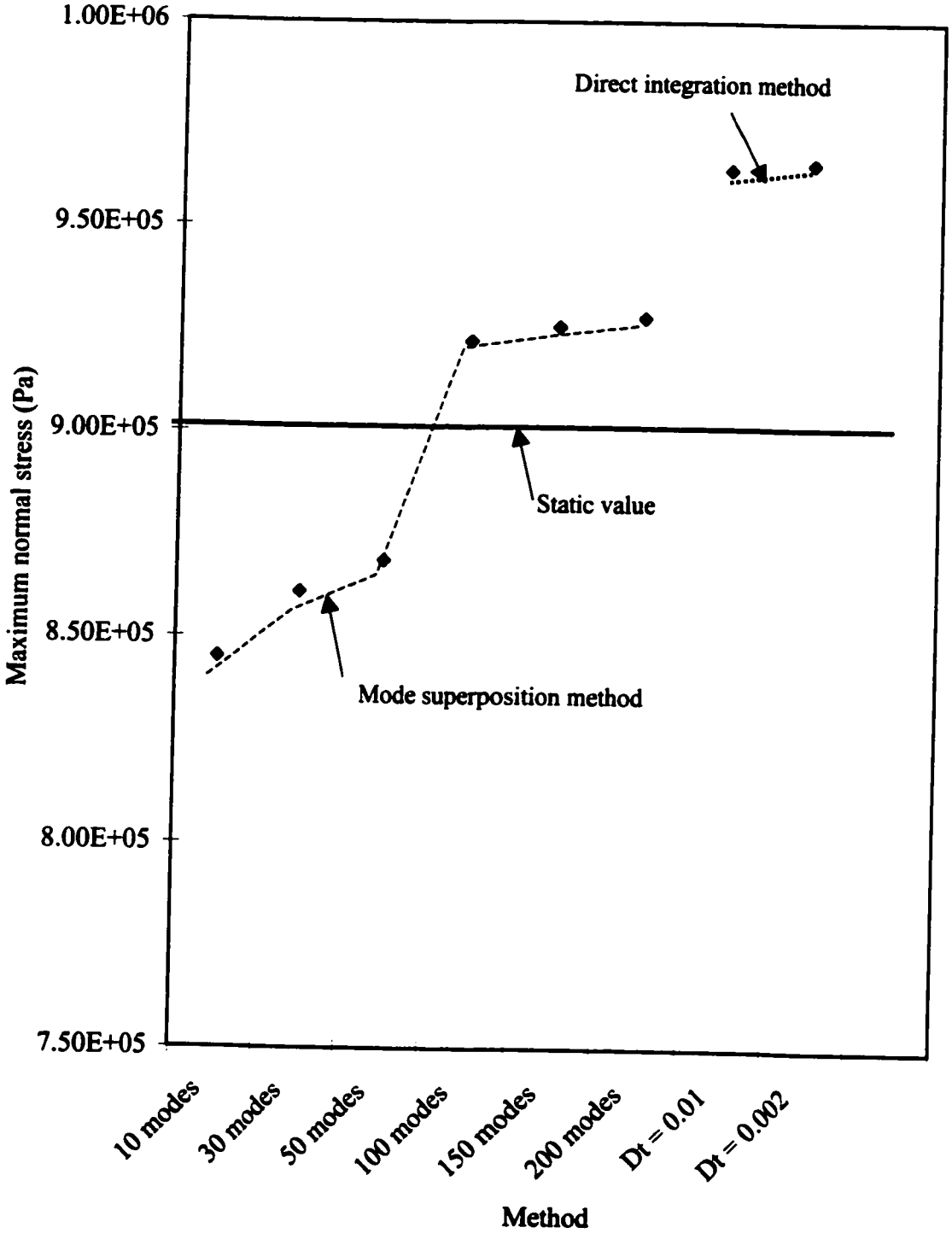

Fig. 5.8. Maximum normal stress of outer-girder mid-span bottom flange of *2l-2c-60* curved bridge (L/R = 1.0, v = 45 km/h, full loading)

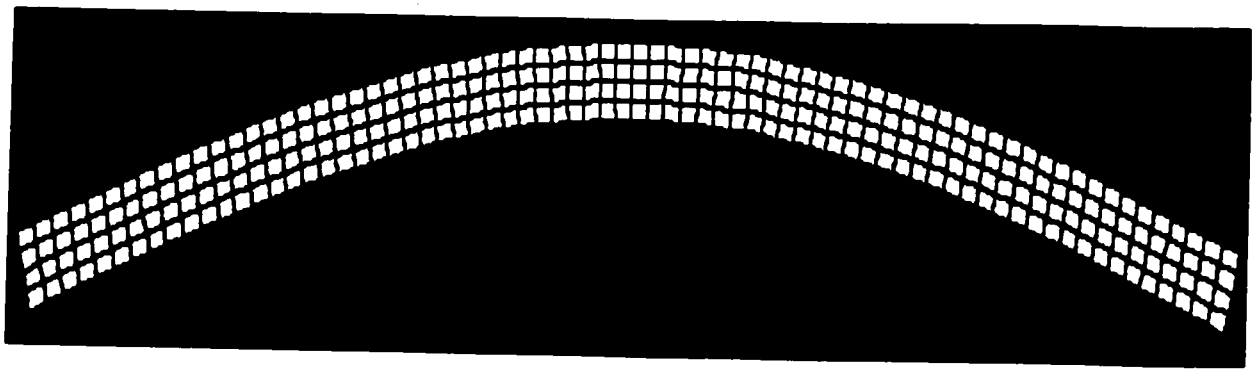

(a) First mode shape (f = 2.46 Hz), LF

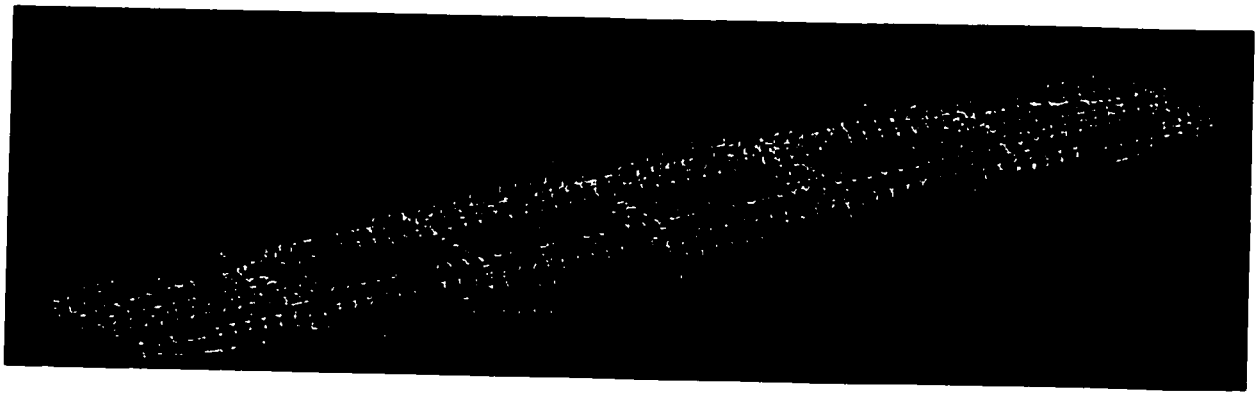

(b) Second mode shape (f = 7.6 Hz), LF-TS

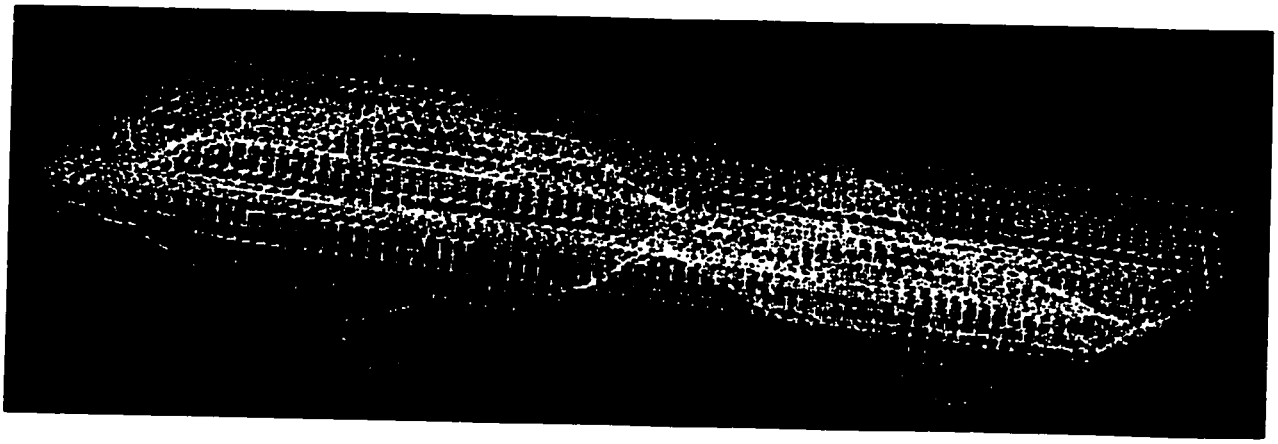

(c) Third mode shape (f = 7.72 Hz), TAS-TF

Fig. 6.1. Mode shapes of 2l-2c-40 straight bridge

Note: LF – Longitudinal Flexural, TS – Symmetric Torsion, TAS – Antisymmetric Torsion

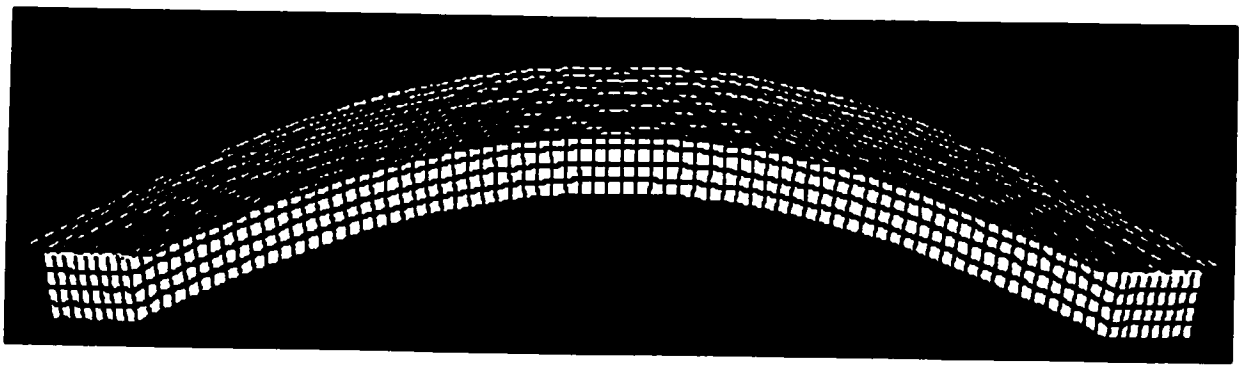

(a) First mode shape (f = 2.03 Hz), LF

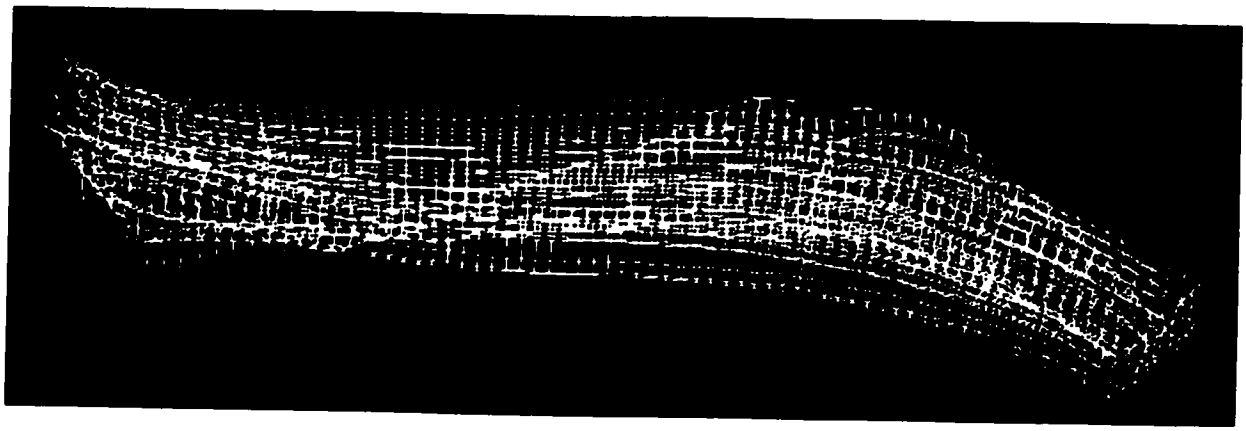

(b) Second mode shape (f = 6.68 Hz), TAS-TF

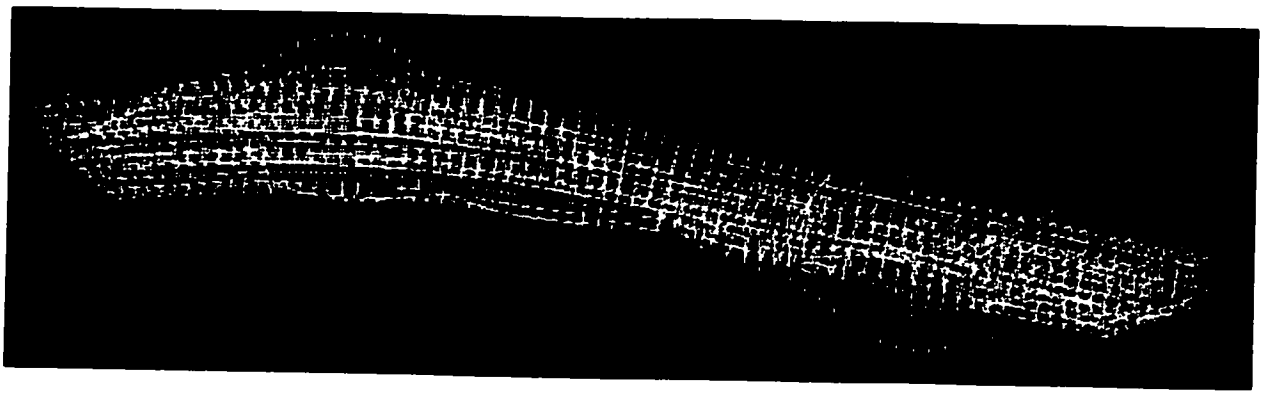

(c) Third mode shape (f = 7.77 Hz), TAS-LF

Fig. 6.2. Mode shapes of 2l-2c-40 curved bridge with L/R = 1.0

Note: LF – Longitudinal Flexural, TF – Transverse Flexural, TAS – Antisymmetric Torsion

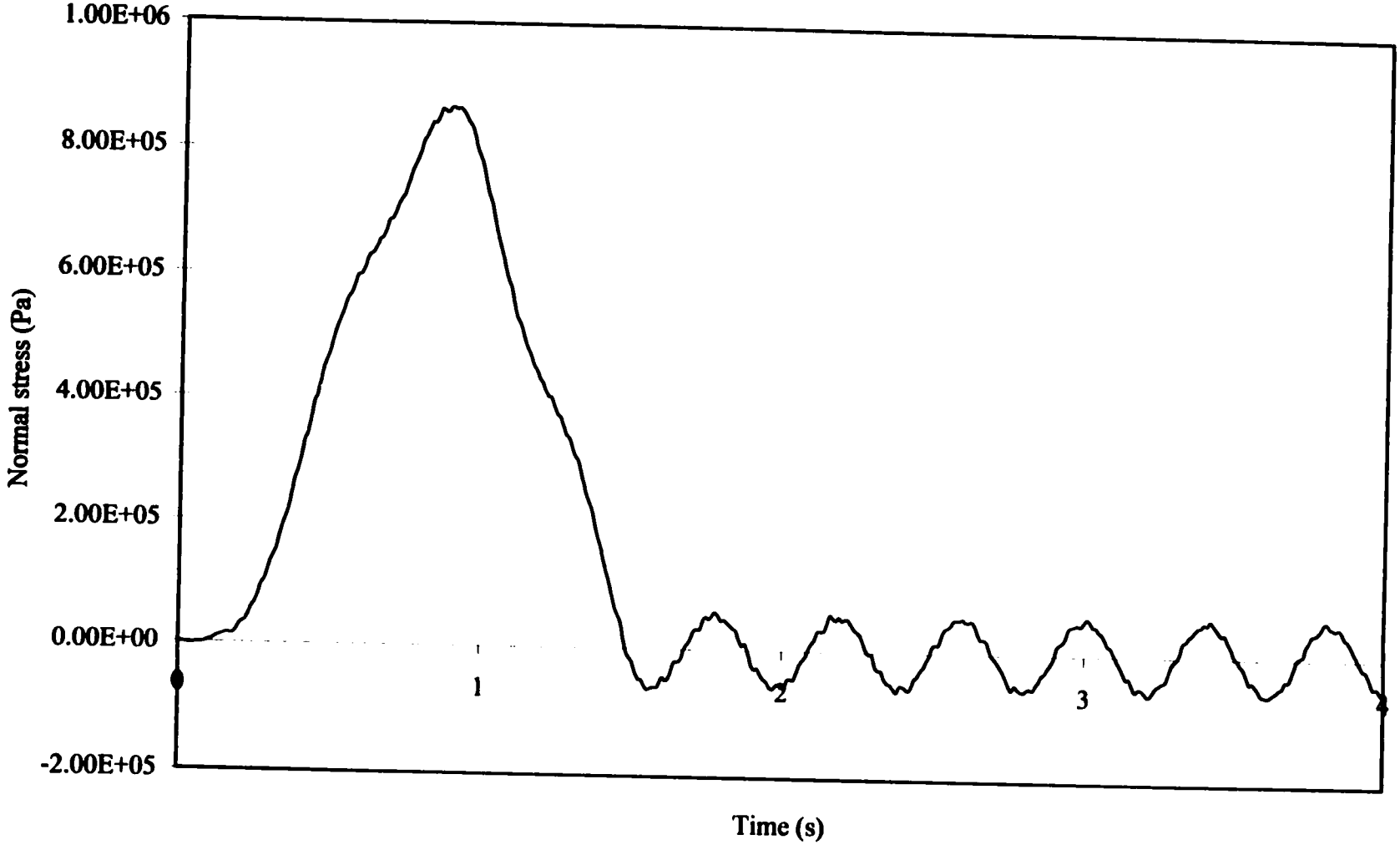

Fig. 6.3a. Normal stress-time history of edge-girder mid-span bottom-flange of *2l-2c-40* straight bridge (v = 110 km/h, full loading)

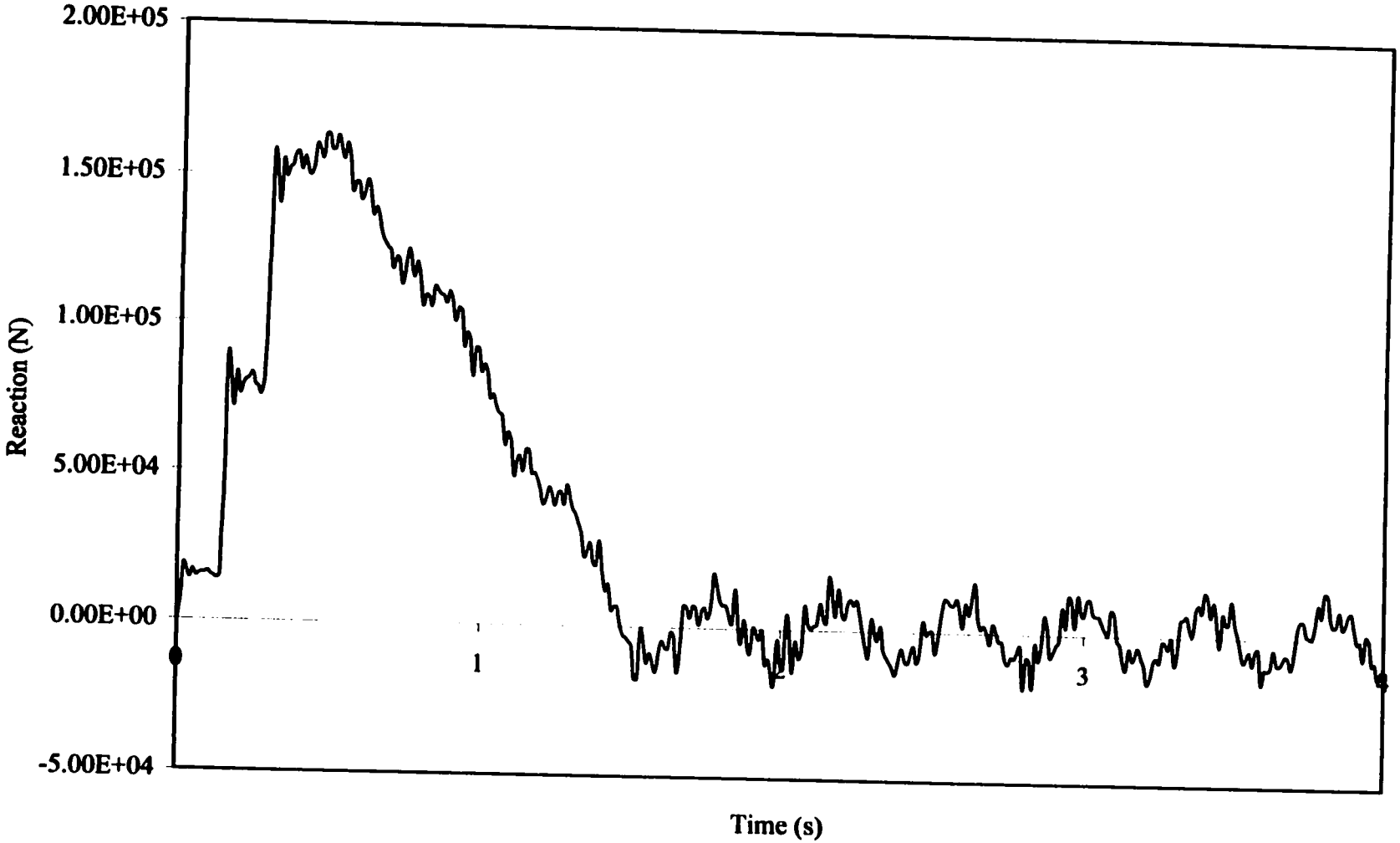

Fig. 6.3b. Reaction-time history of edge-web of *2l-2c-40* straight bridge
(v = 110 km/h, full loading)

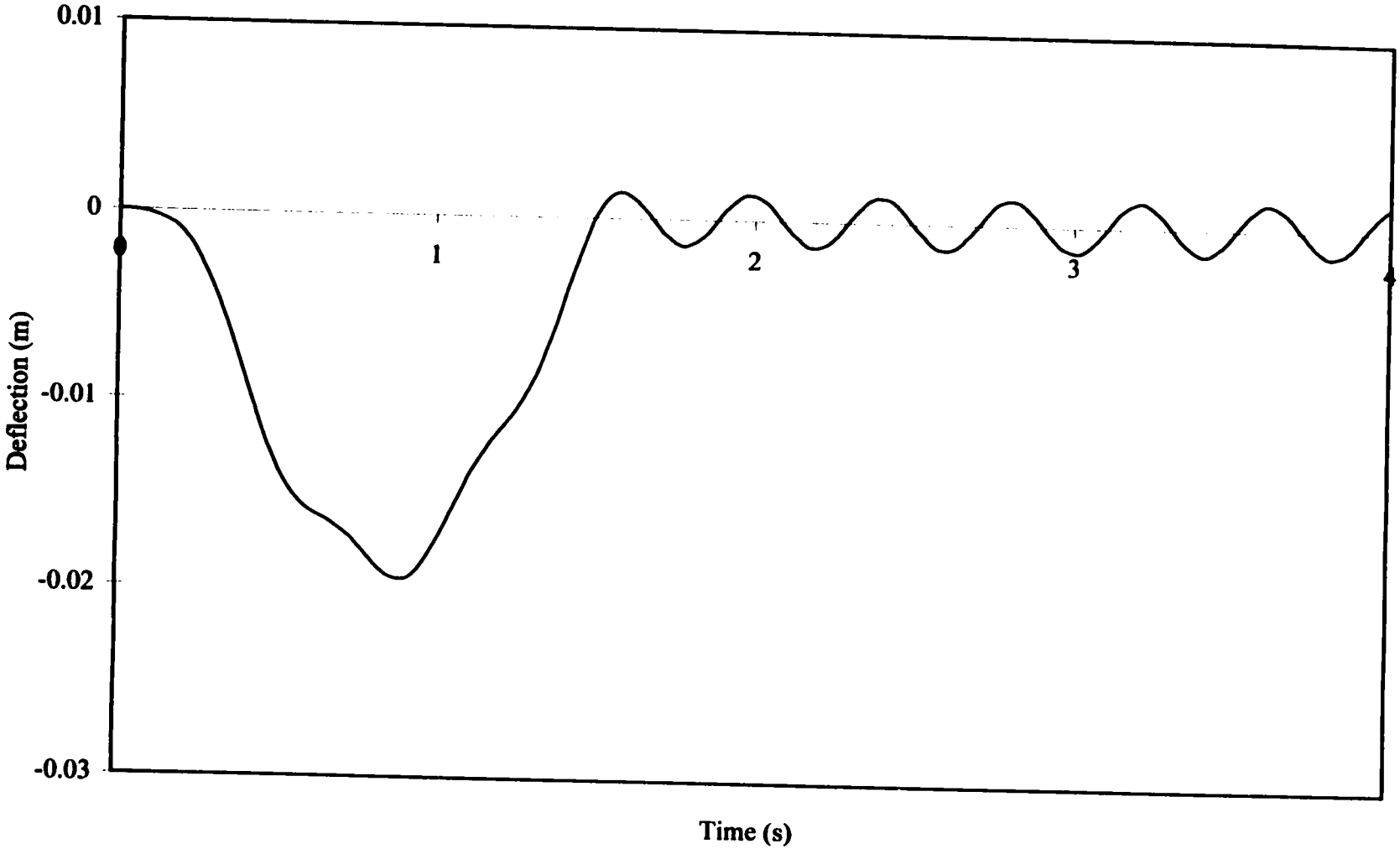

Fig. 6.3c. Deflection-time history of edge-web mid-span of *2l-2c-40* straight bridge (v = 110 km/h, full loading)

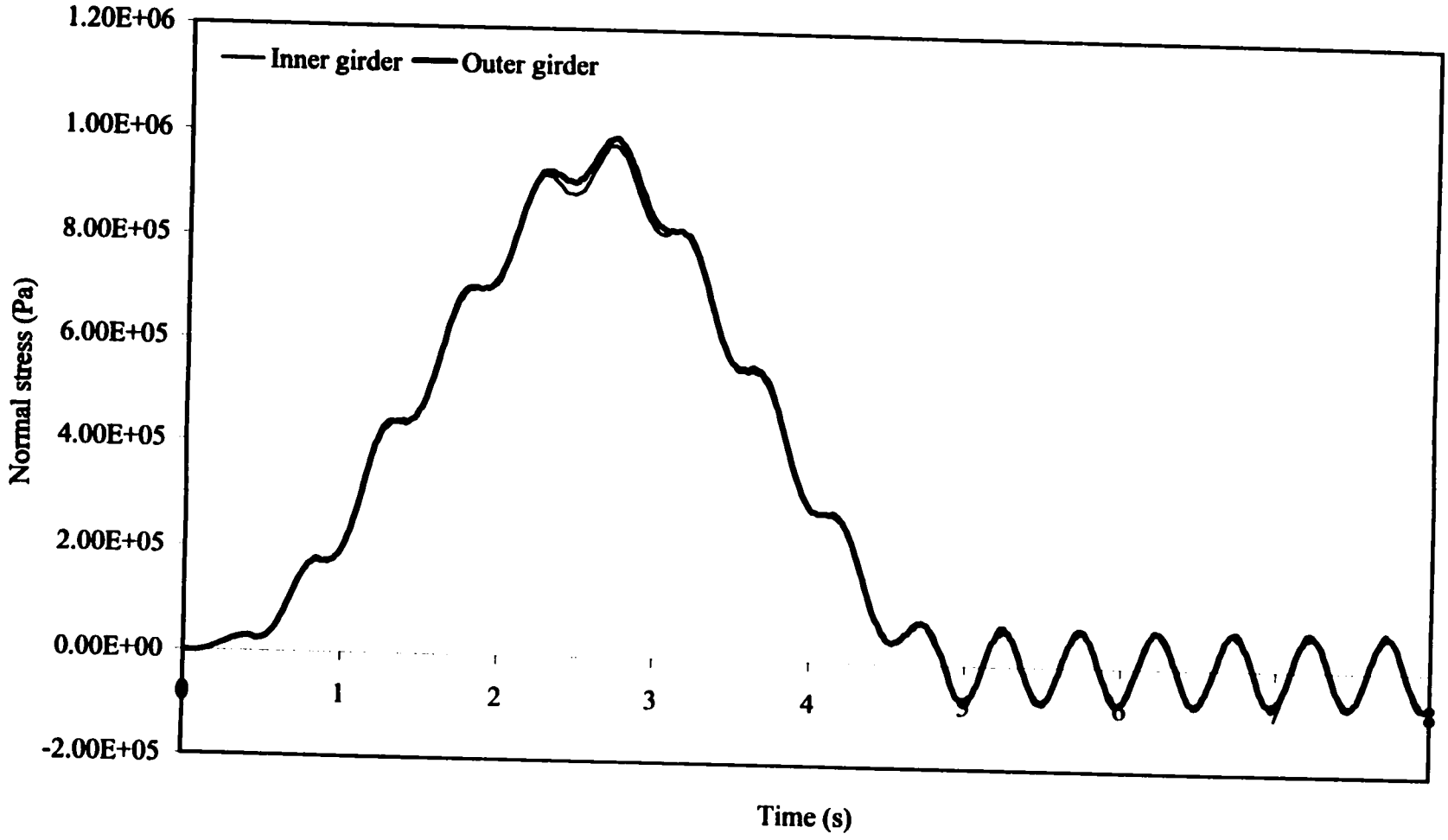

Fig. 6.4a. Normal stress-time history of mid-span bottom-flange of *2l-2c-40* curved bridge (L/R = 1.0, v = 37 km/h, full loading)

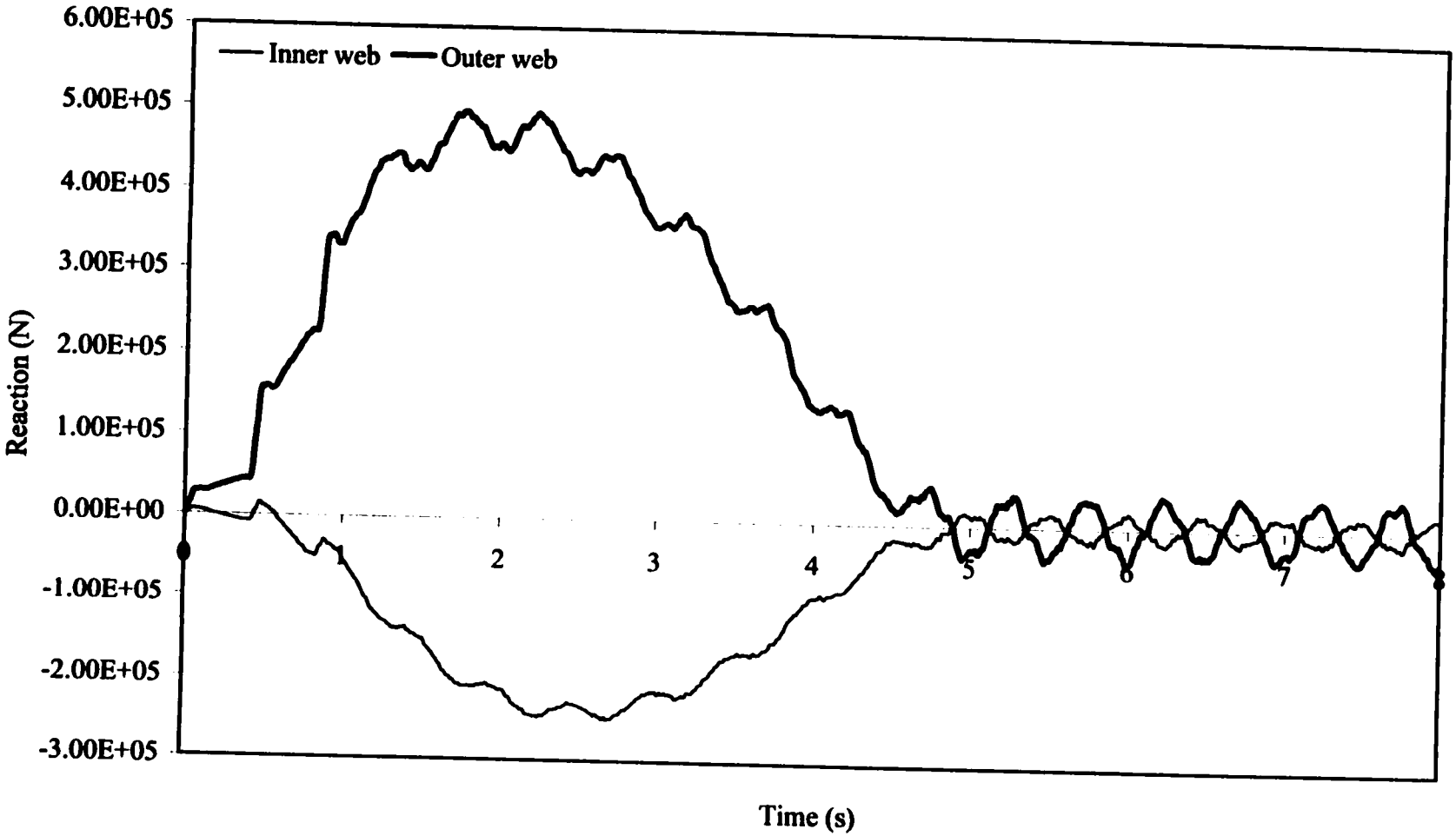

Fig. 6.4b. Reaction-time history of *2l-2c-40* curved bridge
(L/R=1.0, v = 37 km/h, full loading)

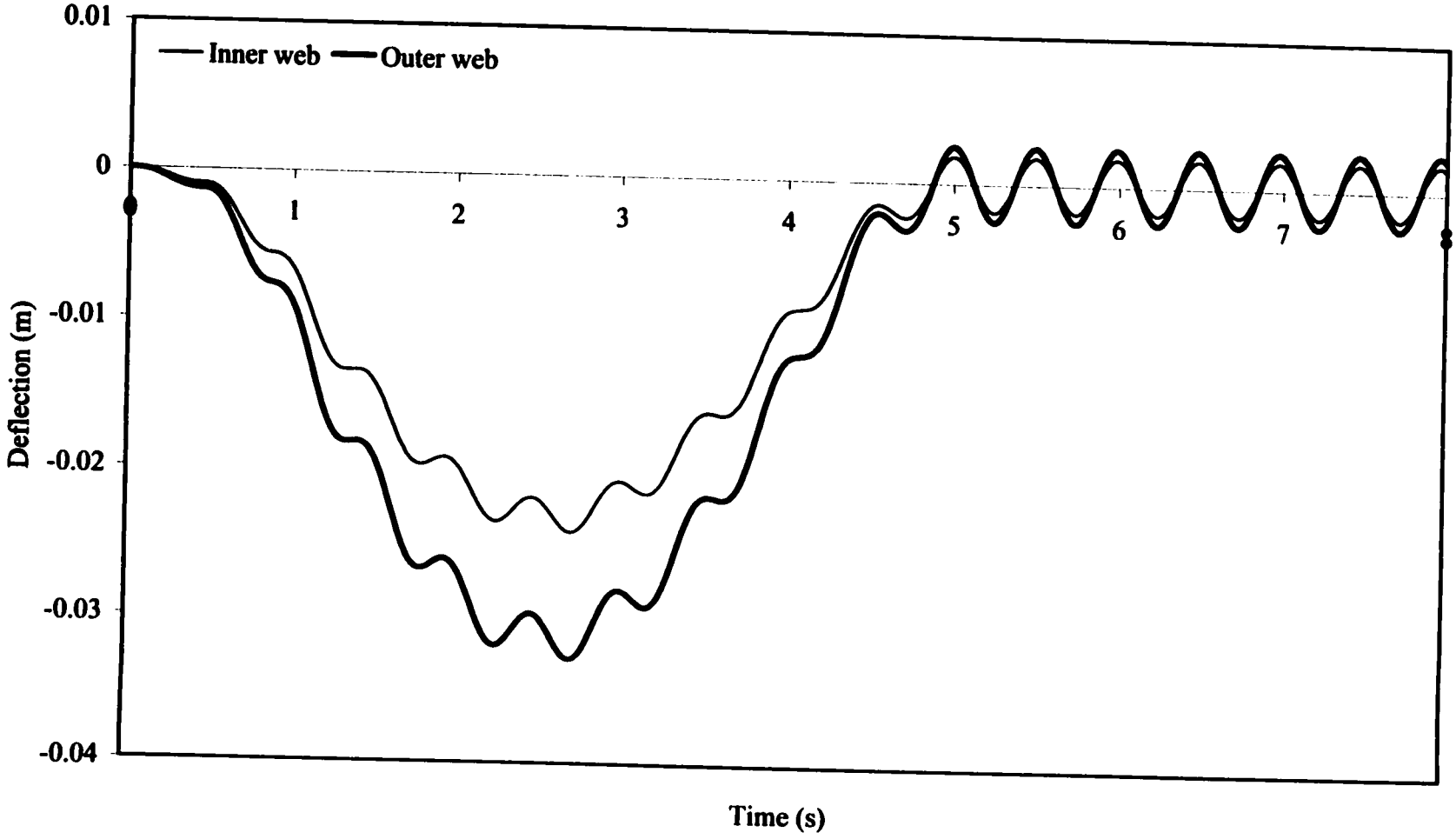

Fig. 6.4c. Deflection-time history of mid-span of *2l-2c-40* curved bridge
(L/R=1.0, v = 37 km/h, full loading)

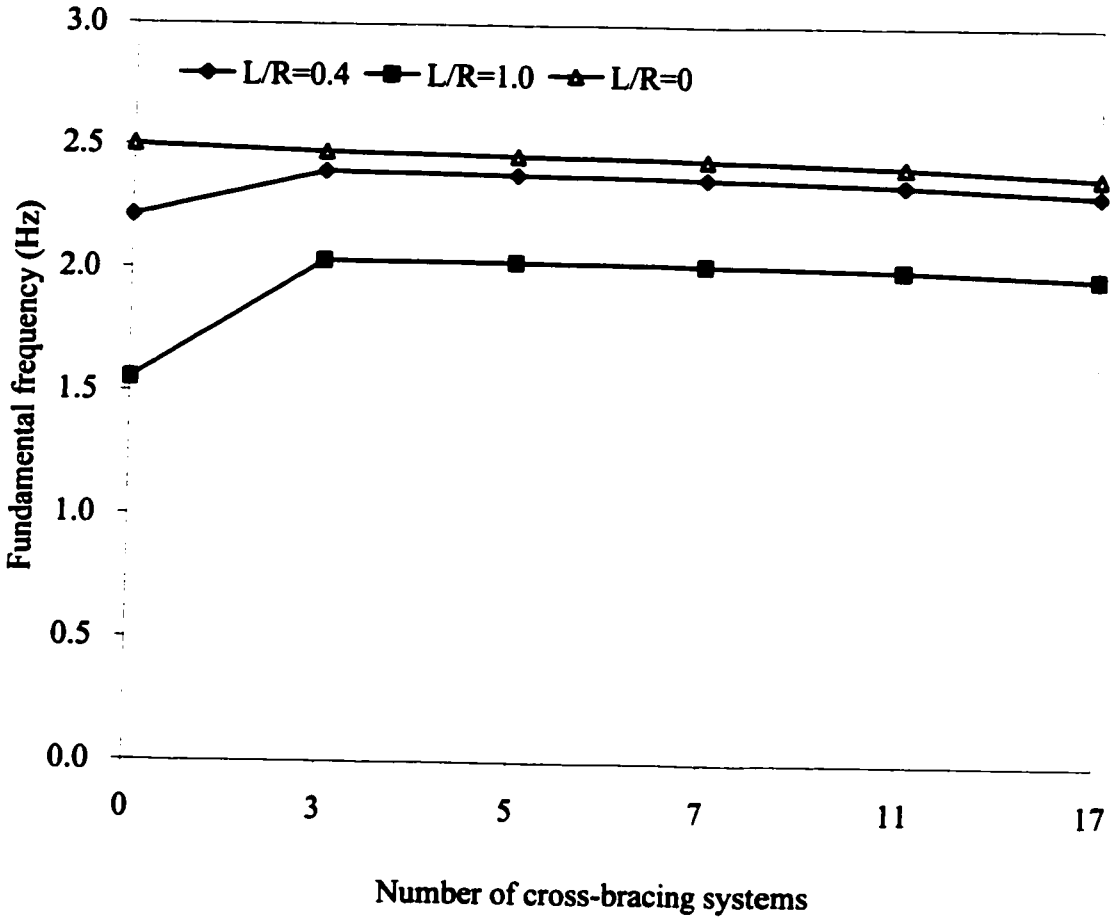

Fig. 6.5. Effect of number of cross-bracing systems on fundamental frequency of *2l-2c-40* bridges (full loading)

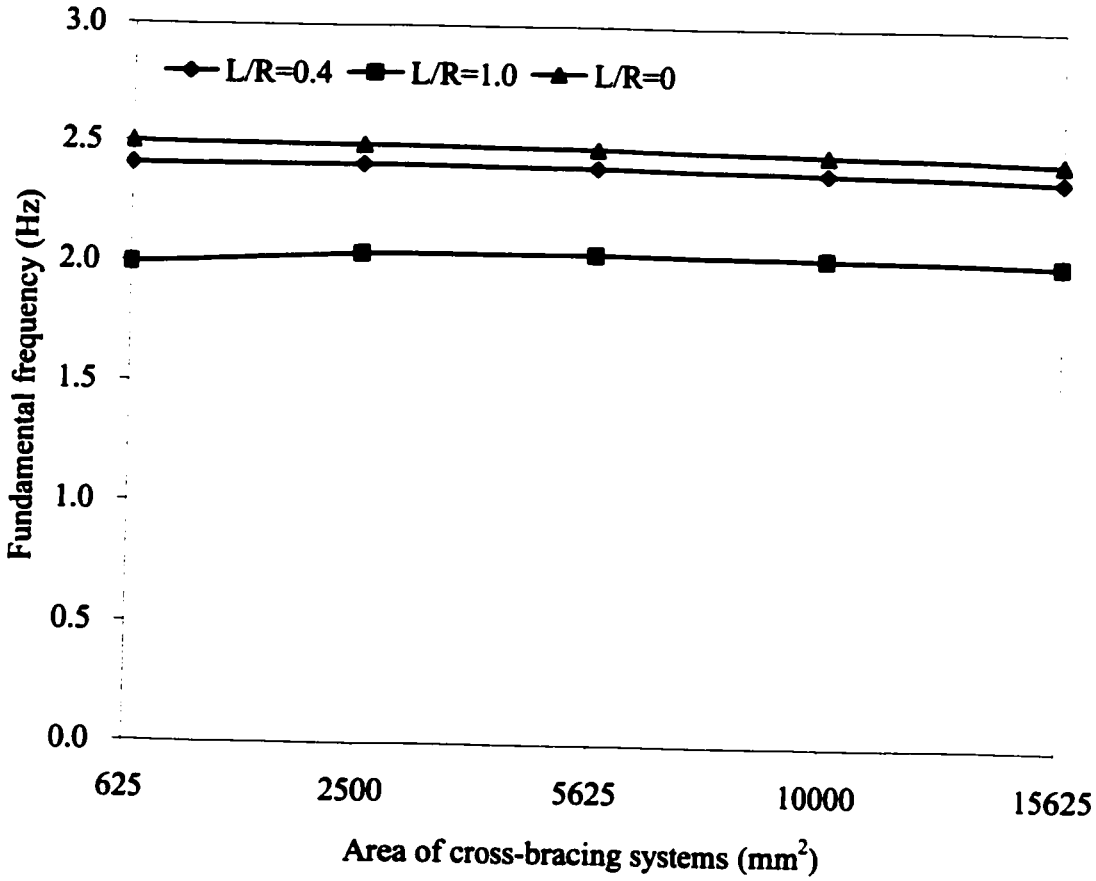

Fig. 6.6. Effect of area of cross-bracing systems on fundamental frequency of *2l-2c-40* bridges (full loading)

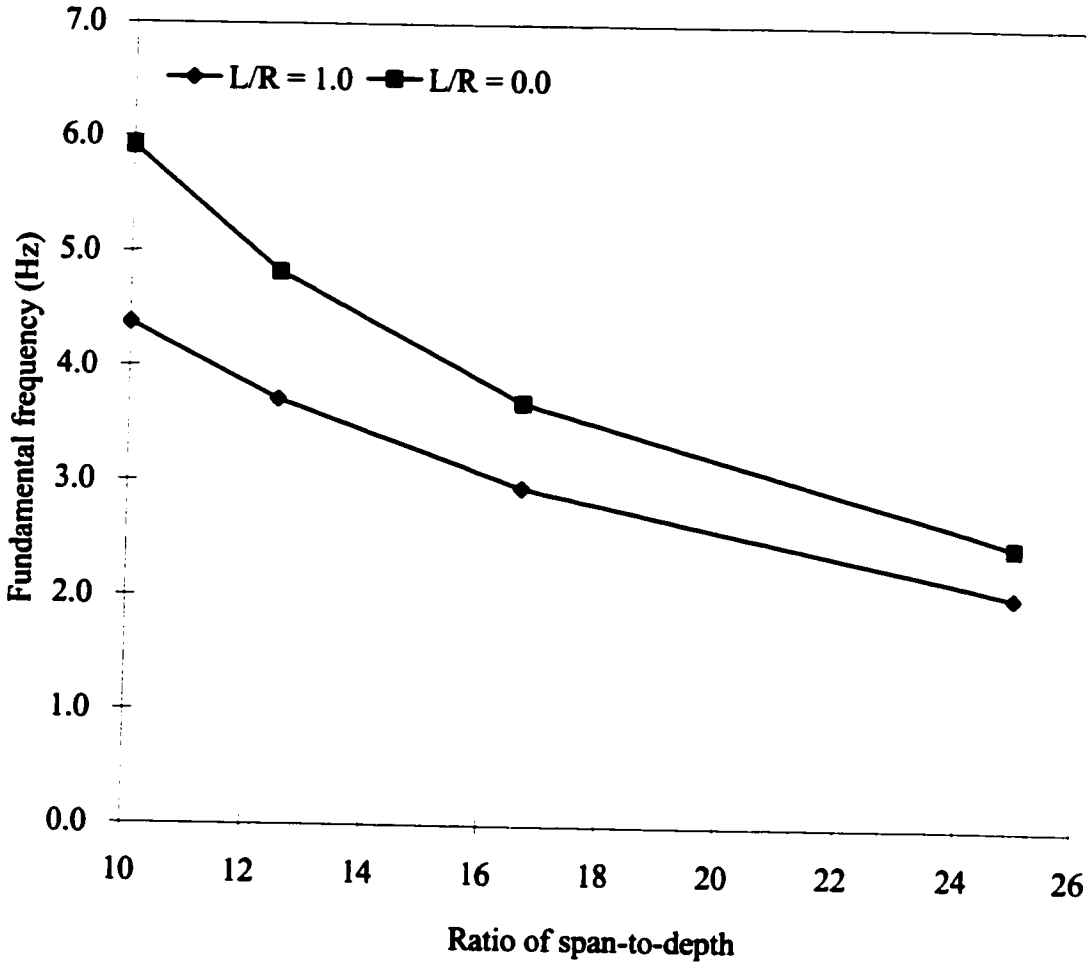

Fig. 6.7. Effect of span-to-depth ratio on fundamental frequency of *2l-2c-40* bridges (full loading)

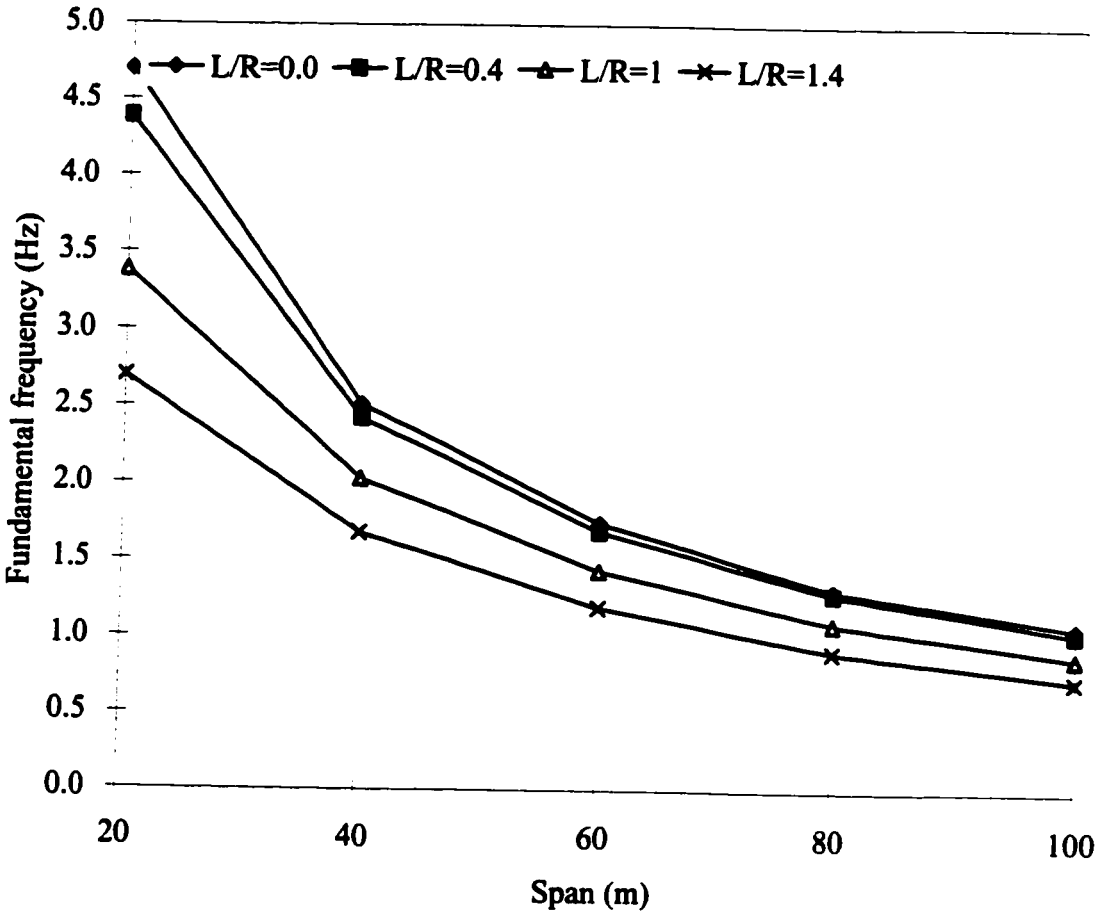

Fig. 6.8. Effect of span on fundamental frequency of *4l-4c* bridges (full loading)

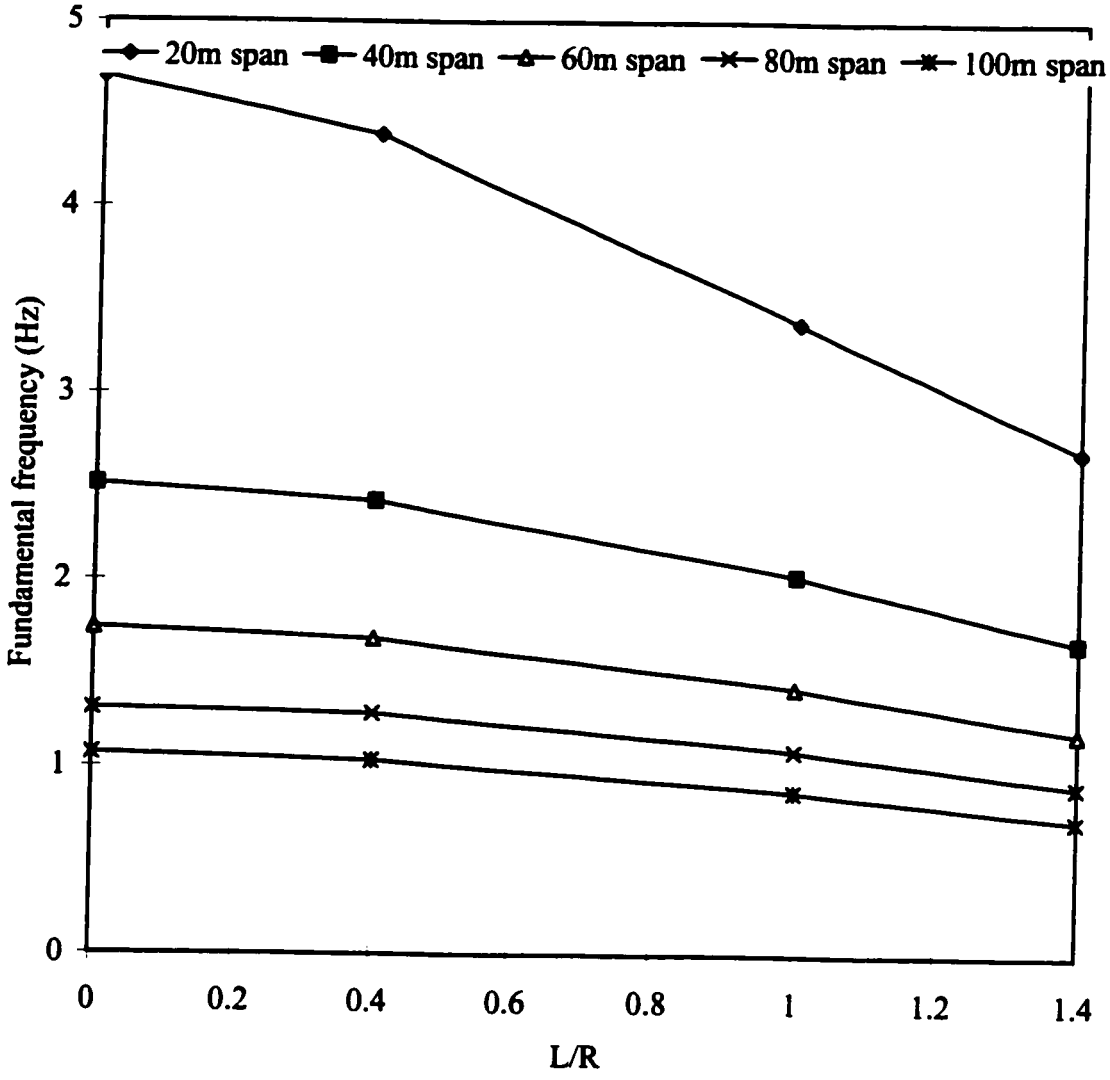

Fig. 6.9. Effect of L/R on fundamental frequency of *4l-4c* bridges (full loading)

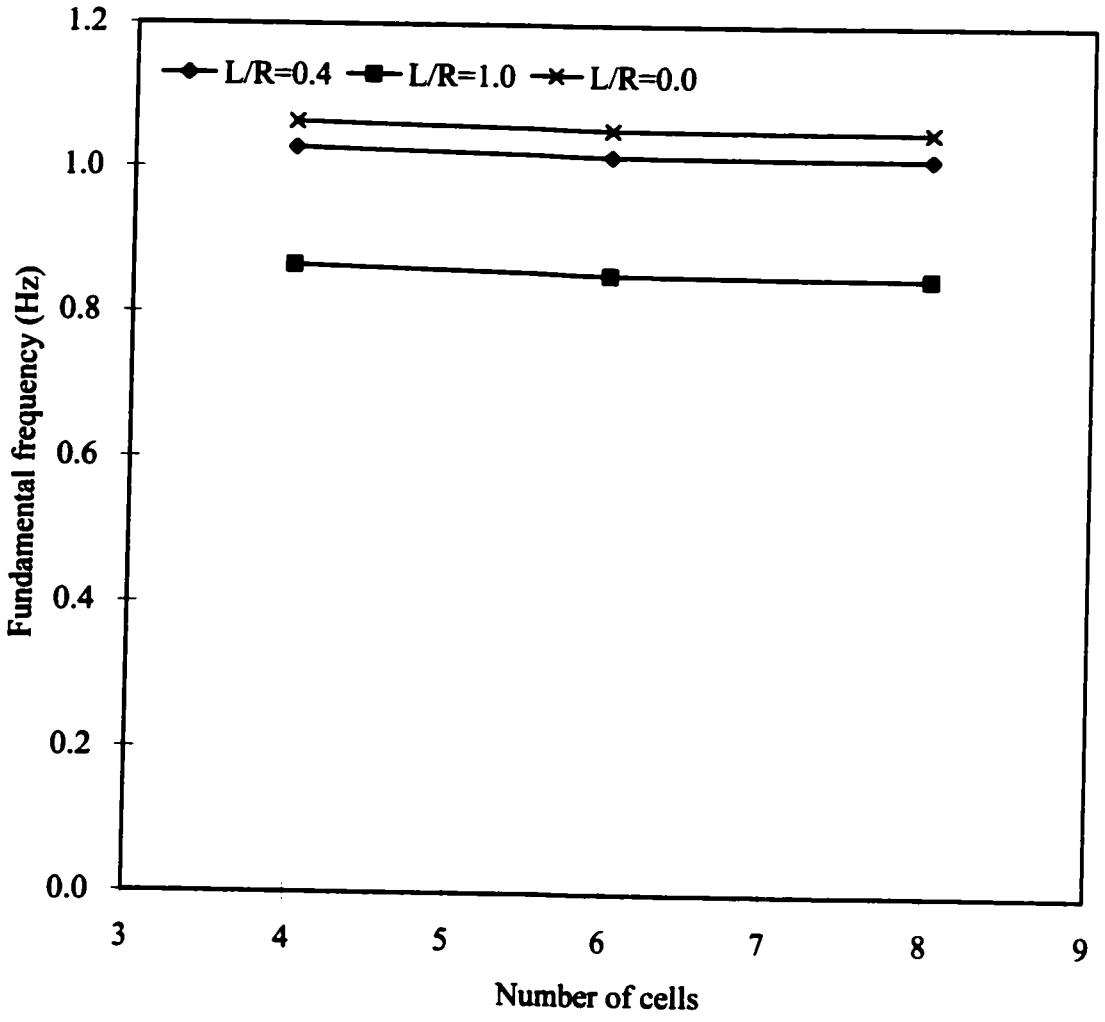

Fig. 6.10. Effect of number of cells on fundamental frequency of *3l-100* bridges (full loading)

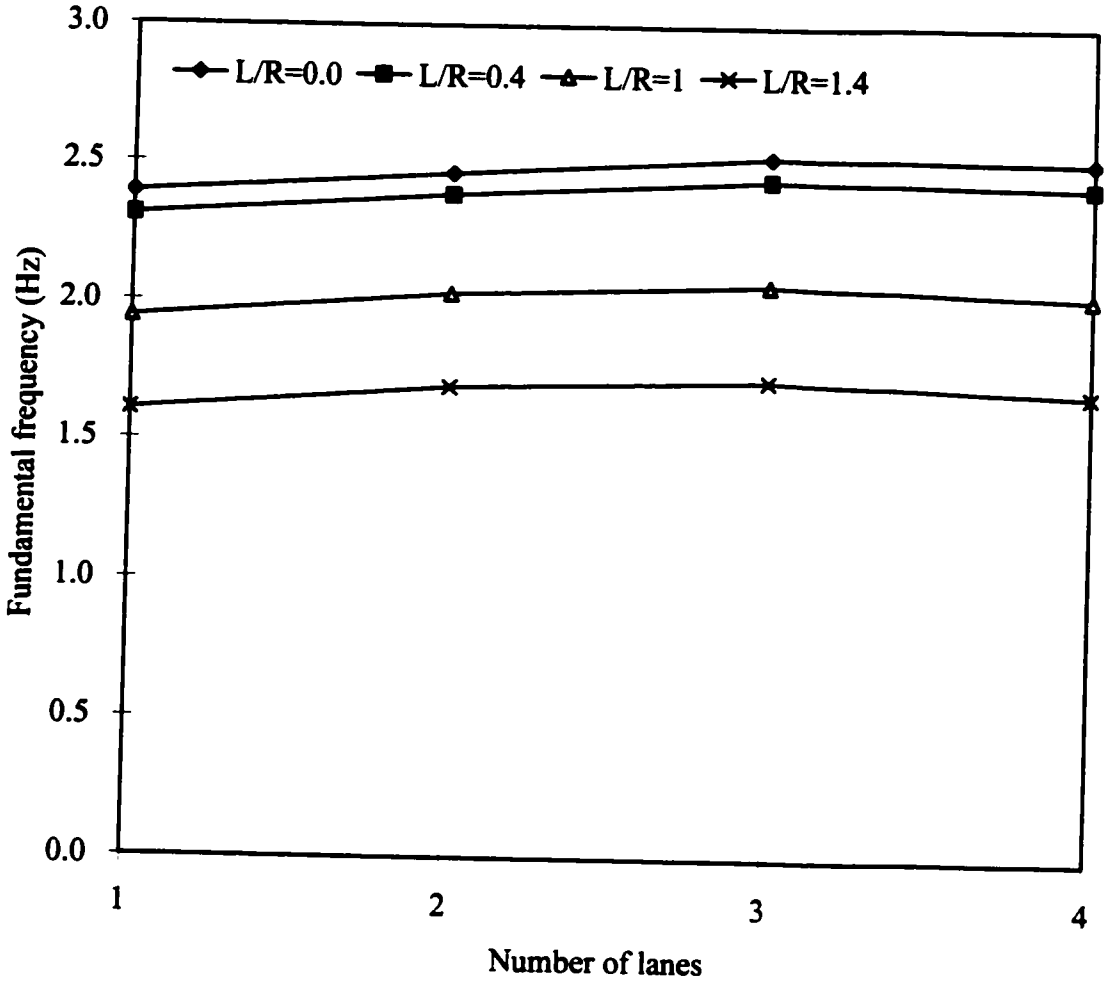

Fig. 6.11. Effect of number of lanes on fundamental frequency of bridges with span 40 (full loading)

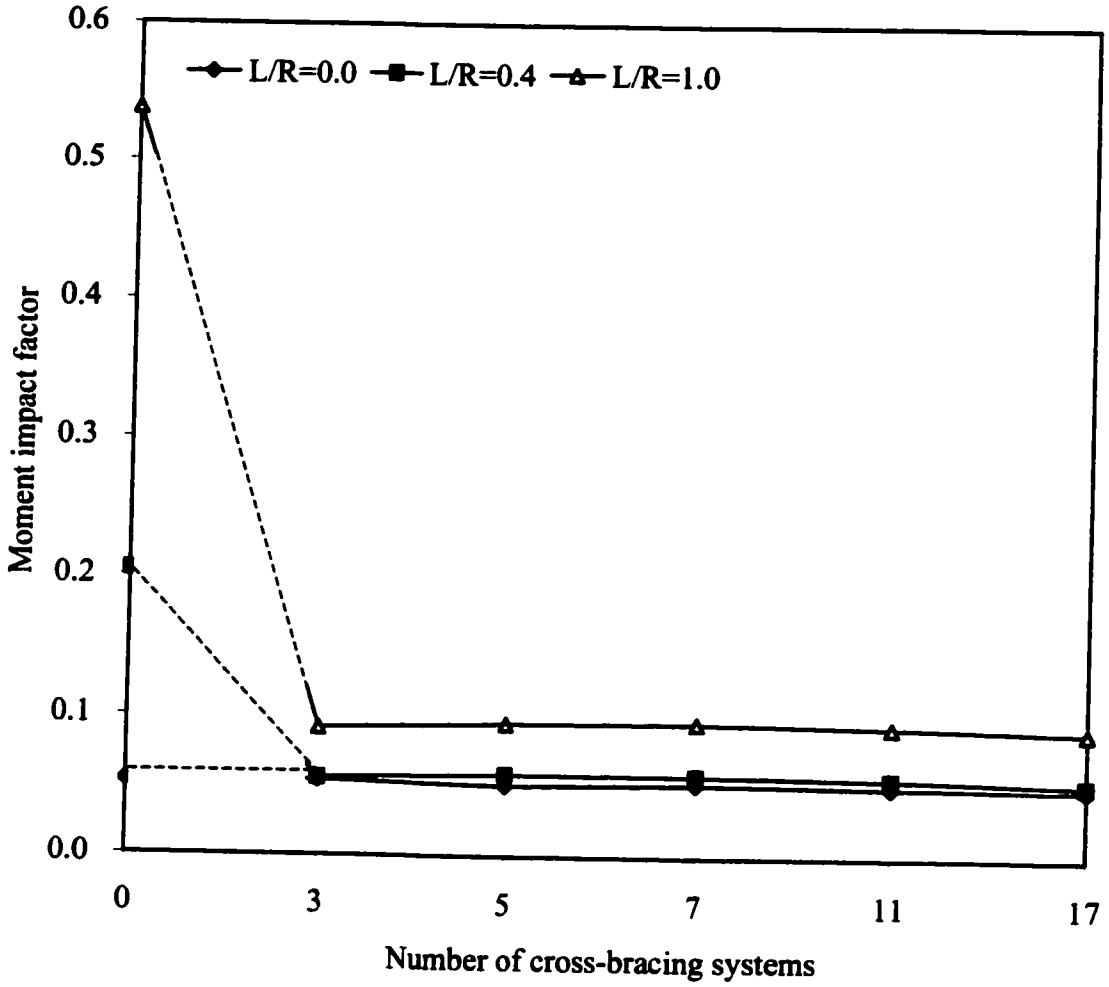

Fig. 7.1. Effect of number of cross-bracing systems on moment impact factor of *2l-2c-40* bridges
(full loading)

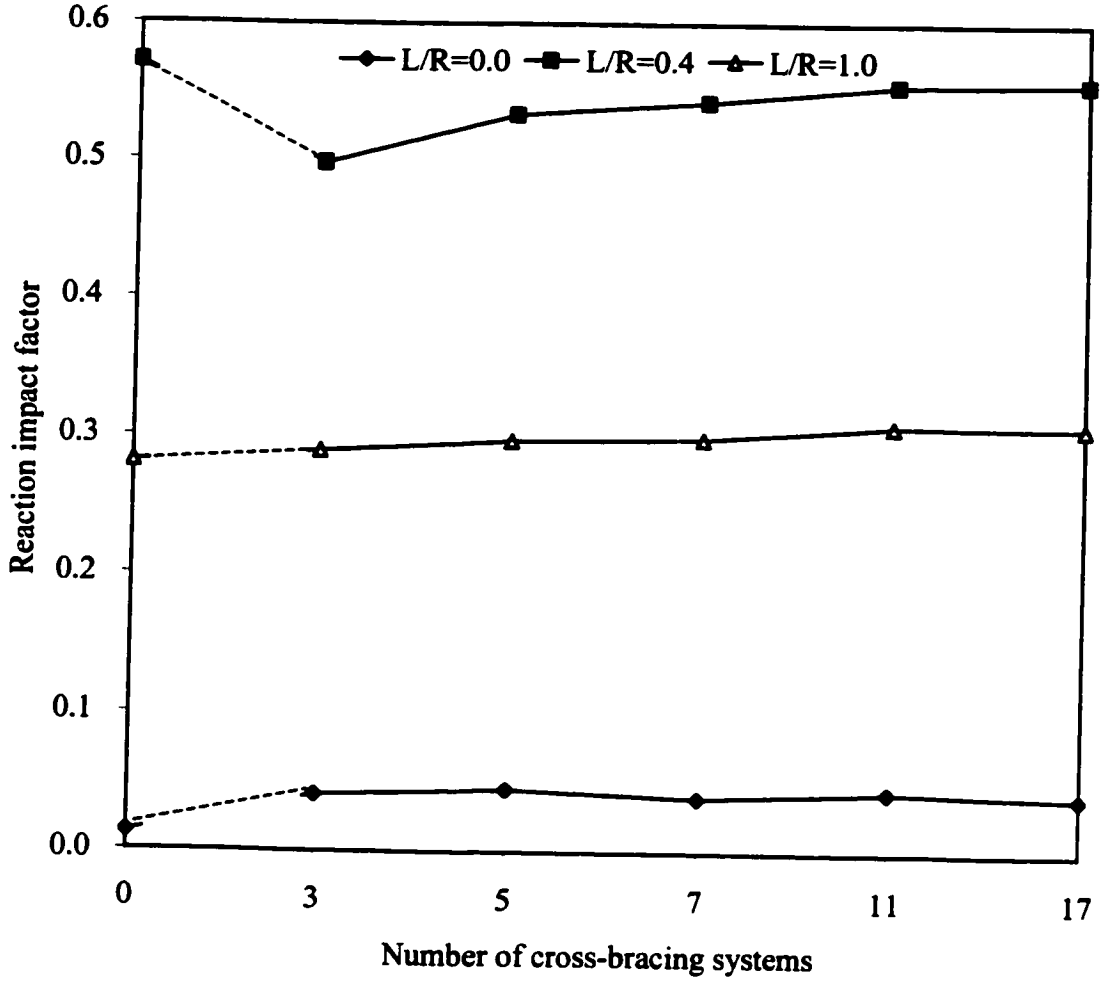

Fig. 7.2. Effect of number of cross-bracing systems on reaction impact factor of *2l-2c-40* bridges
(full loading)

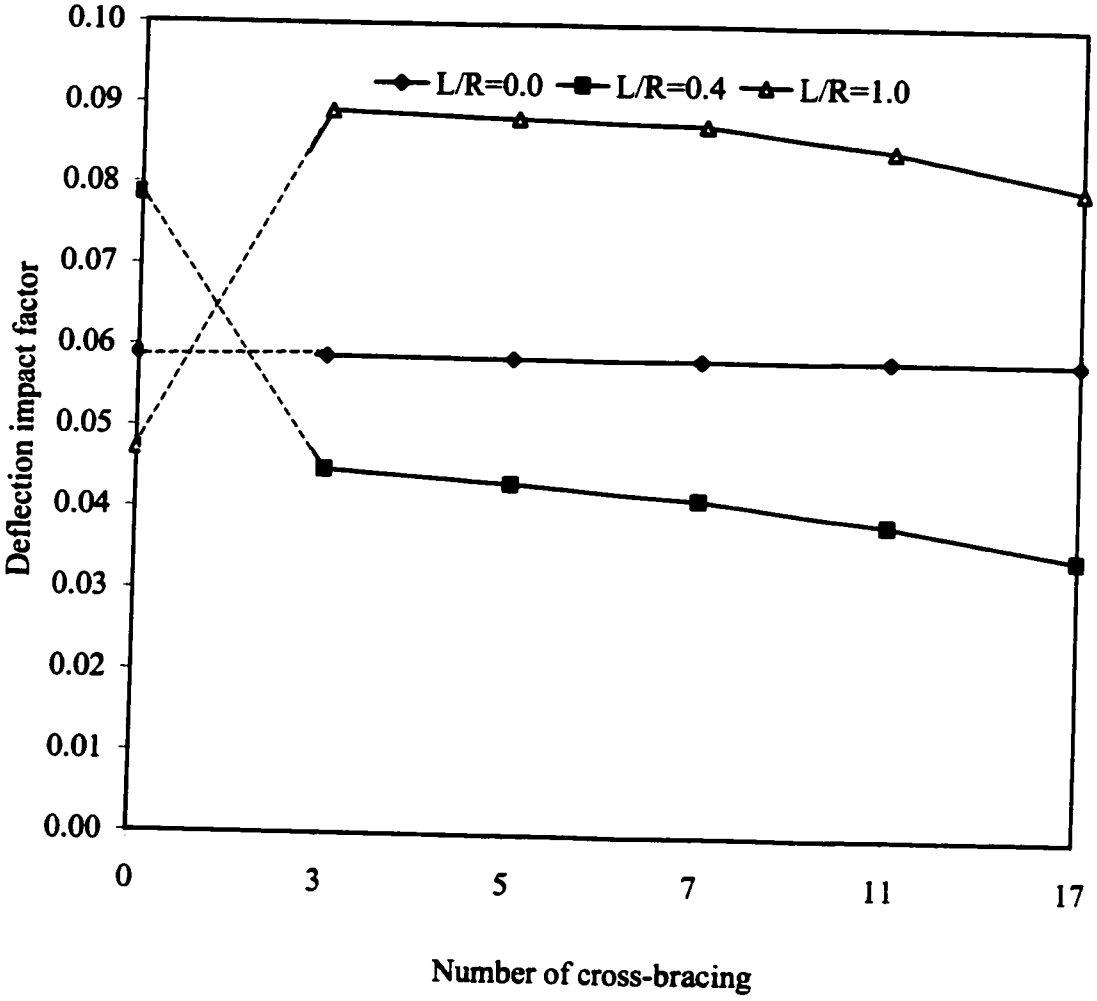

Fig. 7.3. Effect of number of cross-bracing systems on deflection impact factor of *2l-2c-40* bridges (full loading)

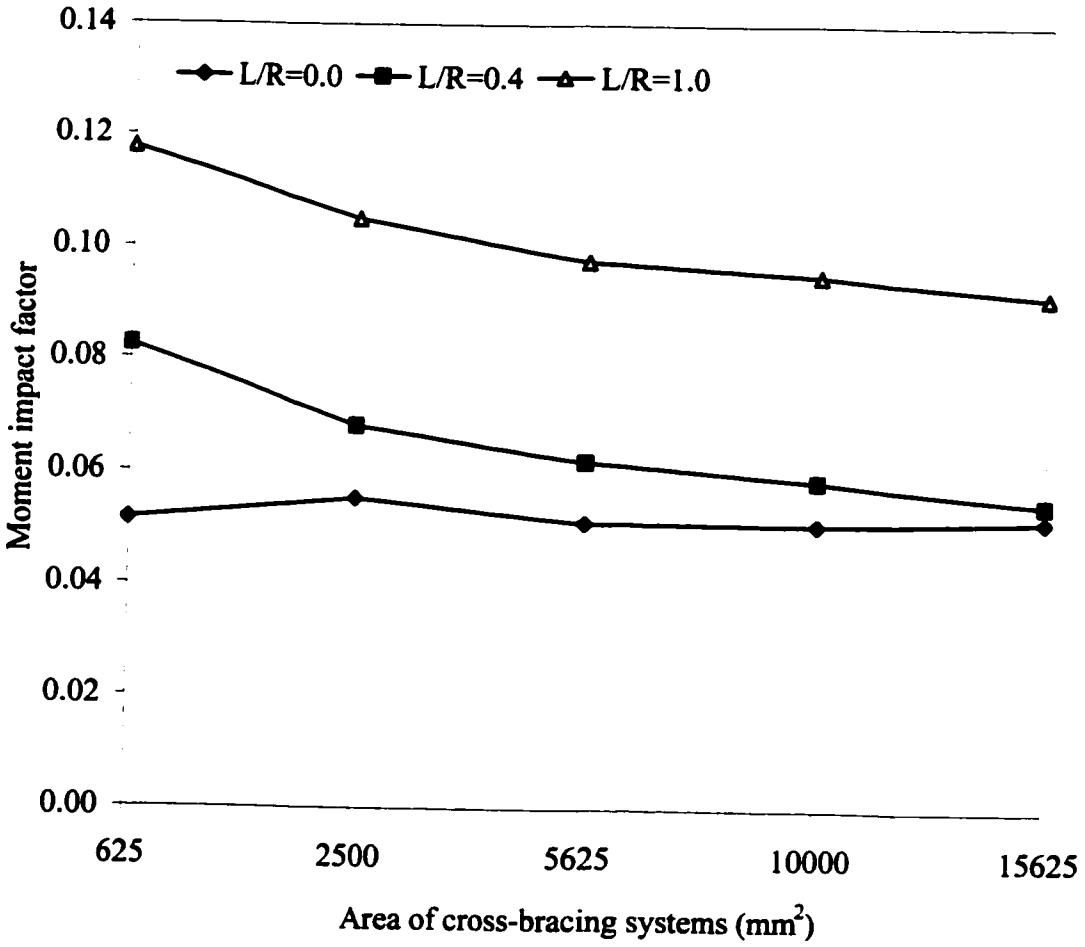

Fig. 7.4. Effect of area of cross-bracing systems on moment impact factor of *2l-2c-40* bridges
(full loading)

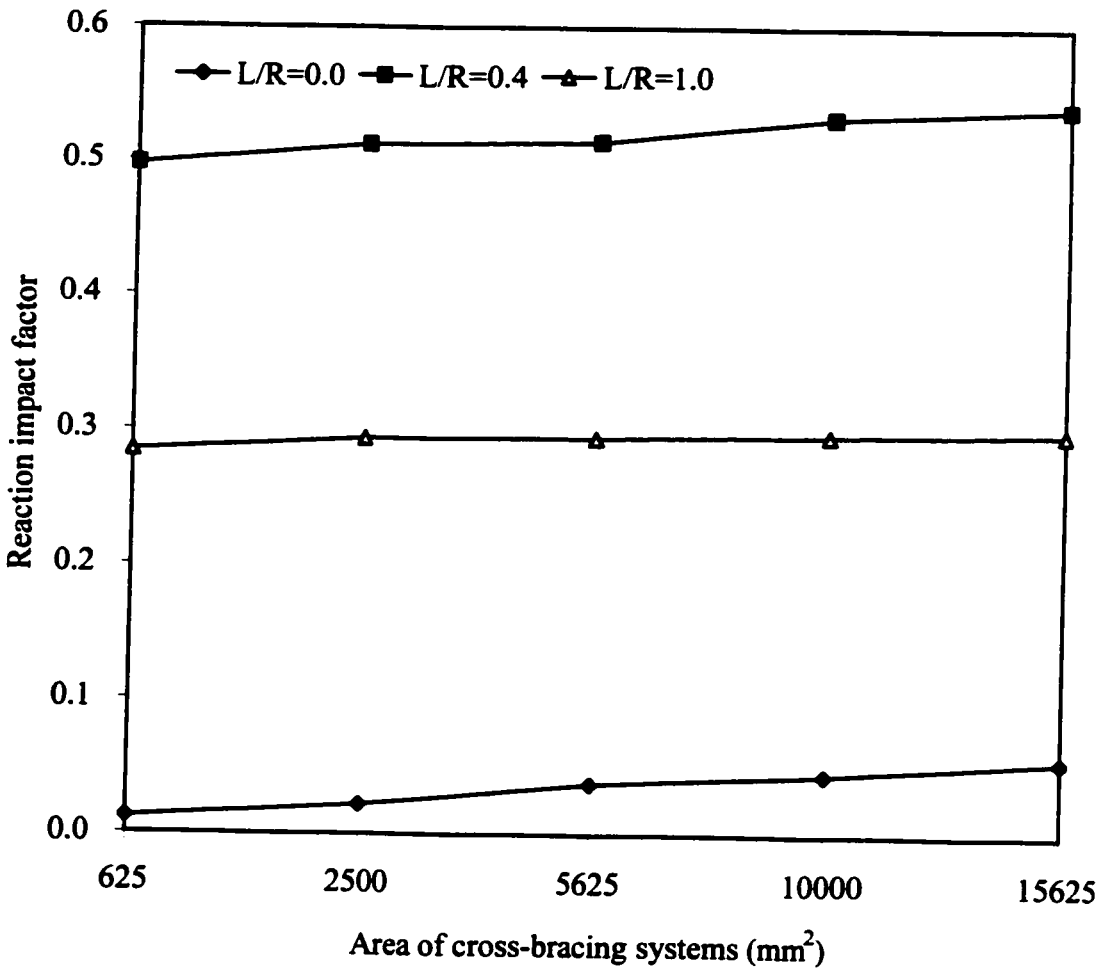

Fig. 7.5. Effect of area of cross-bracing systems on reaction impact factor of *2l-2c-40* bridges
(full loading)

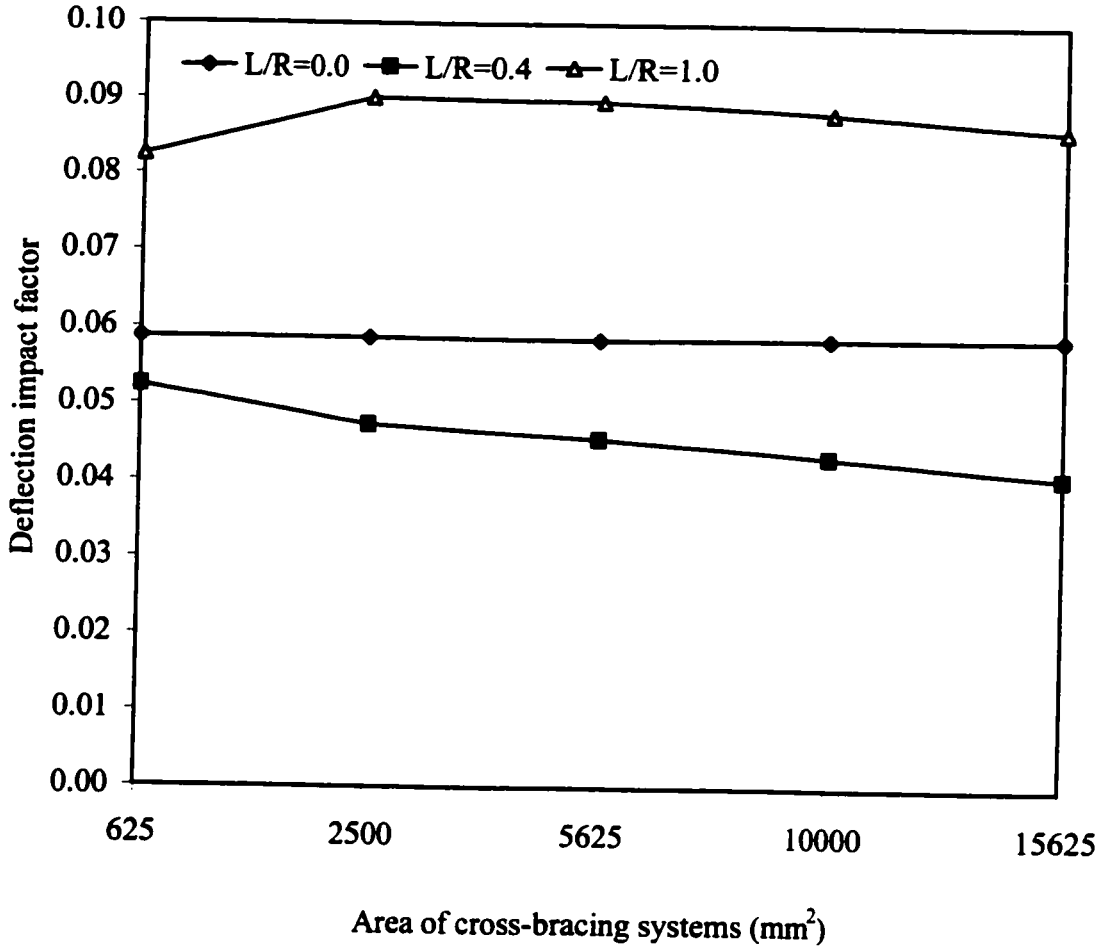

Fig. 7.6. Effect of area of cross-bracing systems on deflection impact factor of *2l-2c-40* bridges
(full loading)

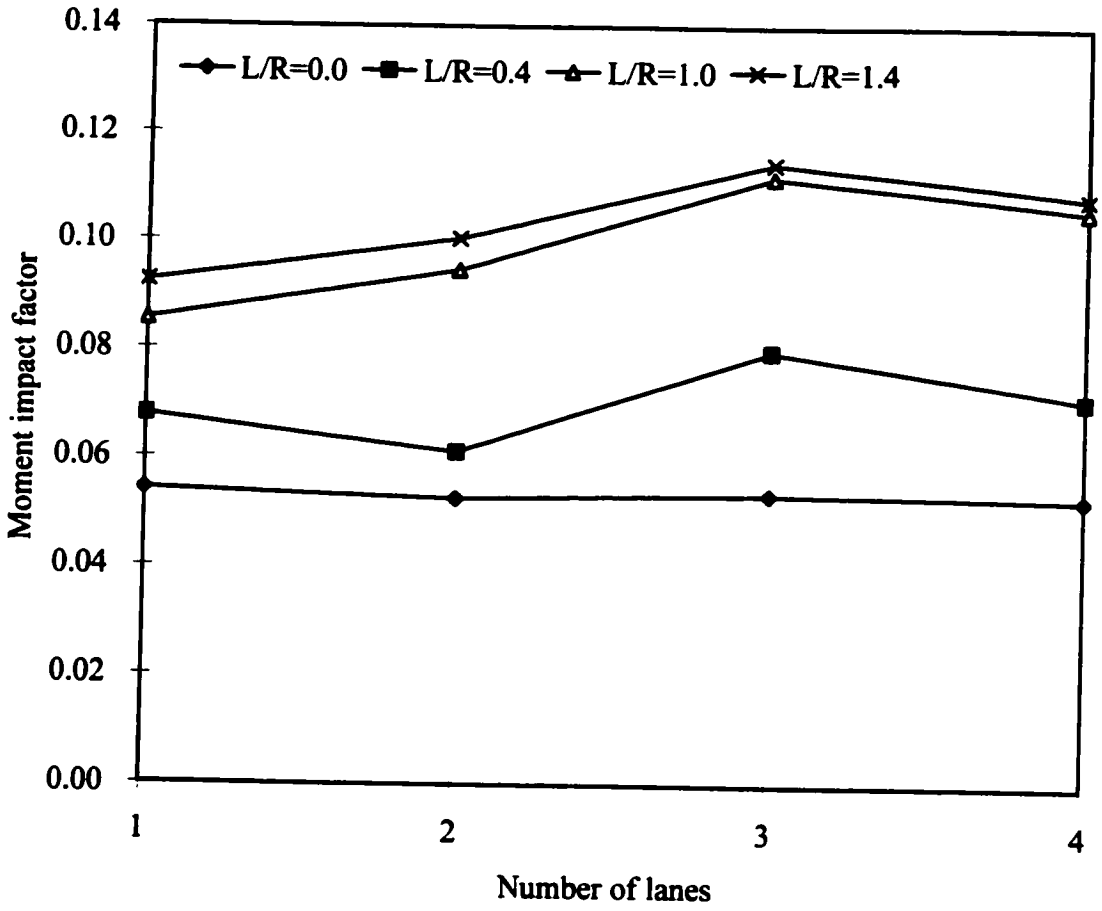

Fig. 7.7. Effect of number of lanes on moment impact factor of *4c-40* bridges (full loading)

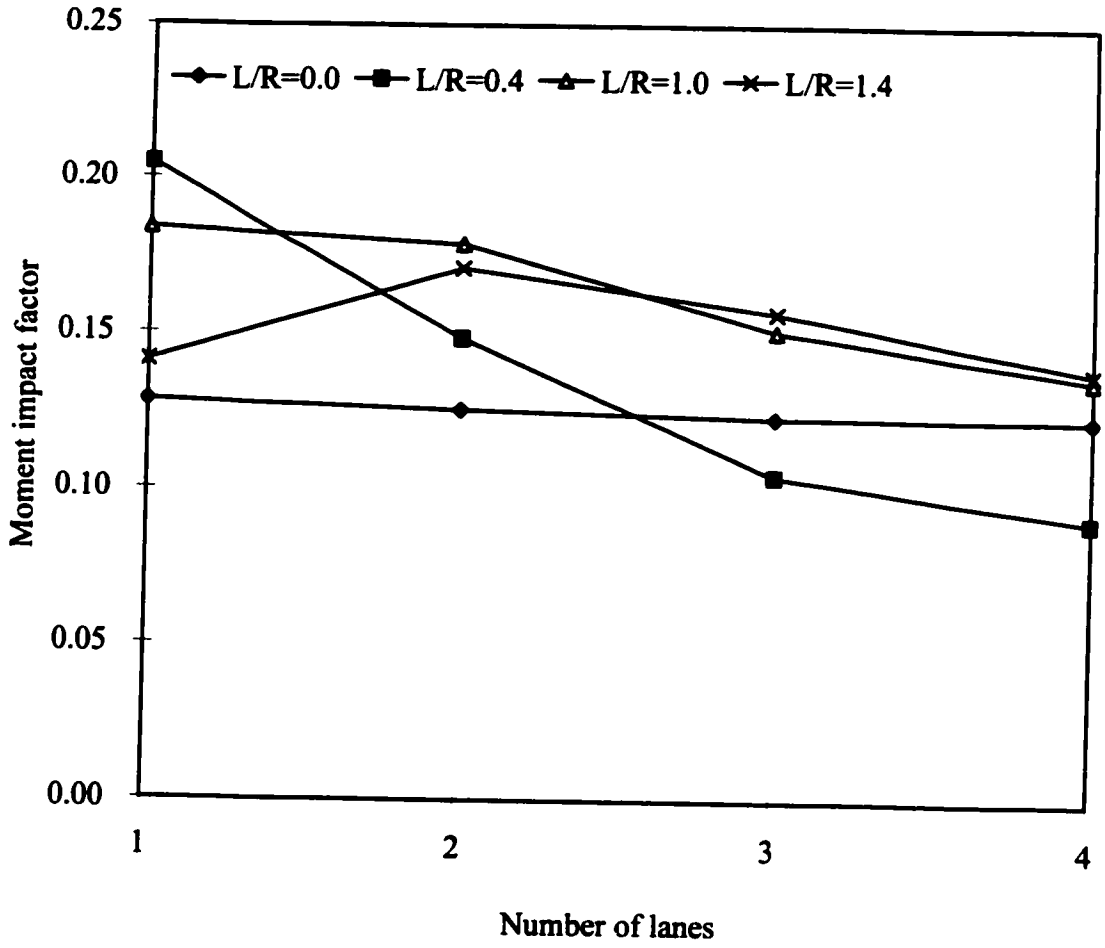

Fig. 7.8. Effect of number of lanes on moment impact factor of *4c-100* bridges (full loading)

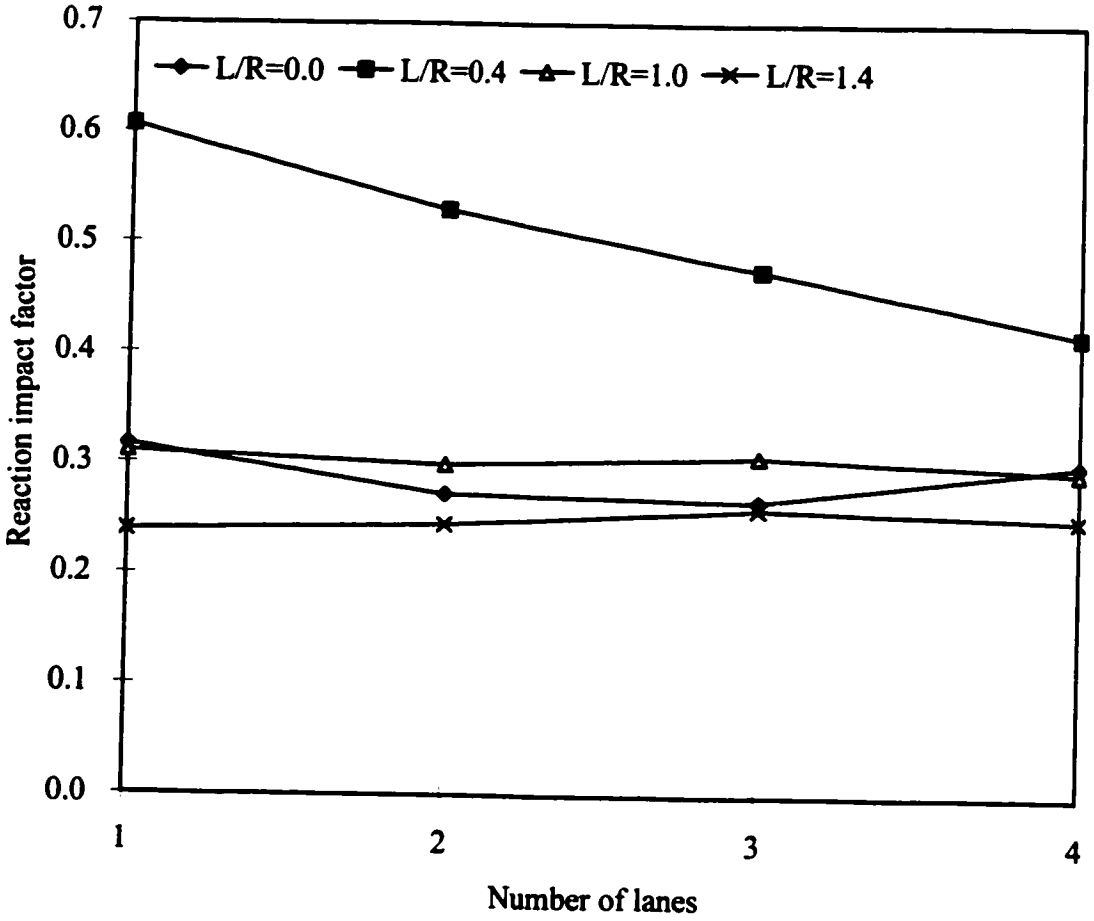

Fig. 7.9. Effect of number of lanes on reaction impact factor of *4c-40* bridges (full loading)

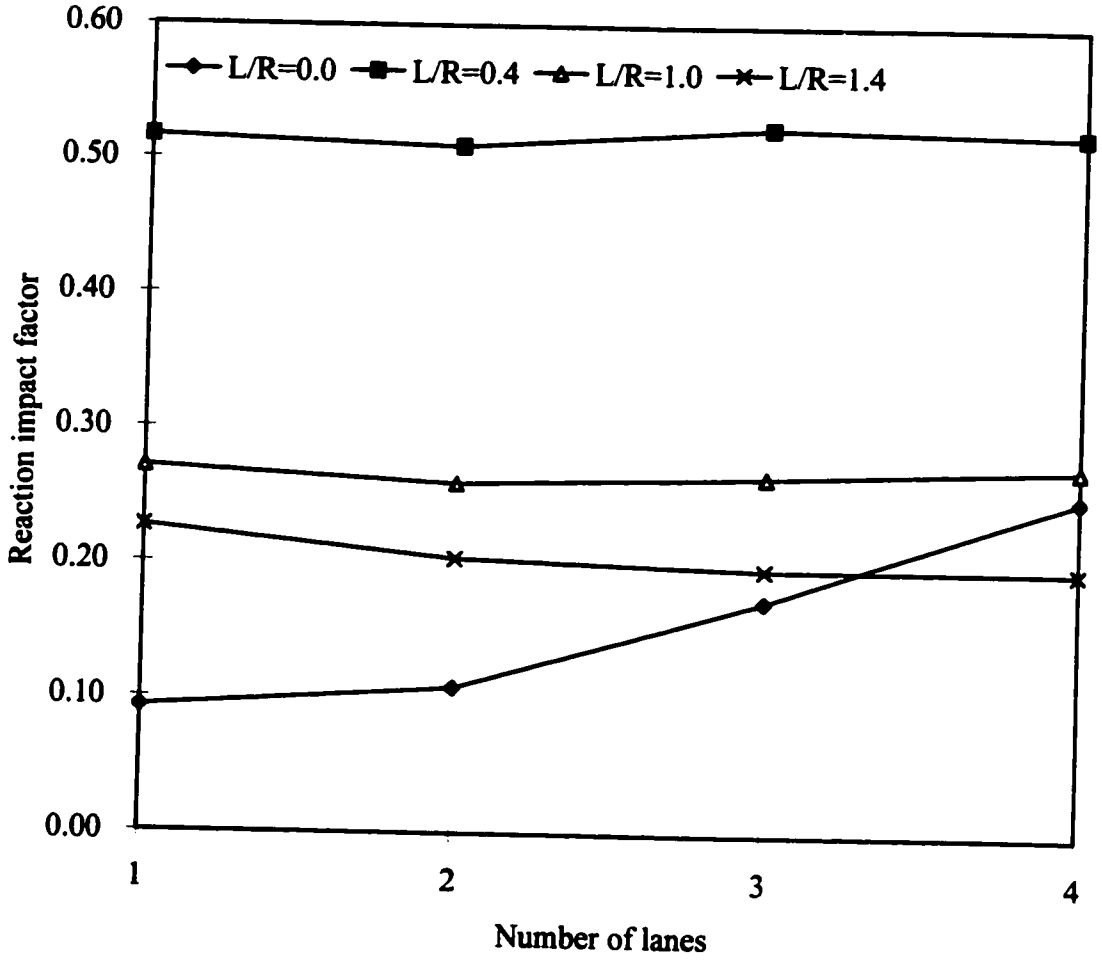

Fig. 7.10. Effect of number of lanes on reaction impact factor
of *4c-100* bridges
(full loading)

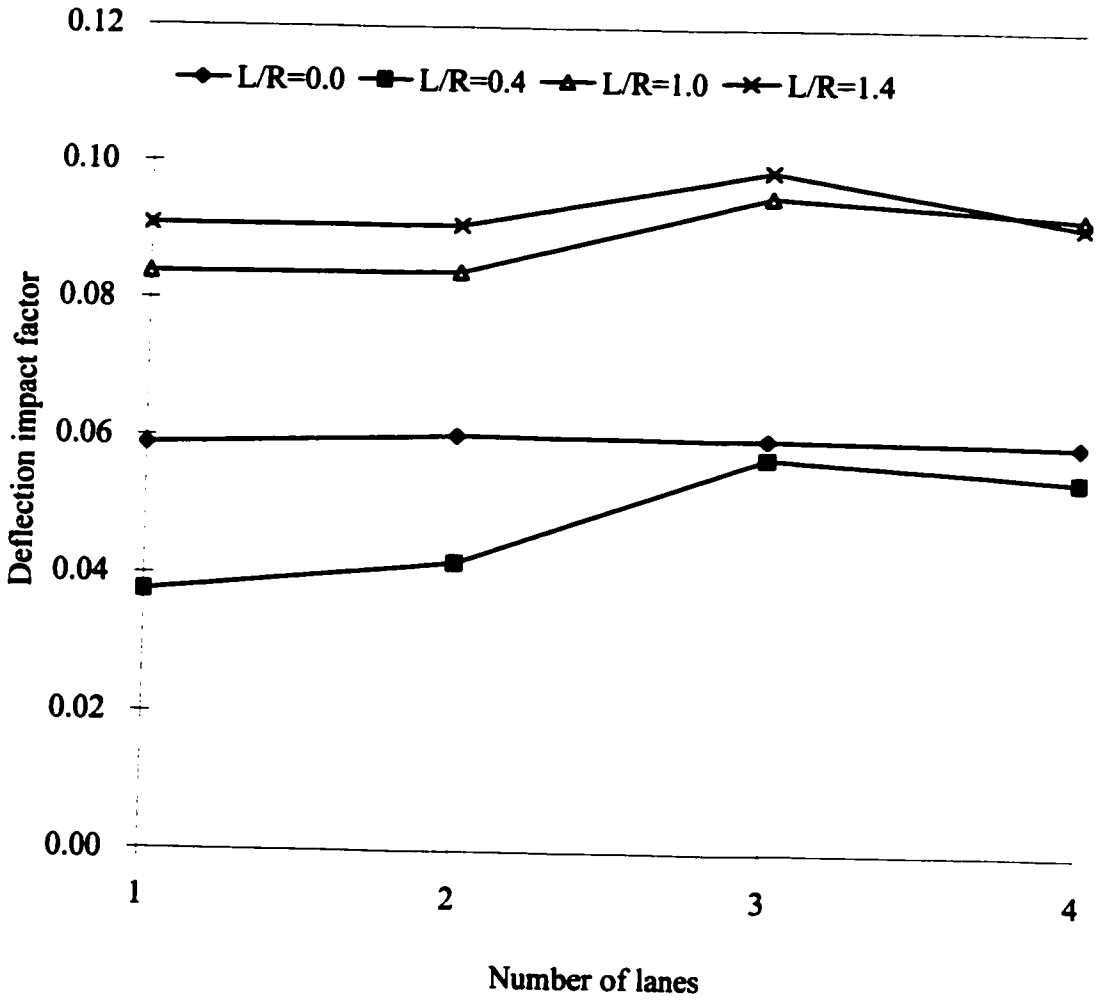

Fig. 7.11. Effect of number of lanes on deflection impact factor of *4c-40* bridges (full loading)

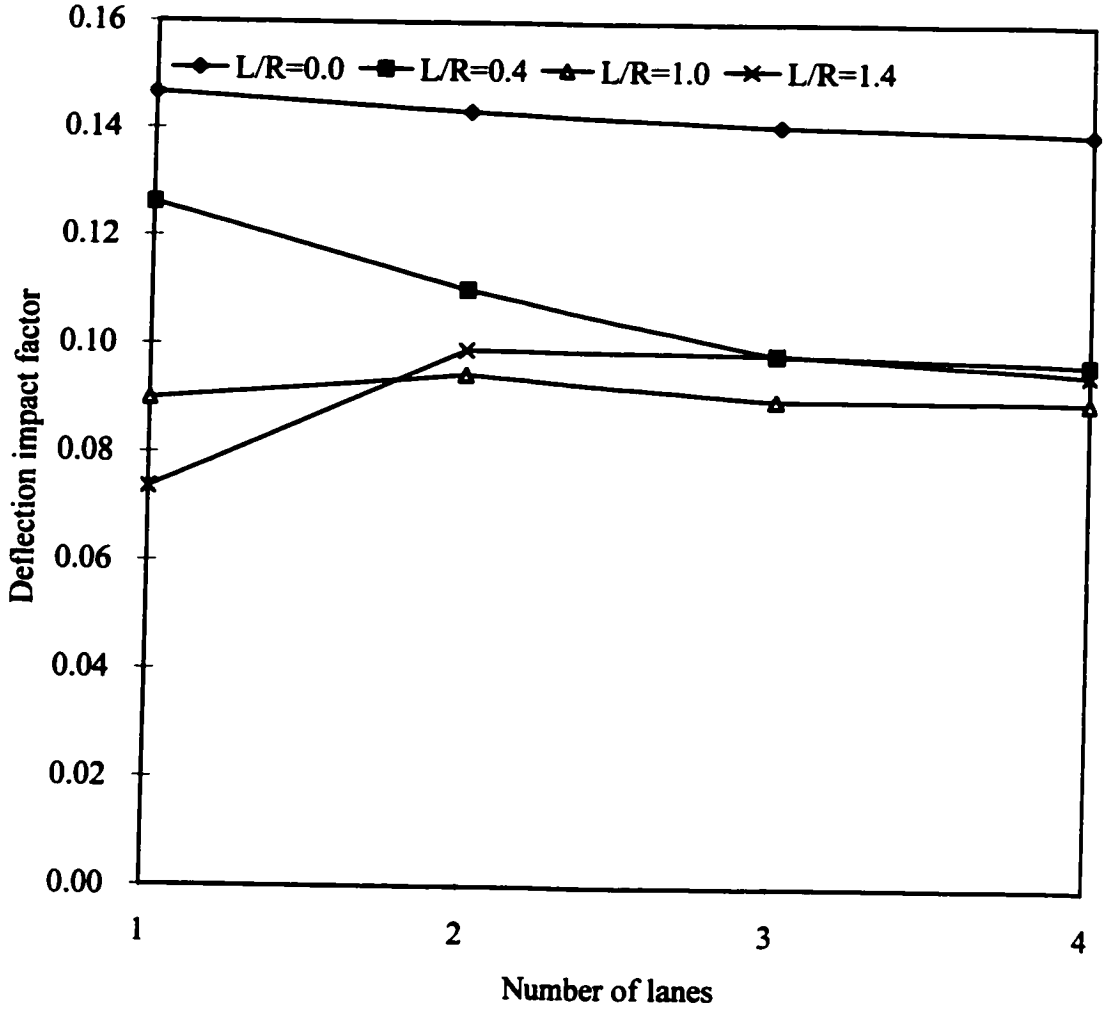

Fig. 7.12. Effect of number of lanes on deflection impact factor of *4c-100* bridges (full loading)

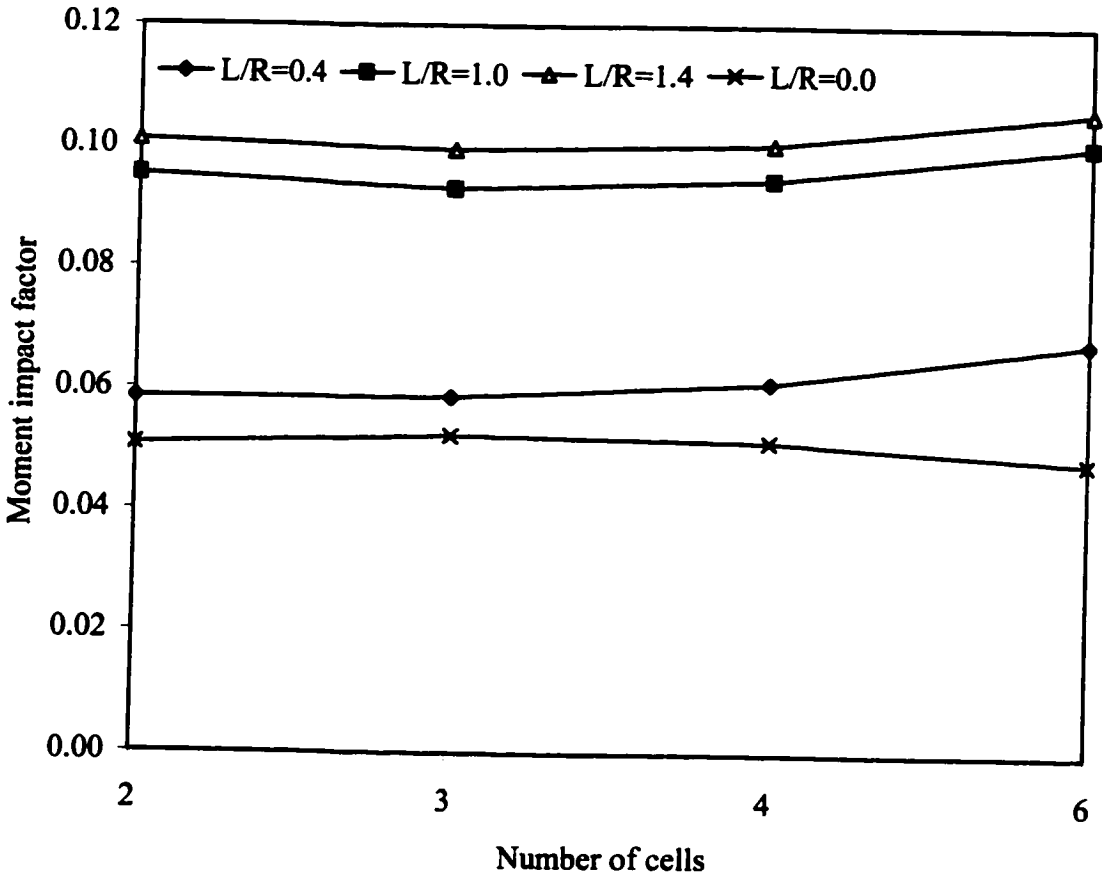

Fig. 7.13. Effect of number of cells on moment impact factor of *2l-40* bridges
(full loading)

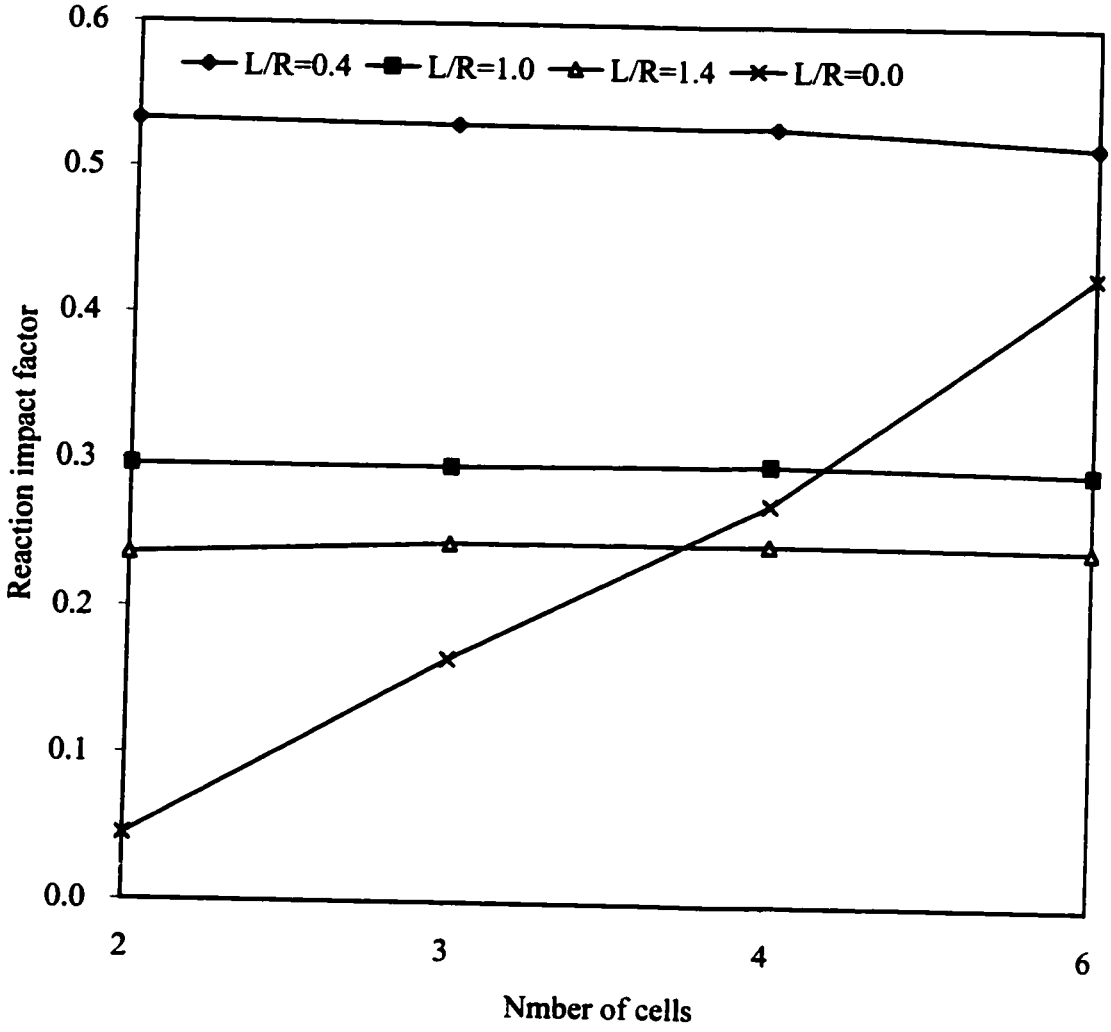

Fig. 7.14. Effect of number of cells on reaction impact factor of *2l-40* bridges
(full loading)

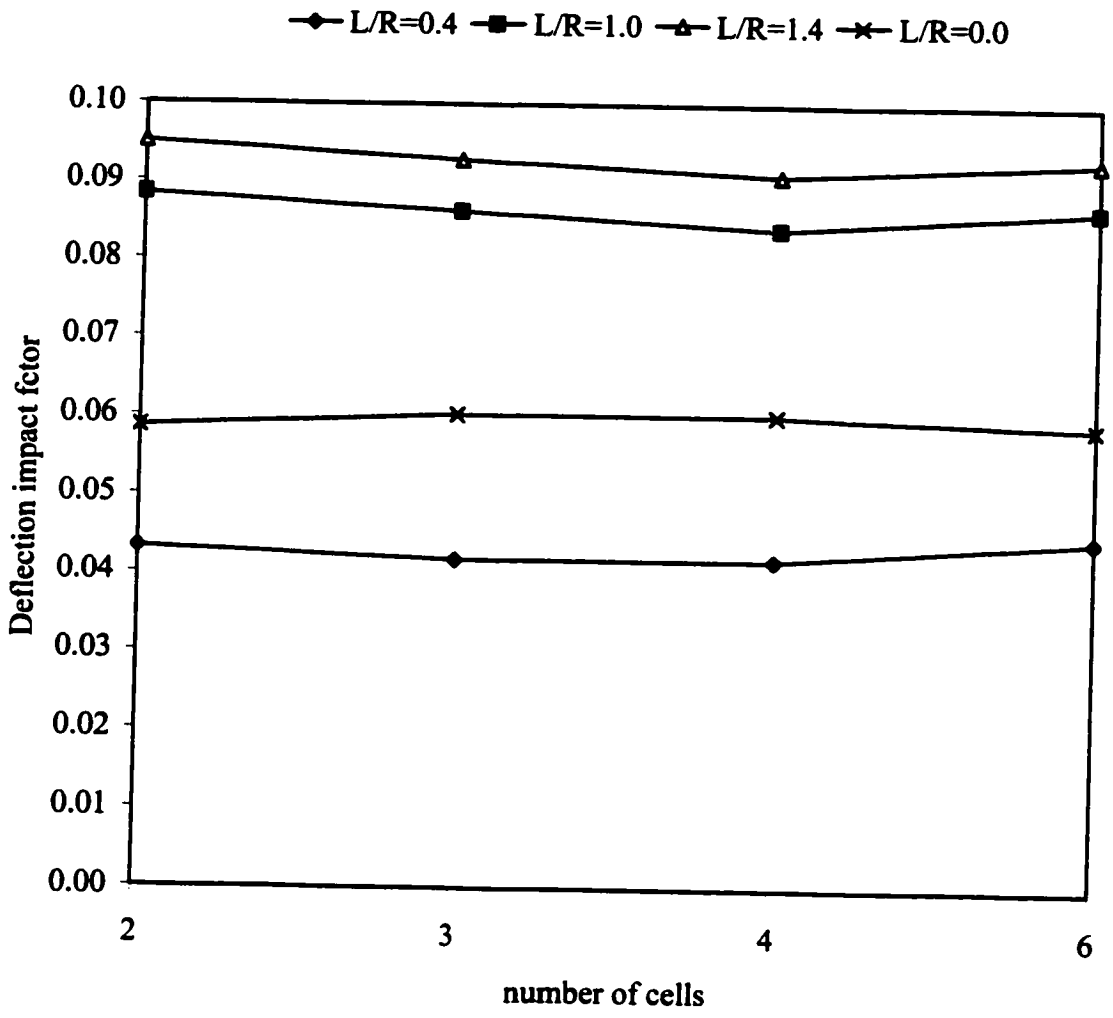

Fig. 7.15. Effect of number of cells on deflection impact factor of *21-40* bridges
(full loading)

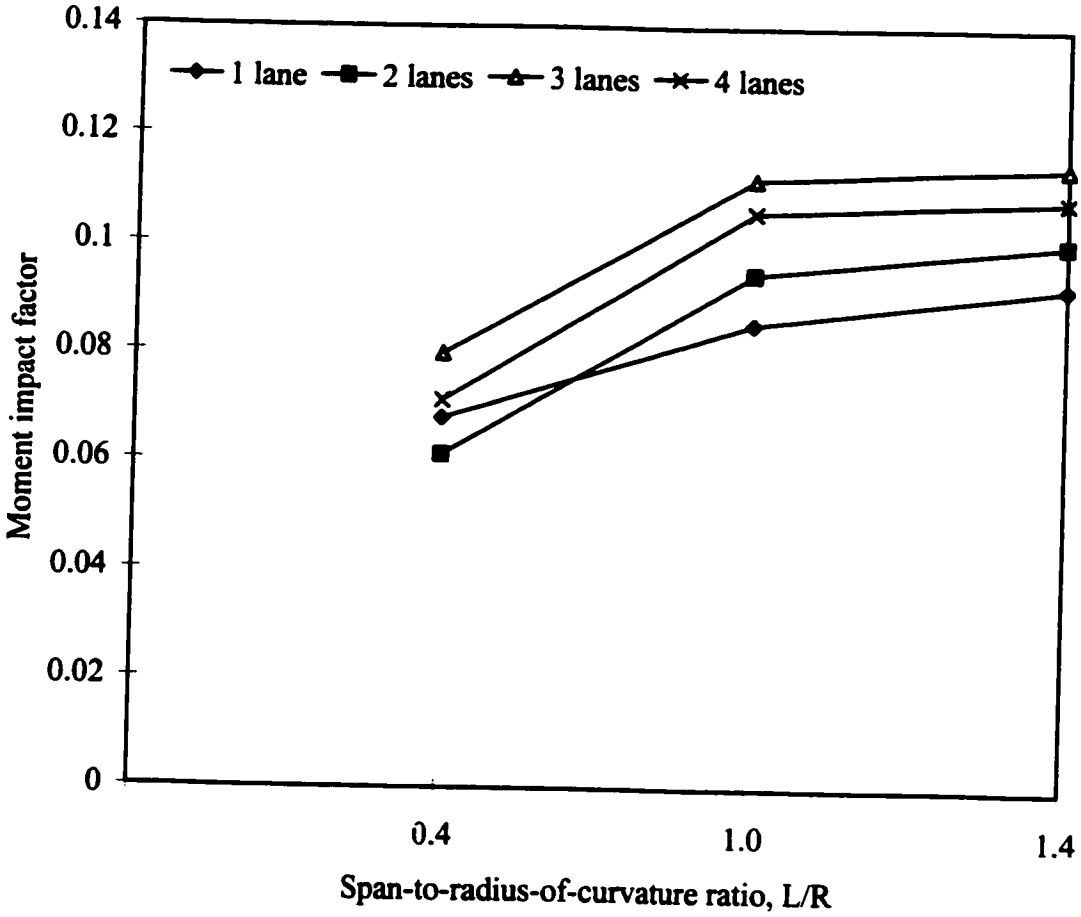

Fig. 7.16. Effect of curvature on moment impact factor
of *4c-40* bridges
(full loading)

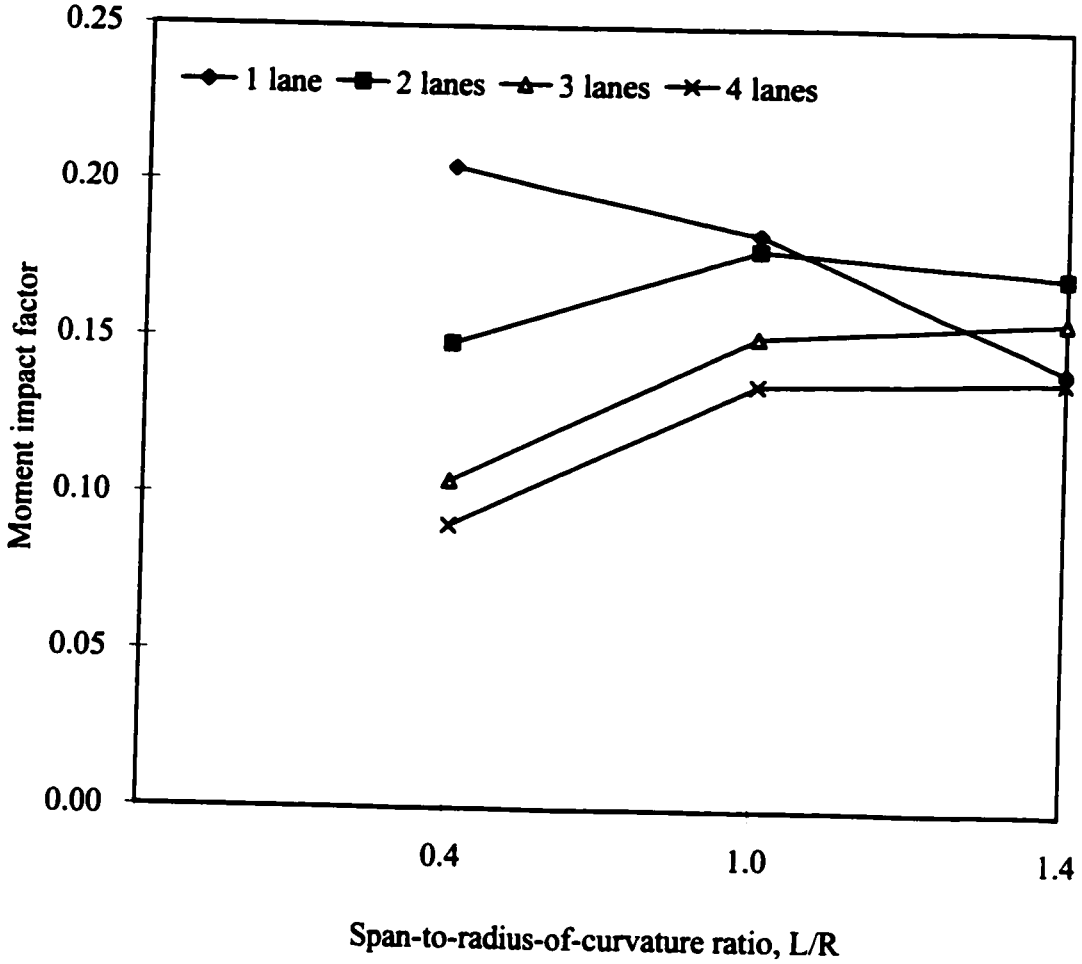

Fig. 7.17. Effect of curvature on moment impact factor
of *4c-100* bridges
(full loading)

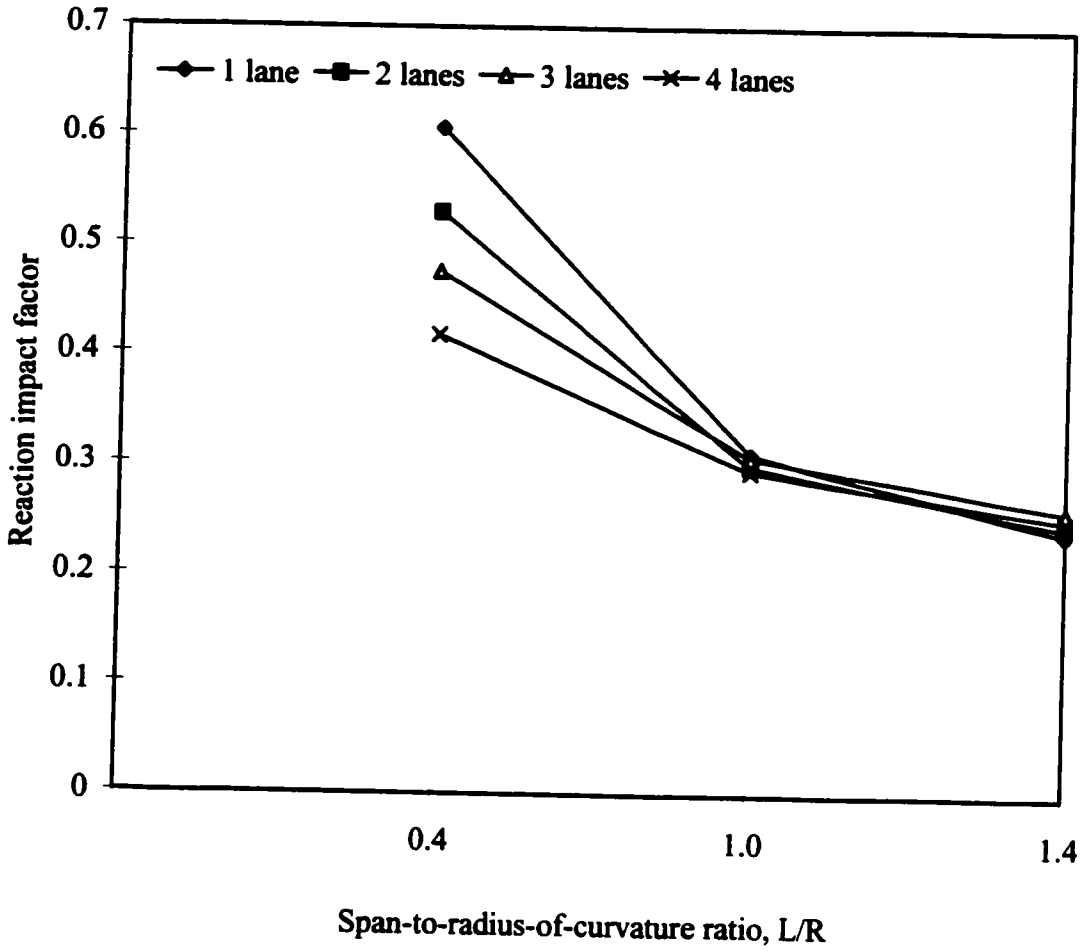

Fig. 7.18. Effect of curvature on reaction impact factor of *4c-40* bridges (full loading)

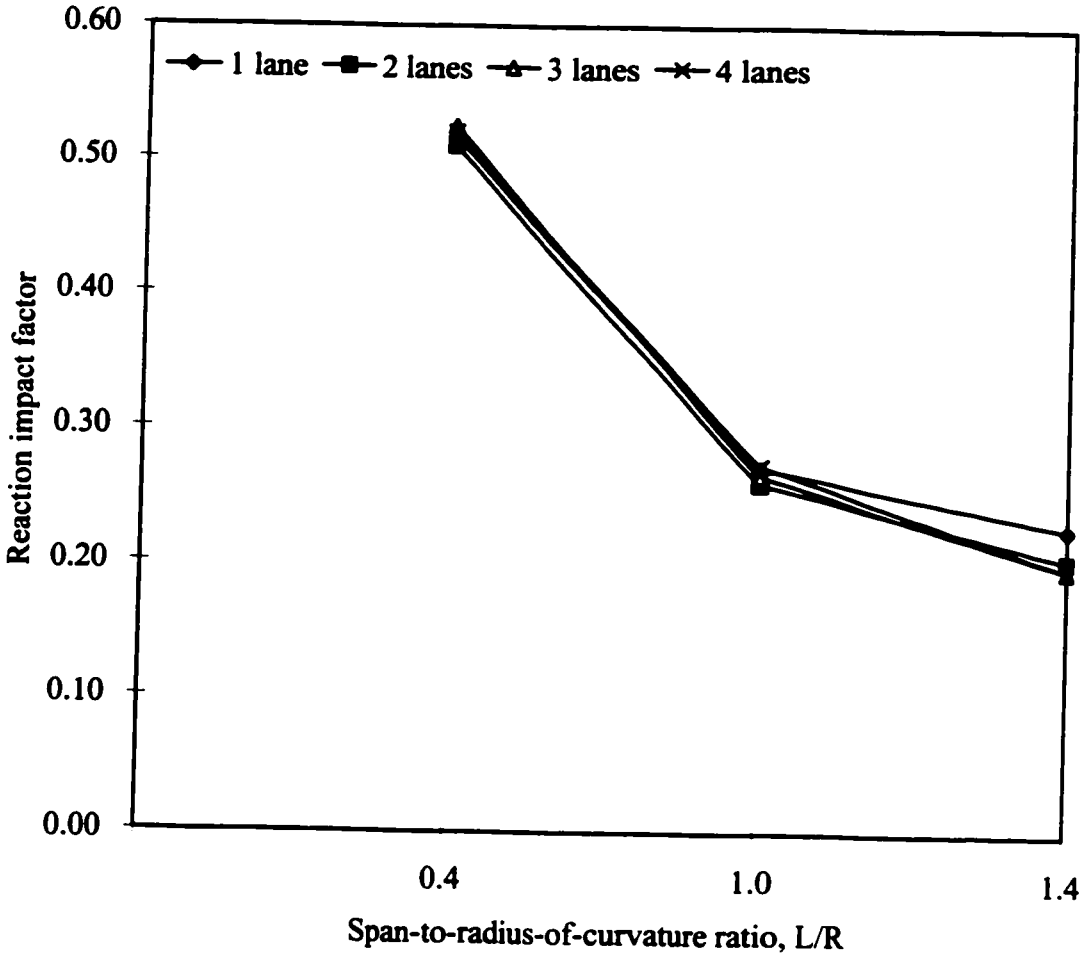

Fig. 7.19. Effect of curvature on reaction impact factor
of *4c-100* bridges
(full loading)

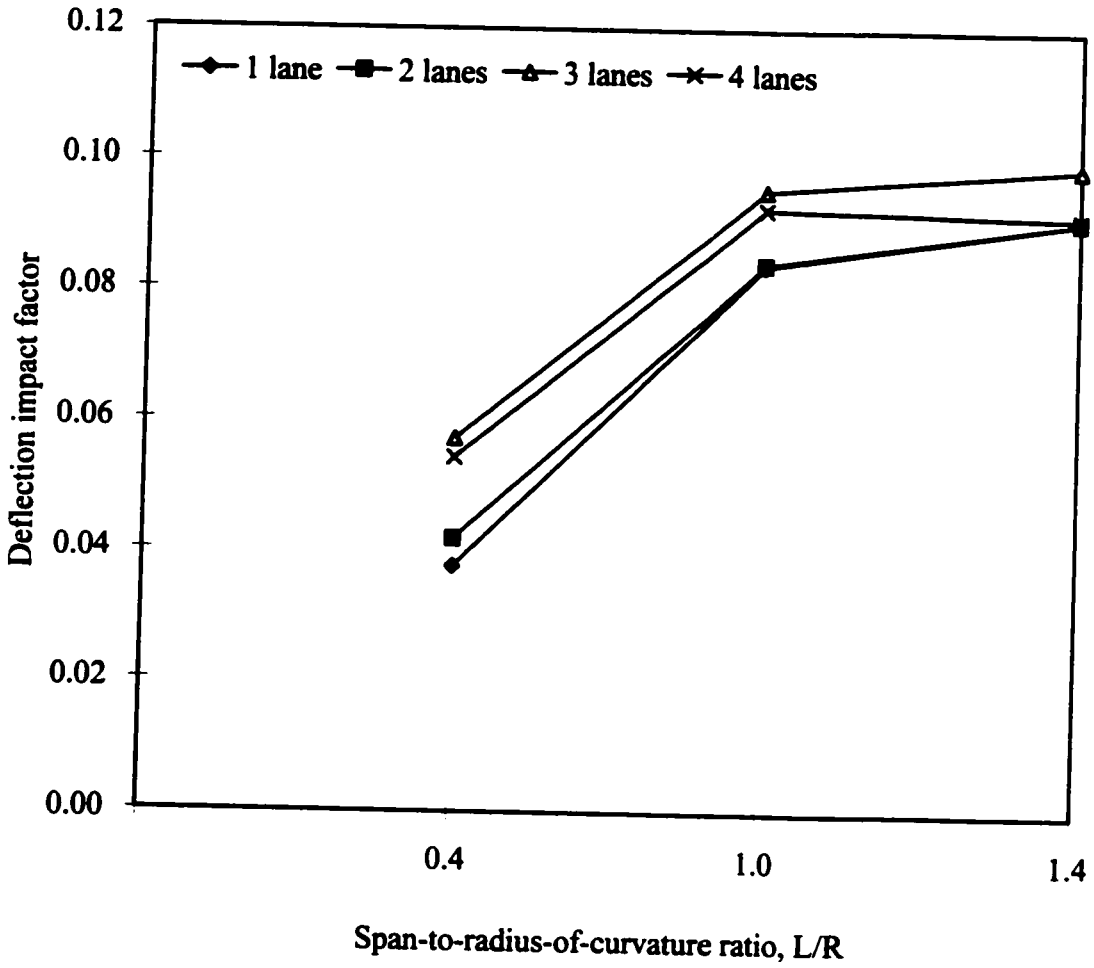

Fig. 7.20. Effect of curvature on deflection impact factor of *4c-40* bridges (full loading)

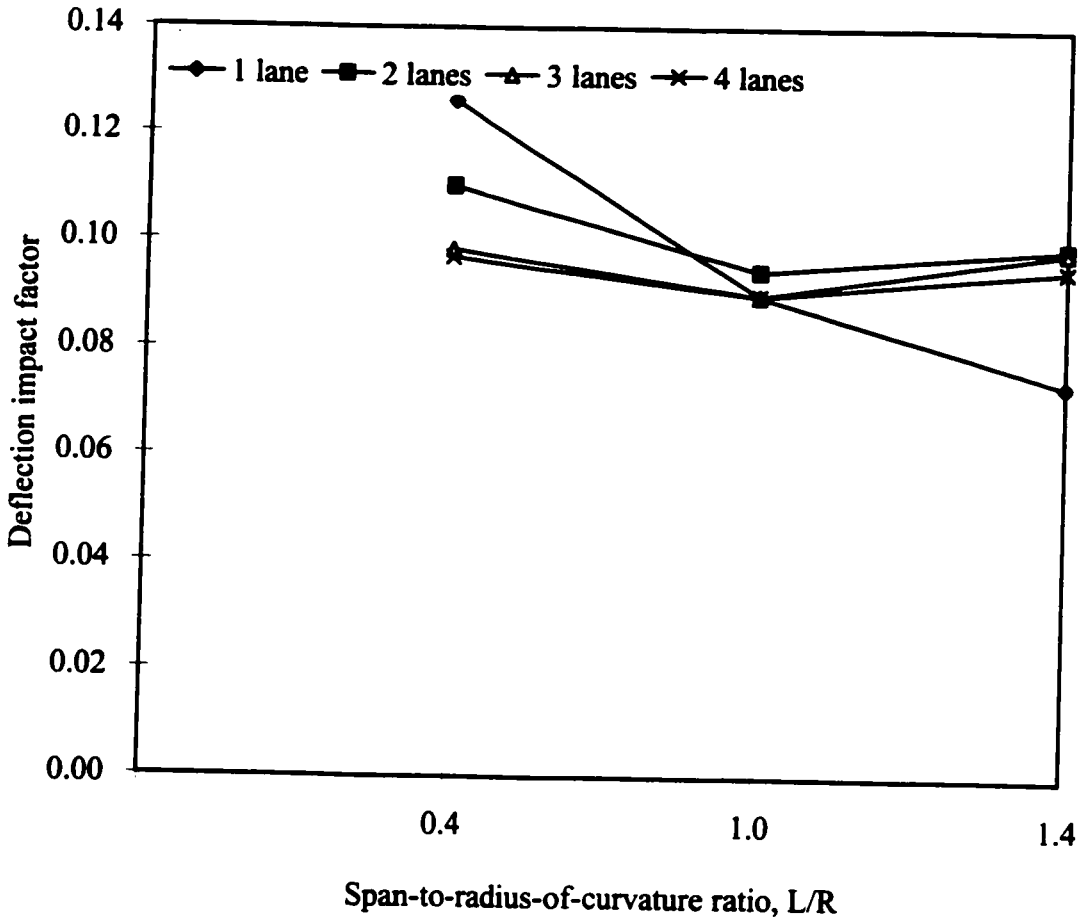

Fig. 7.21. Effect of curvature on deflection impact factor
of *4c-100* bridges
(full loading)

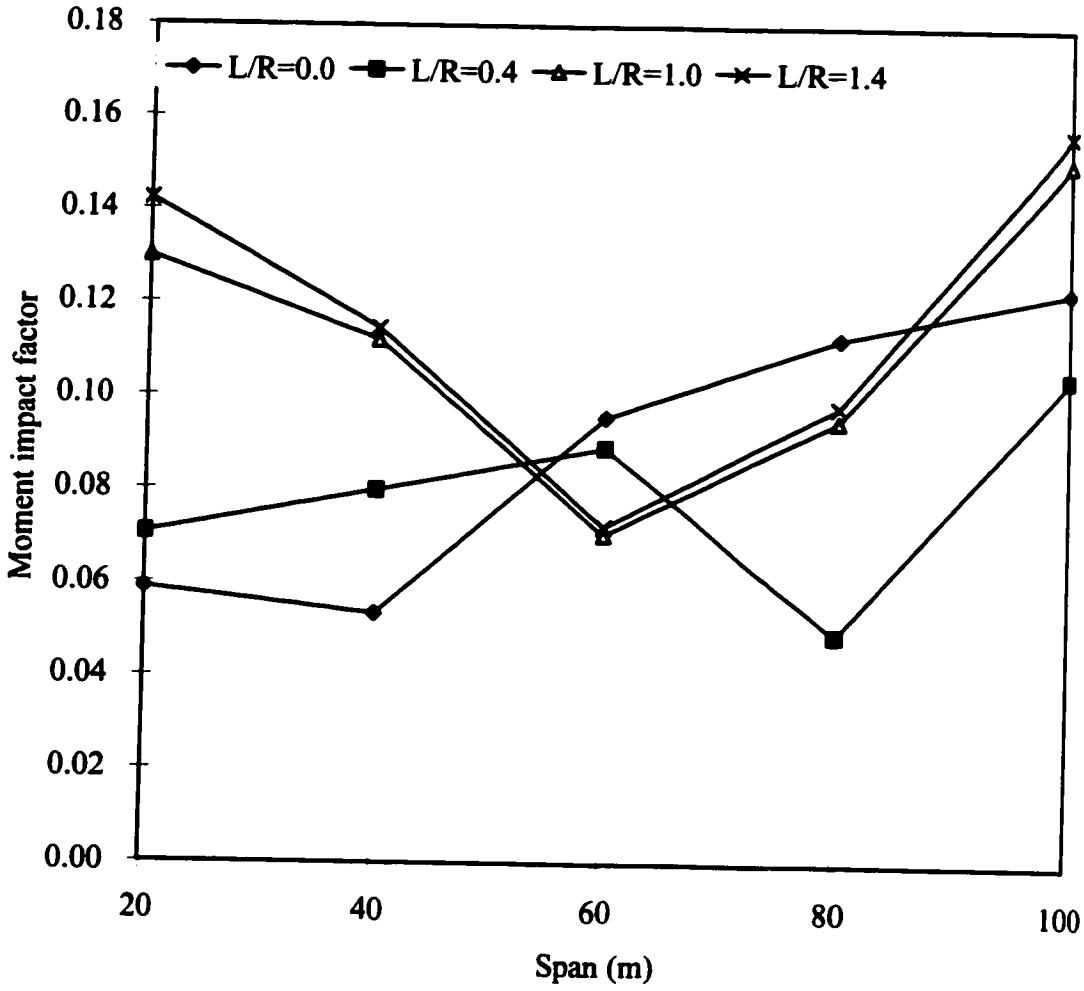

Fig. 7.22. Effect of span on moment impact factor
of *3l-4c* bridges
(full loading)

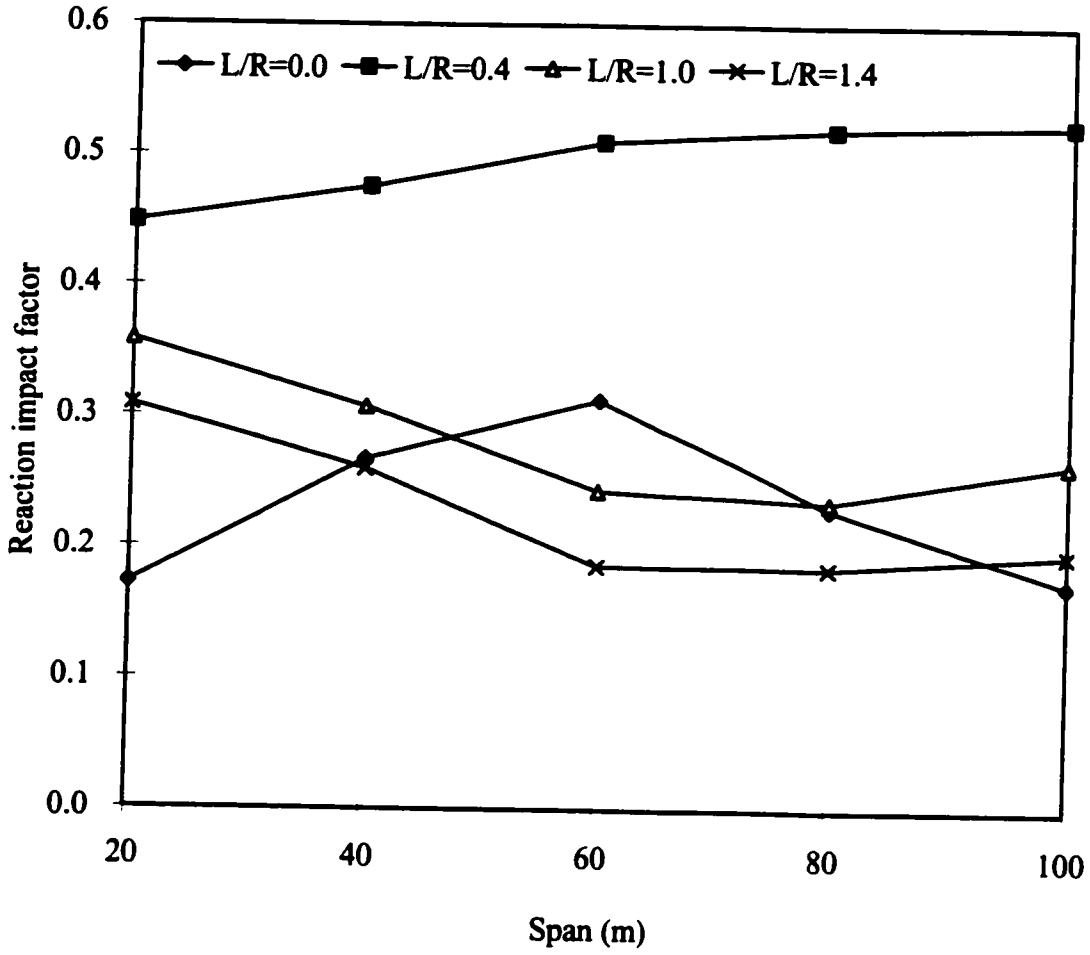

Fig. 7.23. Effect of span on reaction impact factor of *3l-4c* bridges (full loading)

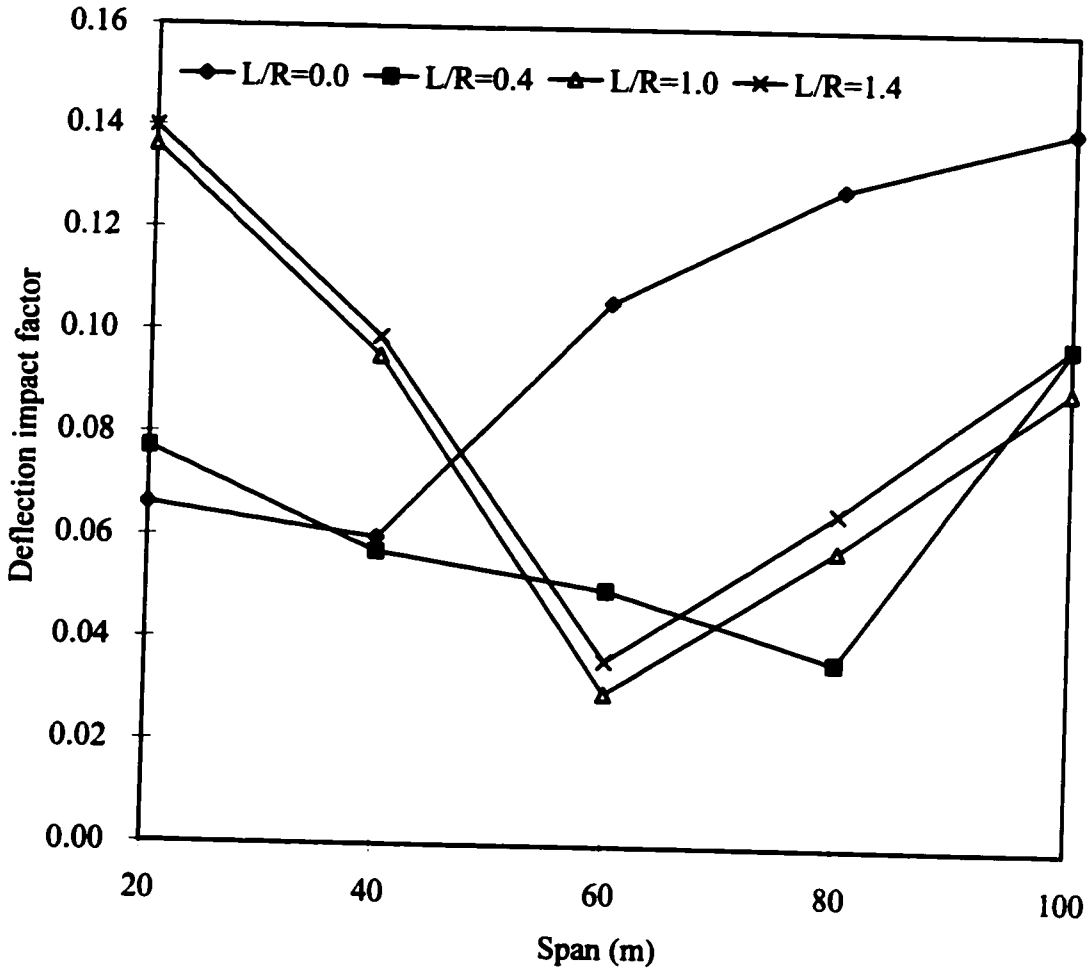

Fig. 7.24. Effect of span on deflection impact factor of *3l-4c* bridges (full loading)

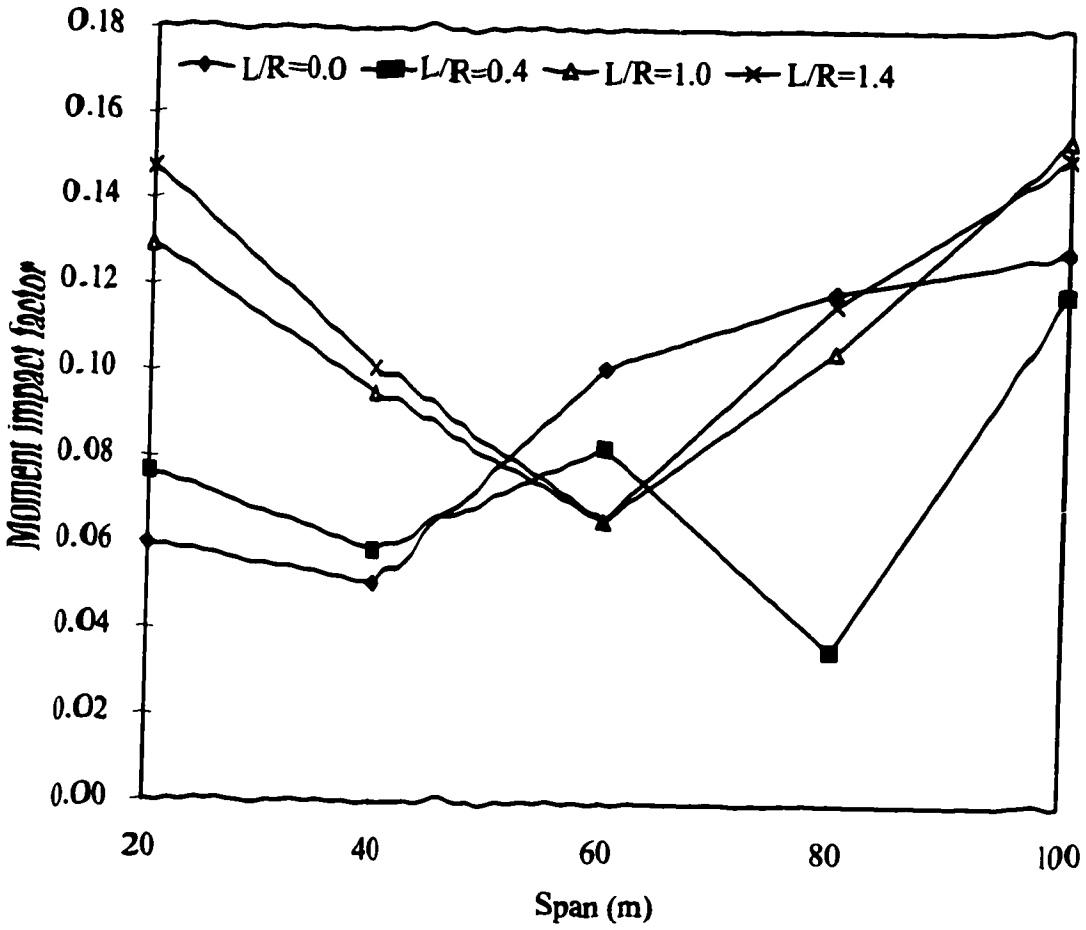

Fig. 7.25. Effect of span on moment impact factor of *2l-2c* bridges (full loading)

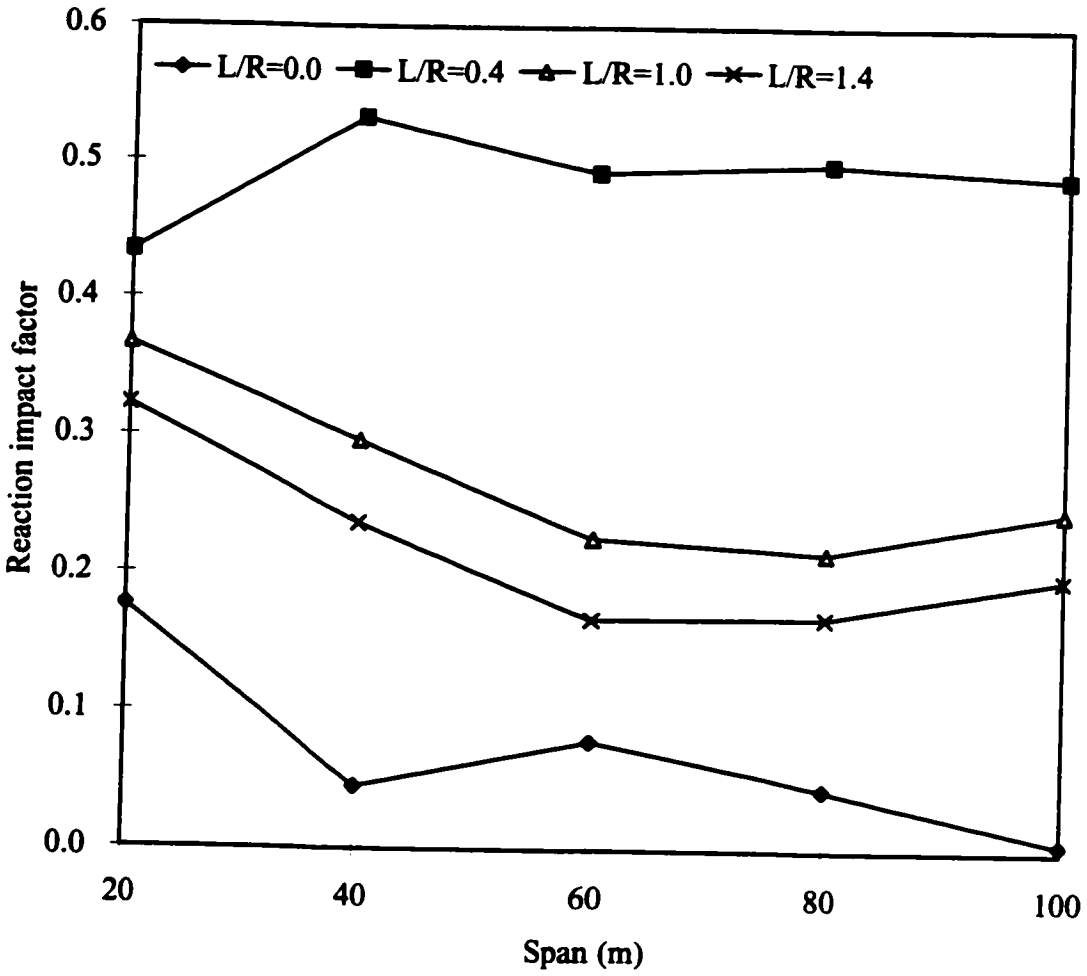

Fig. 7.26. Effect of span on reaction impact factor of *2l-2c* bridges (full loading)

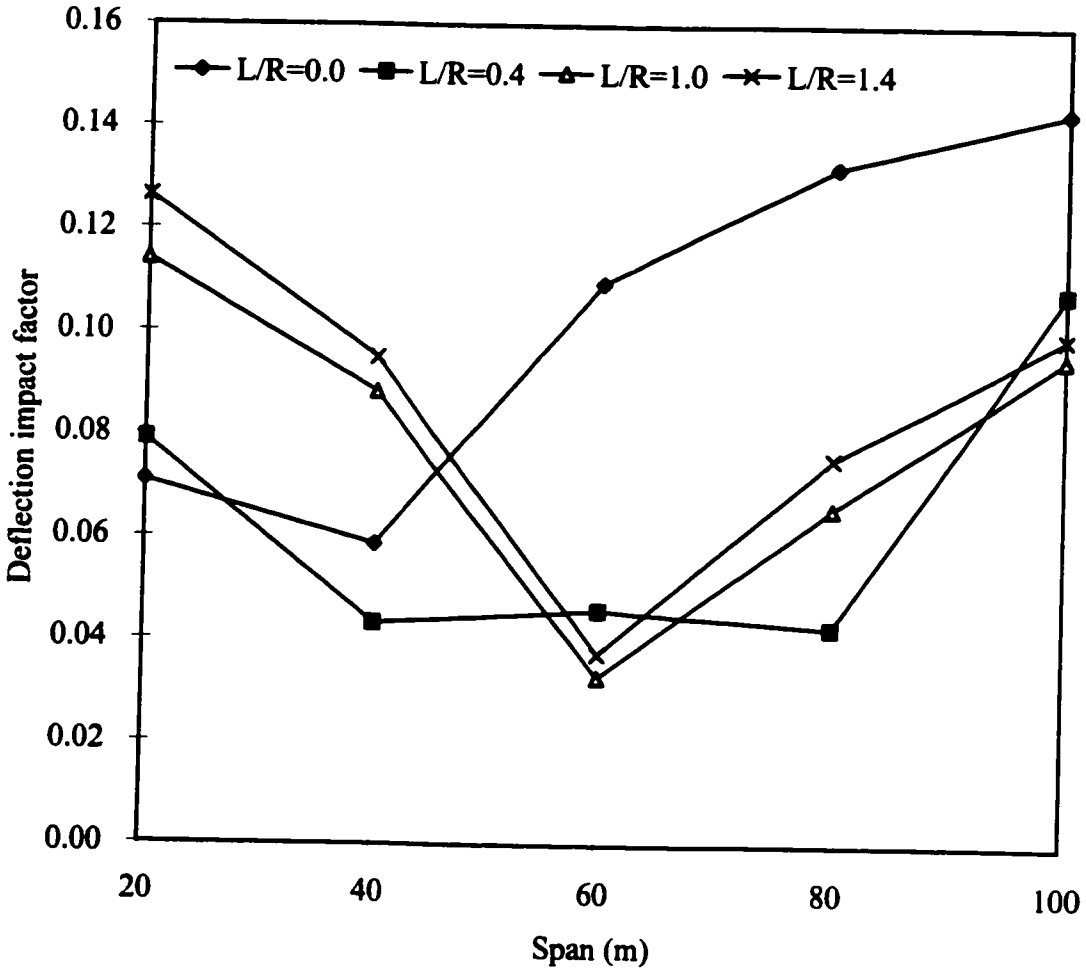

Fig. 7.27. Effect of span on deflection impact factor of *2l-2c* bridges (full loading)

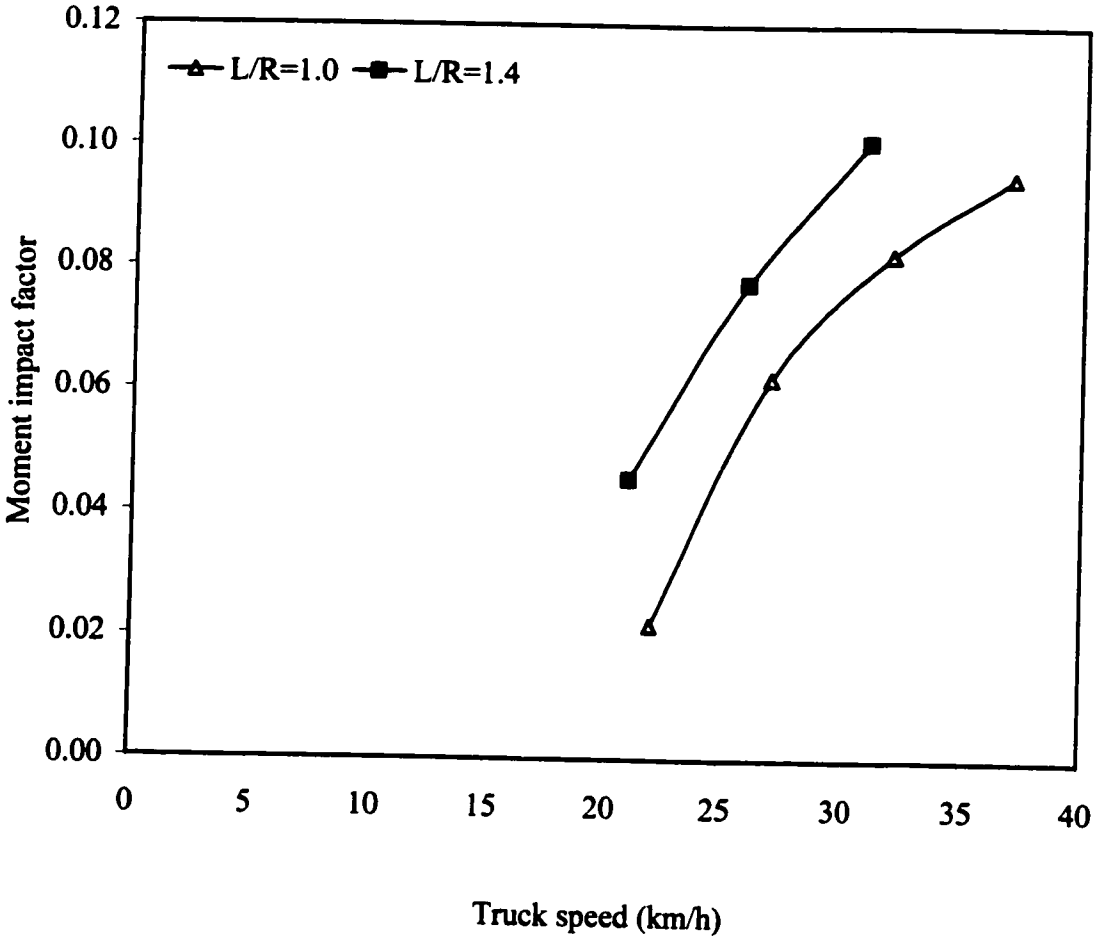

Fig. 7.28. Effect of truck speed on moment impact factor of *2l-2c-40* bridges (full loading)

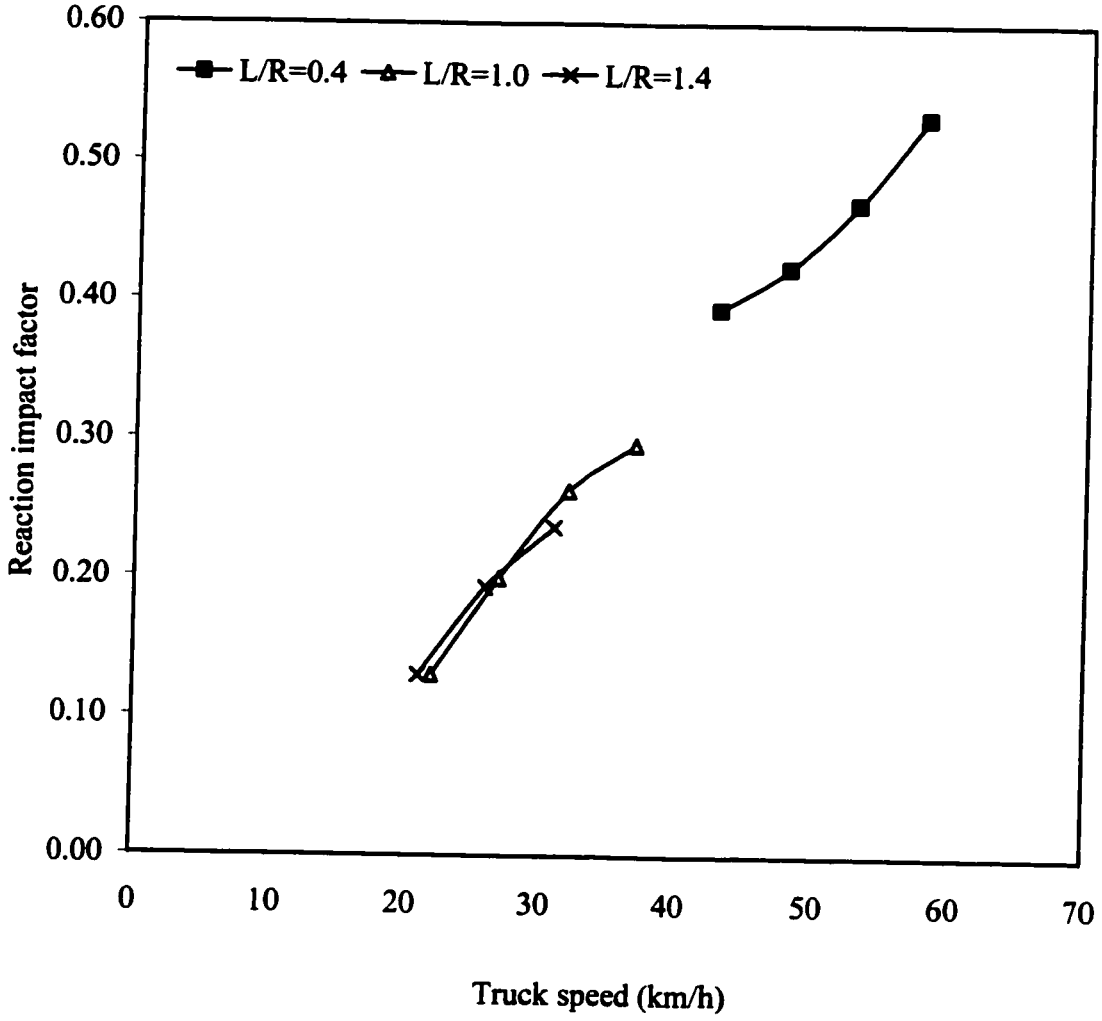

Fig. 7.29. Effect of truck speed on reaction impact factor of *2l-2c-40* bridges (full loading)

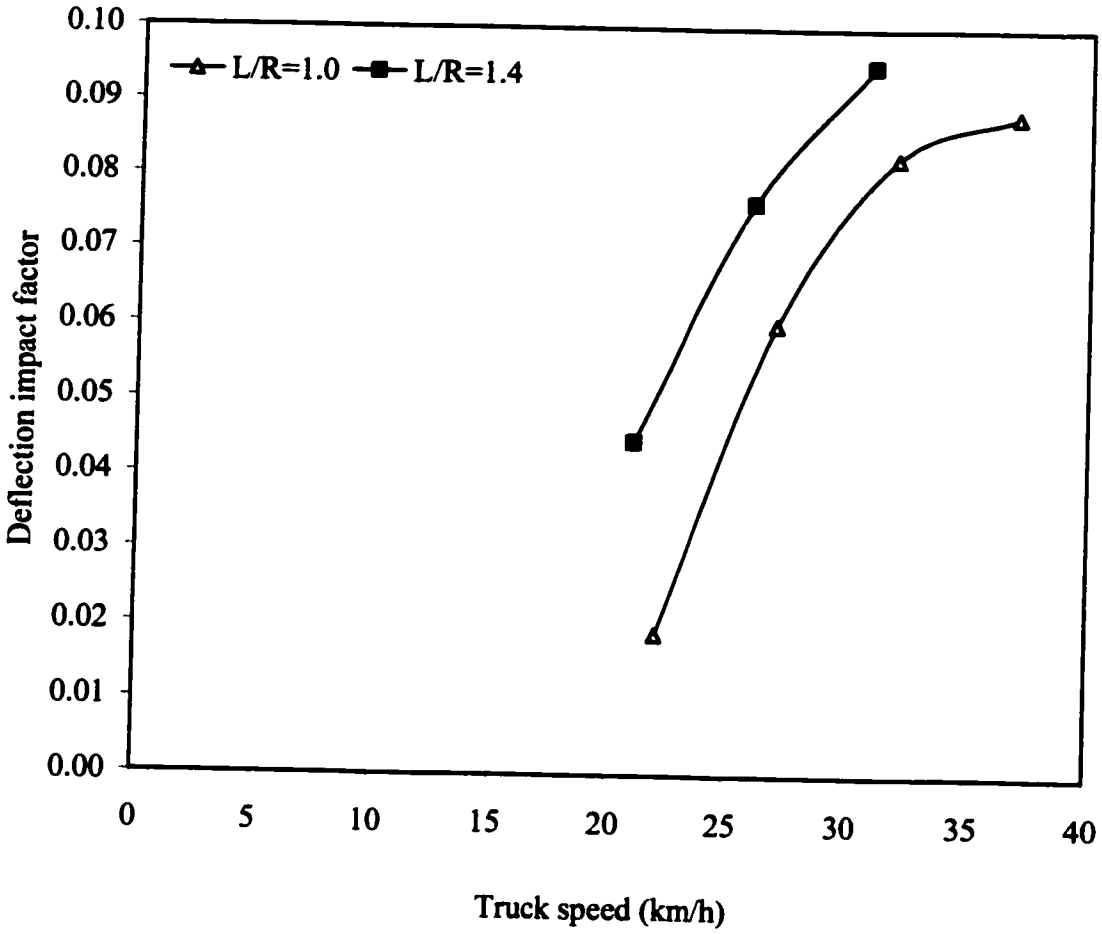

Fig. 7.30. Effect of truck speed on deflection impact factor of *2l-2c-40* bridges (full loading)

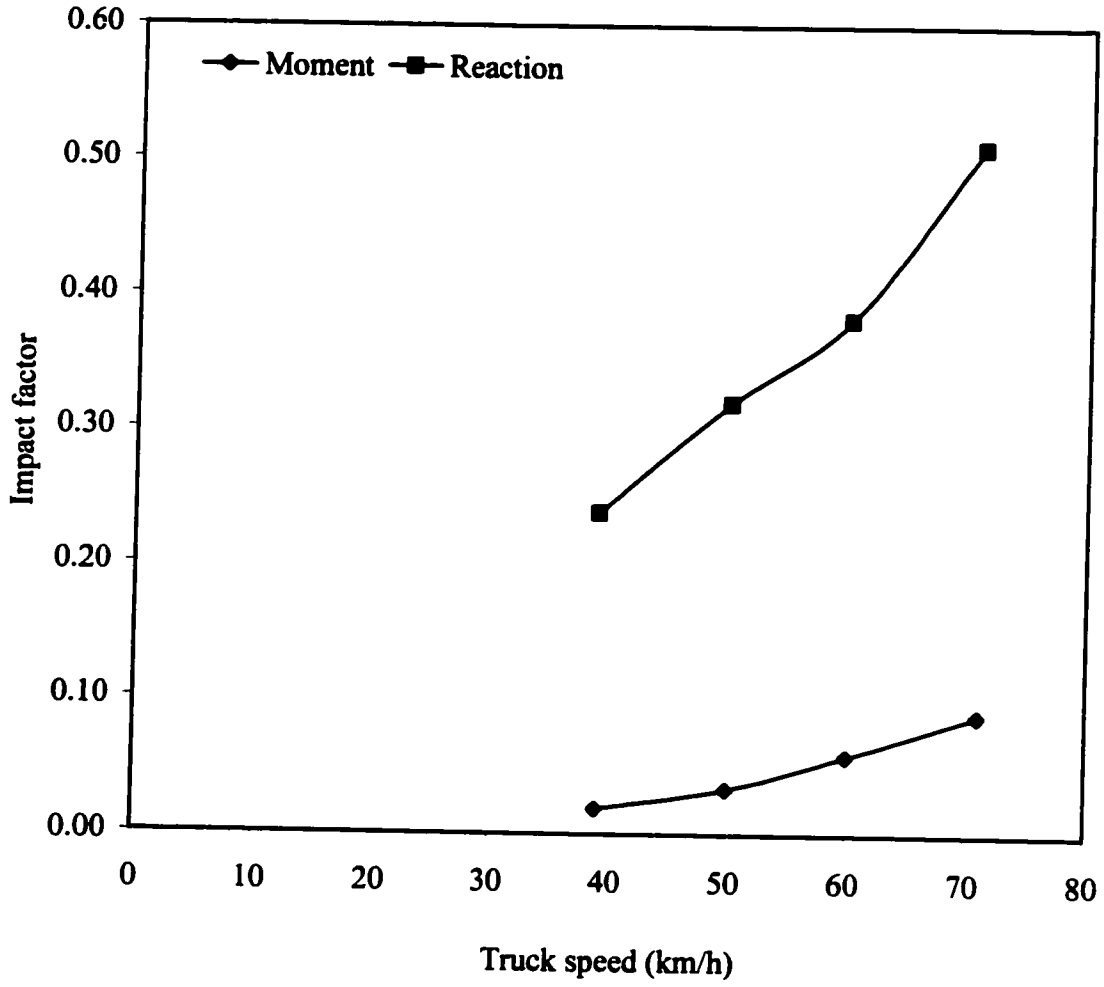

Fig. 7.31. Effect of truck speed on impact factor of
3l-4c-60 bridges with L/R=0.4
(full loading)

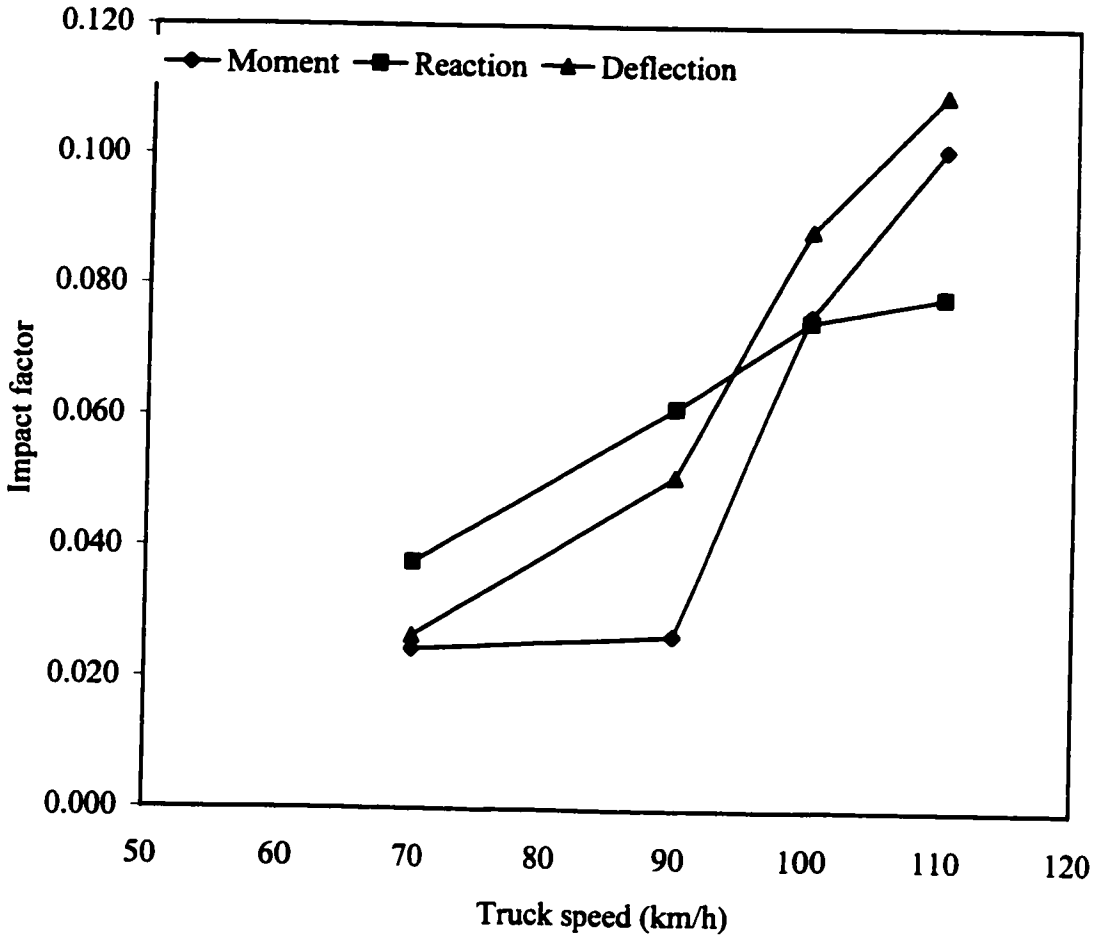

Fig. 7.32. Effect of truck speed on impact factor
of *2l-2c-60* straight bridges
(full loading)

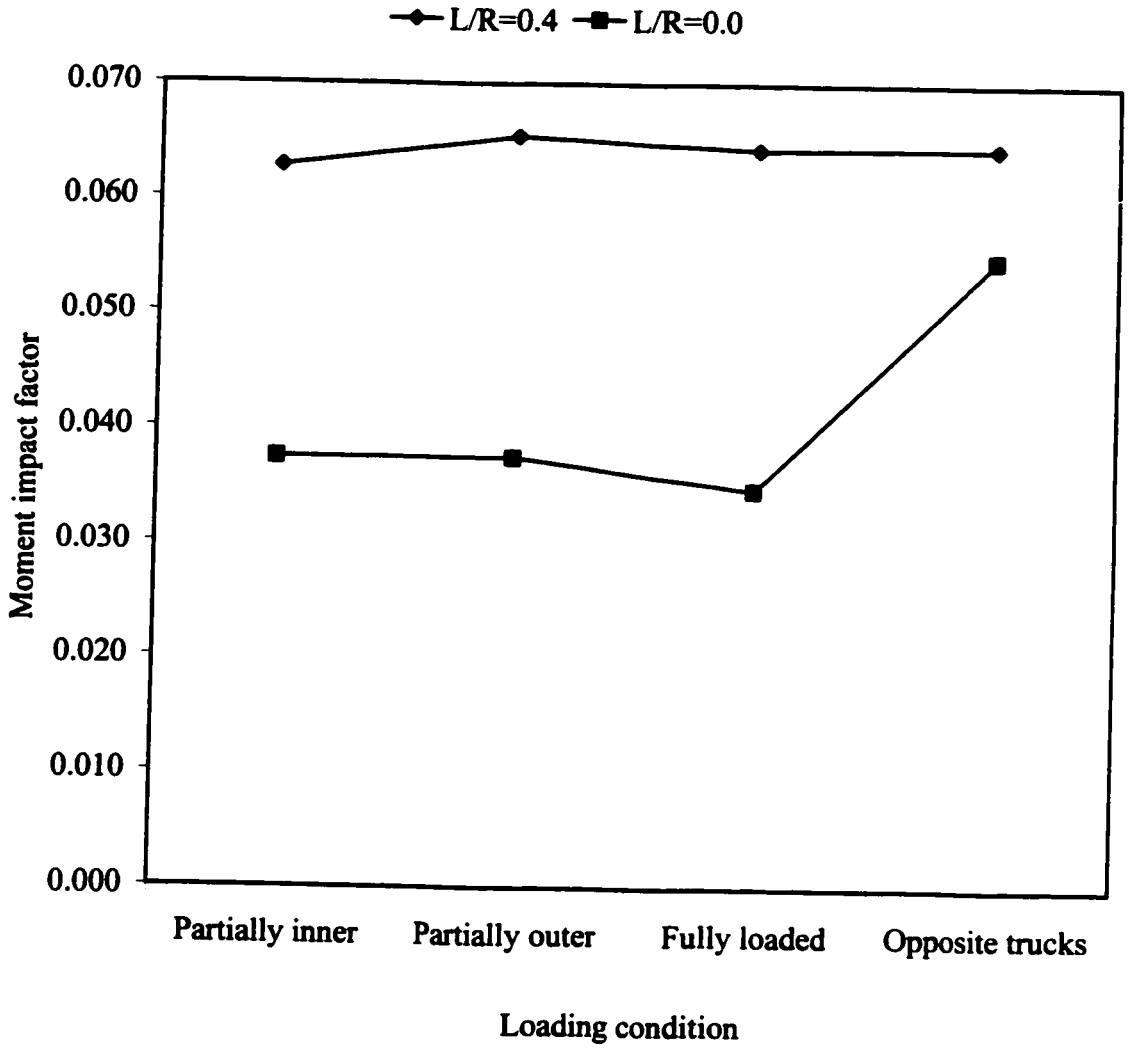

Fig. 7.33. Effect of loading condition on moment impact factor of *2l-2c-40* bridges

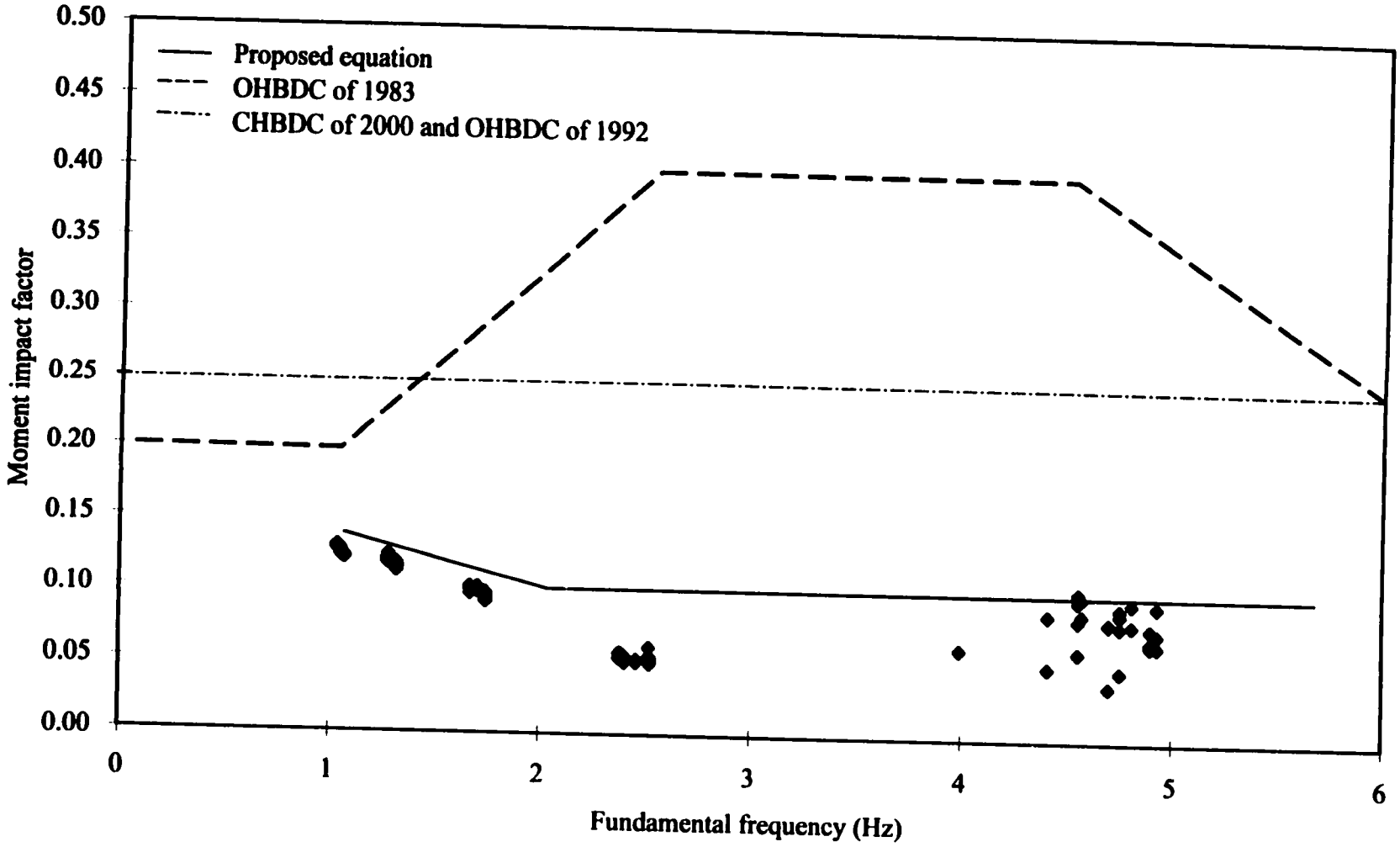

Fig. 7.34. Moment impact factor versus fundamental frequency of straight bridges

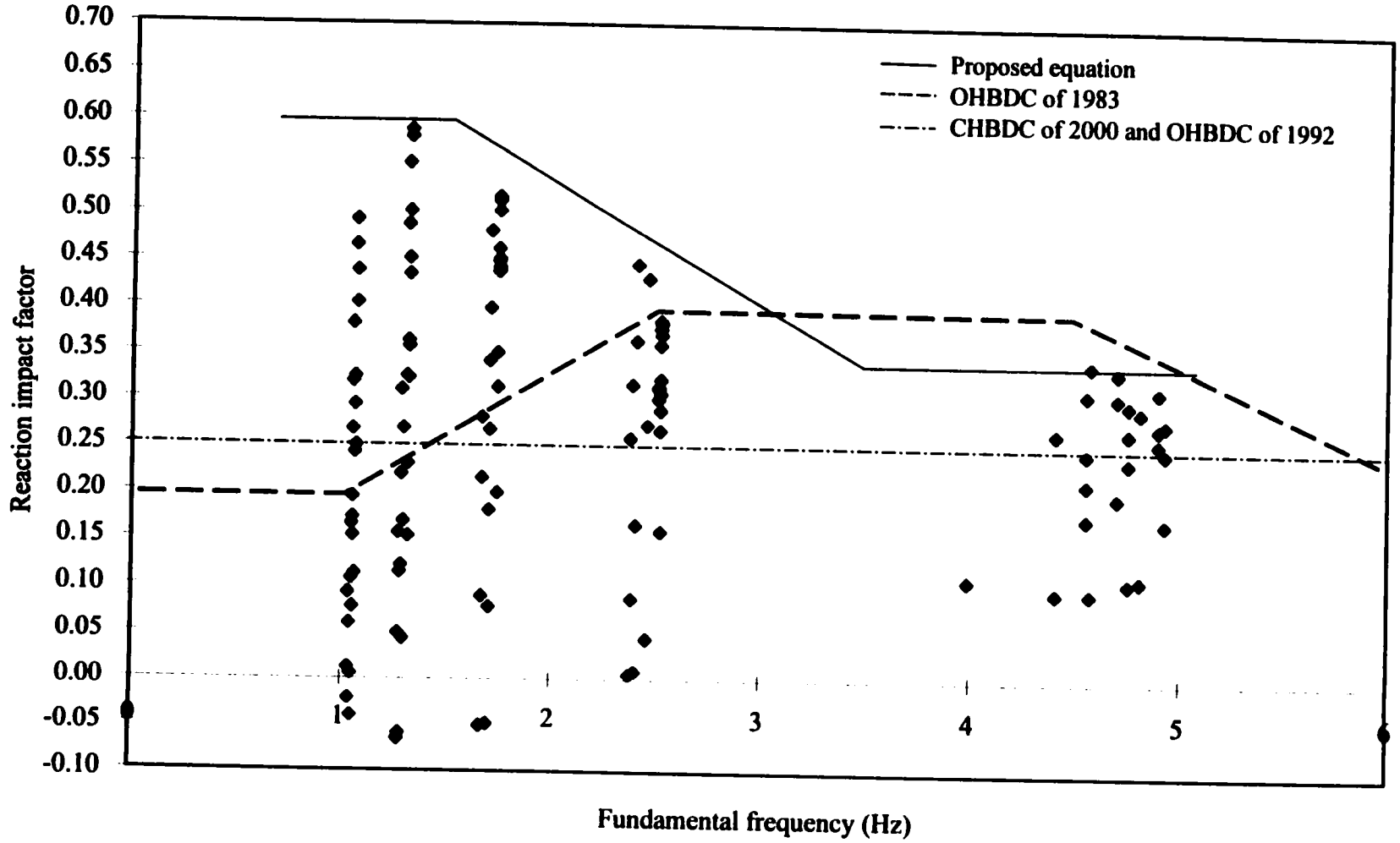

Fig 7.35. Reaction impact factor versus fundamental frequency of straight bridges

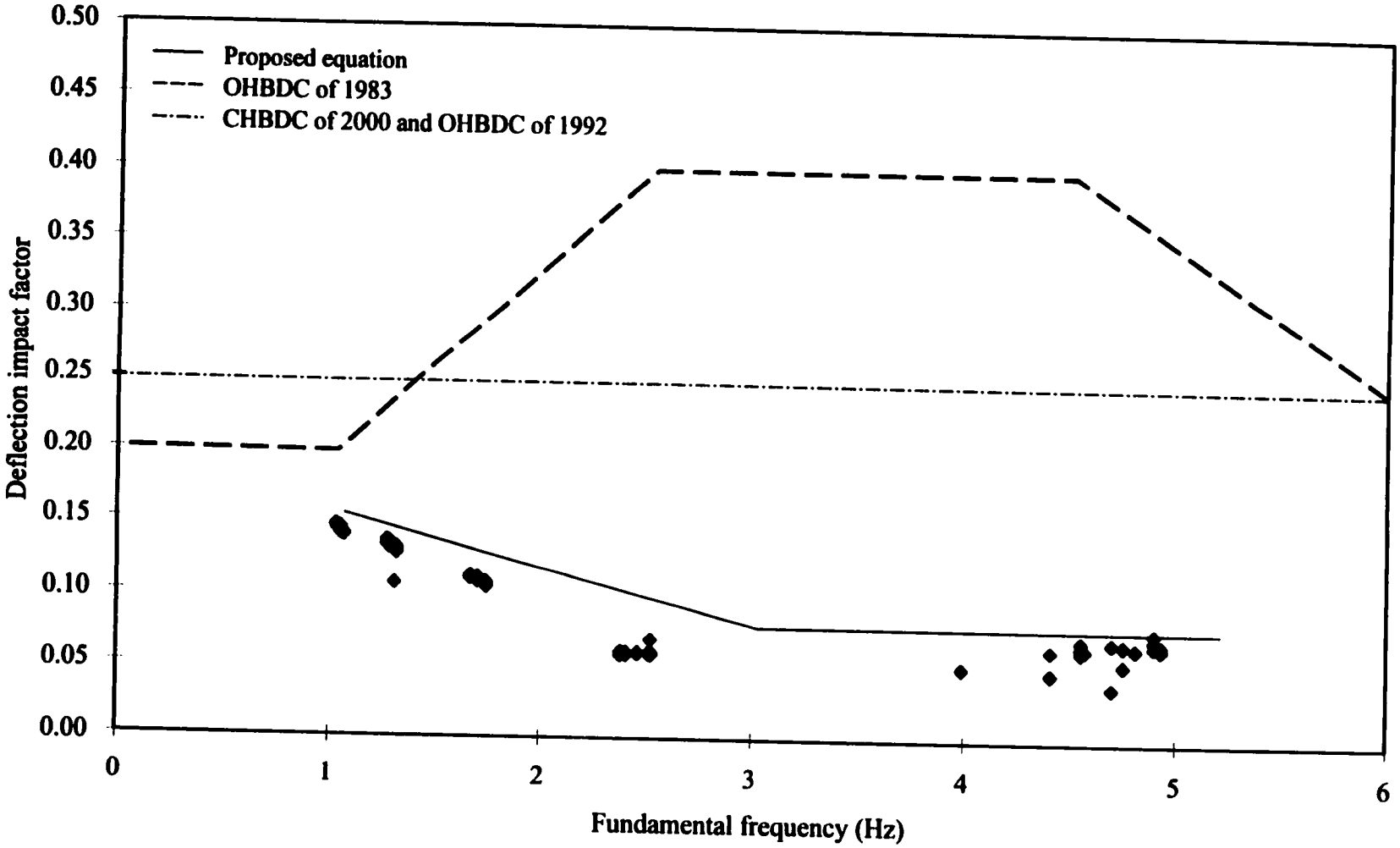

Fig. 7.36. Deflection impact factor versus fundamental frequency of straight bridges

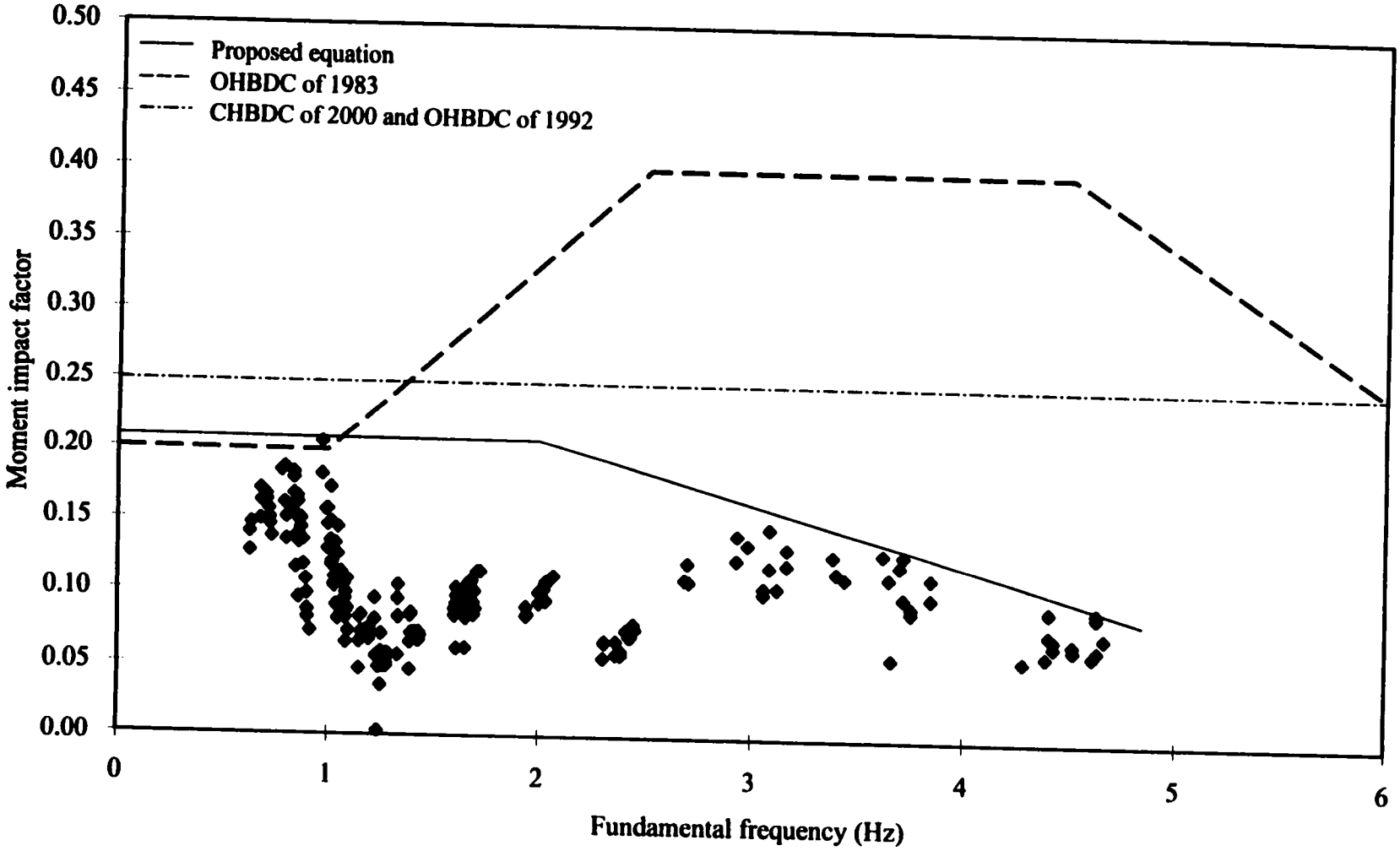

Fig. 7.37. Moment impact factor versus fundamental frequency of curved bridges

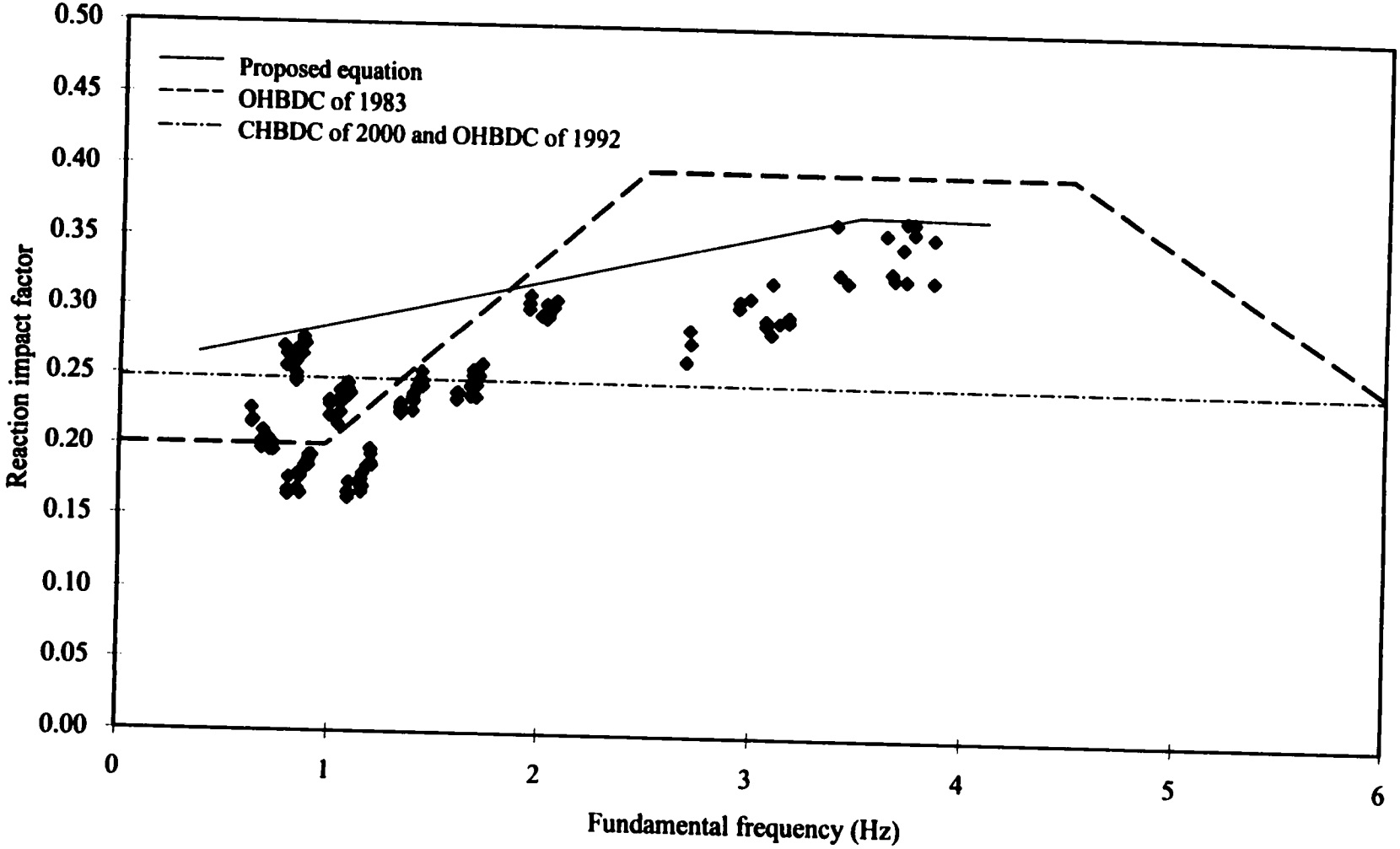

Fig. 7.38. Reaction impact factor versus fundamental frequency of curved bridges with L/R >=1.0

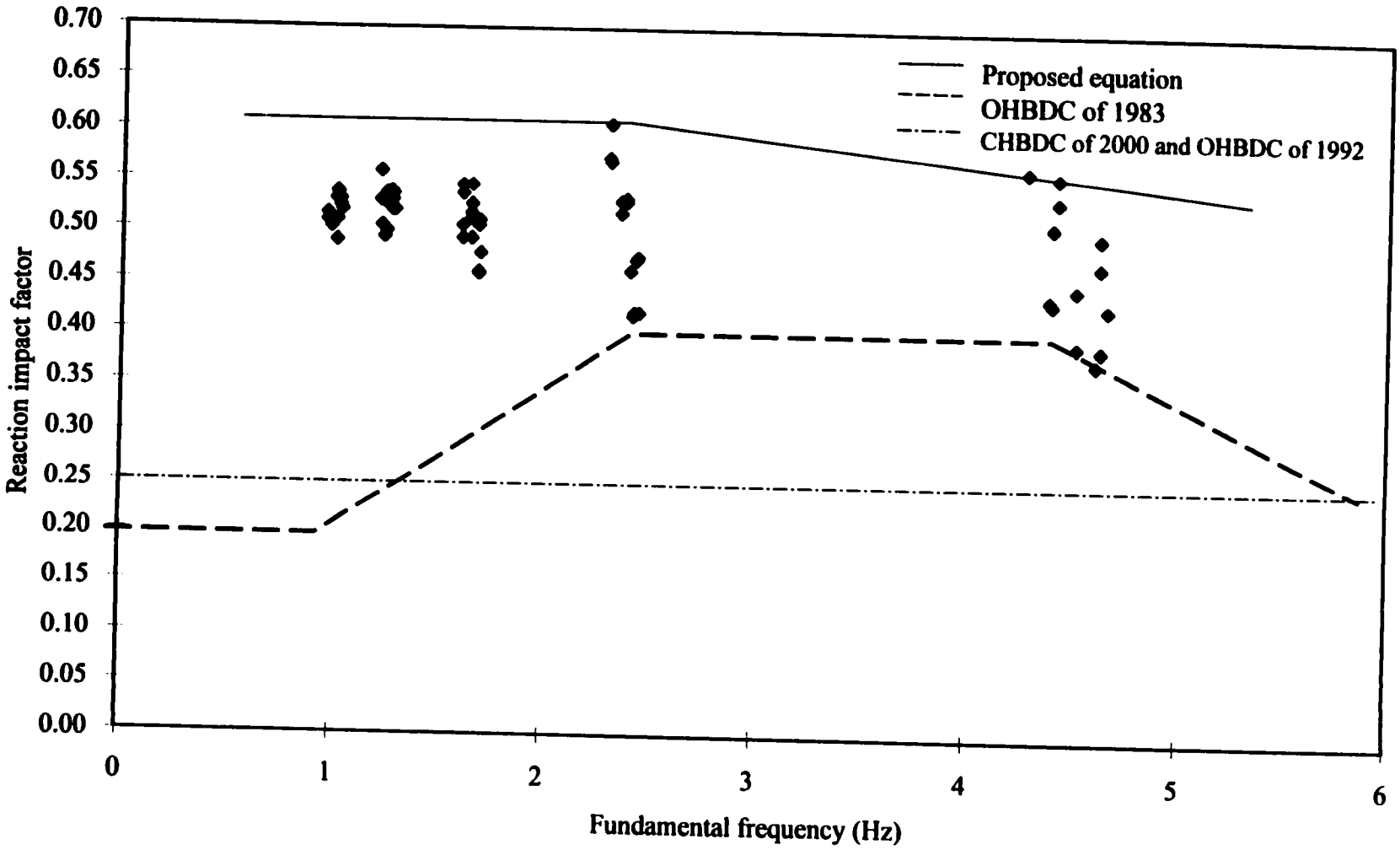

Fig. 7.39. Reaction impact factor versus fundamental frequency of curved bridges with L/R < 1.0

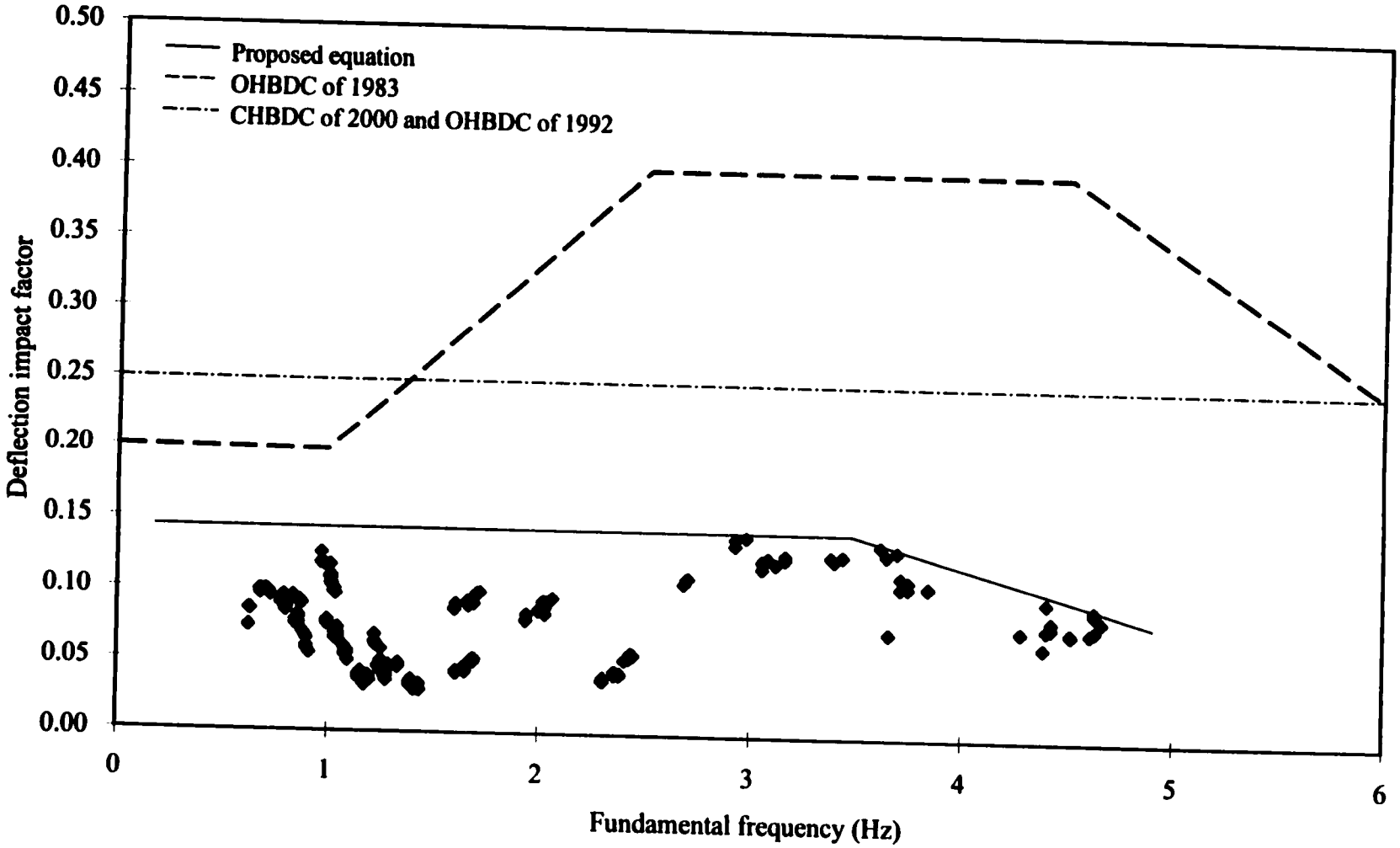

Fig. 7.40. Deflection impact factor versus fundamental frequency of curved bridges

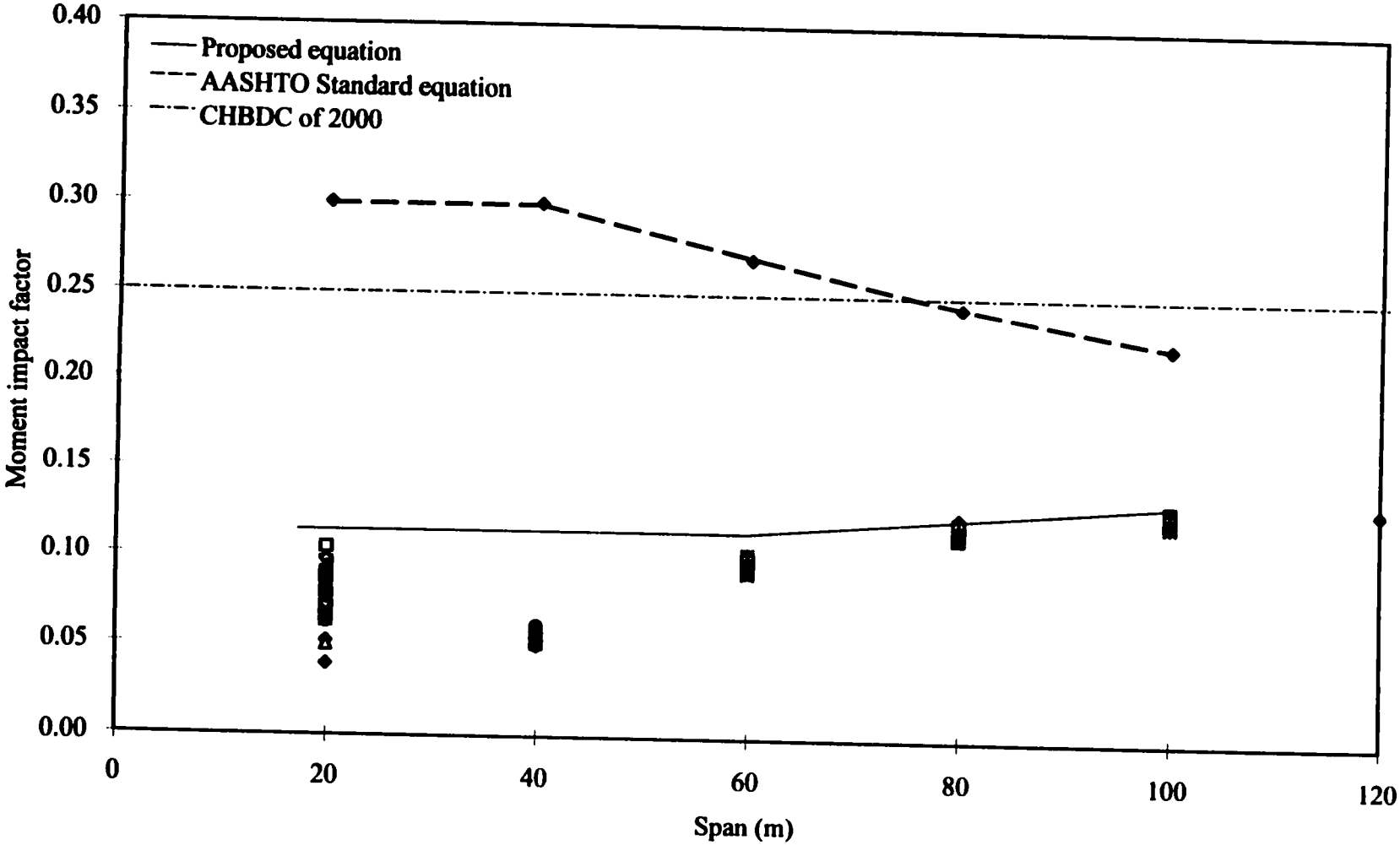

Fig. 7.41. Moment impact factor versus bridge span of straight bridges

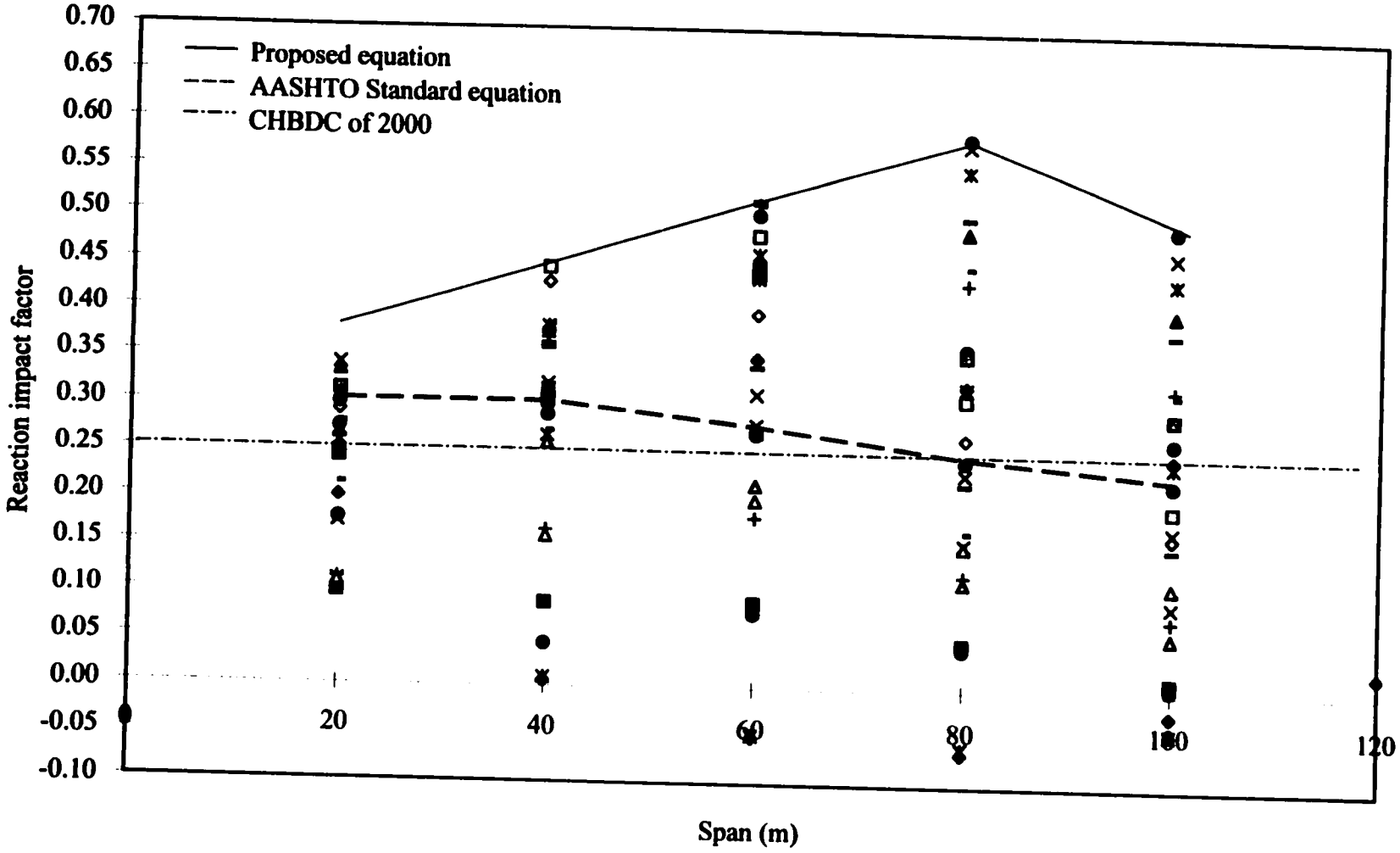

Fig. 7.42. Reaction impact factor versus bridge span of straight bridges

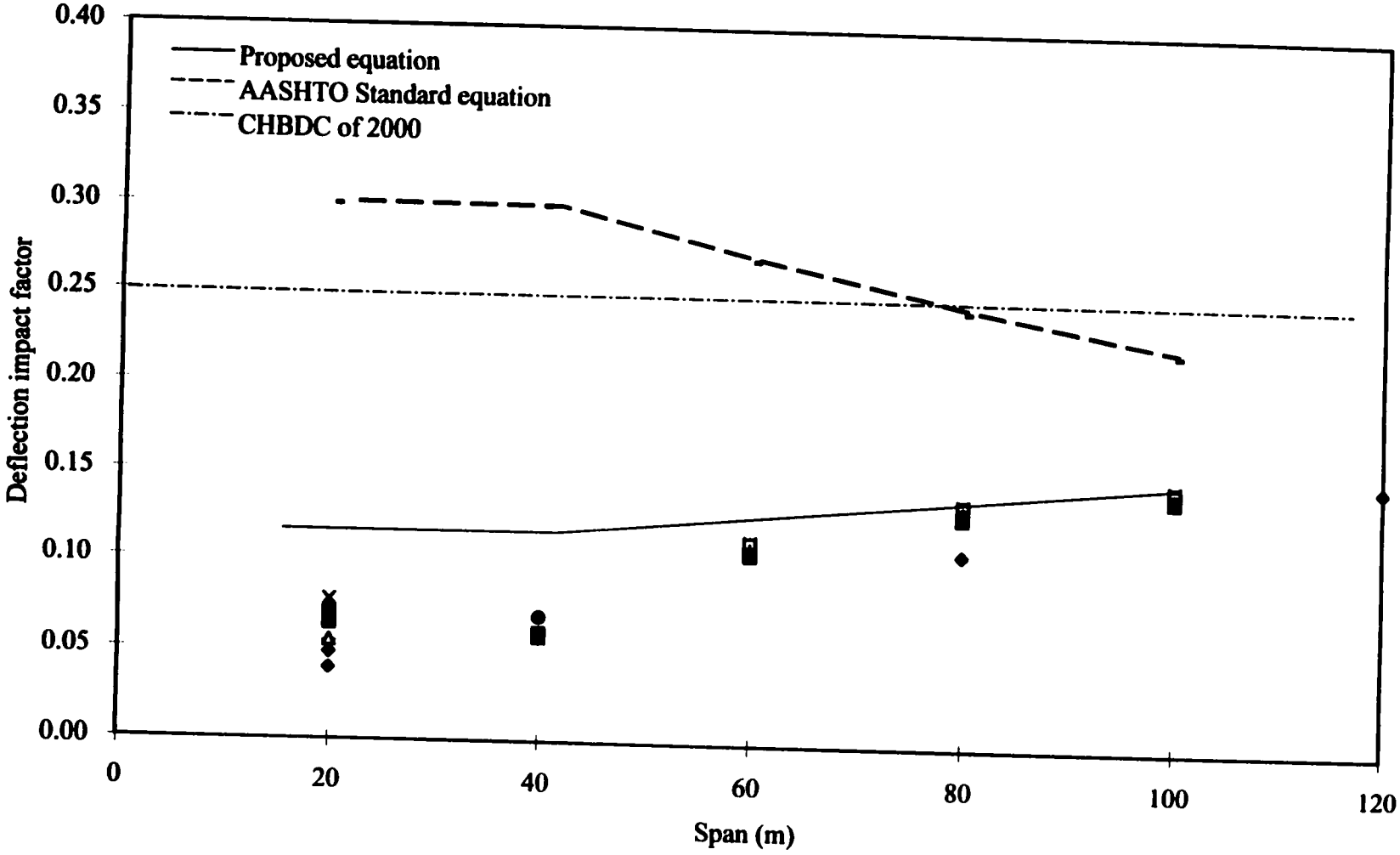

Fig. 7.43. Deflection impact factor versus bridge span of straight bridges

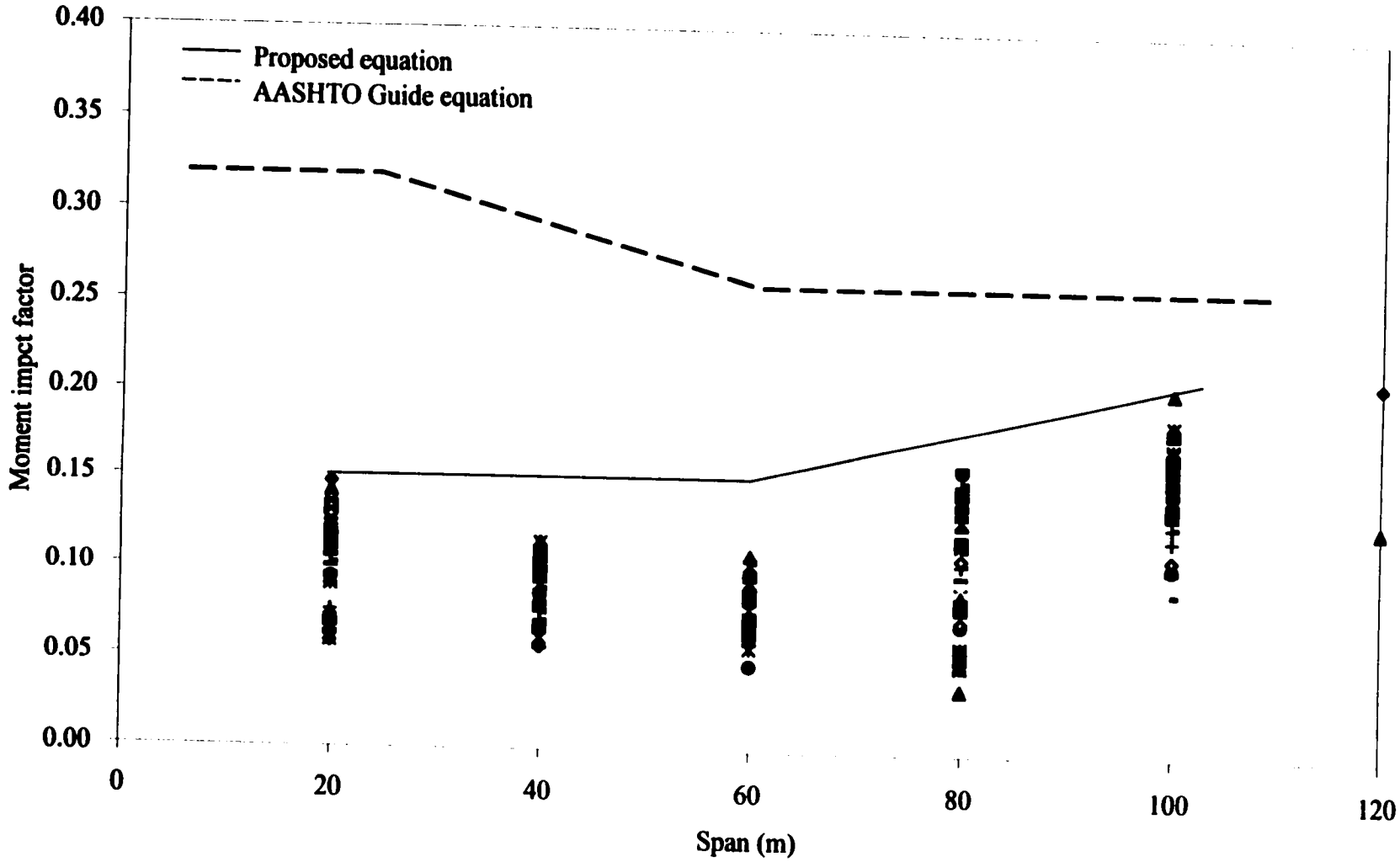

Fig. 7.44. Moment impct factor versus bridge span of curved bridges

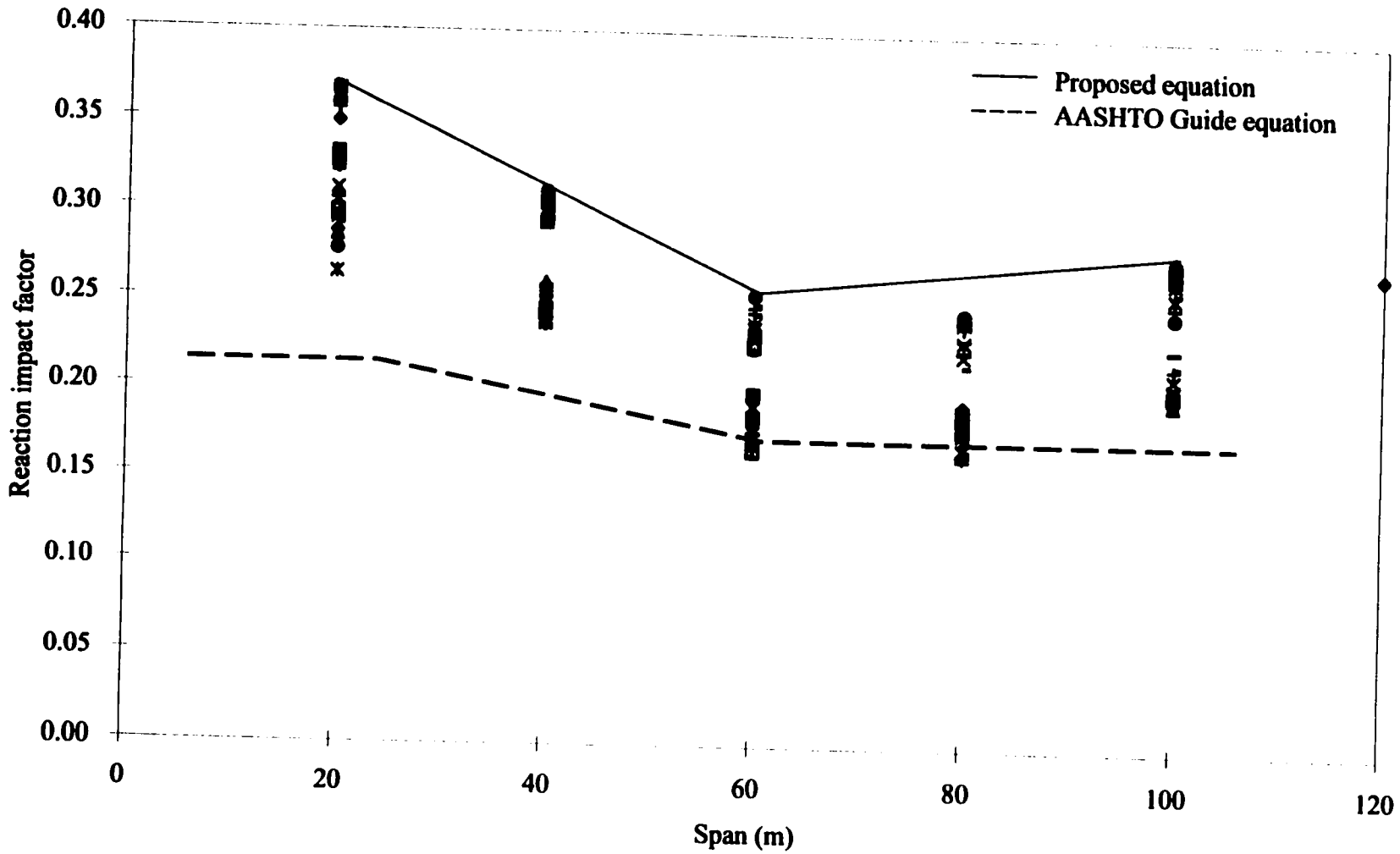

Fig. 7.45. Reaction impact factor versus bridge span of curved bridges with L/R >= 1.0

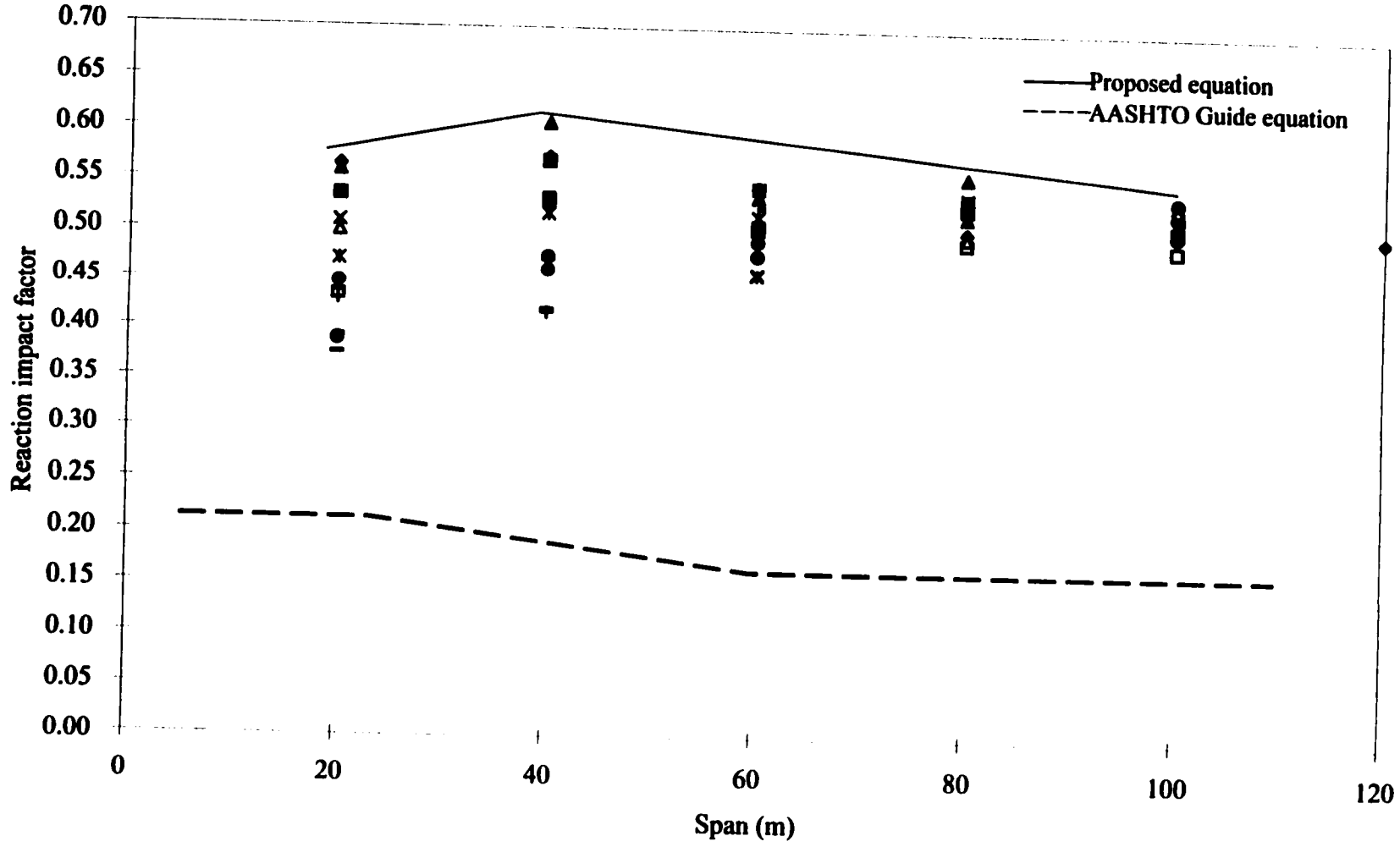

Fig. 7.46. Reaction impact factor versus bridge span of curved bridges with L/R<1.0

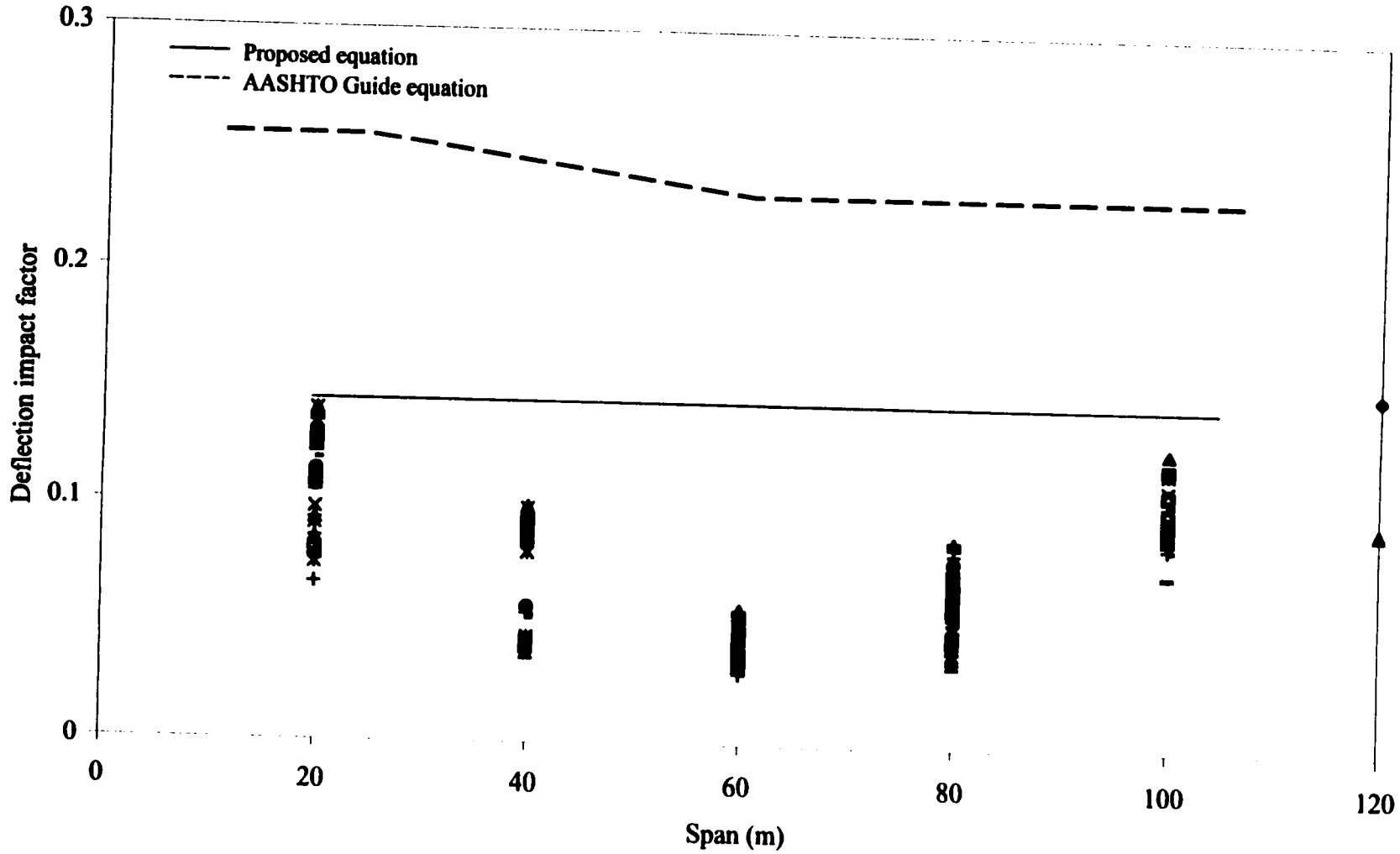

Fig. 7.47. Deflection impact factor versus bridge span of curved bridges

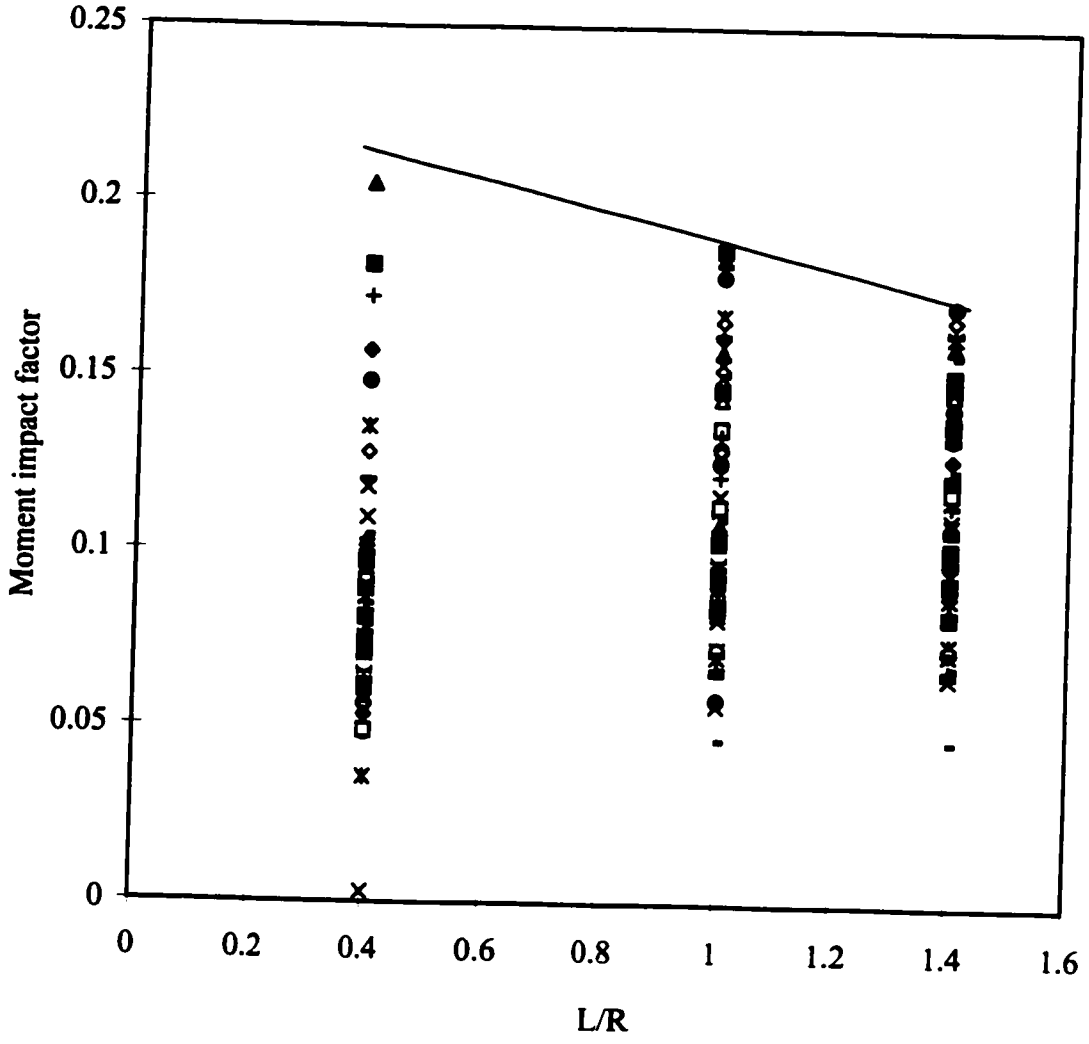

Fig. 7.48. Moment impact factor versus L/R of curved bridges

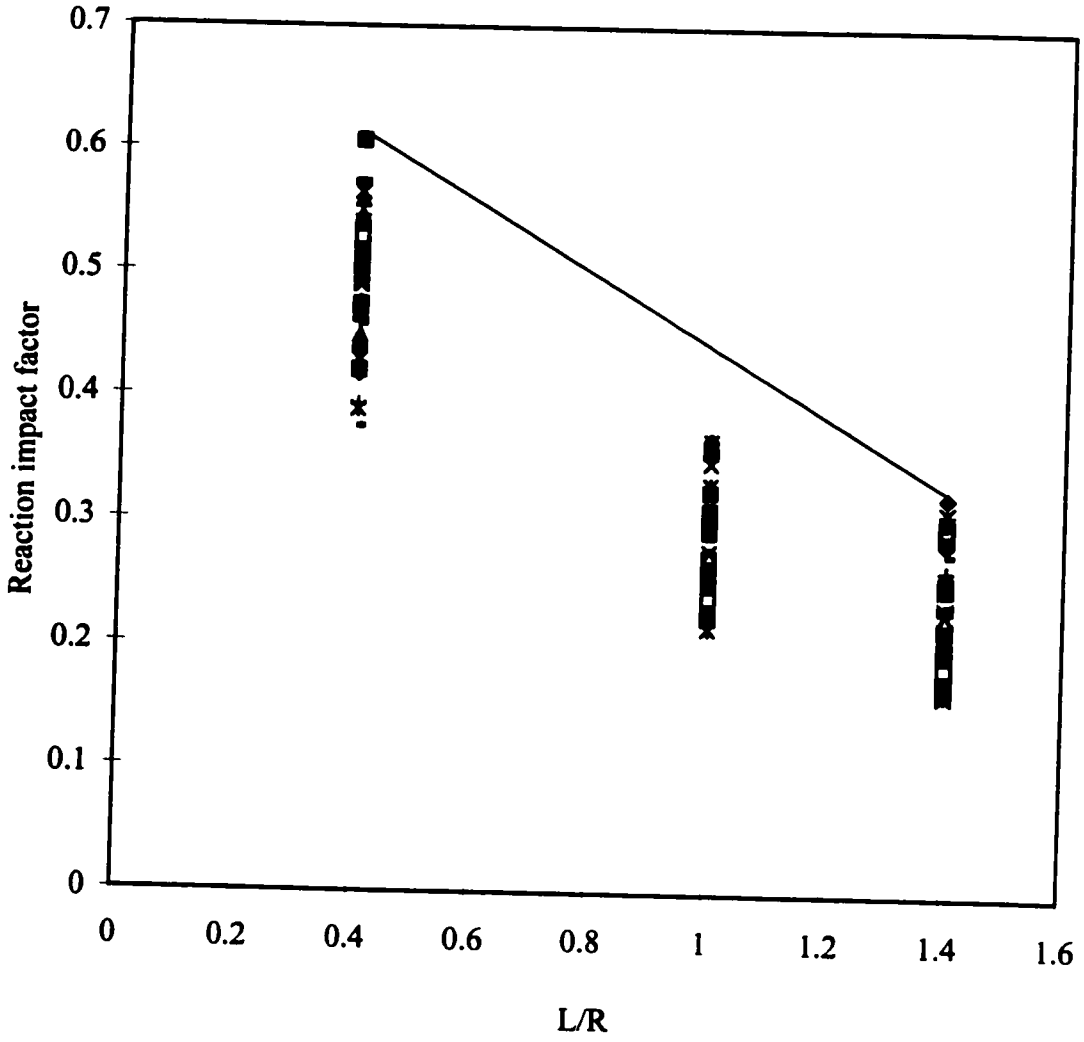

Fig. 7.49. Reaction impact factor versus L/R of curved bridges

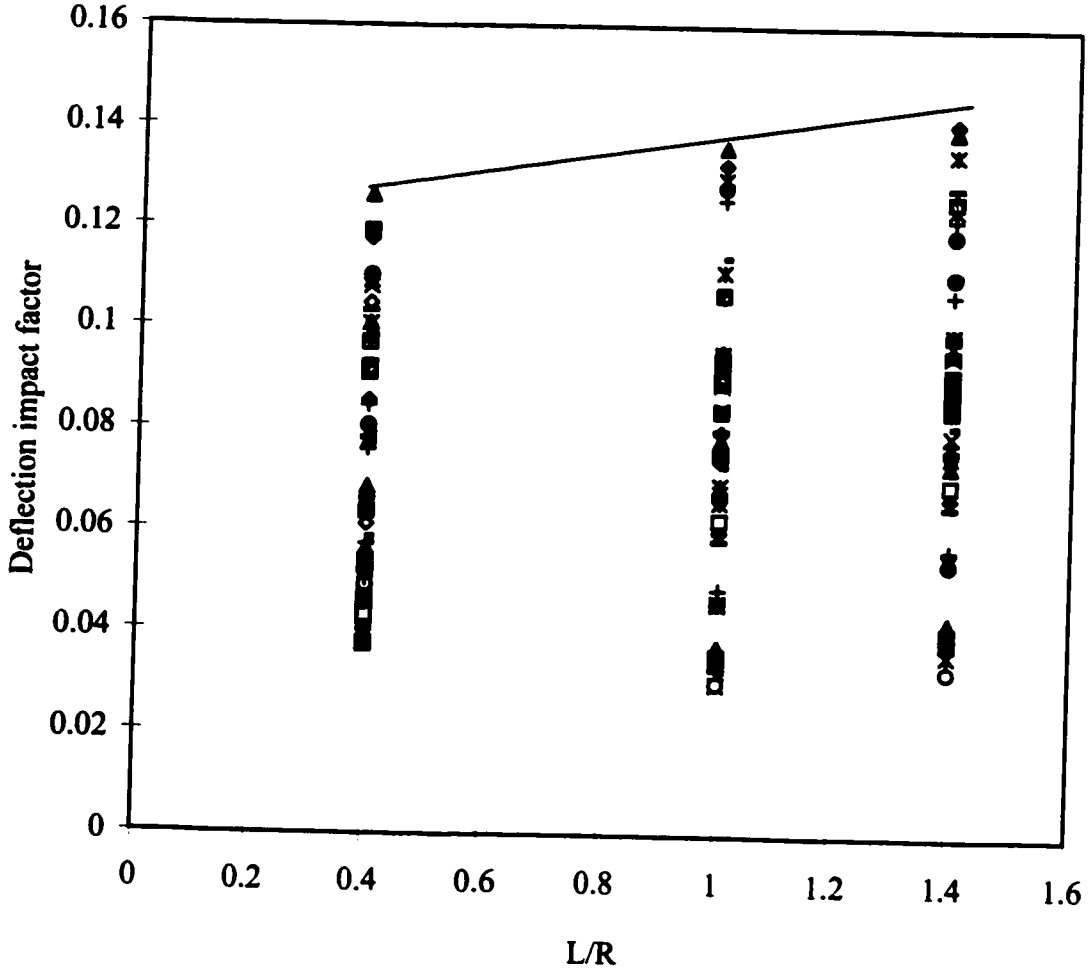

Fig. 7.50. Deflection impact factor versus L/R of curved bridges

APPENDIX 1

Impact Factors Recommended by AASHTO for Horizontally Curved Box Girder Bridges

(1980 Edition)

Quantity	Impact factor, I
Reactions	1.00
Direct stresses in box web and bottom flanges	0.35
Direct stresses in slab	0.30
Shear stresses in box web	0.50
Stresses in diaphragms	0.50
Deflections	0.30

The impact factors are valid within the following parameter values:

$100 \text{ ft} \leq L \leq 300 \text{ ft}$

$300 \text{ ft} \leq R \leq 1000 \text{ ft}$

$v \leq 70$ mph

Number of box girders ≤ 3

Number of continuous spans ≤ 2

Weight of vehicle $\leq 0.30 \times$ Weight of bridge

Where: L = span length (ft)

R = radius of center line of bridge (ft)

v = speed of vehicle (mph)

APPENDIX 2

Impact Factors Recommended by AASHTO for Horizontally Curved Box Girder Bridges

(1993 Edition)

Quantity	Impact function	Limits	
		L (ft)	R_c (ft)
Primary bending moment	$I_M = 0.320$ $I_M = 0.360 - L/2{,}000$ $I_M = 0.260$	$L \leq 80'$ $80' < L \leq 200'$ $200' < L$	$160' \leq R_C \leq 800'$
	$I_M = 0.285$ $I_M = 0.315 - L/2{,}667$ $I_M = 0.240$	$L \leq 80'$ $80' < L \leq 200'$ $200' < L$	$800' < R_C$
Torsion	$I_T = 0.275$ $I_T = 0.291 - L/5{,}000$	$L \leq 80'$ $80' < L$	$160' \leq R_C \leq 800'$
	$I_T = 0.260$ $I_T = 0.308 - L/1{,}667$	$L \leq 80'$ $80' < L$	$800' < R_C$
Shear	$I_S = 0.215$ $I_S = 0.243 - L/2{,}857$ $I_S = 0.173$	$L \leq 80'$ $80' < L \leq 200'$ $200' < L$	$160' \leq R_C$
Reactions	$I_R = 0.275$ $I_R = 0.310 - L/2{,}222$ $I_R = 0.220$	$L \leq 80'$ $80' < L \leq 200'$ $200' < L$	$160' \leq R_C \leq 800'$
	$I_R = 0.225$ $I_R = 0.253 - L/2{,}857$ $I_R = 0.183$	$L \leq 80'$ $80' < L \leq 200'$ $200' < L$	$800' < R_C$
Deflections	$I_D = 0.255$	All L	$160' \leq R_C \leq 800'$
	$I_D = 0.255$ $I_D = 0.271 - L/5{,}000$ $I_D = 0.231$	$L \leq 80'$ $80' < L \leq 200'$ $200' < L$	$800' < R_C$

The impact factors are valid within the following parameter values:

$v \leq 70$ mph

$2 \leq$ Number of box girders ≤ 4

Number of continuous spans ≤ 4

Weight of vehicle $\leq 0.30 \times$ Weight of bridge

Where: L = span length (ft)

R_C = radius of center line of bridge (ft)

v = speed of vehicle (mph)

I_M = Impact factor for bending moment

I_T = Impact factor for torsion

I_S = Impact factor for shear

I_R = Impact factor for reactions

I_D = Impact factor for deflections

APPENDIX 3

Typical 'ABAQUS' Input Data

```
*HEADING
2LANE 2CELL CURVED SIMPLY SUPPORTED L=60, L/R=1, V=45km/h, full loading
**RESTART, WRITE
**DATA CHECK
*PREPRINT, ECHO=YES,MODEL=NO,HISTORY=NO
**
** ******************Reference nodes *******
**
** ********* Origin nodes *****************
*NODE
1,0,0,0
10001,0,0,-0.1390
50001,0,0,-2.5040
** ******** Slab corner nodes *************
2,     -26.5362, 48.5742
26,    -30.9949, 56.7357
7202, 26.5362, 48.5742
7226, 30.9949, 56.7357
** ******** Cell corner nodes *************
10006,-27.2793, 49.9344,-0.1390
50006,-27.2793, 49.9344,-2.5040
17206, 27.2793, 49.9344,-0.1390
57206, 27.2793, 49.9344,-2.5040
** ***************************
10022,-30.2518, 55.3755,-0.1390
50022,-30.2518, 55.3755,-2.5040
17222, 30.2518, 55.3755,-0.1390
57222, 30.2518, 55.3755,-2.5040
** ***************************
*NGEN,NSET=ORIGIN
10001,50001,10000
**
```

```
** ****** NODE GEN. FOR END DIAPHRAGM *****
** NFILL third parameter: 4*cells
**
*NGEN, NSET=NENDI
10006,50006,10000
17206,57206,10000
*NGEN, NSET=NENDO
10022,50022,10000
17222,57222,10000
*NFILL,NSET=NEND
NENDI, NENDO, 8, 2
*NGEN,NSET=NEND
2,26,2
7202,7226,2
**
** ******* Support nodes ******************
**
*NGEN,NSET=LEFT6
50006,50022,8
*NGEN,NSET=RIGHT6
57206,57222,8
**
** ***************NODE GEN. FOR TOP SLAB***
** NFILL third parameter: 4*(cells+1)
**
*NGEN, NSET=NPLI,LINE=C
2, 7202, 100,1
*NGEN, NSET=NPLO,LINE=C
26, 7226, 100,1
*NFILL, NSET=NPLATET
NPLI, NPLO, 12, 2
**
** **************NODE GEN. FOR TOP FLANGE **
** NFILL third parameter: cells
**
*NGEN,NSET=TOPFLNGI,LINE=C
10006,17206,100,10001
*NGEN,NSET=TOPFLNGO,LINE=C
10022,17222,100,10001
*NFILL, NSET=NTOPFLNG
```

```
TOPFLNGI,TOPFLNGO, 2, 8
**
** ********** NODE GEN. FOR WEBS *****
** First and second NFILL third parameter: cells
**
*NGEN, NSET=NWEBTI, LINE=C
10006,17206,100,10001
*NGEN, NSET=NWEBTO, LINE=C
10022,17222,100,10001
*NFILL, NSET=NWEBT
NWEBTI, NWEBTO, 2, 8
*NGEN, NSET=NWEBDI, LINE=C
50006,57206,100,50001
*NGEN, NSET=NWEBDO, LINE=C
50022,57222,100,50001
*NFILL, NSET=NWEBD
NWEBDI, NWEBDO, 2, 8
*NFILL, NSET=NWEB
NWEBT, NWEBD, 4, 10000
**
** ********* NODE GEN FOR BOTTOM FLANGE ***
** NFILL third parameter: 4*cells
**
*NGEN,NSET=NBOTFLI,LINE=C
50006,57206,100,50001
*NGEN,NSET=NBOTFLO,LINE=C
50022,57222,100,50001
*NFILL, NSET=NPLATEB
NBOTFLI, NBOTFLO, 8, 2
**
** ********* NODE GEN FOR CROSS BRACING ***
** NFILL third parameter: cells-1
**
*NGEN, NSET=NBRACEI, LINE=C
30010, 37210, 900,30001
*NGEN, NSET=NBRACEO, LINE=C
30018, 37218, 900,30001
*NFILL, NSET=NBRACE
NBRACEI, NBRACEO, 1, 8
**
```

```
** *** **** ELEMENT GEN. FOR TOP SLAB *****
** First label tangential direction, then radical direction
** ELGEN parameter: 1,72,100,1, 4*(cells+1) ,2,72
**
*ELEMENT,TYPE=S4R
1,2,102,104,4
*ELGEN,ELSET=ESLABT
1,72,100,1,12,2,72
**
** ***** ELEMENT GEN. FOR BOTTOM FLANGE ***
** ELGEN parameter: 3001,72,100,1, 4*cells, 2,72
**
*ELEMENT,TYPE=S4R
3001,50006,50106,50108,50008
*ELGEN,ELSET=ESLABB
3001,72,100,1,8,2,72
**
** ******* ELEMENT GEN. FOR TOP FLANGE ****
** ELGEN parameter: 6001,72,100,1, cells+1, 8,72
**
*ELEMENT,TYPE=B31H
6001,10006,10106
*ELGEN,ELSET=ETOPFL
6001,72,100,1,3,8,72
**
** ******* ELEMENT GEN. FOR WEBS **********
** ELGEN parameter: 7001,72,100,1,4,10000,72, cells+1, 288
**
*ELEMENT,TYPE=S4R
7001,20006,20106,10106,10006
*ELGEN,ELSET=EWEB
7001,72,100,1,4,10000,72,3,8,288
**
** ***** ELEMENT GEN. FOR END DIAPHRAGM ***
** ELGEN parameter: 10001, 4*cells, 2,1,4,10000, 4*cells, 2,7200, 16*cells
**
*ELEMENT,TYPE=S4R
10001,20006,20008,10008,10006
*ELGEN,ELSET=EDIAPH
10001,8,2,1,4,10000,8,2,7200,32
```

```
**
** ********** END FLANGE ELEMENTS ********
** ELGEN parameter: 11001, 4*cells,2,1,2,7200, 4*cells
**
*ELEMENT,TYPE=B31H
11001,10006,10008
*ELGEN,ELSET=ENDFL
11001,8,2,1,2,7200,8
**
** ***** ELEMENT GEN. FOR TRUSS ELEMENTS **
** Element No: 11101,11201,11301,11401,11501
** ELGEN parameters: 11101, cells, 8,1, braces, 7200/(braces+1), cells
**
*ELEMENT,TYPE=B31H
11101,10906,30910
11201,30910,50914
11301,10914,30910
11401,30910,50906
11501,10906,10914
*ELGEN,ELSET=EBRACE
11101,2,8,1,7,900,2
11201,2,8,1,7,900,2
11301,2,8,1,7,900,2
11401,2,8,1,7,900,2
11501,2,8,1,7,900,2
**
** ********** Local support nodes *********
**
*NSET,NSET=NREACT
LEFT6,RIGHT6
*TRANSFORM,NSET=NREACT,TYPE=C
0,0,-10,0,0,10
*TRANSFORM,NSET=NPLATET,TYPE=C
0,0,-10,0,0,10
**
** *************** MATERIAL PROPERTIES *****
**
*MATERIAL,NAME=STEEL
*ELASTIC
200E9,.3
```

```
*DENSITY
7800
*MATERIAL,NAME=CON
*ELASTIC
27E9,.20
*DENSITY
2400
**
** ********** SECTION TYPE **********
**
*BEAM SECTION,SECTION=RECT,ELSET=ETOPFL,MATERIAL=STEEL
.053,.45
5,5
*BEAM SECTION,SECTION=RECT,ELSET=ENDFL,MATERIAL=STEEL
.053,.45
5,5
*BEAM SECTION,SECTION=RECT,ELSET=EBRACE,MATERIAL=STEEL
.1,.1
5,5
**********
*SHELL SECTION,ELSET=EDIAPH,MATERIAL=STEEL
.024,5
*SHELL SECTION,ELSET=ESLABB,MATERIAL=STEEL
.017,5
*SHELL SECTION,ELSET=ESLABT,MATERIAL=CON
.225,5
*SHELL SECTION,ELSET=EWEB,MATERIAL=STEEL
.024,5
**
** ********** MULTI POINT CONSTRAINT ******
** NFILL third parameter: cells
**
*NGEN,NSET=NTOPI,LINE=C
6,7206,100,1
*NGEN,NSET=NTOPO,LINE=C
22,7222,100,1
*NFILL, NSET=NTOP
NTOPI, NTOPO, 2, 8
*NGEN,NSET=NBOTI,LINE=C
10006,17206,100,10001
```

```
*NGEN,NSET=NBOTO,LINE=C
10022,17222,100,10001
*NFILL, NSET=NBOT
NBOTI, NBOTO, 2, 8
*NGEN,NSET=NTOP
6,22,2
7206,7222,2
*NGEN,NSET=NBOT
10006,10022,2
17206,17222,2
*MPC
BEAM,NTOP,NBOT
**
** ****************************************
**
*BOUNDARY
LEFT6,1,3
RIGHT6,1
RIGHT6,3
**
****** Defining the load amplitude*****
**
*AMPLITUDE, NAME=LOAD1,VALUE=RELATIVE
0.000, 0.00, 0.068, 0.25, 0.137, 0.00, 0.342, 0.00
0.410, 1.00, 0.478, 0.00, 0.683, 0.00, 0.752, 1.00
0.820, 0.00
*AMPLITUDE, NAME=LOAD2,VALUE=RELATIVE
0.068, 0.00, 0.137, 0.25, 0.205, 0.00, 0.410, 0.00
0.478, 1.00, 0.547, 0.00, 0.752, 0.00, 0.820, 1.00
0.888, 0.00
*AMPLITUDE, NAME=LOAD3,VALUE=RELATIVE
0.137, 0.00, 0.205, 0.25, 0.273, 0.00, 0.478, 0.00
0.547, 1.00, 0.615, 0.00, 0.820, 0.00, 0.888, 1.00
0.957, 0.00
*AMPLITUDE, NAME=LOAD4,VALUE=RELATIVE
0.205, 0.00, 0.273, 0.25, 0.342, 0.00, 0.547, 0.00
0.615, 1.00, 0.683, 0.00, 0.888, 0.00, 0.957, 1.00
1.025, 0.00
*AMPLITUDE, NAME=LOAD5,VALUE=RELATIVE
0.273, 0.00, 0.342, 0.25, 0.410, 0.00, 0.615, 0.00
```

```
0.683, 1.00, 0.752, 0.00, 0.957, 0.00, 1.025, 1.00
1.093, 0.00
**
** ****** STEP BEGINNING ******************
**
*STEP, INC=1000
*DYNAMIC, ALPHA=0.0, NOHAF
.01,3.3
*CLOAD, AMPLITUDE=LOAD1
108, 3, -31973
112, 3, -85493
114, 3, -32154
116, 3, -24753
120, 3, -110427
108, 1, 18460
112, 1, 14292
114, 1, 8336
116, 1, 14292
120, 1, 18460
*CLOAD, AMPLITUDE=LOAD2
208, 3, -31973
212, 3, -85493
214, 3, -32154
216, 3, -24753
220, 3, -110427
208, 1, 18460
212, 1, 14292
214, 1, 8336
216, 1, 14292
220, 1, 18460
*CLOAD, AMPLITUDE=LOAD3
308, 3, -31973
312, 3, -85493
314, 3, -32154
316, 3, -24753
320, 3, -110427
308, 1, 18460
312, 1, 14292
314, 1, 8336
316, 1, 14292
```

```
320, 1, 18460
*CLOAD, AMPLITUDE=LOAD4
408, 3, -31973
412, 3, -85493
414, 3, -32154
416, 3, -24753
420, 3, -110427
408, 1, 18460
412, 1, 14292
414, 1, 8336
416, 1, 14292
420, 1, 18460
*CLOAD, AMPLITUDE=LOAD5
508, 3, -31973
512, 3, -85493
514, 3, -32154
516, 3, -24753
520, 3, -110427
508, 1, 18460
512, 1, 14292
514, 1, 8336
516, 1, 14292
520, 1, 18460
*OUTPUT,HISTORY,FREQUENCY=0
*OUTPUT,FIELD,FREQUENCY=0
*ELSET,ELSET=EMIDBOT,GEN
3037, 3541, 72
*EL PRINT, ELSET=EMIDBOT, SUMMARY=NO
SF1
*EL PRINT,ELSET=EBRACE, SUMMARY=NO
SF1
*NODE PRINT,NSET=LEFT6, SUMMARY=NO
RF3
*NSET,NSET=NMIDOUT,GEN
53606,53622,8
*NODE PRINT,NSET=NMIDOUT, SUMMARY=NO
U3
*ENDSTEP
```

APPENDIX 4

Program for Processing Output Data from ABAQUS

```
/* Reading and processing ABAQUS .dat file */
/* Dynamic data processing */
/* Direct integration with first 10 steps special */

#include <stdio.h>
#include <math.h>
#include <string.h>

#define INCRE 2000

void fileData(int nCell1, int span1);
void readFile(FILE *ifptr, int type);
void maxFile(void);
void resultFile(FILE *rfptr, char *iFile);
void historyFile(FILE *hfptr, char *iFile);

float result[INCRE][785], max[2][20];
int number[785], total;
int increment, nMoment, nCross, nSupport;

#pragma hdrstop
#include <condefs.h>

#pragma argsused
int main(int argc, char **argv)
{
    char inFile[30],
         resFile[30] = "",
         hisFile[30] = "",
         *res = ".r_s",
         *his = ".t_h";
    int nCell, span, nType;
```

```
    FILE *infptr, *resfptr, *hisfptr;

    printf("Please input the input file name: ");
    scanf("%s", inFile);
    strcat(resFile, inFile);
    strcat(resFile, res);
    strcat(hisFile, inFile);
    strcat(hisFile, his);

   if ((infptr = fopen(inFile, "r")) == NULL)
        printf("File could not be opened\n");
   if ((resfptr = fopen(resFile, "w")) == NULL)
        printf("File could not be opened\n");
   if ((hisfptr = fopen(hisFile, "w")) == NULL)
        printf("File could not be opened\n");
   else {
        printf("Please input the type of bridge: \n");
        printf("   0 for straight,\n   1 for curved bridge: ");
        scanf("%d", &nType);
        printf("Please input the number of bridge cells: ");
        scanf("%d", &nCell);
        printf("Please input the span of bridge: ");
        scanf("%d", &span);
        printf("Please input the number of increment: ");
        scanf("%d", &increment);
        printf("nType = %d\n", nType);

        fileData(nCell, span);
        readFile(infptr, nType);
        maxFile();
        resultFile(resfptr, inFile);
        historyFile(hisfptr, inFile);
   }

   printf("Program is finished successfully!!\n");
   getchar();
   getchar();
   return 0;
}
```

```
/* Determine the basic data */

void fileData(int nCell1, int span1)
{
    switch (nCell1) {
        case 1:
            nMoment = 4;
            nSupport = 2;
            break;

        case 2: case 4: case 6: case 8:
            nMoment = 8;
            nSupport = 3;
        break;

        case 3: case 5: case 7: case 9:
            nMoment = 8;
            nSupport = 4;
            break;

        default:
            printf("Error!! Please reinput the cell number!!\n");
  }

  switch (span1) {
      case 20:
          nCross = nCell1 * 5 * 3;
          break;

      case 40:
          nCross = nCell1 * 5 * 5;
          break;

      case 60:
          nCross = nCell1 * 5 * 7;
          break;

      case 80:
          nCross = nCell1 * 5 * 11;
          break;
```

```
            case 100:
                nCross = nCell1 * 5 * 17;
                break;

            default:
                printf("Error!! Please reinput the span of bridge!!\n");
        }

        total = nMoment + nCross + 2 * nSupport;

        printf("nCell = %d\n", nCell1);
        printf("span = %d\n", span1);
        printf("nMoment = %d\n", nMoment);
        printf("nCross = %d\n", nCross);
        printf("nSupport = %d\n", nSupport);
}

/* Read input file */

void readFile(FILE *ifptr, int type)
{
    int i, j, num1;
    char s[30];
    float num2, num3;

    for (j = 0; j <= 9; j++) {
        for (i = 1;i <= 51; i++)
            fscanf(ifptr, "%s", s);

        for (i = 0; i <= nMoment - 1; i++) {
            fscanf(ifptr, "%d%f%f", &num1, &num2, &num3);
            result[j][i] = num3;
            number[i] = num1;
        }

        for (i = 1;i <= 18; i++)
            fscanf(ifptr, "%s", s);

        for (i = nMoment; i <= nMoment + nCross - 1; i++) {
```

```
            fscanf(ifptr, "%d%f%f", &num1, &num2, &num3);
            result[j][i] = num3;
            number[i] = num1;
        }

        for (i = 1;i <= 26; i++)
            fscanf(ifptr, "%s", s);

        switch (type) {
            case 0:
                for (i = nMoment + nCross;
                    i <= nMoment + nCross + nSupport - 1; i++) {
                    fscanf(ifptr, "%d%f", &num1, &num2);
                    result[j][i] = num2;
                    number[i] = num1;
                }

                for (i = 1; i <= 16; i++)
                    fscanf(ifptr, "%s", s);

            break;

            case 1:
                for (i = nMoment + nCross;
                    i <= nMoment + nCross + nSupport - 1; i++) {
                    fscanf(ifptr, "%d%s%f", &num1, s, &num2);
                    result[j][i] = num2;
                    number[i] = num1;
                }

                for (i = 1; i <= 19; i++)
                    fscanf(ifptr, "%s", s);

            break;
        } /* End of switch */

        for (i = nMoment + nCross + nSupport; i <= total - 1; i++) {
            fscanf(ifptr, "%d%f", &num1, &num2);
            result[j][i] = num2;
            number[i] = num1;
```

```
    }
}

for (j = 10; j <= increment - 1; j++) {
    for (i = 1;i <= 52; i++)
        fscanf(ifptr, "%s", s);

    for (i = 0; i <= nMoment - 1; i++) {
        fscanf(ifptr, "%d%f%f", &num1, &num2, &num3);
        result[j][i] = num3;
        number[i] = num1;
    }

    for (i = 1;i <= 18; i++)
        fscanf(ifptr, "%s", s);

    for (i = nMoment; i <= nMoment + nCross - 1; i++) {
        fscanf(ifptr, "%d%f%f", &num1, &num2, &num3);
        result[j][i] = num3;
        number[i] = num1;
    }

    for (i = 1;i <= 26; i++)
        fscanf(ifptr, "%s", s);

    switch (type) {
        case 0:
            for (i = nMoment + nCross;
                i <= nMoment + nCross + nSupport - 1; i++) {
                fscanf(ifptr, "%d%f", &num1, &num2);
                result[j][i] = num2;
                number[i] = num1;
            }

            for (i = 1; i <= 16; i++)
                fscanf(ifptr, "%s", s);

        break;

        case 1:
```

```
                    for (i = nMoment + nCross;
                         i <= nMoment + nCross + nSupport - 1; i++) {
                         fscanf(ifptr, "%d%s%f", &num1, s, &num2);
                         result[j][i] = num2;
                         number[i] = num1;
                    }

                    for (i = 1; i <= 19; i++)
                         fscanf(ifptr, "%s", s);

               break;
          }  /* End of switch */

          for (i = nMoment + nCross   + nSupport; i <= total - 1; i++) {
               fscanf(ifptr, "%d%f", &num1, &num2);
               result[j][i] = num2;
               number[i] = num1;
          }
     }


     fclose(ifptr);
}

/* Find the maximum and the minimum and write result to file */

void maxFile(void)
{
     int i, j;
     float m[INCRE][9];

     for (i = 0; i <= increment - 1; i++)
          for (j = 0; j <= 8; j++)
               m[i][j] = 0;

     for (i = 0; i <= increment - 1; i++) {
          switch (nSupport) {
               case 2:
                    m[i][0] = result[i][0] + result[i][1];
                    m[i][2] = result[i][2] + result[i][3];
```

```
                m[i][1] = m[i][0] + m[i][2];
                m[i][3] = result[i][nMoment + nCross];
                m[i][5] = result[i][nMoment + nCross + 1];
                m[i][4] = (m[i][3] + m[i][5]) / 2;
                m[i][6] = result[i][nMoment + nCross + nSupport];
                m[i][8] = result[i][nMoment + nCross + nSupport + 1];
                m[i][7] = (m[i][6] + m[i][8]) / 2;
                break;

            case 3:
                m[i][0] = result[i][0] + result[i][1];
                m[i][1] = result[i][2] + result[i][3] + result[i][4] +
                          result[i][5];
                m[i][2] = result[i][6] + result[i][7];
                m[i][3] = result[i][nMoment + nCross];
                m[i][4] = result[i][nMoment + nCross + 1];
                m[i][5] = result[i][nMoment + nCross + 2];
                m[i][6] = result[i][nMoment + nCross + nSupport];
                m[i][7] = result[i][nMoment + nCross + nSupport + 1];
                m[i][8] = result[i][nMoment + nCross + nSupport + 2];
                break;

            case 4:
                m[i][0] = result[i][0] + result[i][1];
                m[i][1] = result[i][2] + result[i][3] + result[i][4] +
                          result[i][5];
                m[i][2] = result[i][6] + result[i][7];
                m[i][3] = result[i][nMoment + nCross];
                m[i][4] = (result[i][nMoment + nCross + 1] +
                          result[i][nMoment + nCross + 2]) / 2;
                m[i][5] = result[i][nMoment + nCross + 3];
                m[i][6] = result[i][nMoment + nCross + nSupport];
                m[i][7] = (result[i][nMoment + nCross + nSupport + 1] +
                          result[i][nMoment + nCross + nSupport + 2]) / 2;
                m[i][8] = result[i][nMoment + nCross + nSupport + 3];
                break;
        } //End of switch
    }

    for (i = 0; i <= increment - 1; i++) {
```

```
                for (j = 0; j <= 5; j++) {
                    if (m[i][j] > max[0][j])
                        max[0][j] = m[i][j];

                    if (m[i][j] < max[1][j])
                        max[1][j] = m[i][j];
                }

                for (j = 6; j <= 8; j++) {
                    if (m[i][j] < max[0][j])
                        max[0][j] = m[i][j];

                    if (m[i][j] >= max[1][j])
                        max[1][j] = m[i][j];
                }
            }

            for (j = 0; j <= increment - 1; j++) {
                for (i = nMoment; i <= nMoment + nCross - 1; i++) {
                    if (result[j][i] > max[0][9]) {
                        max[0][9] = result[j][i];
                        max[0][11] = number[i];
                    }

                    if (result[j][i] < max[0][10]) {
                        max[0][10] = result[j][i];
                        max[0][12] = number[i];
                    }
                }
            }
        }

/* Write result to output file */

void resultFile(FILE *rfptr, char *iFile)
{
    int i, j;

    for (i = 0; i <= 1; i++) {
        for (j = 0; j <= 12; j++)
```

```
                fprintf(rfptr, "%.4e ", max[i][j]);

            fprintf(rfptr, "%s\n", iFile);
        }
    /*
        for (i = 0; i <= increment - 1; i++) {
            for (j = 0; j <= total - 1; j++)
                fprintf(rfptr, "%d %.4f\n", number[j], result[i][j]);

            fprintf(rfptr, "\n\n");
        }
    */
        fclose(rfptr);
    }

    /* Write time history to output file */

    void historyFile(FILE *hfptr, char *iFile)
    {
        int i;

    /*      fprintf(hfptr, "inner_m inner_s inner_d\n"); */

        fprintf(hfptr, "0 0 0 0 0 0 %s\n", iFile);

        for (i = 0; i <= increment - 1; i++) {
            fprintf(hfptr, "%.4e %.4e %.4e %.4e %.4e %.4e",
                result[i][0] + result[i][1],
                result[i][nMoment - 2] + result[i][nMoment - 1],
                result[i][nMoment + nCross],
                result[i][nMoment + nCross + nSupport - 1],
                result[i][nMoment + nCross + nSupport],
                result[i][total - 1]);
            fprintf(hfptr, "\n");
        }

        fclose(hfptr);
    }
```

VITA AUCTORIS

Xuesheng Zhang

1968 Born on the 19th of March in Hubei Province, P.R. China.

1989 Graduated with B.Eng. degree in Civil Engineering from Huazhong University of Science and Technology, Wuhan, P.R.China.

1989 Worked as a Civil Engineer at Wuhan Iron and Steel Design and Research Institute, Wuhan, P.R. China.

1996 Graduated with M.Sc. degree from Institute of Engineering mechanics, Harbin, P.R. China.

1996 Worked as a Civil Engineer at Shenzhen Municipal Company, Shenzhen, P.R. China.

2000 Enrolled in the Faculty of Graduate Studies and Research, University of Windsor, Windsor, Ontario, Canada, in a program leading to the degree of Master of Applied Science in Civil Engineering.